2016

Elucidating Proteasome Catalytic Subunit Composition and Its Role in Proteasome Inhibitor Resistance

Kimberly C. Carmony
University of Kentucky, kim.carmony@gmail.com
Digital Object Identifier: http://dx.doi.org/10.13023/ETD.2016.173

STUDENT AGREEMENT:

I represent that my thesis or dissertation and abstract are my original work. Proper attribution has been given to all outside sources. I understand that I am solely responsible for obtaining any needed copyright permissions. I have obtained needed written permission statement(s) from the owner(s) of each third-party copyrighted matter to be included in my work, allowing electronic distribution (if such use is not permitted by the fair use doctrine) which will be submitted to UKnowledge as Additional File.

I hereby grant to The University of Kentucky and its agents the irrevocable, non-exclusive, and royalty-free license to archive and make accessible my work in whole or in part in all forms of media, now or hereafter known. I agree that the document mentioned above may be made available immediately for worldwide access unless an embargo applies.

I retain all other ownership rights to the copyright of my work. I also retain the right to use in future works (such as articles or books) all or part of my work. I understand that I am free to register the copyright to my work.

REVIEW, APPROVAL AND ACCEPTANCE

The document mentioned above has been reviewed and accepted by the student's advisor, on behalf of the advisory committee, and by the Director of Graduate Studies (DGS), on behalf of the program; we verify that this is the final, approved version of the student's thesis including all changes required by the advisory committee. The undersigned agree to abide by the statements above.

Kimberly C. Carmony, Student

Dr. Kyung Bo Kim, Major Professor

Dr. David Feola, Director of Graduate Studies

ELUCIDATING PROTEASOME CATALYTIC SUBUNIT COMPOSITION AND ITS ROLE IN PROTEASOME INHIBITOR RESISTANCE

DISSERTATION

A dissertation submitted in partial fulfillment of the
requirements for the degree of Doctor of Philosophy in the
College of Pharmacy
at the University of Kentucky

By
Kimberly C. Carmony

Lexington, Kentucky

Director: Kyung Bo Kim, Ph.D., Associate Professor of Pharmaceutical Sciences

Lexington, Kentucky
2016

ABSTRACT OF DISSERTATION

ELUCIDATING PROTEASOME CATALYTIC SUBUNIT COMPOSITION AND ITS ROLE IN PROTEASOME INHIBITOR RESISTANCE

Proteasome inhibitors bortezomib and carfilzomib are FDA-approved anticancer agents that have contributed to significant improvements in treatment outcomes. However, the eventual onset of acquired resistance continues to limit their clinical utility, yet a clear consensus regarding the underlying mechanisms has not been reached.

Bortezomib and carfilzomib are known to target both the constitutive proteasome and the immunoproteasome, two conventional proteasome subtypes comprising distinctive sets of catalytic subunits. While it has become increasingly evident that additional, 'intermediate' proteasome subtypes, which harbor non-standard mixtures of constitutive proteasome and immunoproteasome catalytic subunits, represent a considerable proportion of the proteasome population in many cell types, less is known regarding their contribution to cellular responses to proteasome inhibitors. Importantly, previous studies in murine models have shown that individual proteasome subtypes differ in sensitivity to specific proteasome inhibitors. Furthermore, research efforts in our laboratory and others have revealed that proteasome catalytic subunit expression levels and activity profiles are altered when human cancer cells acquire resistance to proteasome inhibitors. We therefore hypothesized that changes in the relative abundances of individual proteasome subtypes contribute to the acquired resistance of cancer cells to bortezomib and carfilzomib.

A major obstacle in testing our hypothesis was a lack of chemical probes suitable for use in identifying distinct proteasome subtypes. We addressed this by developing a series of bifunctional proteasome probes capable of crosslinking specific pairs of catalytic subunits colocalized within individual proteasome complexes and compatible with immunoblotting-based detection of the crosslinked subunit pairs. We confirmed the utility of these probes in discerning the identities of individual proteasome subtypes in a multiple myeloma cell line that abundantly expresses catalytic subunits of both the constitutive proteasome and immunoproteasome. Our findings indicate that constitutive proteasomes, immunoproteasomes, and intermediate proteasomes co-exist within these cells and support conclusions drawn from previous studies in other cell types.

We also established non-small cell lung cancer cell line models of acquired bortezomib and carfilzomib resistance in which to test our hypothesis. Using immunoblotting and proteasome activity assays, we discovered that changes in the expression levels and activities of individual catalytic proteasome subunits were associated with the emergence of acquired resistance to bortezomib or carfilzomib. These

changes were inhibitor-dependent and persisted after the selective pressure of the inhibitor was removed. Finally, results obtained using our bifunctional proteasome probes suggest that the altered abundance of an intermediate proteasome subtype is associated with acquired proteasome inhibitor resistance. Collectively, our results provide evidence linking changes proteasome composition with acquired proteasome inhibitor resistance and support the hypothesis that such changes are involved in resistance mechanisms to these inhibitors.

Keywords: Proteasome Inhibitor, Bortezomib, Carfilzomib, Proteasome Subtype, Bifunctional Proteasome Probe

Kimberly C. Carmony

April 18, 2016

ELUCIDATING PROTEASOME CATALYTIC SUBUNIT COMPOSITION AND ITS ROLE IN PROTEASOME INHIBITOR RESISTANCE

By

Kimberly C. Carmony

Kyung Bo Kim, Ph.D.
Director of Dissertation

David Feola, Pharm.D., Ph.D.
Director of Graduate Studies

April 18, 2016

To my family

ACKNOWLEDGEMENTS

I am grateful to a number of people who played instrumental roles throughout this journey. I would first like to thank my advisor, Dr. Kyung Bo Kim, for his constant guidance, encouragement, patience, and support. I truly appreciate all of the opportunities he has given me and all he has taught me. Second, I would like to thank Dr. Wooin Lee, who has given her advice and support whenever I have asked. I am also grateful to Dr. Penni Black, Dr. Todd Porter, and Dr. Jerold Woodward for serving on my advisory committee; their unique perspectives have also been essential in shaping my graduate studies. Additionally, I would like to thank Dr. Luke Bradley for agreeing to serve as the external examiner for my dissertation defense.

I would like to thank all of the faculty and staff at the College of Pharmacy. Special thanks to Dr. Jim Pauly and Dr. Linda Dwoskin for allowing me to rotate in their laboratories. I am grateful to Catina Rossoll, Ned Smith, Chris Porter, Lou Dunn, Todd Sizemore, Jay Young, Kristi Moore, Janice Butner, and Dimple Hatfield for their support over the years.

I also thank my colleagues for their friendship and support: Dr. Marie Wehenkel, Dr. Hyosung Lee, Dr. Eun Ryoung Jang, Kyunghwa Kim, Dr. Ying Wu, Dr. Lalit Kumar Sharma, Do-Min Lee, Na-Ra Lee, Dr. Nilay Thakkar, Dr. Donghern Kim, Dr. Songhee Han, Zachary Miller, Lin Ao, Ji Eun Park, Kyungbo Kim, Youngran Lim, Min Jae Lee, Changwe Park, Yujin Jang, Dr. Qingquan Zhao, Allie Milam, James Marks, Daniel Machado, and Courtney Ford. Special thanks to chemists Dr. Lalit Kumar Sharma, Dr. Ying Wu, Do-Min Lee, and Ji Eun Park for providing the probes and substrates used in my experiments, and to Ji Eun Park and Min Jae Lee for their assistance with the indicated experiments described in Chapters 4 and 5.

Finally, I thank my family, especially my parents and husband, for their patience and encouragement throughout my graduate studies.

TABLE OF CONTENTS

LIST OF TABLES

LIST OF FIGURES

1 INTRODUCTION

1.1 Discovery and Characterization of the Ubiquitin-Proteasome Pathway

The decades leading up to the discovery of ubiquitin-dependent protein degradation were characterized by marked paradigm shifts regarding the regulation of intracellular protein levels. Until it was shown in the early 1940s that proteins are continuously turned over (i.e., degraded and resynthesized), they were regarded as stable entities [1, 2]. In the 1950's, the discovery of the lysosome and its apparent protein-degrading capabilities led many researchers to readily accept a new paradigm in which this organelle was solely responsible for cellular protein turnover [1, 2]. However, the unraveling of the ubiquitin-dependent pathway, beginning in the late 1970s and extending through the 1980s, provided a satisfying explanation for a number of observed properties of protein degradation that were seemingly incompatible with the acknowledged non-selective, ATP-independent mechanism of lysosomal degradation—most notably, it explained why different cellular proteins are degraded at different rates, the differential effects of lysosomal protease inhibitors on distinct protein groups, as well as the ATP requirement for intracellular protein degradation. Thus, a second major paradigm shift resulted in which ubiquitin-dependent proteolysis was deemed responsible for degrading the vast majority of cellular proteins [1, 2]. Largely in the pages of *The Journal of Biological Chemistry* and *Proceedings of the National Academy of Sciences*, Aaron Ciechanover, Avram Hershko, and Irwin Rose documented their discoveries that allowed them to elucidate this pathway, for which they were awarded the Nobel Prize in Chemistry in 2004 [1, 2].

Targeting a protein for ubiquitin-dependent degradation, they found, involves its covalent linkage with a chain composed of multiple copies of the ubiquitin protein [3]. Proteins are polyubiquitinated in a multistep process involving a series of three enzymes: an E1 ubiquitin-activating enzyme [4-6], an E2 ubiquitin-conjugating enzyme, and an E3 ubiquitin ligase enzyme [7]. A K48-linked polyubiquitin chain, in which the C-terminal glycine residue of the incoming ubiquitin is linked with lysine at position 48 of the ubiquitin at the end of the growing chain, appears to serve as the earmark for degradation [8, 9]. Additionally, a tetraubiquitin chain appears to be the minimal signal capable of targeting a protein for ubiquitin-dependent degradation [10] (Figure 1.1).

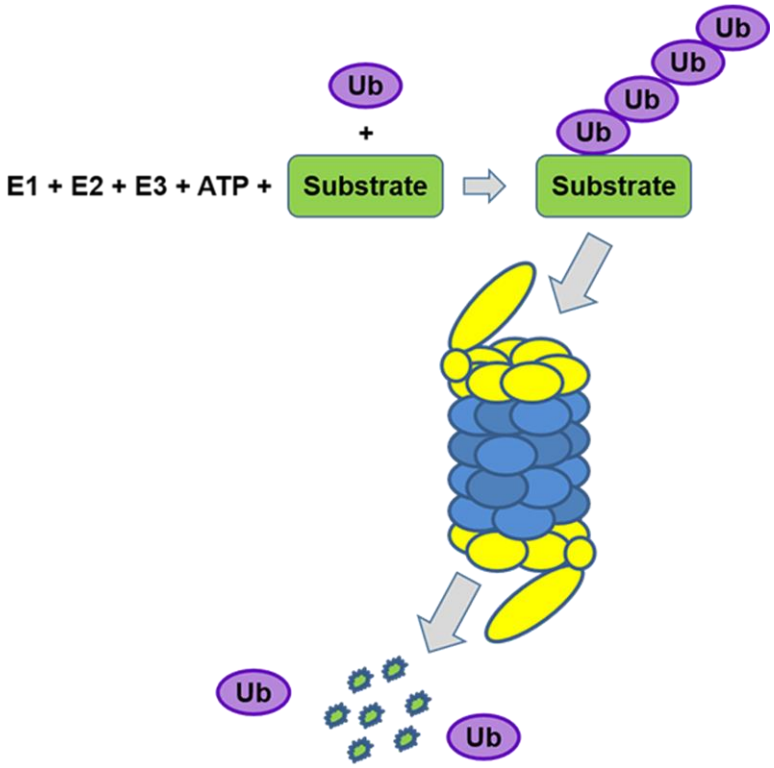

Figure 1.1 Ubiquitin proteasome pathway-mediated protein degradation
A polyubiquitin chain is covalently linked to a target protein (substrate) via a series of three enzymes: an E1, an E2, and an E3. This polyubiquitin chain is recognized by the proteasome, which degrades the protein to short peptides and releases free ubiquitin. The 19S caps are schematically depicted in yellow, and the 20S core in blue.

Wilk, Pearce, and Orlowski were the first researchers to purify and characterize the endopeptidase we now know as the 20S proteasome, which serves as the degradative machinery of the ubiquitin-dependent pathway [11]. It was found to efficiently cleave bonds between leucine and the chromogenic group p-nitroaniline within the synthetic chromogenic substrates Cbz-Gly-Gly-Leu-pNA and Cbz-Gly-Gly-Tyr-Leu-pNA. Conversely, it was unable to hydrolyze model trypsin, chymotrypsin, carboxypeptidase, and aminopeptidase substrates [11]. Further studies with chromogenic peptide substrates revealed that the proteasome possesses three main catalytic activities—a chymotrypsin-like (CT-L) activity, a trypsin-like (T-L) activity, and a peptidylglutamyl-peptide bond hydrolyzing (PGPH) activity—by which it cleaves peptide bonds on the carboxyl side of hydrophobic, basic, and acidic amino acids, respectively [12, 13]. The PGPH activity was later renamed the ‘caspase-like’ (C-L) activity when it was discovered that the active sites responsible for this activity prefer to hydrolyze peptide bonds after aspartates over those that follow glutamates [14]. Two additional catalytic activities were subsequently

discovered: a branched chain amino acid preferring (BrAAP) activity and a small neutral amino acid preferring (SNAAP) activity, which cleave on the carboxyl side of branched chain and small neutral amino acids, respectively [15].

1.2 Proteasome Structure and Proteasomal Degradation of Proteins

Proteasomes interact with polyubiquitinated substrate proteins of the ubiquitin-proteasome pathway (UPP) via ubiquitin-binding subunits of the 19S regulatory caps that associate with the ends of the 20S proteasome core [16-18] (Figure 1.1). The 19S cap also contains components that remove the polyubiquitin chain to facilitate recycling of ubiquitin, unfold the protein, and assist entry of the unfolded protein into the 20S core [19-23]. The core itself is an annular complex built of four axially stacked heptameric rings. Each outer or inner ring is composed of seven α-subunits or seven β-subunits, respectively. The seven α-subunits of the *T. acidophilum* 20S proteasome are all identical, as are the seven β-subunits [24, 25]. However, in eukaryotes, seven distinct α-subunits (α1-α7) and seven distinct β-subunits (β1-β7) comprise each α-ring and β-ring, respectively, with each of these subunits occupying a fixed position within the complex [16, 26, 27]. The N-terminal tails of the α-rings form a gate that must be opened for a substrate to gain access to the 20S core, thereby providing one of several protective barriers against unregulated proteolysis. Interactions between the 19S cap and the 20S core open this gate [28]. The catalytically active subunits, which are members of the N-terminal nucleophile (Ntn) hydrolase family [29], reside in the β-rings. As all seven β-subunits of the *T. acidophilum* proteasome are identical, they are all catalytically active [30]. On the other hand, of the seven distinct β-subunits of eukaryotic proteasomes, only three—β1, β2, and β5—have proteolytic activities [31-33]. The active sites of the catalytic β-subunits are formed at subunit-subunit interfaces and are sequestered within the inner chamber of the core complex, providing further protection against uncontrolled degradation of cellular proteins [30, 33]. Additionally, the catalytic β-subunits are synthesized as precursors containing N-terminal propeptides; they become active only once their propeptides are removed to liberate the catalytic threonine residues of their new N-termini [34-37]. Removal of these propeptides occurs via an autocatalytic mechanism only within the fully assembled proteasome complex, providing yet another protective mechanism to ensure that these subunits cannot degrade proteins at random prior to their proteasome incorporation [36, 38-41]. Upon entry of a substrate protein into the core particle, the active sites begin cleaving its peptide bonds, thereby degrading it to peptide fragments ~3-22 amino acids

in length [42, 43] (Figure 1.1). Most of the products produced by proteasomal proteolysis are then further hydrolyzed by cytosolic peptidases to single amino acids [44]. Alternatively, a small percentage of these products serve as antigens for presentation on MHC class I molecules, either directly or following further peptidase-mediated processing of their N-termini [43, 45-47].

By analyzing the hydrolysis of fluorogenic peptide model substrates by yeast mutants, Heinemeyer et al. were able to assign the C-L activity to β1, the T-L activity to β2, and the CT-L activity to β5 [31]. These conclusions were further supported by crystallography data, which identified amino acid 45 within the S1 specificity pocket of each of the yeast proteasome's catalytic subunits as a major determinant of that subunit's cleavage site preferences [33]. For example, Arg45 of β1's S1 pocket explains the preference of this subunit for cleaving peptide bonds after acidic amino acids. Alternatively, Gly45 of β2 renders its S1 pocket quite spacious, and with Glu53 forming the bottom of this pocket, β2 prefers cleaving peptide bonds after large, basic residues. Finally, Met45 of β5 contributes to the preference of β5 for cleaving peptide bonds after hydrophobic amino acids [33, 48]. The nature of each S1 pocket is further modulated by amino acid residues of an adjacent subunit within the β-ring. In addition to their C-L and CT-L activities, respectively, both β1 and β5 were concluded responsible for the BrAAP activity, and β5 for the SNAAP activity [49]. However, assessments made using fluorogenic peptide substrates may provide an oversimplified view of the cleavage site specificities of these subunits when they degrade longer peptides [50]. Proteasomes containing catalytic subunits β1, β2, and β5 appeared to be expressed in nearly all cell types and tissues examined and are therefore referred to as 'constitutive proteasomes' (Figure 1.2).

It became evident soon after its discovery that the UPP mediates the degradation of short-lived and abnormal proteins [51-53]. Certain short-lived regulatory proteins were found to depend on the UPP for their timely degradation, revealing a key role of this pathway in regulating various cellular processes such as progression through the cell cycle and cell survival and differentiation [54-56]. As will be discussed further below, the development and discovery of selective inhibitors of the proteasome allowed these UPP functions to be confirmed and additional roles to be identified. Furthermore, the contribution of the UPP to various pathological processes underlying human diseases has stimulated interest in targeting its components, particularly the proteasome, for therapeutic purposes.

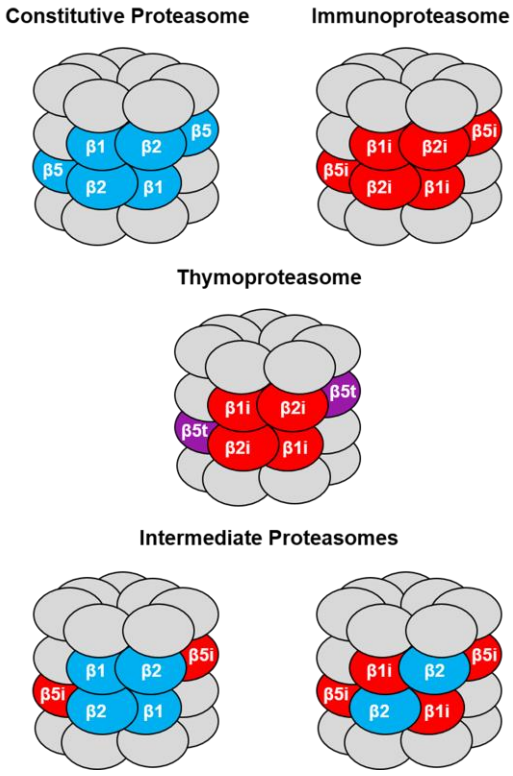

Figure 1.2 Proteasome subtypes
Five distinct proteasome subtypes that can be distinguished by their catalytic subunit compositions have been identified in mammalian cells.

1.3 Immunoproteasome and Thymoproteasome

1.3.1 Immunoproteasome

In the 1980s, Monaco et al. discovered a previously uncharacterized class of murine proteins that could be immunoprecipitated from macrophages by an antiserum against the MHC H-2^d haplotype, yet differed both biochemically and genetically from known MHC-encoded proteins. They were found to range in molecular weight from ~15-30 kDa and were thus named 'low molecular weight proteins' (or 'LMPs') [57]. High levels of the LMPs were detected in macrophages, and lower levels in lymphocytes and fibroblasts [57]. They were shown to exist in a large (580 kDa) complex held together by noncovalent bonds. A similar complex was also detected in the human U937 cell line [58]. The genes encoding two of the LMPs, initially named LMP-2 and LMP-7, mapped to the MHC class II complex in close proximity to the TAP1 and TAP2 genes [59, 60], whose products transport cytoplasmic peptides into the endoplasmic reticulum (ER) for assembly on newly-generated MHC class I molecules. The resulting MHC class I-peptide complexes are transported via the Golgi apparatus to the cell surface, where the antigen

is presented for recognition by cytotoxic ($CD8^+$) T cells of the adaptive immune system [61, 62]. In 1991, Brown et al. provided evidence indicating that the LMP complex was in fact a subtype of the proteasome [60]. Based on the high level of LMPs in antigen-presenting cells and the ability of the immunomodulatory cytokine IFNγ to upregulate the MHC-encoded LMPs as well as TAP1 and TAP2, these researchers proposed that the LMP-2- and LMP-7-containing proteasome complex may function in the processing of foreign antigens, producing antigenic peptides for subsequent transport by TAP1 and TAP2 and, finally, presentation to T cells [59, 60].

Findings from a subsequent study conducted by Brown et al. led them to propose a model in which distinct subtypes of proteasomes are formed by the incorporation of unique subunits into a core complex otherwise comprising subunits common to all proteasomes, permitting proteasome functionality to adapt as needed to meet cellular demands [63]. This was further supported by the results of subsequent studies, which showed that the IFNγ-inducible subunits replaced their 'constitutive subunit' homologs upon *de novo* proteasome biogenesis. Among the first of these was conducted by Aki et al., who demonstrated that the levels of LMP-2 and LMP-7 in intact proteasome complexes strongly increased in human SW620 colon carcinoma cells following IFNγ treatment, while a strong decrease in the levels of subunits 'X' and 'Y' occurred concomitantly [64]. X and Y were identified as previously-reported constitutive subunits β5 and β1, which bear high homology to LMP-7 and LMP-2, respectively [65]. Based on these observations, IFNγ was concluded to cause a replacement of the β5 and β1 subunits by LMP-2 and LMP-7 to form a proteasome complex termed the 'immunoproteasome', a name chosen due to its IFNγ-inducibility and its proposed role in producing antigenic peptides for presentation on MHC class I molecules [65]. Current nomenclature refers to LMP-2 as 'β1i' and LMP-7 as 'β5i'. Additional evidence for such subunit replacement was provided by Früh et al., who showed that an increase in proteasome-incorporated β1i led to a selective decrease in the incorporation of β1, whereas an increase in incorporated β5i led to a decrease only in incorporation of β5. They concluded that these changes likely resulted from a competition between two homologous subunits for a single position within the assembling proteasome complex, with the relative concentration of each competitor determining the outcome [66].

IFNγ stimulation of cells was also found to alter the catalytic activities of proteasome complexes. Specifically, it increased the CT-L and T-L activities and decreased the C-L activity. It was therefore proposed that the IFNγ-induced incorporation

of β1i and β5i into proteasome complexes may result in the functional changes observed [64, 67]. These changes indicated that, in comparison with constitutive proteasomes, immunoproteasomes would less efficiently produce peptides with acidic C-termini and more efficiently produce those with basic and hydrophobic C-termini. As MHC class I molecules preferentially bind peptides with basic and hydrophobic C-termini, this further supports a role for immunoproteasomes in adaptive immune responses [64, 67].

To more precisely identify how the incorporation of each of the IFNγ-inducible subunits (referred to hereafter as 'immunosubunits') impacted these catalytic activities, a series of experiments with transfected cell lines was conducted. Transfecting lymphoblasts or HeLa cells with β5i increased the proteasome's CT-L activity, but its C-L activity remained unaltered, whereas transfecting with β1i decreased proteasomal C-L activity while leaving the CT-L activity unaltered. Transfecting these cells with either β5i or β1i led to an increase in the proteasome's T-L activity [68].

Alternatively, transfecting HeLa cells with β1 increased C-L activity but left the T-L and CT-L activities unchanged [69]. Together with the opposing results obtained with the β1i transfectant [68], this indicates that β1 bears the C-L activity of the proteasome, and that its decreased presence in proteasomes leads to the reduced C-L activity observed following β1i transfection or IFNγ stimulation [68, 69]. Likewise, transfecting a lymphoblast cell line with β5 resulted in decreased CT-L and T-L activity, but left the C-L activity unaltered [69], contrasting what was observed for the β1i and β5i transfectants [68]. These results indicate that the reduced β5 levels in intact proteasomes following β5i transfection or IFNγ stimulation leads to the increased CT-L and T-L activities that were observed under these conditions [68, 69].

A third immunosubunit, 'multicatalytic endopeptidase complex-like 1' ('MECL-1'), was later found to replace β-subunit 'Z' in mouse and human proteasomes following IFNγ stimulation [70, 71]. Unlike β1i and β5i, the gene encoding MECL-1 is located outside of the MHC [72]. Based on the homology of Z to yeast β2, it is now more commonly called 'β2', and its immunosubunit homolog, MECL-1, is called 'β2i'. It was speculated that these subunits modulate the proteasome's T-L activity [70]. These three subunit exchanges (β1i for β1, β5i for β5, and MECL-1 for Z) were the only three noted following IFNγ stimulation [70]; thus, pure immunoproteasomes contain the three immunosubunits in place of their constitutive homologs (Figure 1.2). Similar observations were made in mouse H6 hepatoma cells [73]. Evidence indicating that these three constitutive subunits and their IFNγ-inducible counterparts are catalytically active, while the remaining β-subunits are not,

suggested that the mammalian proteasome has evolved towards a reduced number of catalytically active subunits and an increase in the diversity of these subunits, imparting a high degree of functional versatility [70].

Crystallography data for the mammalian constitutive proteasome and immunoproteasome provided structural explanations for the observed differences in catalytic activities between these two proteasome subtypes [74, 75]. In comparison with that of β1, β1i's S1 specificity pocket has a reduced size and polarity, leading to a shift away from C-L activity towards CT-L and BrAAP activity [74, 75]. Major structural differences between the S1 pockets of β2 and β2i were not observed, in accordance with both having T-L activity [74, 75]. Finally, differences in the conformation of Met45 between β5 and β5i's S1 pockets result in a smaller S1 pocket in β5 and a larger one in β5i. Therefore, although both subunits have CT-L activity, β5 has an increased preference for cleaving after small hydrophobic residues such as Ala, while β5i has a stronger preference for cleaving after larger hydrophobic residues [75]. These differences facilitated the recent development of fluorogenic peptide substrates that are selectively hydrolyzed by individual constitutive subunits or immunosubunits [76].

Early studies in which the expression levels of the immunosubunits were examined across various cell lines and tissues yielded results consistent with the proposed roles of these subunits in adaptive immunity. β1i, β2i, and β5i mRNA levels were high in mouse thymus, spleen, and lymph nodes, moderate in lung, and substantially lower in other non-lymphoid tissues (e.g., liver, kidney, heart, brain, and muscle) [77, 78]. Levels of the mRNAs encoding each constitutive subunit and its immunosubunit counterpart across the various tissues were inversely correlated [78]. Consistent with the high mRNA levels detected, mouse spleen contained an exceptionally high proportion of immunosubunit-containing proteasomes, while the proportion of these proteasomes was lower in heart, kidney, and liver [77]. Mouse thymus also contained high levels of immunosubunit-containing proteasomes, and lung was found to contain an intermediate level of immunosubunits [78]. Constitutive expression of the β2i protein was also detected in freshly isolated human white blood cells [79].

In line with their constitutive expression predominantly in tissues involved in the immune system, the immunosubunits were found to be most highly expressed in cells of hematopoietic origin. β1i and β5i mRNA levels were high in mouse RMA T cell and RHW macrophage cell lines. Lower levels were detected in mouse NIH 3T3 fibroblasts and human hepatocytes, although also in the human CEM T cell line [77]. Additionally, higher

β2i mRNA levels were detected in human B cell lines IM9 and Reh than in human HeLa cervix carcinoma and MCF7 breast adenocarcinoma cells [79], and β2i protein levels were undetectable in HeLa, HeLa S3, human Caco-2 colon adenocarcinoma cells, and human ECV304 endothelial cells prior to IFNγ stimulation [79]. Conversely, although basal expression of β1i and β5i mRNAs was not detectable in the SW620 colon carcinoma cell line, it was also not detected in the J111 monocytic leukemia cell line. Furthermore, basal expression of β5i mRNA was detected in two renal carcinoma cell lines (ACHN and KPK-1), whereas basal β1i mRNA expression was only detected in ACHN (and not KPK-1) cells [64]. In agreement with their mRNA levels, higher basal amounts of the β5i protein were detected in the renal carcinoma cell lines than in the SW620 and J111 cell lines. These results indicate that the basal expression of β1i and β5i is cell type-specific [64], and, at least in cancer cells, not necessarily restricted to immune-related cells. However, immunosubunit protein levels are not always consistent with the levels of their corresponding mRNAs. For example, despite the relatively high β1i and β5i mRNA levels in liver, this tissue was found to have a low proportion of β1i- and β5i-containing proteasomes. It was suggested that the high mRNA levels in liver might allow proteasome composition to be readily adjusted when required [77]. Additionally, although stimulation of mouse RMA T cells with IFNγ led to a marked increase in β1i and β5i mRNA levels, β5i protein levels (which were already readily detectable prior to stimulation) remained relatively unchanged [77].

IFNγ was shown to induce expression of immunosubunit mRNAs in human SW620 colon carcinoma, J111 monocytic leukemia, and KPK-1 and ACHN renal carcinoma cell lines [64, 71] and in the mouse H6 hepatoma cell line [73], whereas the other proteasome α- and β-subunit-encoding mRNAs examined were not significantly affected [64, 71, 73]. Additionally, IFNγ stimulation increased β2i mRNA in HeLa cervix carcinoma and MCF7 breast adenocarcinoma cells, but increased it to a much lesser extent in B cell lines IM9 and Reh in which it was already constitutively expressed at higher levels [79]. β2i protein expression also increased following IFNγ treatment in HeLa, HeLa S3, Caco-2 colon adenocarcinoma, and ECV304 endothelial cells; in ECV304 cells, this was associated with the incorporation of β2i into proteasome complexes [79]. The basal and IFNγ-inducible levels of the processed β2i protein in the Reh and Daudi cells matched relatively well with the mRNA levels observed in these B cell lines [79].

Proteasomes are known to produce most of the antigenic peptides presented on MHC class I molecules [80, 81], and many of the observations described above led

researchers to propose that immunoproteasomes specifically function in producing such peptides. This notion was further supported by demonstrations that immunoproteasomes produce immunodominant epitopes derived from ovalbumin [43] or a lymphocytic choriomeningitis viral protein [82] more efficiently than constitutive proteasomes. Overexpressing all three immunosubunits in mouse fibroblast cells increased the presentation of the latter epitope to $CD8^+$ T cells [82].

Studies conducted with immunosubunit-deficient mice provided additional evidence suggesting that immunoproteasomes produce MHC class I ligands more efficiently than constitutive proteasomes. β5i-deficient mice displayed reduced cell surface levels of MHC class I molecules and ineffectively presented a peptide derived from an endogenous antigen, indicating defective production of antigenic peptides [83]. In line with these results, β5i-deficient mice were unable to survive *Toxoplasma gondii* infection under conditions that spared wild-type mice, which was speculated to result from defects in antigen processing [84]. Furthermore, antigen presenting cells isolated from β1i-deficient mice appeared to present an influenza A viral epitope less efficiently than those obtained from wild-type mice. Accordingly, the anti-influenza $CD8^+$ T cell response is inferior in β1i-deficient mice [85]. In contrast to β5i-deficient mice [83, 86], β1i-deficient mice had fewer $CD8^+$ T cells than wild-type mice [85]. β2i-deficient mice also had fewer $CD8^+$ splenocytes as well as a defective $CD8^+$ T cell response to two lymphocytic choriomeningitis viral protein-derived epitopes, with the reduced response to one epitope being attributable to an altered T cell repertoire [87]. β1i may also protect against tumorigenesis by assisting the antitumor immune response [88]. Alternatively, a study assisted by mice lacking both β2i and β5i expression revealed a potential protective role of immunosubunit upregulation in peripheral tissues under inflammatory conditions against the development of $CD8^+$ T cell-mediated autoimmune diseases [89].

However, while these observations seemed to indicate that immunoproteasomes specifically function in producing MHC class I ligands, other findings indicated that they are actually dispensable for this process. For example, in cell lines lacking the genes encoding β1i, β5i, TAP1, and TAP2, reintroducing TAP1 and TAP2 is sufficient to restore MHC class I-mediated antigen presentation to normal levels [90, 91]. Later studies demonstrated that the impact of a given constitutive subunit or immunosubunit on antigen presentation depends on the sequence of each particular antigenic epitope [92-95]. In fact, some antigenic peptides are actually better produced by constitutive proteasomes, due to either the poor efficiency with which immunoproteasomes produce the correct

C-terminus or the tendency of immunoproteasomes to internally cleave the peptide [95-97]. In line with these results, the $CD8^+$ T cell response against infection with Sendai virus was not reduced in β1i-deficient mice in comparison with wild-type mice, contrasting the impaired response to influenza infection [85]. $CD8^+$ T cell responses to lymphocytic choriomeningitis virus were also largely unimpaired, as was the immunodominance hierarchy, in mice lacking β1i or β5i expression [98]. These findings indicate that understanding which peptides are efficiently and inefficiently produced by each proteasome subtype is beneficial for tumor immunotherapy and vaccine development [95, 96].

The immunosubunits appear to contribute to the adaptive immune system in other ways as well. They have, for example, been found to hold regulatory roles in T cell survival and proliferation [86, 87, 93, 99, 100], T helper cell differentiation [101, 102], and pro-inflammatory cytokine production [101, 103-106]. However, constitutive expression of immunosubunits has also been observed in immunoprivileged tissues, including the retina [107] and brain [107-109], as well as in other non-hematopoietic cells such as aortic endothelial cells [110], suggesting roles for these subunits aside from immune responses. Indeed, immunosubunits appear to be important for the efficient elimination of oxidatively-damaged proteins under conditions of oxidative stress [111, 112] and for regulating cardiac muscle mass [113]. They are also upregulated in response to injury of the retina and brain, suggesting that they may help repair cellular damage to protect against injury [107]. β1i was found to play a role in cell signaling, as it appeared to be important for proteolytic processing events involved in activating the transcription factor NF-κB [88, 114], although this has been disputed by findings obtained in our laboratory and elsewhere [115-118].

1.3.2 Thymoproteasome

Functional proteasomes are essential for the survival of yeast [119]. Because the human T2 cell line, which contains a homozygous deletion of the MHC class II region containing the genes encoding the immunosubunits [120], can survive without expressing immunosubunits, Ortiz-Navarrete et al. suggested that human cells may express multiple specialized proteasome complexes, with the one containing the immunosubunits being better suited for antigen processing [121]. Further supporting this idea of specialized proteasomes, Murata et al. identified a third homolog of the β5 subunit that incorporates into otherwise immunoproteasomes (containing β1i and β2i). The resulting proteasome

complexes were termed ‘thymoproteasomes’ due to the exclusive expression of this newly-identified β5 subunit, ‘β5t’, in cortical thymic epithelial cells [122] (Figure 1.2). In contrast to the S1 specificity pockets of β5 and β5i, which include Met45 and are largely composed of hydrophobic residues, β5t’s S1 pocket includes Thr45 and is predominantly composed of hydrophilic amino acids, indicating that the CT-L activity of β5t should be less pronounced than that of β5 and β5i. Indeed, these β5t-containing proteasome complexes were shown to have lower CT-L activity than those containing either β5 or β5i, making them less effective in producing peptides with hydrophobic C-termini, which tend to bind tightly to MHC class I molecules. These low-affinity MHC class I-binding peptides appear to play an important role in the positive selection of developing $CD8^+$ T cells, a critical process that determines which of these cells will continue on in the developmental program [122].

Immature thymocytes develop into mature T cells in the thymus, during which they undergo both negative and positive selection processes to ensure that only immunocompetent T cells are released into the peripheral lymphoid organs. During positive selection, self peptides complexed with self MHC molecules are presented on the surface of cortical thymic epithelial cells to immature thymocytes as they move through the thymic cortex. Those thymocytes bearing T cell receptors capable of appropriately interacting with these complexes are positively selected to continue their development, as they will be able to interact with self MHC molecules in the periphery, and the remaining thymocytes undergo programmed cell death. In the subsequent process of negative selection, self peptides complexed with MHC molecules are again presented to the developing thymocytes on medullary thymic epithelial cells and other antigen-presenting cells in the thymic medulla, although, in this case, apoptosis is induced in thymocytes that interact with the self peptide-MHC complexes too intensely to eliminate these autoreactive cells from the body.

Thymoproteasomes appear to produce a unique array of MHC class I-binding peptides with distinctive properties important for the positive selection process [123-125]. As thymoproteasomes have a higher propensity to produce peptides that bind to MHC class I molecules with relatively low affinity, the looser interaction between these peptide products and MHC class I molecules on the surface of cortical thymic epithelial cells may dampen the intensity with which thymocytes interact with these complexes, helping to ensure that the positively-selected thymocytes will not further mature into T cells that will then react with normal self peptide-MHC complexes encountered in the periphery [122,

126]. Additionally, it has been proposed that the presentation of this thymoproteasome-specific set of peptides during positive selection may safeguard against mature T cells mounting autoimmune responses against these same peptides in the periphery [127]. Indeed, $CD8^+$ T cells of thymoproteasome-deficient mice tend to be more reactive against self peptides [124]. Whatever the mechanism, thymoproteasomes are obviously crucial for $CD8^+$ T cell development. β5t-deficient mice have substantially fewer $CD8^+$ thymocytes than wild-type mice and are unable to survive an influenza virus infection that is not lethal to control mice [122-124], stressing that differences in proteasome composition can have major biological consequences.

1.4 Development of Proteasome Inhibitors

To further examine the catalytic activities and cellular functions of the proteasome, researchers sought to develop small molecules capable of inhibiting its activity more specifically. Most of the proteasome inhibitors that have been developed to date are composed of a short peptide sequence followed by a C-terminal pharmacophore that reacts with the catalytic threonine residues of the proteasome's active sites. Interactions between the side chains of such inhibitors and the specificity pockets of each active site determine their subunit binding preferences. Therefore, the amino acid sequence of a given inhibitor largely determines whether it will act as a broad-spectrum proteasome inhibitor that targets most or all of the active sites, or a subunit-selective one that selectively targets the active site of a single subunit and/or its constitutive subunit or immunosubunit homolog. The five main classes of inhibitors include the peptide aldehydes, peptide boronates, β-lactones, peptide vinyl sulfones, and peptide epoxyketones (Figure 1.3).

1.4.1 Peptide Aldehydes

Peptide aldehydes were the first synthetic proteasome inhibitors to be developed [128] (Figure 1.3 A). These inhibitors reversibly bind the proteasome's active sites by forming hemiacetal adducts with their catalytic threonine residues [30, 33]. Peptide aldehyde inhibitors were used to make many important discoveries regarding the functional roles of proteasomes. These studies revealed, for example, that proteasomes are responsible for degrading most intracellular proteins and producing most antigenic peptides presented on MHC class I molecules [80]. Additionally, they were used to demonstrate that the tumor suppressor protein p53 [129] and the cyclin-dependent kinase

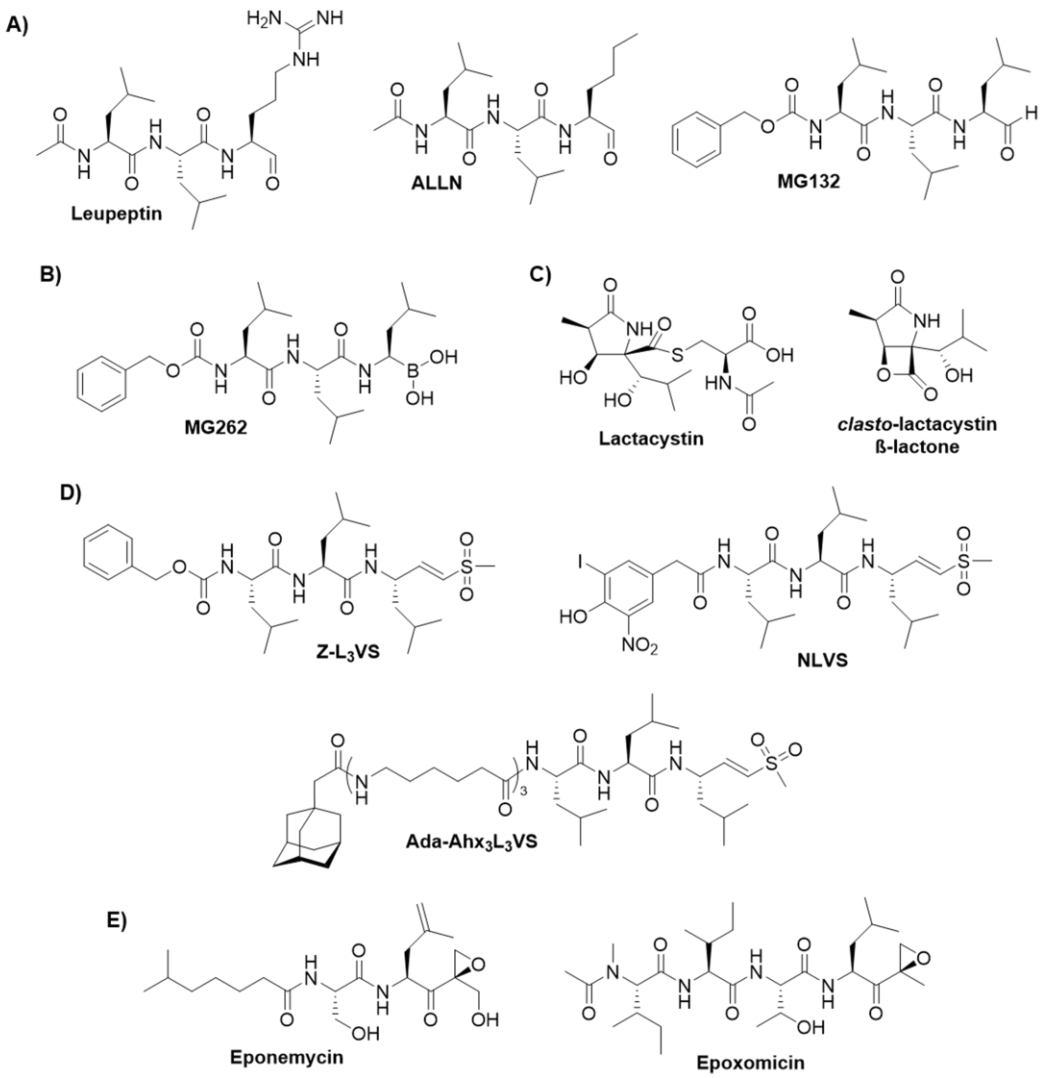

Figure 1.3 Representative members of the five major classes of proteasome inhibitors

A) Peptide aldehydes. Leupeptin (a natural product that selectively inhibits the proteasome's T-L activity) and ALLN and MG132 (synthetic inhibitors that selectively inhibit its CT-L activity) are shown. MG132 targets the proteasome more selectively than do leupeptin and ALLN. **B) Peptide boronates.** MG262, the boronate analog of MG132, is shown. **C) β-lactones.** The natural products *clasto*-lactacystin β-lactone (together with its precursor, lactacystin) and marizomib are shown. **D) Peptide vinyl sulfones.** Z-L_3VS and NLVS selectively inhibit the proteasome's CT-L activity. Ada-Ahx$_3$L$_3$VS is an N-terminally extended peptide vinyl sulfone that operates as a broad spectrum proteasome inhibitor. **E) Peptide epoxyketones.** The natural products eponemycin and epoxomicin are shown. Eponemycin preferentially targets β1i, β5, and β5i, and epoxomicin β5, β5i, β2, and β2i.

inhibitor $p27^{Kip1}$ [130] are proteasome substrates, confirming an important role of the proteasome in regulating the cell cycle. Further studies revealed a role of the proteasome in regulating apoptosis [131, 132]. Peptide aldehydes were also found to block activation of NF-κB by preventing the proteolytic processing of the inactive NF-κB precursor protein p105 and the TNFα-induced degradation of the NF-κB inhibitor IκBα, demonstrating that the proteasome is essential for the activation of this important transcription factor [133]. As NF-κB regulates the expression of numerous genes involved in inflammation, immune responses, and protection from apoptosis, these observations suggest that proteasome inhibitors may be of therapeutic benefit in treating inflammatory diseases as well as cancers [133, 134]. Consistent with a potential anticancer effect, inhibiting proteasome activity via peptide aldehyde inhibitors was shown to induce apoptosis in cancer cells [135-139]. Perhaps the most widely used inhibitor of this class is MG132 [140, 141] (Figure 1.3 A). Other notable peptide aldehyde proteasome inhibitors include the natural product leupeptin, which selectively inhibits the proteasome's T-L activity [12], and the synthetic inhibitor ALLN [80] (Figure 1.3 A). However, the use of peptide aldehyde inhibitors is limited by their off-target inhibition of cysteine and serine proteases, instability, and low bioavailability [142, 143].

1.4.2 Peptide Boronates

Peptide boronates were developed as a second class of synthetic, reversibly-binding proteasome inhibitors and are more potent than their aldehyde counterparts [142] (Figure 1.3 B). The empty *p*-orbital of the boronate pharmacophore can readily accept a lone pair of electrons from the oxygen atom of the proteasome's catalytic threonine residue to form a stable tetrahedral adduct [142, 144]. Although peptide boronates are known to inhibit serine proteases, hydrogen bonding between a boronate hydroxyl group and the N-terminal amino group of the proteasome's catalytic threonine further stabilizes the tetrahedral adduct, thereby giving rise to the high affinity of this class of inhibitors for the proteasome's active sites and contributing to their selectivity for the proteasome over serine proteases [142, 145]. Notable peptide boronates include the boronate analog of MG132, known as MG262 (Figure 1.3 B) [142], and, of special interest, bortezomib, which was the first proteasome inhibitor to receive FDA approval [146] (Figure 1.9).

1.4.3 β-Lactones

Natural products have also served as important proteasome inhibitors. Initial interest in the *Streptomyces* metabolite lactacystin was piqued after the discovery of its abilities to block cell cycle progression and stimulate neurite outgrowth [147] (Figure 1.3 C). Results of a subsequent study identified the proteasome as the cellular target of this inhibitor [148]. Lactacystin, which converts to its active form, *clasto*-lactacystin β-lactone, via spontaneous hydrolysis in aqueous solution [149], was found to preferentially bind to the β5 subunit and, accordingly, to inhibit the proteasome's CT-L activity (Figure 1.3 C). It also inhibited the T-L and C-L activities at slower rates [148]. Accordingly, 100 μM lactacystin was shown to covalently modify all of the constitutive and immunosubunits [81]. β-lactone inhibitors inactivate the catalytic threonine by esterifying its hydroxyl [33]. However, they were also found to inhibit some serine proteases [150, 151]. Lactacystin was used to confirm the proteasome's role in degrading intracellular proteins and producing peptides presented on MHC class I molecules [81]. In fact, treatment of cells with nontoxic doses of lactacystin and the peptide epoxyketone proteasome inhibitor epoxomicin could alter the presentation of specific antigenic epitopes, suggesting that proteasome inhibitors may be useful therapeutics for autoimmune diseases [152]. Like peptide aldehydes and peptide boronates, lactacystin was shown to induce apoptosis in malignant cells [153-156]. A second natural product β-lactone, marizomib (also known as salinosporamide A or NPI-0052), is currently in clinical development [157] (Figure 1.9).

1.4.4 Peptide Vinyl Sulfones

Peptide vinyl sulfones comprise a class of synthetic, irreversibly-binding proteasome inhibitors (Figure 1.3 D). A Michael addition reaction between the hydroxyl group of the catalytic threonine residue and the double bond of the vinyl sulfone pharmacophore serves as the mechanistic basis for inhibition [158]. An initial report described the peptide vinyl sulfone carboxybenzyl-LLL-vinyl sulfone (Z-L_3VS) and its ^{125}I-labeled nitrophenol derivative (^{125}I-NIP-L_3VS (or ^{125}I-NLVS)) as cell-permeable inhibitors that preferentially target the CT-L activity but inhibit the remaining activities at higher concentrations [158] (Figure 1.3 D). Peptide vinyl sulfones proved useful for studying how the peptide sequence of an inhibitor influences its subunit binding preferences [159, 160]. Furthermore, the vinyl sulfone pharmacophore itself was shown to confer enhanced binding selectivity toward the β5 subunit over epoxyketone inhibitors of the same peptide sequence [161]. Due to their ability to form irreversible covalent bonds with the

proteasome's catalytic threonine residues along with their ease of synthesis and amenability to modification, peptide vinyl sulfone inhibitors, including the broad-spectrum proteasome inhibitor Ada-Ahx$_3$L$_3$VS [162] (Figure 1.3 D), have often been converted to activity-based probes for use in purifying or visualizing active proteasome subunits [158, 163]. However, as they were initially developed as cysteine protease inhibitors, they tend to react with these proteases in addition to the proteasome [158, 161, 164].

1.4.5 Peptide Epoxyketones

Natural products eponemycin and epoxomicin are members of the peptide epoxyketone class of proteasome inhibitors [165, 166] (Figure 1.3 E). These inhibitors were isolated from a *Streptomyces* or *Actinomycete* strain, respectively, and identified as compounds with antitumor activity against B16 murine melanoma [167, 168], with their biological activity later being attributed to proteasome inhibition [165, 166]. Inhibitors of this class target the proteasome's catalytic activities irreversibly and with an unparalleled degree of specificity [166, 169]. Upon binding of the epoxyketone pharmacophore to the catalytic threonine, a six-membered morpholino ring is formed, which requires both the catalytic threonine's hydroxyl group and its free α-amino group [170]. Such an adduct cannot be formed with serine and cysteine proteases because their catalytic residues lack a free α-amino group, providing the basis for the remarkable proteasome specificity of this class of inhibitors [170]. Specific structural differences in eponemycin and epoxomicin contribute to their differential subunit binding preferences [171]: eponemycin preferentially binds β1i, β5, and β5i [165, 171], while epoxomicin targets β5, β5i, β2, and β2i [166]. As will be discussed below, many synthetic peptide epoxyketones have been developed for use as research tools, and, ultimately, as therapeutic agents. Carfilzomib, the second proteasome inhibitor to receive FDA approval for use as an anticancer agent, belongs to this inhibitor class [172] (Figure 1.9).

1.4.6 Subunit-Selective Proteasome Inhibitors

While proteasome researchers had begun to better understand the substrate binding preferences of each of the proteasome's catalytic subunits, the contribution to the proteolytic process or unique cellular functions of each individual subunit remained largely undefined. This prompted the design and synthesis of a variety of subunit-selective inhibitors (Figures 1.4 and 1.5). The development of these inhibitors also provided the

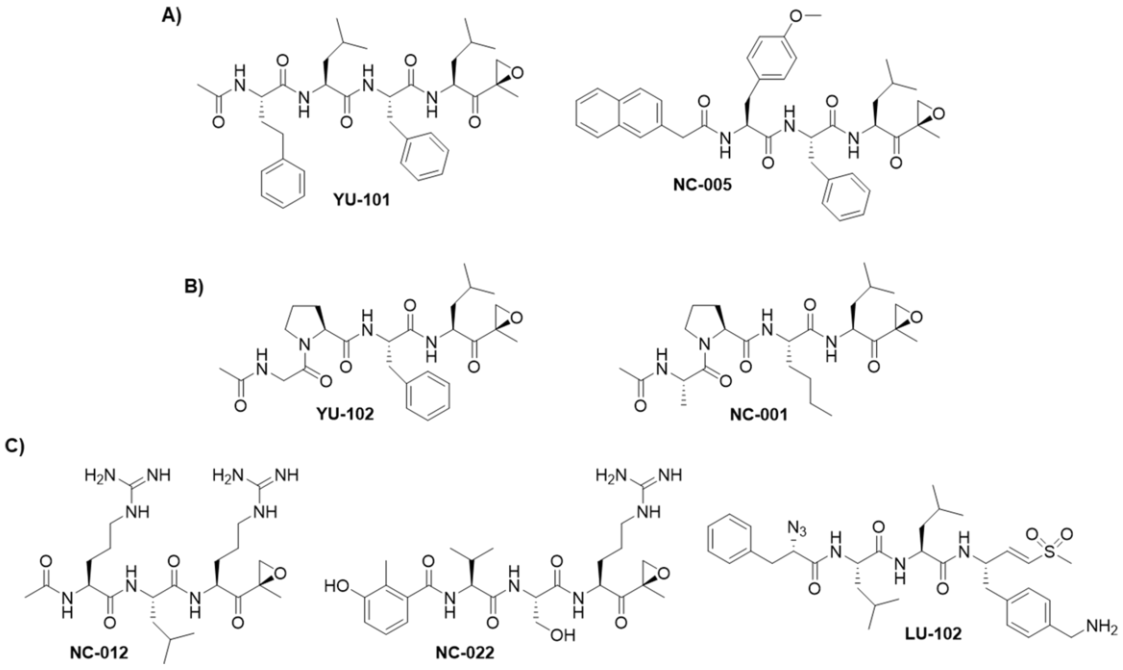

Figure 1.4 Inhibitors that selectively target homologous pairs of catalytic proteasome subunits
A) β5/β5i-selective inhibitors. The peptide epoxyketone inhibitors YU-101 and NC-005 are shown. **B) β1/β1i-selective inhibitors.** The peptide epoxyketone inhibitors YU-102 and NC-001 are shown. While YU-102 was initially found to selectively inhibit the proteasome's C-L activity, our laboratory later revealed its preference for binding immunosubunit β1i over constitutive subunit β1. **C) β2/β2i-selective inhibitors.** The peptide epoxyketone inhibitors NC-012 and NC-022, and the peptide vinyl sulfone inhibitor LU-102, are shown.

tools required to challenge the prevailing notion that inhibiting the proteasome's CT-L activity was of exclusive importance in mediating proteasome inhibitor-induced cytotoxicity.

a. β5/β5i-Selective Inhibitors

The second-generation tetrapeptide epoxyketone YU-101 was synthesized in effort to develop a proteasome-specific inhibitor that potently and selectively targets the CT-L activity [173] (Figure 1.4 A). The potency and selectivity of YU-101 was found to exceed that of epoxomicin, dihydroeponemycin, bortezomib, *clasto*-lactacystin β-lactone, and NLVS [173]. Furthermore, YU-101 was found to have anti-proliferative and anti-inflammatory effects [173]. Derivatization of this inhibitor would later yield the second FDA-approved proteasome inhibitor carfilzomib [174]. Subsequently, Britton et al. sought to develop a proteasome inhibitor with even greater selectivity for the CT-L activity than YU-101. To this end, they used a previously-reported CT-L-selective peptide aldehyde

inhibitor [175] as a reference compound in designing the peptide epoxyketone inhibitor NC-005 (Figure 1.4 A). This inhibitor was concluded to inhibit the CT-L activity with similar potency as YU-101, but with greater selectivity, allowing the CT-L activity to be inhibited almost completely without inhibiting the C-L or T-L activities [176]. However, the cytotoxic effects of NC-005 in most of the cancer cell lines tested were optimal at concentrations at which the T-L and/or C-L activity was co-inhibited, demonstrating that inhibiting the CT-L activity alone is not sufficient to achieve maximal anticancer activity [176].

b. β1/β1i-Selective Inhibitors

Another second-generation epoxyketone proteasome inhibitor, YU-102, was initially concluded to selectively inactivate the C-L activity of the bovine reticulocyte 20S proteasome [177] (Figure 1.4 B). Later work with this inhibitor in our laboratory revealed that YU-102's preferred target is the immunosubunit β1i, followed by the constitutive subunit β1 [178]. YU-102 inefficiently stabilized the proteasome reporter substrate Ub^{G76}-GFP in transfected HeLa cells and had poor anti-proliferative activity, suggesting that selectively inhibiting the β1-type subunits is insufficient to markedly impact protein degradation [177]. Several years later, van Swieten et al. reported a β1/β1i-selective peptide vinyl sulfone inhibitor (Ac-APnLL-VSPhOH) that appeared to inhibit β1i more potently than β1 [179]. An epoxyketone analog of this inhibitor, NC-001, was subsequently synthesized and shown to be a cell-permeable yet potent and selective inhibitor of the β1 and β1i subunits [176] (Figure 1.4 B). Exclusively inhibiting the C-L activity with NC-001 was not cytotoxic to multiple myeloma cells but, at concentrations inhibiting at least 90% of the C-L activity, sensitized these cells to the cytotoxic effects of the β5/β5i-selective inhibitor NC-005, further demonstrating the importance of inhibiting more than one type of proteasome activity for optimal anticancer activity [176].

c. β2/β2i-Selective Inhibitors

Mirabella et al. developed three T-L-selective peptide epoxyketone proteasome inhibitors [180]. The first, NC-002 (Ac-LLR-ek), is the epoxyketone derivative of the peptide aldehyde cysteine protease inhibitor leupeptin (Figure 1.3 A), which, in the context of the proteasome, selectively inhibits its T-L activity [12]. The second, NC-012 (Ac-RLR-ek) (Figure 1.4 C), is an epoxyketone derivative of the T-L-selective fluorogenic peptide substrate, Ac-RLR-AMC [181]. The third, NC-022 (Hmb-VSR-ek) (Figure 1.4 C), was designed using a peptide vinyl-ester that was previously reported to inhibit the

proteasome's T-L activity [182] as a reference compound. All three of these compounds were found to selectively inhibit β2 and β2i [180]. Among these three inhibitors, NC-012 was found to inhibit the T-L activity of purified 26S proteasomes most potently and selectively but displayed the weakest impact on this activity when tested in a multiple myeloma cell line, presumably reflecting low cell-permeability. Instead, NC-022 was chosen as the most potent cell-permeable T-L-selective inhibitor for use in further cell-based studies. These studies demonstrated that selectively inhibiting the T-L activity is not toxic to multiple myeloma cells but sensitizes these cells to the cytotoxic effects of inhibiting the CT-L activity with equivalent or greater efficacy compared with the C-L-selective inhibitor NC-001, indicating that the T-L active sites may be better co-targets for drugs than the C-L ones [180].

Due to the low synthetic yields, apparently inconsistent degrees of cell permeability across multiple cell lines, and chemical instability of the arginine-containing T-L-selective peptide epoxyketones, these researchers subsequently developed a new β2/β2i-selective inhibitor, LU-102 [183] (Figure 1.4 C). In comparison with the peptide epoxyketones, this peptide vinyl sulfone inhibitor is easier to synthesize, is more cell-permeable, and more potently inhibits the proteasome's T-L activity [183]. Like NC-022, LU-102 was not toxic to multiple myeloma cells but sensitized them to the cytotoxic effects of bortezomib and carfilzomib [183, 184]. However, this compound also inhibits cathepsins and therefore its use requires further experimental controls to validate that any observed biological effects result from inhibiting the proteasome's T-L activity [183].

d. β5-Selective Inhibitors

The β5-selective peptide epoxyketone inhibitor PR-825 was discovered in a medicinal chemistry effort to develop orally bioavailable carfilzomib analogs and was shown to be 14-fold selective for β5 over β5i [185] (Figure 1.5 A). PR-825 was subsequently used to differentiate the effects of selective inhibition of β5 versus β5i on the production of pro-inflammatory cytokines by activated PBMCs and on disease progression in a mouse model of rheumatoid arthritis [101], and to demonstrate the importance of inhibiting β5i, but not β5, in producing therapeutic effects in a mouse model of multiple sclerosis [106].

PR-893 (also referred to as CPSI) was the second β5-selective peptide epoxyketone to be reported (Figure 1.5 A). This compound inhibits β5 over β5i and β1i with 21-fold and 13-fold selectivity, respectively. Higher concentrations also inhibit β1, β2,

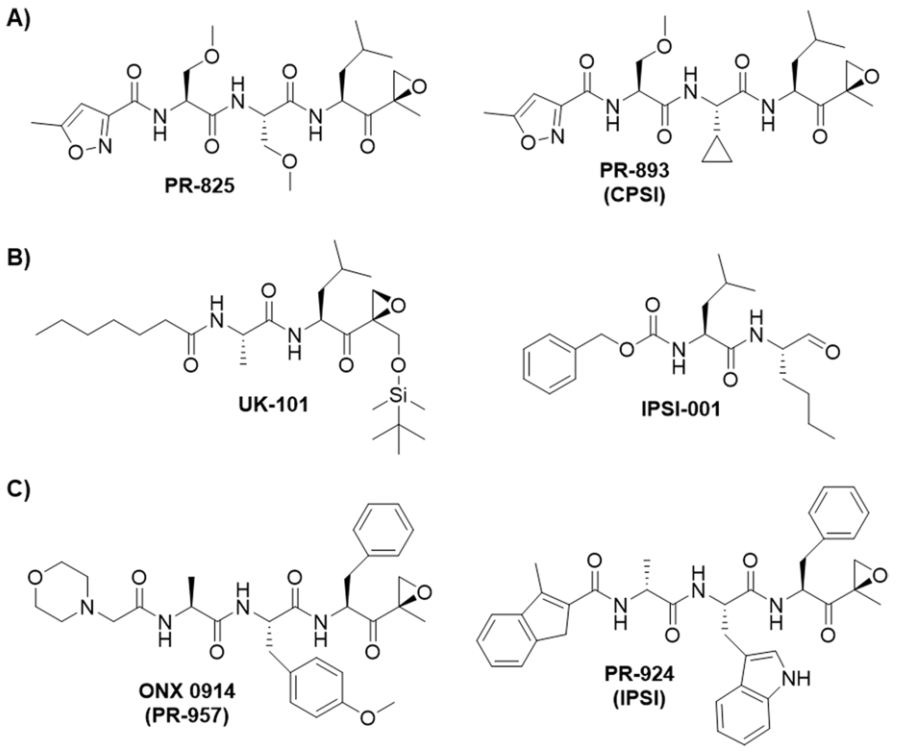

Figure 1.5 Subunit-selective proteasome inhibitors
A) β5-selective inhibitors. The peptide epoxyketone inhibitors PR-825 and PR-893 are shown. **B) β1i-selective inhibitors.** The peptide epoxyketone inhibitor UK-101 and the peptide aldehyde inhibitor IPSI-001 are shown. IPSI-001 is also a calpain inhibitor. **C) β5i-selective inhibitors.** The peptide epoxyketones ONX 0914 and PR-924 are shown.

and β2i [186]. Using PR-893 as a research tool to evaluate the cellular consequences of selective β5 inhibition revealed that, in contrast with dual inhibition of β5 and β5i, inhibiting β5 alone was insufficient to induce proteasome substrate accumulation or cytotoxicity in hematologic cancer cells [186]. Furthermore, in contrast to dual inhibition or inhibition of β5i alone, selectively inhibiting β5 with PR-893 did not substantially inhibit IFNα production by bone marrow cells [187].

1.4.7 Immunosubunit-Selective Inhibitors

Although the immunoproteasome was initially believed to primarily function in producing antigenic peptides for presentation on MHC class I molecules, the results of other studies suggested that it was, in fact, not required for MHC class I-mediated antigen presentation [90, 91] and, as discussed above, may have additional cellular functions. These observations fueled efforts to generate immunosubunit-selective inhibitors for use as molecular probes to investigate the functional roles of immunoproteasomes and their

individual catalytic subunits. Additionally, findings implicating the immunosubunits in the pathogenesis of autoimmune diseases [101, 104, 188-191] and cancers [192-195], and the low levels of these subunits in many non-diseased cells, stimulated interest in examining whether immunosubunit-selective inhibitors could make effective therapeutic agents.

a. β1i-Selective Inhibitors

Building upon knowledge gained form evaluating the structure-activity relationships of natural product peptide epoxyketones epoxomicin and eponemycin, our laboratory developed the first immunosubunit-selective inhibitor to be reported: the β1i-selective peptide epoxyketone inhibitor UK-101 [192] (Figure 1.5 B). Cancer cells with high β1i-levels were found to be more sensitive to the antiproliferative effects of UK-101 than those deficient in this immunosubunit, suggesting that β1i may play an important growth-regulatory role in cancer cells in which it is abundantly expressed [192]. UK-101 was also found to significantly inhibit tumor growth in a mouse xenograft model of prostate cancer [195].

The dipeptide aldehyde calpain inhibitor IPSI-001 (also known as calpeptin) was also found, in the context of the proteasome, to selectively inhibit β1i [193] (Figure 1.5 B). This inhibitor, which exhibited a 100-fold selectivity towards the CT-L activity of the immunoproteasome over that of the constitutive proteasome, was shown to induce apoptosis in bortezomib-sensitive and -resistant multiple myeloma cell lines and patient samples, and in samples from patients with other hematologic cancers, while having less pronounced effects than bortezomib on the viability of non-hematopoietic cells. Its pro-apoptotic activity was attributed to proteasome—rather than calpain—inhibition. Because of its aldehyde pharmacophore and low potency, further optimization of IPSI-001 will be required to obtain a β1i inhibitor suitable for clinical development [193].

b. β5i-Selective Inhibitors

The tripeptide epoxyketone PR-957 (now known as ONX 0914) was the first β5i-selective inhibitor to be reported [101] (Figure 1.5 C). When tested for its subunit binding preferences in a human leukemia cell line expressing both constitutive subunits and immunosubunits, ONX 0914 was found to display 20- and 40-fold selectivity for β5i over secondary targets β5 and β1i, respectively, while also inhibiting β2, β2i, and β1 at high concentrations. In PBMCs, which predominantly express immunosubunits, greater than

80% β5i inhibition was achievable by ONX 0914 treatment without substantially inhibiting β1i or β2i [101]. ONX 0914 was shown to inhibit the production of pro-inflammatory cytokines by activated monocytes, as well as the activation and differentiation of T helper cells, indicating that β5i is a potential therapeutic target for treating inflammatory diseases. This was further corroborated by the anti-inflammatory efficacy of ONX 0914 in mouse models of rheumatoid arthritis, in contrast to the β5-selective inhibitor PR-825, which lacked efficacy, and the β5/β5i-selective inhibitor carfilzomib, which was only moderately effective [101]. ONX 0914 also reduced disease severity and/or suppressed disease progression in mouse models of colitis [104], lupus [187], and multiple sclerosis [106], further supporting the potential therapeutic benefits of β5i inhibitors in treating autoimmune diseases.

A second β5i-selective peptide epoxyketone proteasome inhibitor, PR-924 (also referred to as IPSI), was subsequently reported [186] (Figure 1.5 C). This inhibitor was found to display 130-fold selectivity towards β5i over β5. It also inhibited β1i at higher concentrations but was not found to substantially inhibit β1, β2, or β2i within the concentration range examined [186]. Experimental results obtained using this compound demonstrated that, similarly to inhibiting β5 alone, inhibiting β5i alone was incapable of inducing proteasome substrate accumulation or producing cytotoxic effects in hematologic cancer cells; inhibiting both subunits was required [186]. Conversely, Singh et al. found PR-924 to inhibit growth and induce apoptosis in multiple myeloma cells without significantly reducing the viability of normal PBMCs [194]. PR-924 was also well-tolerated, exerted antitumor activity, and prolonged survival in mouse xenograft models. The results of the latter study, therefore, provided a rationale for the clinical development of PR-924 for anti-myeloma therapy [194].

1.4.8 Bifunctional Proteasome Inhibitors

Several bifunctional compounds containing two reactive groups have also been developed in effort to obtain potent and/or subunit-selective proteasome inhibitors. Among the first of these was Mal-βAla-Val-Arg-H, a peptide aldehyde inhibitor designed to selectively target the T-L activity [196] (Figure 1.6 A). Like other peptide aldehydes, the aldehyde warhead was intended to react with β2's catalytic threonine residue, while the N-terminal maleinimide moiety was expected to react with the thiol group of Cys118 of

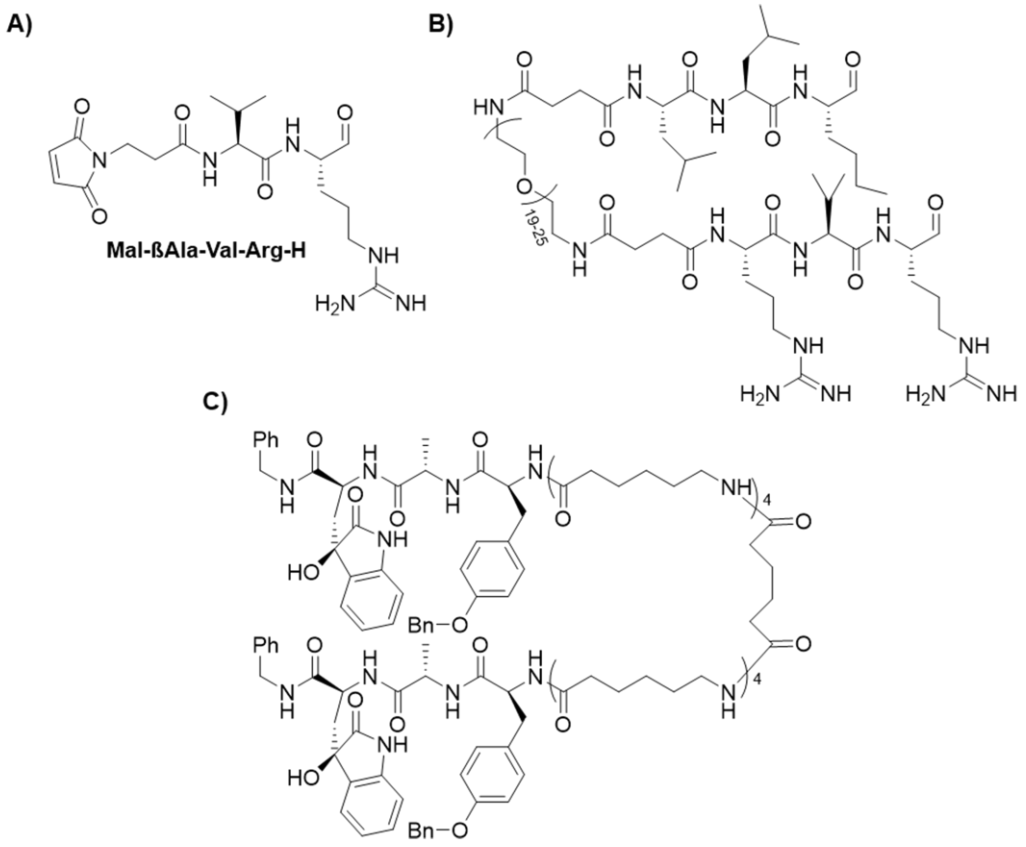

Figure 1.6 Bifunctional proteasome inhibitors
A) Mal-βAla-Val-Arg-H is an inhibitor comprising two functional groups designed to covalently modify distinct residues of the β2 active site. The aldehyde pharmacophore targets the catalytic threonine, while the N-terminal maleinimide moiety targets a cysteine residue unique to the β2 active site. **B)** A heterobifunctional compound comprising a β5-selective (LLnL-H) and a β2-selective (RLR-H) inhibitor coupled by a polydisperse PEG linker. **C)** A homobifunctional inhibitor derived from a linear mimic of the noncovalent proteasome inhibitor TMC-95A. The two inhibitor moieties were coupled via a monodisperse polyaminohexanoic acid linker.

β3—which protrudes into β2's S3 specificity pocket—to further increase the inhibitor's concentration in the β2 active site. The ethylene spacer was selected based on the optimal spacer length determined via molecular modeling, and the Val-Arg sequence was chosen based on the Bz-Phe-Val-Arg-AMC substrate used to selectively measure the proteasome's T-L activity [196]. As anticipated, Mal-βAla-Val-Arg-H inhibited the T-L activity of the yeast proteasome with an IC_{50} value of 0.5 μM, exhibiting a more than 200-fold selectivity over the CT-L and C-L activities [196]. Activity assay and crystal structure data indicate that the P1 Arg first interacts with the S2 specificity pocket of β2, leading to the reaction of the aldehyde group with β2's catalytic threonine residue. This positions

the maleinimide group for reaction with Cys118's thiol within the S3 specificity pocket of this subunit, which results in the sustained presence of the inhibitor in the β2 active site [196].

This same research group subsequently reported bifunctional compounds comprising two peptide aldehyde proteasome inhibitors N-terminally coupled via poly(ethylene glycol) (PEG) linkers. These included both homobifunctional inhibitors containing two identical inhibitory moieties, which were intended to simultaneously inhibit the two identical active sites on opposing β-rings within a single 20S proteasome complex, and a heterobifunctional inhibitor, which was designed to simultaneously inhibit two different active sites [197]. The crystal structure-derived distances between individual active sites within the yeast proteasome complex were used to select a linker of the appropriate length to facilitate simultaneous binding of the two inhibitory moieties to the desired active sites. PEG was chosen as a spacer because its flexibility and linearity allows it to mimic an unfolded polypeptide chain and therefore gain entry into the 20S proteasome core while, in contrast to an actual polypeptide chain, being resistant to proteolysis [197]. The two homobifunctional inhibitors developed met the intended goal of increasing inhibitory potency towards the targeted catalytic subunits. One homobifunctional inhibitor, which was derived from the peptide aldehyde Ac-LLnL-H and designed to target the two β5 subunits within a 20S proteasome complex, was found to inhibit the CT-L activity of the yeast proteasome with an IC_{50} value of 17 nM, and another, derived from Ac-RVR-H and designed to target the two β2 subunits, inhibited the T-L activity with an IC_{50} of 71 nM. These values represent potency increases of more than 100-fold over the respective PEGylated monomeric inhibitors, which was achieved while avoiding detectable inhibition of the non-targeted catalytic activities (IC_{50} values >100 μM). The heterobifunctional compound, which was constructed from the same monomeric inhibitors and designed to simultaneously target β5 and β2, was found to inhibit the CT-L and T-L activities with IC_{50} values of 31 and 97 nM, respectively, without substantially inhibiting the C-L activity (IC_{50} >100 μM) [197] (Figure 1.6 B). Although the crystallography data obtained did not allow the simultaneous binding of two active sites to be confirmed, the inhibitory potency of the heterobifunctional compound toward the CT-L and T-L activities was increased to a similar extent as that of the homobifunctional compounds if the stoichiometry of the inhibitory moieties is considered (i.e., the heterobifunctional inhibitor is ~2-fold less potent against a given activity than the homobifunctional inhibitor targeting that activity) [197].

A second research group extended this approach to develop homobifunctional inhibitors built from two linear mimics of a noncovalent proteasome inhibitor known as TMC-95A [198, 199]. The more active of the two bifunctional compounds described in the initial report, in which the two inhibitors were coupled via a polydisperse PEG linker, inhibited the CT-L activity of the rabbit 20S proteasome with 783-fold increased potency (IC_{50} value of 0.18 μM) compared with the reference compound [198]. Alternatively, the homobifunctional inhibitors described in the second report were composed of two units of a different linear TMC-95A mimic coupled by monodisperse polyaminohexanoic acid linkers [199] (Figure 1.6 C). These compounds potently inhibited both the CT-L (IC_{50} values between 19.1 and 25.9 nM) and T-L (IC_{50} values between 12.4 and 20.2 nM) activities of purified human constitutive proteasomes, while the C-L activity was targeted more weakly (IC_{50} values between 336 and 590 nM). These values indicate 123-167-fold (CT-L), 355-577-fold (T-L), and 19-34-fold (C-L) increases in inhibitory potency relative to the monomeric reference compound. Four of these bifunctional inhibitors were also found to inhibit the CT-L activity in HEK-293 cells more potently (IC_{50} values ranging from 0.472-0.756 μM) than the reference compound (IC_{50} value of 7.97 μM) [199]. Collectively, these results indicate that applying the principle of multivalency to proteasome inhibitor design can successfully improve the potency of proteasome inhibitors towards multiple active sites.

1.4.9 Activity-Based Probes

By attaching a reporter group to an inhibitor that binds covalently and irreversibly to the proteasome's catalytic threonine residues, many researchers have converted existing proteasome inhibitors to activity-based probes (ABPs) for use in functional studies [163]. Various reporter groups, such as biotin, radioisotopes, or fluorophores, can be attached to enable probe-bound proteasome subunits to be purified by affinity chromatography or visualized by techniques such as western blotting, in-gel fluorescence, or fluorescence microscopy (Figure 1.7). Both active and inactive forms of the proteasome's catalytic subunits are often present in cells; as only active subunits can be bound by ABPs, the use of these probes ensures that only the active forms of these subunits are detected when working with complex biological samples. This approach, therefore, overcomes a major limitation of traditional antibody-based approaches, since antibodies bind to both inactive and active forms of catalytic proteasome subunits [163].

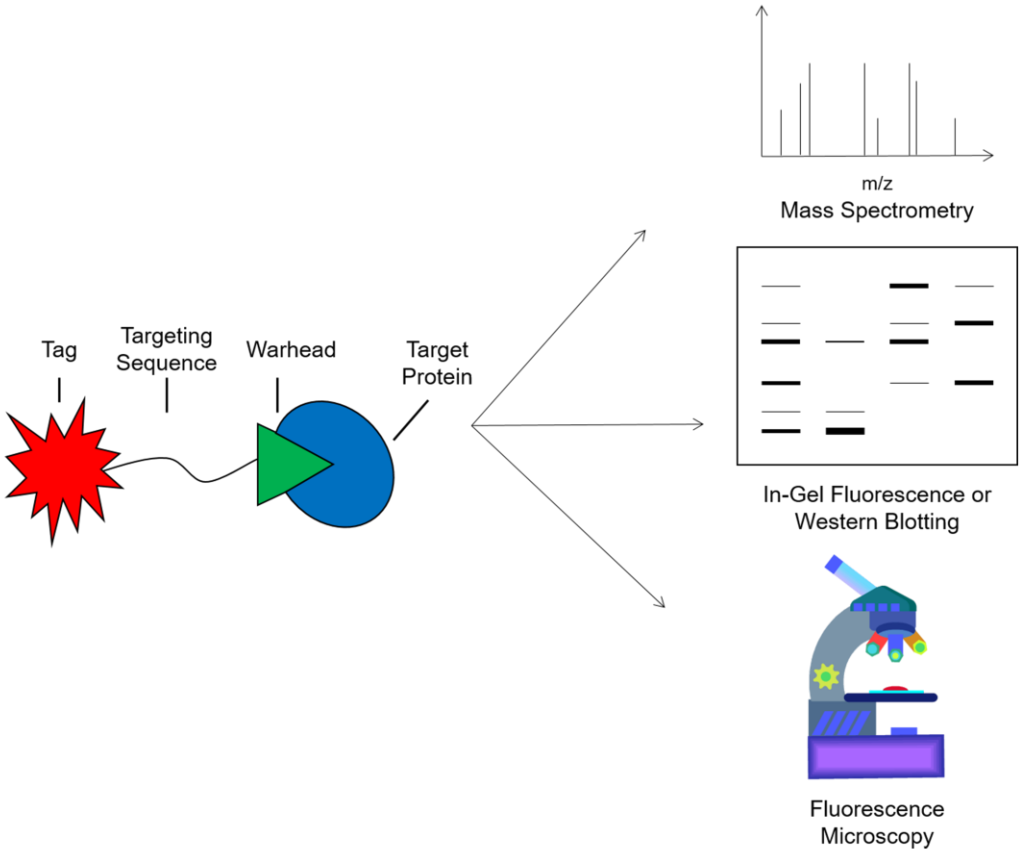

Figure 1.7 Activity-based probes and their utility
Structural representation of an ABP, which is composed of a targeting sequence that directs the probe to the targeted enzyme, a reactive chemical warhead which binds irreversibly to the enzyme's catalytic residues, and a tag for identification or visualization of probe-bound enzymes. Biotin-tagged ABPs can be used for affinity purification and mass spectrometry-based identification of probe targets, as well as for visualization of these targets by streptavidin affinity blotting. Radiolabeled and fluorescent ABPs can be used to visualize target proteins by in-gel fluorescence. Additionally, cell-permeable fluorescent ABPs can be used to monitor enzyme activity in living cells or tissue samples via fluorescence microscopy. *This figure was published in our previous report [163].*

^{125}I-labeled peptide vinyl sulfones were among the first proteasome-targeting ABPs to be developed [158]. They were used alongside fluorogenic peptide substrates in determining which catalytic subunits of the mammalian proteasome were responsible for each of its distinct activities [159, 160] and in examining the influence of inhibitor substituents on their subunit-selectivity profiles [159, 160, 162]. Many peptide vinyl sulfone- and peptide epoxyketone-based ABPs have since been developed, most of which were derived from broad-spectrum inhibitors that generally target all of the proteasome's active sites and contain fluorophores and/or biotin rather than radiolabels as reporter

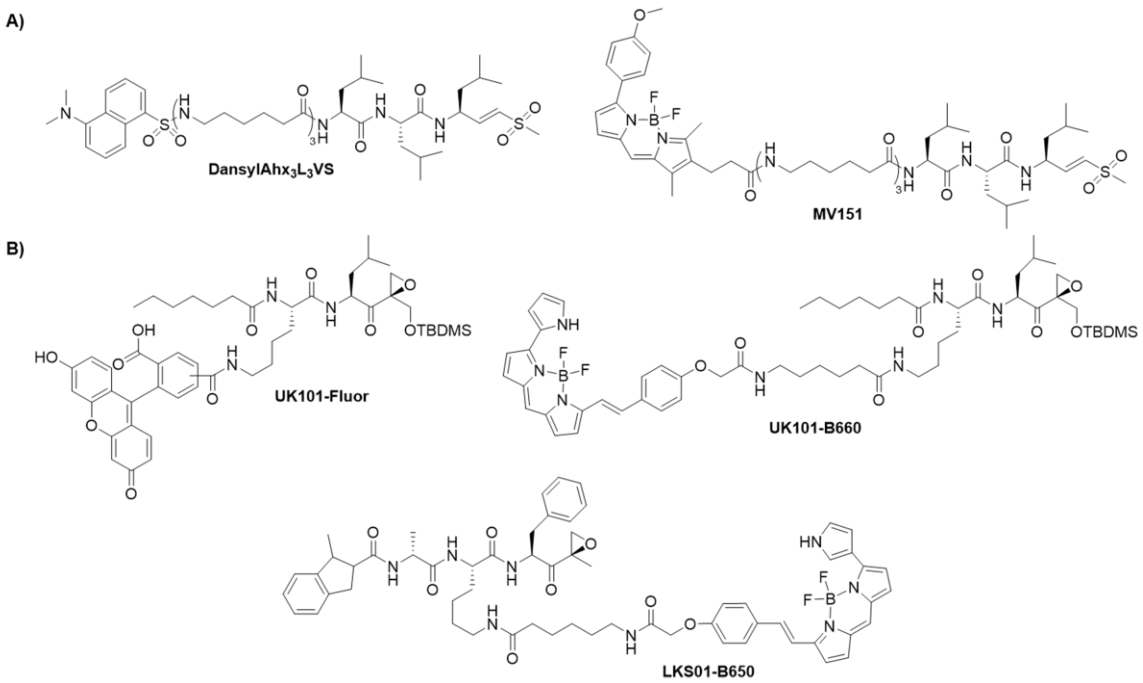

Figure 1.8 Proteasome-targeting activity-based probes
A) Broad-spectrum activity-based probes. DansylAhx$_3$L$_3$VS and MV151 are peptide vinyl sulfones labeled with the dansyl-sulfonamidohexanoyl hapten or the fluorophore Bodipy TMR, respectively. Catalytic proteasome subunits covalently modified by the former can be detected via immunoblotting with antibodies directed against the dansyl moiety, whereas those modified by the latter can be detected via in-gel fluorescence or fluorescence microscopy. **B) Immunosubunit-selective activity-based probes.** Fluorescent derivatives of the β1i-selective inhibitor UK-101 and the β5i-selective inhibitor LKS01 were previously developed in our laboratory. These probes allow catalytically active β1i or β5i to be visualized via in-gel fluorescence or fluorescence microscopy. UK101-B660 and LKS01-B650 are labeled with the near-infrared Bodipy 650/665 fluorophore and may therefore be compatible with *in vivo* imaging.

groups [163]. Perhaps the most widely utilized among these probes include dansyl-Ahx$_3$L$_3$VS [200] and Bodipy TMR-Ahx$_3$L$_3$VS (known as MV151) [201], the latter of which can be used in *in vivo* studies [201] (Figure 1.8 A). The most common application of the broad-spectrum ABPs has been to examine the subunit binding preferences of both existing and newly-developed proteasome inhibitors [158-162, 180, 192, 200-207]. Results from such investigations have assisted the development of both subunit-selective and broad-spectrum proteasome inhibitors and ABPs [159-162, 180, 192, 206]. Proteasome-targeting ABPs may also be useful in evaluating the clinical efficacy of proteasome inhibitors [204, 208].

The utility of these probes in monitoring proteasome activity profiles also renders them suitable for use in investigating proteasome functions. Results obtained with peptide

vinyl sulfone-based ABPs demonstrated that proteasome activity patterns vary substantially across primary leukemia samples and that proteasome activity increases when cell lines acquire bortezomib resistance, thereby enabling higher residual activity to be maintained following bortezomib treatment [184, 204, 209]. Additional studies in which proteasome-targeting ABPs were utilized uncovered a relationship between Bcr-Abl-mediated malignant transformation and proteasome activity in cell line models [210] and indicated roles of the proteasome in programmed cell death and defense responses in Arabidopsis plants [205]. Another study showed that disease-associated prion protein aggregates inhibit proteasome activity [211]. Finally, findings obtained with peptide epoxyketone- and peptide vinyl sulfone-based ABPs confirmed that the thymoproteasome subunit β5t has catalytic activity and demonstrated that this subunit differs from β5 and β5i in its substrate and inhibitor binding preferences. These results support the hypothesis that β5t is involved in generating peptides for the positive selection of developing T cells [212].

In addition to the broad-spectrum probes discussed above, subunit-selective ABPs have also been developed. Some of these bind both a particular constitutive subunit and its immunosubunit counterpart [176, 179, 180], while others can selectively bind a particular immunosubunit. Probes of the latter sort can be used to assess the functions of immunosubunit-containing proteasomes in normal and diseased cells. β1i- and β5i-selective ABPs developed in our laboratory facilitate the subcellular localization of the catalytically active forms of these immunosubunits via fluorescence microscopy, and those containing a near-infrared (NIRF) fluorophore may be suitable for use in animal studies [213, 214] (Figure 1.8 B). The high β1i levels detected in multiple cancer types [192, 193, 195] suggest its potential to serve as a tumor biomarker; therefore, β1i-selective ABPs may be useful as imaging probes for cancer screening or monitoring disease progression [213].

The use of ABPs has allowed researchers to obtain valuable information regarding proteasome function and inhibitor efficacy. Importantly, results obtained from such studies continue to provide insight into ways in which clinical responses to proteasome inhibitor therapy can be improved. A more detailed discussion of proteasome-targeting ABPs can be found in our review article [163].

1.5 Proteasome Assembly

Proteasomes are assembled in an ordered, chaperone-assisted process that begins with the formation of the α-rings. A heterodimeric chaperone complex comprising proteasome assembling chaperones-1 and -2 (PAC1-PAC2) serves as a scaffold upon which α-rings are built to prevent improper α-subunit aggregation [215]. A second heterodimeric chaperone complex, PAC3-PAC4, also assists in α-ring formation [216, 217]. Fully-assembled α-rings then serve as scaffolds for β-ring assembly. During this process, β2 and the assembly chaperone proteasome maturation protein (POMP) first associate with an α-ring. β3 is incorporated next, and the PAC3-PAC4 complex is concomitantly released [217]. Additional β-subunits continue to incorporate—β4, then β5, then β6, then β1, and finally β7—to form a half proteasome, with the propeptides of β2 and β5 and β2's C-terminal tail acting as intramolecular chaperones to aid in this process [217]. POMP, together with β7's C-terminal tail, then facilitate the dimerization of two half proteasomes, the propeptides of β1, β2, β5, β6, and β7 are removed, and POMP, PAC1, and PAC2, serving as the first substrates of the now fully-assembled 20S proteasome complex, are degraded [216, 217]. In mammals, the propeptides of the catalytically active β-subunits appear to be removed in a two-step autocatalytic mechanism, with an initial *trans*-autocatalytic step in which a neighboring β-subunit trims the propeptide to a specific length and a final *cis*-autocatalytic step involving Thr1 O^{γ} and Lys33 of the subunit undergoing processing [39]. As mentioned above, removing the propeptides from the catalytically active subunits only upon completion of 20S proteasome assembly serves as a safety mechanism to protect against unregulated cleavage of cellular proteins by these subunits that may otherwise occur prior to their incorporation into the complex [36, 38-41].

Immunosubunits can, alternatively, become incorporated in place of their constitutive counterparts during the β-ring assembly process. Unlike incorporation of β1, which occurs at a relatively late step, co-incorporation of β1i and β2i was concluded to be the initial step in immunoproteasome β-ring assembly [217-219]. This is followed by incorporation of β3. Either β4 or β5i can be incorporated immediately after β3, followed by the incorporation of the other. Bai et al. suggested that the addition of β5i prior to β4 may contribute to the preferential assembly of immunoproteasomes over constitutive proteasomes when all six catalytic subunits are simultaneously expressed [219]. Addition of β6, and, finally, β7, complete the assembly of the immunoproteasome β-ring. Assembly chaperones were concluded to play the same roles in immunoproteasome assembly as in constitutive proteasome assembly [219].

While it has been concluded that cooperative assembly mechanisms encourage the assembly of pure constitutive proteasomes or pure immunoproteasomes, assembly of intermediate proteasome subtypes comprising mixtures of constitutive proteasome and immunoproteasome catalytic subunits has also been reported [220-223]. However, there seem to be restrictions governing which combinations of constitutive proteasome and immunoproteasome catalytic subunits can be co-incorporated into a single 20S proteasome complex. For example, it was found that β2i is not incorporated into proteasomes independently of β1i, indicating that all β2i-containing proteasome complexes also contain β1i [220, 221, 223]. Additionally, proper maturation of β1i- and β2i-containing proteasomes requires incorporation of β5i, indicating that β5i is present in all mature 20S proteasome complexes that contain any of the immunosubunits [221]. Conversely, β1i can incorporate into proteasome complexes without co-incorporation of β2i [223]. Furthermore, β5i can incorporate into proteasome complexes containing either constitutive subunits or immunosubunits [220-223]. Collectively, these findings suggest that the formation of four distinct 20S proteasome subtypes—pure constitutive proteasomes composed of β1, β2, and β5, pure immunoproteasomes composed of β1i, β2i, and β5i, and two subtypes of intermediate proteasomes composed of β1, β2, and β5i or β1i, β2, and β5i—is permitted, whereas the formation of subtypes comprising β2i with constitutive subunits or β5 with immunosubunits is precluded [223] (Figure 1.2).

1.6 Intermediate Proteasomes

An initial clue to the existence of intermediate proteasomes was obtained via immunoprecipitation experiments conducted by Brown et al. The $P388D_1$ murine macrophage cell line simultaneously harbored proteasomes either containing or lacking immunosubunit β1i, both of which also contained β5i, demonstrating that intermediate proteasome subtypes containing β5i without β1i can form in these cells [63]. The H6 hepatoma cell line, conversely, exclusively contained proteasomes lacking β1i, but these differed from the β1i-deficient subtype identified in $P388D_1$ cells by their lack of β5i as well as a third component, which was present in both subtypes from $P388D_1$ cells. Additionally, while β1i-containing proteasomes were detected in H6 cells following IFNγ stimulation, these subtypes also differed from the β1i-containing proteasomes of $P388D_1$ cells in the continued absence of this component. Therefore, at least four distinct subtypes of proteasomes were identified [63]. Whether or not additional proteasome subtypes aside from these four existed could not be determined in this study due to a lack of appropriate

research tools. However, the difference in the proportion of $\beta1i^+$ and $\beta1i^-$ proteasome subtypes between the two cell lines and the differential extent to which the $\beta1i^+$ subtypes could be upregulated by IFNγ (they were only weakly upregulated in $P388D_1$ cells under these conditions) led the authors to suggest that proteasome subtypes with unique subunit compositions have specialized biological functions [63].

A subsequent report by Dahlmann et al. described the detection of intermediate proteasome subtypes in murine tissues [224]. Although rat muscle tissue predominantly contained constitutive proteasomes, substantial amounts of intermediate proteasomes of composition β1-β2-β5i and β1/β1i-β2-β5i were detected. While only low levels of pure immunoproteasomes were detected in muscle, this was the most abundant subtype present in rat spleen. Intermediate proteasomes of subtype β1-β2i-β5i and β1/β1i-β2i-β5i were also detected in spleen [224]. Since then, results of many studies have indicated the presence of intermediate proteasomes in various non-diseased tissues and cancer cells derived from both murine and human sources [186, 225-229]. For example, ELISA-based quantification demonstrated that normal human tissues contain considerable quantities of intermediate proteasomes; intermediate proteasome subtypes of catalytic subunit composition β1-β2-β5i or β1i-β2-β5i constituted between one-third and one-half of the total proteasomes in liver, kidney, small intestine, and colon. They were also found to comprise 9-17% of the total proteasomes in melanoma cell lines (most of which were of catalytic subunit composition β1-β2-β5i) and ~20% of proteasomes in NCI-H460 non-small cell lung carcinoma and L363 myeloma cell lines (most or all of which were of composition β1i-β2-β5i) [226].

Consistent with the notion that individual subtypes may be specialized to assist in specific cellular functions, each subtype seems to differ from the rest in its activity profile and tissue and subcellular distribution patterns [224-235]. With regards to antigen presentation, results from several studies indicate that intermediate proteasome subtypes support the enhanced diversification of antigenic peptides presented on MHC class I molecules [226, 236-238]. Importantly, specific intermediate proteasome subtypes are indispensable for the production of certain tumor antigens; therefore, identifying which proteasome subtypes are present in cells should be helpful for the development of immunotherapy-based approaches [226]. Distinguishing proteasome compositions have also been associated with diseases such as Crohn's disease and ulcerative colitis, suggesting their potential to serve as disease biomarkers [191]. Finally, as distinct proteasome subtypes appear to differ in their sensitivities to specific proteasome inhibitors

[231, 232], identifying which proteasome subtypes are present in diseased cells could ultimately guide the selection of the appropriate proteasome inhibitor to selectively target those subtypes more effectively while minimizing toxicity to healthy cells [232, 239].

1.7 Development of Proteasome Inhibitors for Clinical Use

Initial interest for developing proteasome inhibitors for clinical use was sparked by the finding that excessive UPP activity was a substantial contributor to muscle wasting in rodent disease models. It was reasoned that inhibiting the proteasome may be able to prevent muscle wasting in human patients suffering from various diseases [240]. Additionally, the discovery of the proteasome's role in activating the transcription factor NF-κB, a key contributor to inflammation and cancer [133], indicated that proteasome inhibitors could be of therapeutic benefit in inflammatory diseases and cancers. However, due to the critical roles of the proteasome in normal cellular function, the potential for proteasome inhibitors to be overly toxic to non-diseased cells remained a prominent concern [240]. Fortunately, several research groups began to discover that proteasome inhibitors were selectively cytotoxic to malignant cells over healthy ones [136-138, 155, 241, 242]. For example, the β-lactone inhibitor lactacystin was shown to preferentially induce apoptosis in B cell chronic lymphocytic leukemia (B-CLL) cells over normal lymphocytes [241], and patient-derived multiple myeloma cells were found to be more susceptible to the growth inhibitory effects of bortezomib than peripheral blood mononuclear cells (PBMCs) isolated from healthy donors [242]. These findings suggested a therapeutic window for proteasome inhibitors in treating cancers; thus, clinically, they have largely been developed as anticancer agents.

1.7.1 Bortezomib

Bortezomib (formerly known as PS-341 and now marketed as Velcade®), a peptide boronate, was the first proteasome inhibitor to receive FDA approval [134] (Figure 1.9 A). Bortezomib preferentially targets the β5 and β5i subunits [174, 180, 207, 243-245], but also targets β1 and β1i at clinically achievable concentrations [200, 204, 207, 243]. Conversely, an increase in T-L activity is frequently observed following bortezomib treatment [145, 203, 207, 243, 245, 246]. Bortezomib induces apoptotic cell death via both caspase-8 and caspase-9-dependent pathways [247]. Activation of caspase-4-dependent apoptosis, which is induced by ER stress, has also been noted following treatment with bortezomib [248].

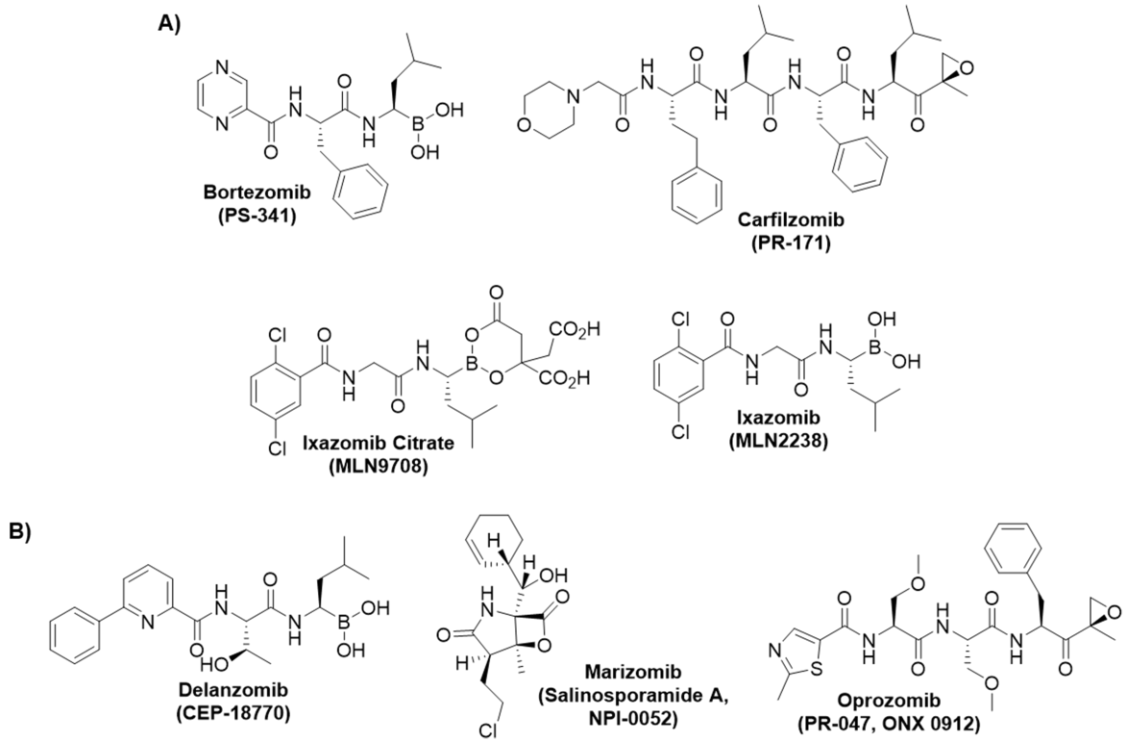

Figure 1.9 Proteasome inhibitors that are FDA-approved or in clinical trials
A) FDA-approved proteasome inhibitors. The peptide boronate bortezomib, the peptide epoxyketone carfilzomib, and the peptide boronate ixazomib were granted FDA approval in 2003, 2012, and 2015, respectively. The peptide boronic ester prodrug of ixazomib, ixazomib citrate, is also shown. **B) Proteasome inhibitors in clinical trials.** The peptide boronate delanzomib, the β-lactone marizomib, and the peptide epoxyketone oprozomib are shown.

Bortezomib was evaluated in the National Cancer Institute's *in vitro* screen and found to produce significant cytotoxic effects in multiple cell lines derived from diverse tumor types. Bortezomib-mediated proteasome inhibition in PC-3 prostate cancer cells led to elevated levels of the cyclin-dependent kinase inhibitor p21 and induced G_2/M-phase cell cycle arrest and apoptosis [134]. The inhibitor also achieved broad tissue distribution in rats and significant antitumor activity in a mouse xenograft model of prostate cancer [134]. Maximum achievable CT-L inhibition following bortezomib administration, as measured in patient blood samples, was found to be ~70-80% [249-253]. Maximal inhibition was detected within 5 minutes following bortezomib treatment, with recovery of activity beginning as early as 4 hours following treatment [252]. Complete recovery was observed within 72 hours following treatment [249, 250, 252]. Since bortezomib-mediated proteasome inhibition is reversible, recovery of proteasome activity can occur via

bortezomib dissociating from the proteasome's active sites, or via new proteasomes being produced by the cell [174].

Based on promising clinical trial results, bortezomib was approved by the FDA in 2003 for treating relapsed or refractory multiple myeloma [254]. It has since been approved for use as a first line agent in treating multiple myeloma and mantle cell lymphoma [255]. Clinical trials of bortezomib for other applications are ongoing [157].

Despite its clinical success, bortezomib-treated patients experience several severe side effects. Peripheral neuropathy is a dose-limiting side effect of bortezomib treatment that may result from off-target inhibition of the neuronal prosurvival serine protease HtrA2/Omi [256]. Intrinsic and acquired resistance are also clinical challenges observed with bortezomib-based therapy [257-260]. Furthermore, while bortezomib is active against solid tumor cells *in vitro* and in xenograft models [134], it has had limited success in treating solid cancers in the clinic [261]. These observations prompted the development of second-generation proteasome inhibitors with improved activity, reduced toxicity, and efficacy in treating bortezomib-resistant cancers. Such inhibitors include second-generation peptide boronates as well as inhibitors falling into other classes. So far, two second-generation inhibitors have received FDA approval: carfilzomib and ixazomib.

1.7.2 Carfilzomib

Modifying the N-terminus of the synthetic epoxomicin analog YU-101 to improve its water solubility later gave rise to the second FDA-approved proteasome inhibitor carfilzomib (formerly called PR-171 and now marketed as Kyprolis®) [174] (Figure 1.9 A). This inhibitor was approved in 2012 for treating relapsed or refractory multiple myeloma [172]. In comparison with bortezomib, carfilzomib inhibits the proteasome's CT-L activity more selectively [174], and slightly differs from bortezomib in its secondary targets; β1i and β2i are the next preferred targets of carfilzomib, which, in contrast to bortezomib, exhibits a distinct aversion to binding β1 [262]. Another difference is that, in contrast to bortezomib, carfilzomib does not substantially cross-react with non-proteasomal proteases [256]. The more selective proteasome inhibitory profile, together with the unparalleled proteasome specificity of the epoxyketone pharmacophore, are potential reasons behind carfilzomib's lower *in vivo* toxicity relative to that of bortezomib [174]. Notably, the incidence of treatment-emergent peripheral neuropathy is substantially lower in carfilzomib-treated patients than those treated with bortezomib [263-268] consistent with the notion that this side effect results from the off-target activity of bortezomib [256].

Carfilzomib's more favorable toxicity profile permits consecutive-day dosing, which prevents complete recovery of proteasome activity between consecutive day doses and therefore achieves a more robust and sustained proteasome inhibition [174, 263, 264, 266]. Applying the consecutive-day dosing schedule to xenograft models of human cancers produced greater anticancer activity than bortezomib (or carfilzomib) administered on bortezomib's clinical dosing schedule (biweekly day 1/day 4, which allows proteasome activity to recover between bortezomib doses) [174, 249, 250, 252]. Furthermore, in comparison with bortezomib, carfilzomib's irreversible binding mechanism also facilitates a more sustained proteasome inhibition following a single, brief exposure, as recovery of proteasome activity following carfilzomib treatment requires *de novo* proteasome production [174]. This has been suggested to contribute to its enhanced anticancer efficacy over that of bortezomib [174, 262] and its ability to overcome bortezomib resistance [262, 263, 266, 267]. However, resistance is still a major clinical challenge, as ~50% of multiple myeloma cases fail to respond to initial treatment with bortezomib or carfilzomib [259, 265], and, as for bortezomib, acquired resistance to carfilzomib emerges in initially responsive patients [269].

Although it was hoped that the advantages offered by carfilzomib over bortezomib would lead to enhanced clinical activity against solid tumors, results of a clinical trial with carfilzomib in this setting were disappointing [268]. However, its tolerable toxicity profile makes it worthwhile to investigate its therapeutic efficacy in higher doses or in combination with other chemotherapeutic agents in patients with solid cancers [268], and further clinical trials are exploring such possibilities [157].

1.7.3 Ixazomib and Delanzomib

A suggested consequence of bortezomib's slowly irreversible binding to the proteasome's active sites is that proteasomes in red blood cells may act as a sink for this inhibitor following its intravenous administration, therefore limiting its tissue distribution and, consequently, its activity in solid tumors. This provided the rationale for the development of ixazomib citrate (previously known as MLN9708), a prodrug which is hydrolyzed to its active form, ixazomib (previously called MLN2238 and now marketed as NINLARO®), in aqueous solution or plasma [270] (Figure 1.9 A). Ixazomib is an N-capped dipeptide boronic acid that preferentially inhibits β5 (IC_{50} value of 3.4 nM). Higher concentrations are required to inhibit the C-L and T-L active sites, with IC_{50} values of 31 nM and 3,500 nM, respectively [270]. In comparison with bortezomib, ixazomib has an

~6-fold shorter proteasome dissociation half-life, which was suggested to largely contribute to its superior tissue distribution [270]. Unlike bortezomib and carfilzomib, ixazomib is orally bioavailable [270], and, unlike bortezomib, it lacks activity against the neuronal protease HtrA2/Omi [271]. Ixazomib has a similar subunit selectivity profile to that of bortezomib, but inhibited the proteasome's CT-L activity in tumor tissue more strongly and displayed greater antitumor activity in xenograft models of both hematologic and solid cancers [270, 271]. It was also active in multiple myeloma cells obtained from bortezomib-resistant patients and in a cell line model of acquired bortezomib resistance [271]. Ixazomib was recently approved (in November of 2015) by the FDA for use, in combination with lenalidomide and dexamethasone, in treating multiple myeloma in patients who have received at least one prior therapy [272]. A second orally-bioavailable peptide boronate, delanzomib (also known as CEP-18770), has also been assessed in clinical trials [245] (Figure 1.9 B). This inhibitor has a subunit selectivity profile similar to that of bortezomib and ixazomib [245, 270]. In a phase I clinical study, CT-L activity in blood was inhibited by only ~45% at the maximum tolerated dose [273]. Further clinical trials of delanzomib were initiated but have since been terminated [157].

1.7.4 Marizomib

A β-lactone proteasome inhibitor is also in clinical development. This inhibitor, marizomib (also known as salinosporamide A or NPI-0052), is a natural product produced by the marine gram-positive actinomycete *Salinospora tropica* [202] (Figure 1.9 B). Its subunit selectivity profile differs from that of bortezomib: marizomib is more potent than bortezomib against the CT-L and T-L activities of purified erythrocyte proteasomes, but is less potent than bortezomib against the C-L activity. Marizomib was found to be more cytotoxic than bortezomib to multiple myeloma cells derived from bortezomib-resistant patients, but was less cytotoxic than bortezomib to non-malignant cells [202]. When these inhibitors were administered intravenously to mice at the maximum tolerated doses, marizomib achieved complete inhibition of the CT-L activity in whole blood, which was sustained for at least 72 hours following administration, whereas bortezomib inhibited this activity less completely, with recovery already beginning to occur 24 hours following administration. Conversely, bortezomib inhibited the C-L activity more strongly than marizomib, which was sustained for at least 72 hours following administration [202]. Importantly, marizomib inhibited the T-L activity by ~50%, whereas a persistent bortezomib-mediated stimulation of this activity was observed; elevated T-L activity

remained detectable 168 hours after treatment [202]. Like the second-generation peptide boronates described above, marizomib is also orally bioavailable. Additionally, marizomib and bortezomib were found to have synergistic cytotoxic activity in multiple myeloma cells [202]. However, like bortezomib, marizomib can also inhibit non-proteasomal proteases [202]. Several clinical trials of marizomib, as a single agent or in combination with others, remain open [157].

1.7.5 Oprozomib

Finally, the tripeptide epoxyketone inhibitor oprozomib (formerly known as PR-047 or ONX 0912) is an orally bioavailable carfilzomib analog that is currently in clinical trials [185] (Figure 1.9 B). Like carfilzomib, oprozomib selectively inhibits β5 and β5i over the remaining catalytic proteasome subunits and does so with similar potency [185, 274]. Additionally, oprozomib was cytotoxic to multiple myeloma cells, including primary cells derived from bortezomib-resistant patients, but was not significantly cytotoxic to nonmalignant PBMCs even at high doses [274]. Administering oprozomib orally on two consecutive days per week at doses that inhibit the CT-L activity by >80% in blood and in the peripheral tissues examined was well-tolerated in mice and, in mouse xenograft models of hematologic and solid cancers, had similar antitumor activity to that of intravenously administered carfilzomib and prolonged survival [185, 274]. Proteasome activity recovered in adrenal and liver within 24-72 hours following oral administration of oprozomib, while no recovery was observed in blood [185]. As observed for a marizomib/bortezomib combination [202], combined treatment of multiple myeloma cells with oprozomib and bortezomib produced synergistic cytotoxic effects [274]. Oprozomib is currently being examined in clinical trials in patients with both hematologic and solid cancers, both as a single agent and in combination regimens [157].

1.8 Proteasome Inhibitor Resistance

Clinical resistance has emerged as a major limitation associated with bortezomib therapy, although the mechanisms responsible remain unclear. Both intrinsic and acquired proteasome inhibitor resistance mechanisms have been investigated in laboratory settings, and wide-ranging conclusions have been drawn. Resistance to a catalytic β-subunit-targeting proteasome inhibitor such as bortezomib could theoretically be conferred by several mechanisms. First, the activity of drug efflux transporters or metabolic enzymes in cancer cells may lead to suboptimal intracellular inhibitor

concentrations and, therefore, to an insufficient extent of proteasome inhibition to promote growth arrest and apoptotic cell death. Second, proteasome substrates may be rerouted to an alternative proteolytic system for degradation, thus mitigating the cytotoxic effects of proteasome inhibition. Third, aberrant apoptotic/survival signaling downstream of proteasome inhibition may allow cells to withstand proteasome inhibitor-induced accumulation of polyubiquitinated proteins. Finally, various mechanisms involving the proteasome complex itself may confer proteasome inhibitor resistance. Of course, these mechanisms are not mutually exclusive; multiple mechanisms may operate simultaneously to confer resistance. Additionally, mechanisms may be inhibitor-specific and therefore capable of being overcome by applying an alternative proteasome inhibitor with different inhibitory properties. A summary of the previously-reported mechanisms of proteasome inhibitor resistance—predominantly focusing on acquired resistance—will ensue.

1.8.1 Role of Drug Efflux Transporters

a. ALLN Resistance

Perhaps the first report of a cell line model of acquired resistance to a proteasome inhibitor came from Sharma et al., who cultured the Chinese hamster ovary cell line CHO-K1 in the presence of gradually increasing concentrations of the synthetic peptide aldehyde inhibitor ALLN (Figure 1.3 A) until it adapted to grow under continuous exposure to 50 μg/mL ALLN [275]. This process was undertaken to understand the apparent contribution of the protease(s) inhibited by ALLN to the degradation of the rate-limiting cholesterol biosynthetic enzyme 3-hydroxy-3-methylglutaryl coenzyme A (HMG-CoA) reductase, and it was hoped that the mechanism by which ALLN resistance was acquired would involve amplifying the protease-encoding gene(s) to facilitate this study. However, the resulting cell line, $ALLN^{r50}$, instead acquired ALLN resistance by amplifying and overexpressing the multidrug resistance gene *mdr1*, which encodes the drug efflux transporter P-glycoprotein (P170) [275]. Overexpression of this ATP-hydrolyzing transmembrane transporter confers resistance to various structurally and functionally diverse chemotherapeutic agents. The multidrug resistance phenotype of $ALLN^{r50}$ cells was exemplified by their more than 10-fold upregulation of P-glycoprotein, cross-resistance to P-glycoprotein substrates doxorubicin, colchicine, and etoposide, and a reduction in their 50-fold ALLN resistance by treatment with the competitive P-glycoprotein inhibitor verapamil. It was therefore concluded that ALLN is a P-glycoprotein substrate,

and that, in ALLN^{r50} cells, overexpression of P-glycoprotein contributes to ALLN resistance by extruding the inhibitor and, consequently, lowering the steady-state ALLN levels available for binding its intracellular targets. Further support for this conclusion was provided by the substantially higher ALLN concentrations required to inhibit the degradation of a chimeric reporter protein in ALLN^{r50} than in parental CHO-K1 cells [275]. In contrast to the results of this study, de Jong et al. found that A2780 ovarian cancer cells selected for 10 μM ALLN resistance overexpressed multidrug resistance-associated protein (MRP)1 instead of P-glycoprotein [276]. Other transporter proteins, including MRP2, 3, 5, breast cancer resistance protein (BCRP), and the lung resistance protein (LRP), were not overexpressed in these cells [276].

b. Epoxomicin Resistance

While ALLN inhibits the proteasome [128], it also inhibits other cellular proteases [277]. However, a multidrug resistance phenotype was also observed in a derivative of the KMS-11 multiple myeloma cell line selected for resistance to the proteasome-specific inhibitor epoxomicin [278]. The resulting cell line, KMS11R, remained viable in the presence of 20 nM epoxomicin but maintained similar bortezomib sensitivity to that of parental KMS-11 cells. Although KMS11R cells exhibited reduced CT-L activity relative to parental KMS-11 cells and lacked mutations in the *PSMB5* gene encoding the catalytic proteasome subunit β5, epoxomicin, unlike bortezomib, was unable to significantly inhibit the proteasome's CT-L activity in KMS11R cells. However, treatment of lysates of parental and epoxomicin-resistant KMS-11 cells led to similar dose-dependent inhibition of proteasome activity in both cell lines, suggesting that epoxomicin's ability to bind the proteasomes of KMS11R cells was not impaired [278]. KMS11R cells incubated in both the absence and presence of epoxomicin for 24 hours were shown to express P-glycoprotein, while parental cells incubated under these same conditions did not, indicating that P-glycoprotein expression was associated with the mechanism of acquired epoxomicin resistance. Overexpression of P-glycoprotein in KMS11R cells led to a 3-5-fold lower uptake of doxorubicin—a known P-glycoprotein substrate—in comparison with parental KMS-11 cells [278]. Treatment with the P-glycoprotein inhibitor verapamil restored epoxomicin sensitivity and doxorubicin uptake to KMS11R cells, further emphasizing a causative role of P-glycoprotein overexpression in epoxomicin resistance and identifying epoxomicin as a P-glycoprotein substrate. Conversely, the lack of cross-resistance of KMS11R cells to bortezomib implies that bortezomib is not a P-glycoprotein

substrate [278]. Results of a study by Ohkawa et al. also suggested that epoxomicin is a P-glycoprotein substrate [279]. In contrast to the findings of Gutman et al. [278], however, the mechanism by which A431 squamous cell carcinoma cells acquired resistance to 12 nM epoxomicin apparently did not involve P-glycoprotein overexpression [279].

c. Carfilzomib/Peptide Epoxyketone Inhibitor Resistance

Based on the above-mentioned studies in support of epoxomicin as a P-glycoprotein substrate, it is unsurprising that the structurally-related proteasome inhibitor carfilzomib was also found to be a substrate of this transporter [280]. CEM T cell leukemia cells overexpressing P-glycoprotein (CEM/VLB) were highly resistant to carfilzomib as well as to the structurally-related proteasome inhibitors ONX 0914 and (to a lesser extent) oprozomib. Slight bortezomib resistance was also observed [280]. The reduced sensitivity of CEM/VLB cells to these inhibitors was associated with the requirement of higher inhibitor concentrations to induce a similar suppression of proteasomal CT-L activity, and resistance and inhibitory efficacy towards the CT-L activity were largely reversed and restored, respectively, by the P-glycoprotein inhibitor reversin 121 (P121). These findings further implicated P-glycoprotein-mediated drug efflux in the causative resistance mechanism [280]. Conversely, cell lines overexpressing the drug transporters MRP1-5 were not significantly resistant to these proteasome inhibitors, and the transporter BCRP was also ruled out as a contributor to resistance, indicating that P-glycoprotein is the major transporter with resistance-conferring potential with respect to these agents [280]. Even the low basal levels of P-glycoprotein's transport activity observed in PBMCs from rheumatoid arthritis patients and healthy controls were sufficient to slightly but significantly reduce the *ex vivo* inhibitory efficiency of carfilzomib and ONX 0914 against the proteasome's CT-L activity, as demonstrated by the stronger suppression of this activity by both inhibitors in the presence of reversin 121. However, these effects were not observed for oprozomib or for bortezomib [280].

Furthermore, H23 lung adenocarcinoma and DLD-1 colon adenocarcinoma cell line models of acquired carfilzomib resistance were found by our laboratory to overexpress P-glycoprotein at both the mRNA and protein levels, which was shown to contribute to the resistance phenotype by a substantial loss of resistance upon treatment with the P-glycoprotein inhibitor verapamil [281]. These cell lines acquired the ability to grow in culture medium containing 500 nM (H23/Carf) or 1,000 nM (DLD-1/Carf) carfilzomib and exhibited marked cross-resistance to the carfilzomib analog YU-101 and the known

P-glycoprotein substrate paclitaxel but retained parental levels of bortezomib sensitivity. Peptide analogs of carfilzomib lacking the epoxyketone pharmacophore were shown to resensitize the carfilzomib-resistant cell lines to carfilzomib, suggesting that such analogs may be useful in combating P-glycoprotein-mediated drug resistance [281]. Consistent with the results obtained in our laboratory [281], KMS-34 multiple myeloma cells cultured for 4 weeks in the presence of a low concentration (6 nM) of carfilzomib exhibited reduced carfilzomib sensitivity that could be restored by inhibiting P-glycoprotein with reversin 121 [282]. Although this cell line already expressed high basal levels of P-glycoprotein mRNA prior to carfilzomib exposure, its reduced carfilzomib sensitivity following culture in carfilzomib-containing medium was associated with increased levels of P-glycoprotein on the cell surface [282]. Furthermore, gene expression profiling detected increased expression of P-glycoprotein mRNA in drug-refractory cells obtained from a multiple myeloma patient following carfilzomib relapse, suggesting the contribution of this transporter to carfilzomib resistance may be of clinical relevance [282]. Additional studies will be required to definitively determine whether P-glycoprotein overexpression is a clinically important mediator carfilzomib resistance.

P-glycoprotein overexpression was also concluded to contribute to the acquired resistance of head and neck squamous cell carcinoma cell line models to 1 μM carfilzomib (R-UMSCC-1 and R-Cal33) [283]. While parental cells did not express detectable levels of P-glycoprotein, both of the resistant cell lines overexpressed this transporter, and the finding that a partial restoration of carfilzomib sensitivity could be achieved by reversin 121 treatment demonstrated that P-glycoprotein overexpression contributes to carfilzomib resistance in these cell lines. However, additional factors must also contribute, as the R-Cal33 cell line expressed much higher levels of P-glycoprotein than did the R-UMSCC-1 cell line but was more sensitive to carfilzomib [283]. In line with this, Bcl-2 was also upregulated in R-UMSCC-1 cells but not in R-Cal33 cells. Furthermore, co-treatment with carfilzomib and the Bcl-2/Bcl-X_L inhibitor ABT-737 led to an ~50% decrease in the carfilzomib IC_{50} in R-UMSCC-1 cells, in contrast to R-Cal33 cells. The authors suggested that elevated levels of Bcl-2 may contribute to the higher degree of acquired carfilzomib resistance exhibited by the R-UMSCC-1 cells, and, therefore, that adding a Bcl-2 inhibitor may be of therapeutic utility in such instances [283]. Additionally, although these carfilzomib-resistant cell lines were highly cross-resistant to oprozomib, they were only moderately cross-resistant to bortezomib, suggesting that bortezomib may be effective in treating carfilzomib- and oprozomib-resistant cancers [283].

d. Bortezomib Resistance

The above mentioned reports by Gutman et al. and Ao et al. demonstrated that bortezomib sensitivity was maintained in P-glycoprotein-overexpressing epoxomicin- and carfilzomib-resistant lines [278, 281], indicating that bortezomib may not be a P-glycoprotein substrate. However, results of other studies on whether or not bortezomib is a substrate of this transporter have yielded mixed results. Verapamil did not influence the sensitivity of P-glycoprotein-overexpressing K562 cells toward bortezomib, but did increase their sensitivity toward the P-glycoprotein substrate daunorubicin, suggesting that the activity of bortezomib is not significantly impacted by P-glycoprotein overexpression [284]. Additionally, results of studies of various cell line models of bortezomib resistance indicated that P-glycoprotein-mediated efflux of bortezomib did not serve as an underlying resistance mechanism [209, 246, 285-290]. Conversely, slight (4.5-fold) bortezomib resistance was observed by Verbrugge et al. in the P-glycoprotein-overexpressing CEM/VLB cell line [280]. Likewise, P-glycoprotein overexpression was shown to reduce bortezomib sensitivity only slightly (2-fold) in HL60/VCR and 8226/Dox6 MDR cell lines relative to parental HL60 and 8226 cells, an effect that was deemed unlikely to be relevant *in vivo* [291]. Bortezomib sensitivity was not affected by overexpression of MRP1, BCRP, or LRP [291].

Results of a study by Rumpold et al. also demonstrated that siRNA-mediated knockdown of P-glycoprotein in the P-glycoprotein-overexpressing cell line K562/Dox resulted in an ~6-fold increase in sensitivity to bortezomib-induced cytotoxicity, whereas sensitivity to the bortezomib analog MLN273 was increased to a greater extent (~26-fold) [292]. Consistent with this divergence, more pronounced differences were observed in the extent of MLN273-mediated inhibition of the proteasome's CT-L activity in the cells in which P-glycoprotein was knocked down versus left intact than those observed for bortezomib-mediated inhibition. These results suggested that, while both inhibitors can be transported by P-glycoprotein, MLN273 is more efficiently transported than is bortezomib [292].

O'Connor et al. also concluded bortezomib to be a substrate of P-glycoprotein. This was based on the reduced sensitivity to bortezomib observed in the P-glycoprotein-overexpressing DLKP-A cell line in comparison with the DLKP parental cell line, which did not overexpress P-glycoprotein, and the synergism with which bortezomib reduced cell viability in combination with the P-glycoprotein inhibitor elacridar in the former cell line [293]. Synergistic effects of this drug combination were also observed in other

P-glycoprotein-mediated multidrug resistant cell lines, including the NCI-Adr/res ovarian cancer and RPMI-Dox40 multiple myeloma cell lines [293]. O'Connor et al. suggested that the degree to which P-glycoprotein is overexpressed may dictate the ability of bortezomib to serve as a P-glycoprotein substrate, as the DLKP-A cell line, with higher P-glycoprotein expression, was less sensitive to bortezomib relative to its parental cell line, but the differences between the sensitivities of the A549-taxol cell line, with lower P-glycoprotein expression, and its parental cell line were much less pronounced. Additionally, the synergistic effects of the bortezomib-elacridar combination were greater in the cell line with higher P-glycoprotein expression than in the cell line with lower P-glycoprotein expression [293]. Consistent with the results of Minderman et al. [291], bortezomib was not found to be a substrate of MRP1 or BCRP [293].

NF-κB activity can induce P-glycoprotein expression in cancer cells [294]. Since proteasome inhibitors attenuate NF-κB signaling, they could potentially block upregulation of P-glycoprotein and thereby reduce the MDR phenotype. In fact, the proteasome inhibitors MG132 and bortezomib were found to reduce expression of P-glycoprotein, increase intracellular accumulation of doxorubicin, and synergize with doxorubicin and paclitaxel in P-glycoprotein-overexpressing MCF7 breast cancer cells (MCF7/ADR); treatment with these inhibitors also caused an increase in cytosolic IκBα levels and a decrease in NF-κB DNA binding [295]. O'Connor et al. also found P-glycoprotein expression in both RPMI-Dox40 and DLKP-A cells, and P-glycoprotein's transport activity in the former, to decrease following treatment with bortezomib, presumably due to a suppressed NF-κB-mediated induction of P-glycoprotein expression [293]. Alternatively, Fujita et al. attributed the reduced P-glycoprotein levels observed in MCF7/ADR cells following treatment with MG132 and bortezomib to increased signaling through the c-Jun pathway, which has been shown to inhibit P-glycoprotein expression in MDR cells, together with decreased and unaltered signaling through the ERK1/2 MAPK and p38-MAPK pathways, respectively, which have been suggested as contributors to the MDR phenotype [295].

1.8.2 Role of Altered Drug Metabolism

After concluding that P-glycoprotein overexpression mediated ALLN resistance in their original ALLN-resistant cell line [275], Inoue et al. generated a second ALLN-resistant CHO cell line, this time also adding verapamil to the culture medium in effort to block P-glycoprotein overexpression. These cells adapted to grow in the presence of 100 μM

ALLN and displayed 30-fold increased ALLN resistance in comparison with the parental CHO cell line [296]. They were also cross-resistant to the ALLN analog ALLM but not to the dipeptide aldehyde protease inhibitor calpeptin or E-64-d, a cysteine protease inhibitor which lacks an aldehyde group. Importantly, this cell line was not cross-resistant to doxorubicin, etoposide, or colchicine, demonstrating that the selection protocol did, in fact, prevent the development of the multidrug resistance phenotype [296]. Instead, the newly-generated ALLN-resistant cells were found to overexpress an aldo-keto reductase, which was accompanied by elevated levels of aldo-keto reductase activity. Aldo-keto reductases are capable of reducing a variety of carbonyl compounds, including xenobiotic aldehydes; thus, the observed aldo-keto reductase upregulation was presumed to contribute to the resistance phenotype by reducing ALLN's aldehyde pharmacophore to a pharmacologically inactive alcohol [296]. As observed for the P-glycoprotein-overexpressing ALLN-resistant cell line [275], higher concentrations of ALLN were required to inhibit the degradation of a reporter substrate in the aldo-keto-reductase-overexpressing ALLN-resistant cell line than in the parental cell line, which, in this case, was concluded to result from metabolic inactivation of ALLN [296]. The ALLN-resistance phenotype of these cells was found to be stable over a 1 month period in the absence of ALLN, whereas the levels of the aldo-keto reductase began to decrease 2 months following removal of the inhibitor [296].

As for bortezomib, Xu et al. demonstrated that DII1-mediated activation of the Notch signaling pathway led to reduced sensitivity of murine and human multiple myeloma cells to the inhibitor, an effect that was attributed to the increased expression of the cytochrome P450 enzyme CYP1A1 and could be abrogated by Notch pathway inhibition [297]. Conversely, microarray data led researchers to conclude that an increase in cytochrome P450-mediated oxidative deboronation of bortezomib was unlikely to contribute to the acquired bortezomib resistance of THP-1 myelomonocytic leukemia and HT-29 colorectal adenocarcinoma cell line models [246, 298].

1.8.3 Role of Alternative Proteolytic Pathways

Culturing EL4 mouse lymphoma cells in the presence of the peptide vinyl sulfone proteasome inhibitor NLVS led to the selection of an NLVS-resistant cell population in which an alternative, AAF-AMC-hydrolyzing, NLVS-insensitive proteolytic complex capable of taking over proteasome functions was concluded to help facilitate continued survival and proliferation under these conditions [299]. Subsequently, Geier et al.

identified tripeptidyl peptidase II (TPPII) as an AAF-AMC-hydrolyzing proteolytic complex with increased activity in EL4 cells selected for resistance to a 6 μM dose of the β-lactone proteasome inhibitor lactacystin and suggested that it may play a role in degrading proteasome substrates when proteasome activity is inhibited [300]. However, as TPPII activity was also detected in parental EL4 cells, Geier et al. concluded it to be most likely that multiple factors, including increased TPPII activity, simultaneously contribute to the lactacystin-resistant phenotype of these cells [300].

Indeed, TPPII was deemed capable of protecting against the cytotoxic effects of NLVS in the NLVS-resistant EL4 cell line by helping to degrade polyubiquitinated proteins [301]. Although Wang et al. discovered that proteasome activity was incompletely inhibited by the concentration of NLVS applied, residual proteasome activity (primarily of the β2 and β2i subunits) alone was concluded to be inadequate for protecting these cells against NLVS-induced cytotoxicity [301]. However, findings of a separate study refuted these conclusions and instead suggested that continued polyubiquitinated protein degradation via residual proteasome activity was essential for the NLVS-resistant cells to survive NLVS exposure [302]. Additionally, the results of several more studies suggested that TPPII was not involved in mechanisms of acquired bortezomib resistance [246, 285, 287]. Whether TPPII actually plays a role in conferring acquired proteasome inhibitor resistance, therefore, remains unresolved.

On the other hand, it may seem much more likely that compensatory activity of the main non-proteasomal proteolytic pathway—that is, the lysosomal/autophagy pathway—would contribute to proteasome inhibitor resistance. In fact, a number of studies have revealed that autophagy can compensate for diminished proteasome activity, which can contribute to insensitivity of cancer cells to proteasome inhibitors [303-305]. Enhanced prosurvival autophagy was identified as a contributor to acquired carfilzomib resistance in two multiple myeloma cell lines selected for resistance to 12 nM carfilzomib—one of which overexpressed P-glycoprotein and one which did not [306]. The results generated in this study supported a model in which the pluripotency reprogramming transcription factor KLF4—which was upregulated in the carfilzomib-resistant cell lines—mediates upregulation of sequestosome 1/p62, a ubiquitin-binding adaptor protein that can direct ubiquitinated proteins to either the proteasomal or the autophagic degradative pathway. This thereby allows ubiquitinated proteasome substrates to be rerouted to autophagosomes for clearance via prosurvival autophagy when proteasome activity is inhibited. Treatment with the autophagy inhibitor chloroquine sensitized both of these

carfilzomib-resistant cell lines to carfilzomib, further implicating this pathway in mediating carfilzomib resistance [306]. Activation of autophagy has also been associated with acquired bortezomib resistance [290]. These findings indicate that targeting both the proteasome and autophagy may be a more effective treatment strategy than targeting the proteasome alone [303-305].

1.8.4 Role of Proteasome-Mediated Mechanisms

The cellular effects of proteasome inhibitors have been shown to be concentration-dependent. For example, while a high concentration of the proteasome inhibitor MG132 induced apoptosis in AT3 prostate carcinoma cells, a lower concentration was not toxic and instead protected against apoptosis induced by Sindbis virus infection, demonstrating that proteasome inhibitors can induce or protect against apoptosis, depending on the concentration applied. These concentration-dependent effects are presumably due to differential degrees of proteasome inhibition achieved at a low versus high inhibitor concentration [307]. In line with this, a 24 hour treatment of human umbilical cord vein cells (HUVECs) with nontoxic doses of the proteasome inhibitors MG132 and MG262 inhibited the CT-L activity of the proteasome by 80%, while the C-L and T-L activities were inhibited by less than 50%. Alternatively, toxic doses inhibited the CT-L activity by 90-97%, the C-L activity by >50%, and the T-L activity by >70% [308]. Furthermore, similar bortezomib-mediated inhibition of proteasome activities did not similarly inhibit protein degradation in a panel of myeloma cell lines, with stronger inhibition of protein degradation leading to greater sensitivity to bortezomib. In most of the myeloma cell lines studied, a >90% reduction in viability by bortezomib required >95% inhibition of the proteasome's CT-L activity, co-inhibition of the C-L activity, and an ~50% inhibition in protein degradation. Unfortunately, this exceeds clinically achievable levels of bortezomib-mediated inhibition [309].

Alternatively, bortezomib's inhibitory efficacy against the CT-L activity was found to differ between two non-small cell lung cancer (NSCLC) cell lines, which was considered to be a contributing factor to their differential sensitivities to this inhibitor [310]. Basal CT-L proteasome activity was slightly lower and was more substantially inhibited by a lower concentration of bortezomib in the intrinsically bortezomib-sensitive NSCLC cell line SW1573 than in the intrinsically bortezomib-resistant H460 NSCLC cell line. Accordingly, G2/M arrest and apoptosis were induced by a lower concentration of bortezomib in SW1573 than in H460 NSCLC cells [310]. However, at higher doses of bortezomib that

similarly inhibited CT-L activity in both cell lines and induced G2/M arrest in H460 cells, a higher percentage of apoptotic H460 than SW1573 cells was observed. Although the extent to which the C-L and T-L activities were inhibited by bortezomib in these cell lines was not reported, these results suggested that induction of apoptosis in NSCLC cells requires sufficient inhibition of proteasome activity to induce G2/M arrest, and, once G2/M arrest has been induced, resistance to apoptosis must be overridden [310].

Collectively, these results (and others described above) suggest that, while mechanisms downstream of the proteasome are probably involved as well, cellular mechanisms leading to suboptimal inhibition of the proteasome's catalytic activities are likely to contribute to proteasome inhibitor resistance. Mutations in the β5-encoding *PSMB5* gene and altered expression levels and activity profiles of the catalytic proteasome subunits have been shown to produce such effects.

a. Bortezomib Resistance

Proteasome Inhibitor Resistance-Conferring PSMB5 Mutations

1. Impact on bortezomib binding

Lu et al. were the first to report a cell line model of acquired proteasome inhibitor resistance in which a mutation in the *PSMB5* gene contributes to the resistance phenotype [311]. In their initial publication, they described two mutations in this gene that they had identified in bortezomib-resistant Jurkat T lymphoblastic lymphoma/leukemia cells: a homogenous yet silent T192C mutation, and a G322A mutation encoding an Ala49Thr amino acid substitution in the β5 subunit. This latter mutation was initially heterogeneous, but became homogenous following further selection with higher bortezomib concentrations, perhaps indicating that the heterogeneity originally observed resulted from polyclonality of the initial culture rather than heterozygosity. Similar results were obtained with three additional bortezomib-resistant cell lines derived from the parental Jurkat cell line, suggesting that the Ala49Thr β5 mutant provides a growth advantage to these cells under bortezomib exposure [311]. Measuring the CT-L activity following bortezomib treatment in parental and bortezomib-resistant cell lines revealed that bortezomib's inhibitory efficacy towards this activity was significantly lower in the bortezomib-resistant cell lines, leading the authors to conclude that the Ala49Thr mutation in the β5 subunit plays a key role in bortezomib resistance by reducing the efficiency with which bortezomib inhibits its activity [311]. In line with this conclusion, introducing the mutant *PSMB5* gene into parental Jurkat cells led to significantly reduced bortezomib-mediated inhibition of the

proteasome's CT-L activity and conferred bortezomib resistance [311]. Overall, the results of this study are consistent with a resistance mechanism in which bortezomib's binding affinity for the conformationally-altered β5 subunit is reduced, leading to reduced bortezomib-mediated inhibition of CT-L activity and, consequently, suppressed G2 cell cycle arrest and apoptosis [311].

Further study of Jurkat sublines adapted to 1,000 nM bortezomib uncovered two additional *PSMB5* mutations: C323T and C326T, leading to Ala49Val and Ala50Val substitutions, respectively, in the β5 subunit [312]. One of these sublines initially contained a mixture of the G322A and C323T mutations, but, upon repeated rounds of selection, the C323T mutation became homogenous. Similarly, two additional sublines were found to contain a mixture of the C323T mutation and a G322A, C3236T conjoined mutation, with the conjoined mutation becoming homogenous upon further rounds of selection. These results led Lu et al. to hypothesize that, when challenged with a high dose (1,000 nM) of bortezomib, the G322A, C326T conjoined mutation provided a growth advantage over the C323T mutation, while this C323T mutation in turn provided a growth advantage over the G322A mutation [312]. Supporting this hypothesis, cells harboring the G322A, C326T conjoined mutation were the most resistant to bortezomib-induced cytotoxicity, those with the C323T mutation were intermediately resistant, and those containing the G322A mutation were the least resistant. This rank order also held true for resistance to bortezomib-mediated inhibition of the proteasome's CT-L activity [312]. As crystallographic studies previously showed that active site constituent amino acids Ala49 and Ala50 of the functional β5 protein are involved in a hydrogen bonding network with the carbonyl oxygen of bortezomib's pyrazine-2-carboxyl side chain [145], amino acid substitutions at these positions likely reduce the number of stabilizing interactions that can occur between bortezomib and the β5 active site, thereby leading to the reduced inhibitory efficacy observed, and, consequently, to bortezomib resistance [311, 312]. Additionally, computational modeling suggested that the Ala49Thr mutation leads to structural changes in the β5 subunit that may lower bortezomib's binding affinity [311]. The G322A point mutation has subsequently been identified in other bortezomib-resistant cell line models, including those derived from the THP-1 myelomonocytic leukemia [246], RPMI 8226 [313], KMS-11, and OPM-2 [314] multiple myeloma, and H460 and A549 NSCLC [289] cell lines, while the C323T mutation was also identified in bortezomib-resistant CCRF-CEM acute lymphoblastic leukemia cells [313].

The bortezomib-resistant THP-1 cell line gained an additional G311T mutation in the *PSMB5* gene while undergoing selection for resistance to 500 nM bortezomib, leading to a second, Met45Ile, substitution in the β5 active site [313]. A heterozygous G311T mutation in the *PSMB5* gene was associated with acquired bortezomib resistance in JY human B lymphoblast cells as well [315]. Franke et al. also observed *PSMB5* mutations in bortezomib-resistant derivatives of the CCRF-CEM and RPMI 8226 cell lines [313]. CCRF-CEM cells selected for resistance to 7 nM bortezomib harbored a G332T point mutation in this gene, leading to a Cys52Phe substitution in the S1 specificity pocket of the β5 active site [313]. The G332T mutation was also detected in SW1573 NSCLC cells resistant to 30 or 150 nM bortezomib [289].

Although Met45 plays an important role in defining the specificity of β5's S1 pocket [33], the Met45Ile substitution was not found by in silico modeling to directly impact bortezomib binding [313]. Analyzing the crystal structure of the bortezomib-bound yeast proteasome revealed that the position of its side chain shifts upon bortezomib binding to allow the S1 pocket to accommodate the P1 leucine side chain [145]. Met45 substitutions may alter the specificity and flexibility of the S1 pocket and, therefore, the dynamics of bortezomib binding [313]. Additionally, although Cys52 may not be directly involved in bortezomib binding, it is located near Met45 [145]. In silico modeling indicated that Cys52Phe would slightly repel bortezomib from β5's S1 specificity pocket [313].

In addition to the G332T mutation, CCRF-CEM cells selected for resistance to a higher concentration (200 nM) of bortezomib gained the C323T mutation in the *PSMB5* gene previously observed by Lu et al. [312], leading to a second amino acid substitution, Ala49Val, in the β5 subunit [313]. While the additional methyl groups contributed by the Ala49Val substitution did not, based on in silico modeling, appear to provide a direct steric barrier to bortezomib binding, this substitution was previously suggested to render β5's S1 pocket less accessible [313, 316].

RPMI 8226 cells selected for resistance to 7 nM bortezomib also contained an A247G *PSMB5* mutation, encoding a Thr21Ala substitution in the β5 subunit. This mutation was initially heterozygous, but became homozygous under continuous bortezomib exposure [313]. Thr21 was also previously concluded to play a direct role in bortezomib binding to β5 [145]. In silico modeling demonstrated that the Thr21Ala substitution causes a hydrogen bond between β5 and bortezomib to be lost, likely resulting in decreased affinity of bortezomib for β5 [313]. The heterozygous A247G mutation of the bortezomib-resistant RPMI 8226 cells was ultimately replaced by a homozygous G322A

mutation (encoding Ala49Thr) during dose escalation to 100 nM bortezomib [313]. When Franke et al. introduced the Ala49Thr substitution into their in silico model, they observed steric clashes with bortezomib's backbone or a constriction of the entrance into the S1 pocket—depending on how the Thr side chain was oriented—that may hinder bortezomib binding [313].

Interestingly, different *PSMB5* mutations were detected in independently-generated bortezomib-resistant CCRF-CEM and THP-1 cell lines [313]. An A310G mutation emerged in the new bortezomib-resistant THP-1 cell line, leading to a Met45Val substitution in the β5 subunit. Alternatively, a G322A mutation was detected in the new bortezomib-resistant CCRF-CEM cell line, resulting in the Ala49Thr substitution observed in the RPMI 8226 and THP-1 cell lines selected for resistance to 100 nM bortezomib. These results led the authors to conclude that β5 mutations are acquired *de novo* consequent to long-term exposure to bortezomib [313]. The A310G mutation was also identified in A549 cells resistant to 40 nM bortezomib, while a second, G322A, mutation was additionally detected in this cell line following selection for resistance to 100 nM bortezomib [289]. The elevated basal levels and suppressed bortezomib-induced accumulation of Mcl-1 and NOXA seen in the A549 cells resistant to 40 nM bortezomib were suggested as potential consequences of alterations in the degradation of specific proteins imposed by the β5 Met45Val substitution [289].

Ri et al. also observed heterozygous G322A (Ala49Thr-encoding) point mutations in the *PSMB5* gene in their bortezomib-resistant KMS-11 and OPM-2 cell lines [314]. However, the resulting amino acid substitutions were not accompanied by upregulation of the β5 protein in these cell lines [314], contrasting the results of other studies of bortezomib-resistant cell lines in which the G322A mutation was found [246, 289, 313]. The Ala49Thr substitution was concluded to result in a slightly impaired bortezomib-mediated inhibition of the CT-L activity in these bortezomib-resistant cell lines, thereby suppressing the bortezomib-induced accumulation of polyubiquitinated proteins and facilitating the evasion of a fatal ER stress response [314].

Acquired bortezomib resistance in HT-29 colorectal adenocarcinoma cell line models was also associated with *PSMB5* mutations [298]. Two *PSMB5* mutations were identified: one encoding a Cys63Phe substitution in the mature β5 protein, and another encoding an Arg24Cys substitution in the β5 propeptide [298]. Cys63 resides outside of the β5 active site but on the same α-helix containing the active site residues Ala49 and Ala50, which are involved in bortezomib binding [145]. Molecular modeling predicted that

the Cys63Phe substitution alters the position of this helix relative to the active site, especially in the bortezomib-bound state, causing bortezomib to adopt an unfavorable conformation in in the β5 active site [298]. The accelerated recovery of the proteasome's CT-L activity following its bortezomib-mediated inhibition in the bortezomib-resistant cell lines suggests that the Cys63Phe substitution may increase bortezomib's dissociation constant with respect to the β5 active site. Conversely, the Cys63Phe substitution was not predicted to substantially impact the binding of epoxomicin to the β5 active site, which was in line with the largely retained sensitivity of the bortezomib-resistant HT-29 cell lines to the epoxomicin analog carfilzomib [298]. On the other hand, the Arg24Cys substitution results from a naturally-occurring polymorphism observed more frequently in patients with multiple myeloma than in the general population [317]. Suzuki et al. proposed that this substitution may contribute to the faster recovery of CT-L activity following its inhibition by bortezomib by influencing propeptide processing [298]. In addition, a mutation in the *PSMB8* gene, encoding a Phe50Ile substitution in the β5i propeptide, was observed in HT-29 cells resistant to 200 nM bortezomib, but how this may contribute to bortezomib resistance was not further discussed [298].

2. Impact on β5's Catalytic Activity

Many of the *PSMB5* mutations identified in the bortezomib-resistant cell lines described above were also concluded to impair β5's catalytic activity. For example, the observed discrepancy between the strong overexpression of the Ala49Thr mutant β5 subunit and the relatively minor increase in basal CT-L activity detected in the bortezomib-resistant THP-1 cell lines described by Oerlemans et al. [246] may have resulted from a reduced ability of the P1 tyrosine of Suc-LLVY-AMC—the substrate used to measure proteasomal CT-L activity in this study—to access the S1 specificity pocket of the mutant β5 subunit, leading to a weaker hydrolysis of this substrate than observed with wild-type β5 [313]. Similarly, de Wilt et al. suggested that the β5 amino acid substitutions identified in their bortezomib-resistant NSCLC cell lines resulted in the reduced CT-L activity observed, despite β5 upregulation [289]. The Ala49Thr substitution was also concluded to reduce the efficiency of β5 labeling by the ABP Bodipy FL-Ahx$_3$L$_3$VS, as this labeling appeared to be prominently reduced in cells selected for resistance to 30 nM bortezomib but rebounded somewhat in cells selected for higher levels of resistance in which greater upregulation of the mutant β5 was observed [246].

Franke et al. used in silico modeling to evaluate how the amino acid substitutions in the β5 active site observed in their bortezomib-resistant cell lines may impair Suc-LLVY-AMC hydrolysis [313]. This analysis indicated that, when Cys52 is replaced by Phe, it displaces the P1 tyrosine side chain of the Suc-LLVY-AMC substrate from β5's S1 specificity pocket, thereby decreasing its binding affinity. The Cys52Phe mutation may also hamper the conformational change in Met45 that is required for substrate binding [313]. Thr21 was not shown by in silico modeling with wild-type β5 to play a direct role in Suc-LLVY-AMC binding, but, due to its proximity to Suc-LLVY-AMC's peptide backbone, a hydrogen bond may form between the two upon minor shifts in conformation, which may explain the negative impact of the Thr21Ala substitution on Suc-LLVY-AMC hydrolysis [313]. The Ala49Thr substitution alters β5's S1 pocket, and in silico modeling suggested it may impair the P1-S1 interaction between Suc-LLVY-AMC and β5, as predicted for bortezomib [313]. The Ala49Val, Cys52Phe and Met45Ile, Ala49Thr double substitutions were predicted to lead to a greater repulsion of Suc-LLVY-AMC's P1 side chain from β5's S1 specificity pocket than the Cys52Phe or Ala49Thr substitution, respectively, alone [313]. Based on their results, Oerlemans et al. and Franke et al. suggested that, as the identified amino acid substitutions in the β5 subunit appear to impair proteasomal CT-L activity, overexpression of the mutant β5 subunits in the bortezomib-resistant cells serves to maintain acceptable levels of this activity [246, 313]. In support of this notion, bortezomib-resistant cells with homozygous β5 mutations showed greater β5 upregulation relative to cells with heterozygous mutations [313]. Verbrugge et al. also suggested that upregulation of the Met45Ile mutant β5 subunit in their bortezomib-resistant JY cells likely reflected this compensatory mechanism [315].

In contrast to the various mutations identified in the β5-encoding gene (and the mutation identified by Suzuki et al. in the β5i-encoding gene), no mutations were detected in the genes encoding β1 or β2 in the bortezomib-resistant CCRF-CEM or RPMI 8226 cells reported by Franke et al. [313]. Additionally, no mutations were detected in the genes encoding β1 or β6 in the bortezomib-resistant multiple myeloma cell lines reported by Ri et al. [314], in the genes encoding β1, β7, or β1i in the bortezomib-resistant HT-29 cell lines reported by Suzuki et al. [298], or in the gene encoding β5i in the bortezomib-resistant JY cells reported by Verbrugge et al. [315].

3. Impact on Cross-Resistance to Alternative Proteasome Inhibitors

In addition to contributing to bortezomib resistance, the amino acid substitutions in the β5 subunit observed in bortezomib-resistant cell lines may also lower the inhibitory efficiency of, and thereby confer cross-resistance to, other active site-targeting proteasome inhibitors. THP-1 cells resistant to up to 200 nM bortezomib and harboring Ala49Thr mutant β5 subunits were cross-resistant to reversibly-binding proteasome inhibitors, including tripeptide aldehydes ALLN and MG-132 and MG-132's boronate analog, MG-262 [246]. THP-1 cells resistant to 50 and 500 nM bortezomib, which harbor only an Ala49Thr substitution or both Ala49Thr and Met45Ile substitutions, respectively, in the β5 active site, were also cross-resistant to the irreversibly-binding proteasome inhibitors ONX 0912, ONX 0914, and carfilzomib, indicating that *PSMB5* mutations contribute to a general resistance to β5/β5i-targeting inhibitors due to an impaired ability of these inhibitors to bind to the β5 active site [280]. Furthermore, bortezomib-resistant cell lines harboring mutant β5 subunits were less sensitive than their parental counterparts to both the β5-inhibitory and cytotoxic effects of PR-924, consistent with a negative impact of these amino acid substitutions on PR-924 binding to β5 and in line with the finding that the cytotoxic effects of this β5i-selective inhibitor require co-inhibition of β5 [186, 318]. Additionally, the observed cross-resistance of bortezomib-resistant NSCLC cell lines to the proteasome inhibitors MG132, carfilzomib, and ONX 0912 was concluded to support a causative role of *PSMB5* mutations in cases of acquired bortezomib resistance [289].

Despite these conclusions, bortezomib-resistant cell lines typically displayed much greater resistance to bortezomib than to alternative reversibly- and irreversibly-binding inhibitors [246, 280, 289, 318]. Furthermore, while introducing the mutant *PSMB5* into parental KMS-11 cells led to suppressed polyubiquitinated protein accumulation, a weakened terminal ER stress response, and protection against growth inhibition and apoptosis following treatment with bortezomib, it conferred a lesser degree of resistance than that observed in the bortezomib-adapted KMS-11 cells [314]. These findings imply that other factors besides amino acid substitutions in the β5 subunit also contribute to the resistance of these cell lines to bortezomib [246, 280, 289, 314, 318]. Finally, although PSMB5 mutations have been identified in a variety of proteasome inhibitor (predominantly bortezomib)-resistant cell line models, such mutations have not yet been linked to clinical cases of proteasome inhibitor resistance [313, 314, 317, 319-321].

Altered Proteasome Subunit Expression Levels

As overexpression of target proteins can confer resistance to targeted therapeutic agents, perhaps an increase in the levels of proteasome subunits can mediate proteasome inhibitor resistance. The observed feedback upregulation of proteasome components following proteasome inactivation in yeast [322, 323], *Drosophila* [324], and mammalian [247, 325-327] cells supports this notion, and, in fact, this response was shown to be important in compensating for impaired proteasome activity [322, 323, 326-328]. Thus, mRNA and/or protein levels of proteasome subunits were often evaluated in cell line models of acquired proteasome inhibitor resistance.

1. mRNA Levels

The *PSMB5* gene encodes the catalytic proteasome subunit β5—the primary constitutive subunit targeted by bortezomib. Of the mRNAs encoding catalytic proteasome subunits, the levels of *PSMB5* mRNA were most frequently reported, and were often found at odds with the β5 protein levels detected in the same cell lines. For example, among a series of bortezomib-resistant THP-1 myelomonocytic leukemia cell lines selected for varying degrees of bortezomib resistance, *PSMB5* mRNA levels ranged from reduced to relatively similar to parental levels in those selected for resistance to 30-200 nM bortezomib, and were only increased in cells resistant to 500 nM bortezomib—the highest concentration applied in this study. This contrasted the β5 protein levels in these cell lines, which were elevated by as much as 60-fold, leading the authors to conclude that the massive upregulation of β5 occurred at the post-transcriptional level [246]. Although this is the most extreme example, similar disparities were also noted by others [209, 288, 329]. Additionally, despite a greater upregulation of *PSMB5* mRNA in RPMI 8226 multiple myeloma cells selected for resistance to 100 nM bortezomib than in those selected for resistance to only 7 nM of the inhibitor, these two cell lines contained similar levels of the β5 protein, again suggesting post-transcriptional control of cellular β5 levels [313]. Conversely, increased levels of *PSMB5* mRNA were observed in bortezomib-resistant CCRF-CEM acute lymphoblastic leukemia [313], RPMI 8226 multiple myeloma [330], JY B lymphoblast [315] and HT-29 colorectal adenocarcinoma cell lines [298], which corresponded to the increased β5 protein levels detected [298, 313, 315, 330].

The upregulation of *PSMB5* mRNA observed in bortezomib-resistant cell lines can be a transient effect of bortezomib exposure. For example, Lu et al. found *PSMB5* mRNA to be increased up to 7-fold in an initial study of bortezomib-resistant Jurkat T

lymphoblastic lymphoma/leukemia cell lines, which was associated with an increase in the proteasome's CT-L activity of up to 6-fold [286]. However, in a subsequent study in which bortezomib-resistant Jurkat cells were withdrawn from bortezomib for more than two months, the levels of both *PSMB5* mRNA and CT-L activity were found to be similar to those detected in parental Jurkat cells, suggesting that *PSMB5* upregulation had been reversed during prolonged culture in the absence of bortezomib [312]. Similarly, both *PSMB5* mRNA and β5 protein levels decreased time-dependently in bortezomib-resistant THP-1 cells following bortezomib withdrawal, further suggesting that the upregulation of these species can be reversed once the selective pressure of bortezomib is removed [246].

PSMB6 (β1-encoding) and *PSMB7* (β2-encoding) mRNA levels were also evaluated in several of these studies. Like *PSMB5* mRNA, the regulation of these species were often found to inadequately represent that of the respective proteins [209, 246, 298]. For instance, while *PSMB6* and *PSMB7* mRNAs were increased above parental levels in bortezomib-resistant HL-60 myeloid leukemia cells, only β2, and not β1, was upregulated at the protein level [209]. This contrasts the results of Suzuki et al., who found that *PSMB7*, but not *PSMB6*, mRNA was upregulated in bortezomib-resistant HT-29 cells, but that both subunits were upregulated 3-4-fold at the protein level [298]. On the other hand, increases in *PSMB6* and *PSMB7* mRNA levels were observed in bortezomib-resistant CCRF-CEM [313] and JY [315] cells, which corresponded to increases in the protein levels of β1 and β2 [313, 315]. However, despite the greater increases in *PSMB6* and *PSMB7* mRNAs in bortezomib-resistant RPMI 8226 cells compared with those observed in bortezomib-resistant CCRF-CEM cells, no major changes were observed in β1 and β2 expression at the protein level [313].

Only three of the above-mentioned reports addressed the levels of mRNAs encoding the immunosubunits. In the bortezomib-resistant THP-1 cells described by Oerlemans et al., *PSMB8* and *PSMB9* mRNAs (which encode β5i and β1i, respectively) were the only β-subunit mRNAs that were substantially downregulated, whereas the levels of *PSMB10* mRNA (which encodes β2i) remained relatively unaltered. However, the protein levels of these subunits were not evaluated for comparison [246]. Verbrugge and colleagues, as well as Suzuki and colleagues, alternatively, did examine immunosubunit expression at both the mRNA and protein levels [298, 315]. In the former case, a slight increase in immunosubunit mRNAs relative to parental levels was observed in bortezomib-resistant JY cells, which was not associated with changes in the levels of the immunosubunit proteins [315]. In the latter case, conversely, no major changes in

immunosubunit mRNA levels were observed in bortezomib-resistant HT-29 cells, whereas, at the protein level, although β1i expression did in fact appear to remain unaltered, β5i and β2i levels were increased 8-fold and 3-4-fold, respectively [298].

Collectively, these findings demonstrate that the levels of the mRNAs encoding the various catalytic proteasome subunits are often poorly predictive of their corresponding protein levels, as previously discussed [331], stressing the importance of evaluating proteasomal protein levels and activity profiles directly rather than using mRNA levels as a surrogate.

2. Protein Levels

As was the case for *PSMB5* mRNA, the protein expression levels of β5 were most frequently examined in bortezomib-resistant cells. Downregulation of this subunit at the protein level was never observed, but, in a few bortezomib-resistant cell lines, it was concluded to remain unchanged from parental levels [287, 290, 314]. However, its levels were increased in almost all bortezomib-resistant cell lines [209, 246, 280, 285, 288, 289, 298, 313, 315, 329, 330, 332, 333].

Many of these studies also assessed the protein levels of constitutive catalytic subunits β1 and β2. It was concluded that the expression of only β1 (in bortezomib-resistant HL-60 myeloid leukemia and ARH-77 plasmacytoid lymphoma cells [209]) or both β1 and β2 (in bortezomib-resistant RPMI 8226 [313] and U266 multiple myeloma [290] and I-45 mesothelioma [287] cells) remained unaltered in several bortezomib-resistant cell lines. Ri et al. also concluded that β1 and β2 levels were unaltered in bortezomib-resistant KMS-11 and OPM-2 multiple myeloma cell lines cultured in the absence of bortezomib [314]. β2 expression was slightly increased in these cell lines following reintroduction of 10 nM bortezomib, contrary to the slight decrease in the levels of this subunit in the parental cell lines under these conditions. However, no such bortezomib-induced changes were noted for β1 or β5 in the parental or bortezomib-resistant cell lines [314]. Conversely, the levels of β2, as well as those of β1 and β5, whether altered with respect to those of the parental cells or not, were concluded to be uninfluenced by whether or not bortezomib-resistant HL-60 myeloid leukemia, ARH-77 plasmacytoid lymphoma, AMO-1 multiple myeloma [209] or I-45 mesothelioma [287] cells were cultured in the presence or absence of bortezomib. For bortezomib-resistant HL-60, ARH-77, and AMO-1 cells, this was suggested to reflect adaptive and not reactive changes in proteasome catalytic subunit content [209]. Irrespective of these findings, β1

and β2 expression, like that of β5, was found to increase when bortezomib resistance was acquired in most cell line models in which it was examined [209, 246, 280, 285, 289, 298, 313, 315, 330, 332].

More varied results were observed in the handful of studies for which immunosubunit levels were reported. All three were found to be reduced in bortezomib-resistant Namalwa Burkitt lymphoma [285], THP-1 myelomonocytic leukemia, RPMI 8226 multiple myeloma, and CCRF-CEM acute lymphoblastic leukemia [280, 332] cell lines, but were increased in bortezomib-resistant H460 and A549 NSCLC cell lines [289]. De Wilt et al. suggested that, while the increased immunosubunit levels detected in their bortezomib-resistant H460 and A549 cell lines contrast the results of Busse et al., who showed that elevated immunosubunit levels were associated with increased (albeit intrinsic) bortezomib sensitivity [334], their finding may be in agreement with the ability of immunoproteasomes to efficiently degrade oxidized proteins [112], which are known to accumulate following bortezomib treatment; thereby, immunoproteasomes may serve a protective role against bortezomib-mediated induction of apoptosis [289]. Alternatively, Niewerth et al. proposed that the increased formation of intermediate proteasomes containing β5i together with β1 and β2 or β1i and β2 following bortezomib withdrawal may be capable of compensating for the weakened CT-L activity of mutant β5 subunit-containing proteasomes [332]. Conversely, no major changes in immunosubunit levels were reported for bortezomib-resistant HL-60 myeloid leukemia [209], JY B lymphoblast [315], or SW1573 NSCLC [289] cells, and, in bortezomib-resistant HT-29 colorectal adenocarcinoma cell lines, β5i and β2i were increased (8- and 3-4-fold, respectively), but β1i remained unaltered from parental levels [298]. The lack of a concerted increase in all three immunosubunits in the bortezomib-resistant HT-29 cells may suggest an increase in intermediate proteasome levels [298]. Lastly, an increase in proteasome-incorporated β5i was observed in the initial study of bortezomib-resistant CCRF-CEM cells, while a decrease was observed in bortezomib-resistant RPMI 8226 cells [313].

In addition to the catalytic subunits of the 20S proteasome, up- or downregulation of other proteasome components was observed in bortezomib-resistant cell lines. An increase in structural 20S proteasome subunits α3, β4 and β6, 19S cap subunits Rpt5 and Rpn2, and in the proteasome maturation protein POMP was observed in bortezomib-resistant Namalwa cells, which, together with the increased β5, β1, and β2 levels detected, suggested a general upregulation of proteasome components and elevated assembly of proteasome complexes [285]. On the other hand, as was observed for the three

immunosubunits, the PA28β subunit of the IFNγ-inducible 11S proteasome activator—an alternative regulatory complex that can associate with the 20S proteasome in place of the 19S cap at either or both ends [335, 336]—was downregulated. This led Fuchs et al. to suggest that the inducible proteasome subunits, unlike the constitutive subunits, are not required for the survival of this cell line in the continuous presence of bortezomib [285]. Conversely, although expression of the three immunosubunits was unaltered in bortezomib-resistant HL-60 cells in comparison with parental HL-60 cells, expression of the PA28α subunit of the 11S activator was elevated, as were the levels of 11S-20S complexes [209]. Furthermore, the increased levels of structural 20S proteasome subunit α7 in bortezomib-resistant NSCLC cell lines was in agreement with the increased levels of assembled proteasome complexes detected [289]. However, while increases in the levels of α7 and assembled proteasome complexes were also detected in bortezomib-resistant CCRF-CEM cells, no major changes in these properties were observed in bortezomib-resistant RPMI 8226 cells [313]. Although THP-1 cells selected for resistance to 100 nM bortezomib did not show substantially elevated α7 levels [246], a later study showed that THP-1 cells selected for resistance to a higher concentration (200 nM) of bortezomib had higher levels of assembled proteasomes than did parental THP-1 cells [332]. Finally, no major changes were observed in the levels of structural 20S proteasome subunit α4 or 19S cap subunit Rpn1 in bortezomib-resistant HL-60 cells [209].

In summary, altered levels of the various proteasome components were commonly detected in cancer cell lines upon acquisition of bortezomib resistance, yet the specific changes observed often differed cell line-dependently. This may suggest that proteasome complexes can adapt in multiple unique ways to allow cancer cells to survive bortezomib exposure. This notion is further evidenced by the findings discussed below.

Altered Proteasome Activities

The levels of individual catalytic activities of the proteasome were also evaluated in many bortezomib-resistant cell line models. The proteasome's CT-L activity was increased in many of these cell lines relative to that of the parental cells [246, 285, 286, 298, 313, 329, 333]. Alternatively, in some cases, no increase [289, 290] or reduced [287, 288, 313] CT-L activity was observed. In the initial study of bortezomib-resistant Jurkat cells, upregulation of *PSMB5* mRNA and the associated increase in CT-L activity were concluded to lead to the high levels of bortezomib resistance established [286]. IκB levels were decreased in a time-dependent manner following bortezomib treatment in one of

these bortezomib-resistant cell lines, indicating that activation of NF-κB under these conditions may also contribute to their resistance phenotype [286]. Subsequently published findings obtained with the bortezomib-resistant Jurkat cells revealed, however, that point mutations in the *PSMB5* gene contributed to the impaired ability of bortezomib to inhibit the CT-L activity of the β5 subunit—whether *PSMB5* mRNA levels and CT-L activity were increased or not—and, therefore, to their reduced bortezomib sensitivity [311, 312]. Conversely, despite the large (up to 60-fold) upregulation of the β5 protein in bortezomib-resistant THP-1 cells, their basal CT-L activity was only increased 1.3-1.4-fold over parental levels, presumably due to the negative impact of the β5 active site substitution identified in these cells on their CT-L activity [246, 313].

Additionally, in agreement with the reduced immunosubunit levels observed in bortezomib-resistant THP-1, RPMI 8226, and CCRF-CEM cells, basal β5i and β1i activities were decreased in these cell lines [318, 332]. On the other hand, despite the presence of active site-mutant β5 subunits, the increased expression of constitutive catalytic subunits detected in these cell lines was accompanied by 2-4-fold higher basal β5 activity [318, 332]. Based on these results and those obtained from experiments involving IFNγ-mediated immunosubunit upregulation and siRNA-mediated immunosubunit downregulation, the authors concluded that downregulation of β5i is a major factor contributing to the acquired resistance of these cell lines to the cytotoxic effects of bortezomib, and that IFNγ-mediated upregulation of immunosubunits could increase the sensitivity of bortezomib-resistant leukemia cells to bortezomib, carfilzomib, and the β5i-selective inhibitor ONX 0914 [332]. They speculated that, since IFNγ increases the levels of both oxidant-damaged proteins, which are in need of proteasomal degradation, and immunoproteasomes, which degrade these substrates more efficiently than do constitutive proteasomes, inhibiting immunoproteasome activity in bortezomib-resistant cells under these conditions ensures the accumulation of polyubiquitinated proteins, providing an explanation for the increased accumulation of these species and enhanced cytotoxicity observed following combined IFNγ stimulation and proteasome inhibition, particularly when ONX 0914 was used as the inhibitor [332].

Increases in proteasomal C-L and T-L activities were also observed in several studies [246, 285, 298, 329], although these activities were concluded to be reduced [333] or largely unaltered [290] in some bortezomib-resistant cell lines. In bortezomib-resistant Namalwa cells, the <1.5-fold increase in the three major proteolytic activities poorly reflected the marked β1, β2, and β5 upregulation observed, leading Fuchs et al. to

conclude that proteasomes in these cells possessed lower levels of these specific activities [285].

The CT-L activity in bortezomib-resistant cell lines was frequently found to be less susceptible to bortezomib-mediated inhibition than that of the parental cells. This has been attributed to increased basal expression and activity of the β5 subunit and/or amino acid substitutions in or near the β5 active site [246, 289, 313, 314]. However, the reduced sensitivities of other proteasome activities to bortezomib-mediated inhibition noted for bortezomib-resistant cell lines harboring *PSMB5* mutations suggest that factors aside from these mutations also underlie their bortezomib-resistant phenotypes. For example, Oerlemans et al. observed a reduced inhibitory efficacy of bortezomib against not only the CT-L activity, but also the C-L and T-L activities, in their bortezomib-resistant THP-1 cell lines. They suggested that, in particular, the enhanced (rather than reduced) T-L activity observed in these cell lines upon exposure to their selective concentrations of bortezomib may compensate for the substantially suppressed CT-L and C-L activities observed under these conditions [246]. Similar conclusions were drawn from results obtained with bortezomib-resistant CCRF-CEM cells [337]. De Wilt et al. also found that higher concentrations of bortezomib were required to inhibit the CT-L and C-L activities of bortezomib-resistant NSCLC cell lines to a comparable extent to that achieved with lower bortezomib doses in the corresponding parental cell lines. Furthermore, even a high concentration (500 nM) of bortezomib did not inhibit the T-L activity of the bortezomib-resistant cell lines, and, as observed for the parental cell lines, low concentrations stimulated the T-L activity [289]. In line with these findings, higher concentrations of bortezomib were required to induce a similar degree of polyubiquitinated protein accumulation in the bortezomib-resistant cell lines to that attained with lower bortezomib concentrations in the parental cell lines; higher bortezomib concentrations were also required to induce G2/M arrest and cell death in the bortezomib-resistant cells than in the parental cells [289]. Doses exceeding the selective bortezomib concentrations were also required to induce polyubiquitinated protein accumulation in bortezomib-resistant THP-1 [246], CCRF-CEM, RPMI 8226 [313], and JY [315] cells. Consistently, higher concentrations of bortezomib were required to provoke loss of mitochondrial membrane potential and apoptosis in bortezomib-resistant THP-1 cells, yet apoptosis was induced by etoposide with similar efficiency in the parental and bortezomib-resistant cells. This suggests that the bortezomib-resistant cells do not display general resistance to apoptosis; only proteasome inhibitor-induced apoptosis is suppressed [246].

Bortezomib also inhibited proteasome activity less efficiently in bortezomib-resistant cell lines devoid of *PSMB5* mutations. The elevated levels of constitutive catalytic subunit expression in bortezomib-adapted AMO-1, HL-60, and ARH-77 cells were consistent with the increased basal levels of active proteasome subunits detected via ABP labeling [204, 209]. These changes were concluded to result in the ability of the bortezomib-resistant cells to retain higher levels of active β5/β1-type subunits in the presence of 20 nM bortezomib than those found in the parental cells under these conditions [204, 209], reflecting an important role of maintaining sufficient levels of active β5- and β1-type subunits in surviving bortezomib exposure [204]. Furthermore, the increased relative β2 activity in bortezomib-resistant AMO-1 cells in comparison with that of parental AMO-1 cells [209, 338] was suggested to indicate that, as previously proposed by Oerlemans et al. [246], maintaining sufficiently high β2 activity in the presence of bortezomib may compensate for the bortezomib-mediated suppression of β1/β1i and β5/β5i activities, thereby allowing cells to bypass the cellular repercussions of bortezomib treatment [338]. This, in turn, is consistent with the ability of β2/β2i-selective inhibitors to sensitize cancer cells, including those with acquired proteasome inhibitor resistance, to the cytotoxic effects of bortezomib and carfilzomib [180, 184]. However, bortezomib did still inhibit β1, β1i, β5, and β5i activities, and to a lesser extent β2 and β2i activities, dose-dependently in bortezomib-adapted AMO-1 cells, consistent with the established bortezomib inhibition profile [338], with a similar proportion of the basal levels of active proteasome subunits being inactivated in the parental and bortezomib-adapted cell lines [184]. These findings indicated to the authors that mutations in the β1/β5 active sites that impede bortezomib binding did not contribute to the bortezomib resistance mechanisms of these cells [209, 338], which was later confirmed directly [184]. As observed for other cell line models both with and without *PSMB5* mutations [246, 289, 313, 315, 330], bortezomib-induced accumulation of polyubiquitinated proteins was suppressed in bortezomib-resistant HL-60 cells in comparison with parental HL-60 cells [209]. Additionally, genes encoding several proteins involved in ER stress and the unfolded protein response (UPR) were found to be downregulated in bortezomib-resistant HL-60 cells [209].

In bortezomib-resistant Namalwa cells, the CT-L activity became resistant to the inhibitory effects of even 50 nM bortezomib, which inhibited most of the CT-L activity in the parental cell line [285]. Conversely, while lactacystin suppressed the CT-L, C-L, and T-L activities in the parental cells, it selectively inhibited the CT-L activity in the bortezomib-

resistant cells. The ability of lactacystin, but not bortezomib, to inhibit the CT-L activity in the bortezomib-resistant cells was suggested to possibly result from the irreversible binding mechanism of this inhibitor to the β5 subunit [285]. Whether or not this cell line harbored a *PSMB5* mutation was not reported.

Alternatively, in addition to their elevated β5 levels and proteasome activities, bortezomib-resistant JEKO and HBL2 mantle cell lymphoma cell lines could successfully withstand a greater bortezomib-mediated reduction in their CT-L activity than could parental cells [329]. Although the extent to which C-L and T-L activities were inhibited by bortezomib in these cell lines was not reported, the authors concluded that these results may suggest that other cellular mechanisms aside from increased proteasome activity are also important contributors to the bortezomib resistance seen. Indeed, it was concluded that, along with the above-mentioned properties, plasmacytic differentiation played an important role in the adaptation of these cells to the presence of bortezomib [329]. All of these factors were concluded to contribute to the enhanced ability of the bortezomib-resistant mantle cell lymphoma cells to deal with the increased protein load placed on the proteasome by bortezomib treatment, thus, in the absence of the increased immunoglobulin synthesis associated with fully-differentiated plasma cells, rendering them less susceptible to bortezomib-induced cytotoxicity [329].

Faster Recovery from Proteasome Inhibition

While inferior inhibition of proteasome activity by a given dose of bortezomib may be one important factor contributing to bortezomib resistance, faster recovery of proteasome activity following an initially similar extent of bortezomib-mediated inhibition appears to be another. Despite the increased β5 expression detected in a bortezomib-resistant RPMI 8226 cell line reported by Kuhn et al., bortezomib maintained the ability to suppress their CT-L activity, suggesting that active site mutations in the β5 subunit do not contribute to the resistance mechanism in these multiple myeloma cells [288]. This was confirmed by sequencing the active site region of the *PSMB5* gene. Although CT-L activity was inhibited by 10 nM bortezomib to a similar extent in both the parental and resistant cell lines at early timepoints, this activity recovered more quickly following bortezomib addition in the latter cell line than in the former [288]. However, while it was acknowledged that multiple mechanisms may contribute to the emergence of bortezomib resistance, the focus of this study was turned to the contribution of elevated IGF-1/IGF-1R signaling, which was concluded to potentially play a key role in bortezomib resistance in multiple

myeloma cells and to possibly be an interesting co-target to examine for bortezomib-based combination regimens. It was suggested that such regimens could ultimately overcome or prevent clinical resistance to proteasome inhibitors in multiple myeloma patients [288].

Similar findings to those obtained by Kuhn et al. were reported for bortezomib-resistant HT-29 colorectal adenocarcinoma cell lines [298]. Despite the elevated expression levels and activities of catalytic proteasome subunits detected in these cell lines, CT-L activity was inhibited to a similar extent in both parental and bortezomib-resistant HT-29 cells following treatment with bortezomib but recovered faster from bortezomib-mediated inhibition. The faster recovery could not be attributed to the expedited production of new proteasomes, since recovery was actually more rapid in the presence of the protein synthesis inhibitor cycloheximide. These results were concluded to suggest that bortezomib's dissociation constant with respect to the β5 active site was increased in the bortezomib-resistant cell line, attributable to the presence of a Cys63Phe mutation near the β5 active site [298]. Conversely, while the CT-L activity was also similarly inhibited in both the parental and bortezomib-resistant cells following treatment with carfilzomib, it recovered more slowly and at similar rates in both cell lines. In this case, recovery was largely prevented by inhibiting protein synthesis, consistent with new proteasome synthesis being required for substantial recovery of proteasome activity in both the parental and bortezomib-resistant cells following exposure to irreversibly-binding inhibitors such as carfilzomib [298]. Additionally, the similar recovery rates of the CT-L activity in parental and bortezomib-resistant cells from carfilzomib-mediated inhibition indicate that β5 mutations that impair bortezomib binding do not necessarily impair binding of carfilzomib to the β5 active site. Consistent with this, computational modeling indicated that the Cys63Phe mutation should not impact epoxomicin binding. Accordingly, the bortezomib-resistant cells remained largely sensitive to carfilzomib; their 3-4-fold decrease in carfilzomib sensitivity was in line with their 3-4-fold increase in proteasome catalytic activities [298]. Resistance of these HT-29 cell lines to bortezomib was attributed to increased proteasome activity, *PSMB5* mutations, and the altered expression of genes associated with stress response and cell survival pathways [298].

In contrast to the unaltered inhibitory efficacy described by Kuhn et al. and Suzuki et al. for their bortezomib-resistant cell lines, 10 nM bortezomib was found slightly less effective in inhibiting the proteasome's CT-L activity in bortezomib-resistant KMS-11 and OPM-2 multiple myeloma cell lines than in their respective parental cell lines [314]. Accordingly, polyubiquitinated proteins accumulated to a lesser extent in the bortezomib-

resistant cell lines than in the parental cell lines following bortezomib treatment. This accumulation was transient in the bortezomib-resistant cell lines, with basal levels of these species being restored within 24 and 48 hours following bortezomib addition in bortezomib-resistant KMS-11 and OPM-2 cells, respectively [314]. Importantly, the suppressed polyubiquitinated protein accumulation was associated with the evasion of fatal ER stress. These results led the authors to conclude that bortezomib's slightly inferior inhibition of the CT-L activity in the bortezomib-resistant cell lines, which was concluded to partially result from a heterogeneous G322A point mutation in the *PSMB5* gene, may have assisted in preventing polyubiquitinated proteins from accumulating to levels sufficient to induce cell death. The results presented in this report are consistent with the conclusion that the G322A mutation in the *PSMB5* gene contributes to a less robust accumulation of polyubiquitinated proteins following bortezomib treatment, which, by protecting against activation of a fatal ER stress response and suppressing subsequent apoptotic signaling, can contribute to acquired bortezomib resistance [314].

Polyubiquitinated proteins also accumulated more weakly, and returned to basal levels more rapidly, in bortezomib-resistant I-45 mesothelioma cells than in parental I-45 cells after treatment with 40 nM bortezomib—the final selection concentration used in developing the bortezomib-resistant cell line [287]. However, since the levels of the constitutive catalytic subunits were concluded to remain unaltered, the basal CT-L activity was found to be slightly decreased rather than increased and was not resistant to bortezomib-mediated inhibition, and no mutations were identified in the coding region of the *PSMB5* gene, the authors concluded that the resistance of this cell line to bortezomib was independent of the commonly-reported proteasome-dependent mechanisms [287]. Instead, it was proposed that the reduced growth rate of these cells in comparison with parental I-45 cells may have been accompanied by a reduced rate of protein synthesis, potentially contributing to the reduced polyubiquitinated protein levels observed [287]. Whatever the cause, bortezomib resistance in this cell line was attributed to reduced polyubiquitinated protein accumulation following bortezomib exposure, resulting in a failure to activate ER stress and the UPR and to stabilize the pro-apoptotic proteins Mcl-1S, NOXA, and p53 [287]. Similarly, the ability of 15 nM bortezomib to inhibit the CT-L activity and induce polyubiquitinated protein accumulation remained unimpaired in two mantle cell lymphoma cell lines (Jeko-1 and Z-138) selected for resistance to 30 nM bortezomib [339]. The bortezomib resistance phenotypes of these cells were attributed to the Hsp90-assisted accumulation of the prosurvival chaperone BiP upon bortezomib

treatment, resulting in activation of the prosurvival arm of the UPR; accordingly, treatment with an Hsp90 inhibitor resensitized the bortezomib-resistant cells to bortezomib [339].

CT-L activity was also inhibited to a similar extent in parental and bortezomib-adapted KMS-11 multiple myeloma cell lines following treatment with 32 nM bortezomib. It was therefore concluded that a mutation of the proteasome could not account for the resistance observed [340]. In bortezomib-adapted KMS-11 sublines, resistance to bortezomib was associated with low levels of XBP-1 mRNA, which may suggest a reduced dependence on the UPR and serve as a predictor of poor response to bortezomib in multiple myeloma cells [340]. Likewise, treatment with 10 nM bortezomib inhibited similar proportions of the CT-L, C-L, and T-L activities in parental and bortezomib-resistant U266 multiple myeloma cells, with the T-L activity being, as expected, relatively resistant to inhibition by bortezomib. Similar proportions of these activities were also inhibited by epoxomicin, MG132, or Tlck (an inhibitor of the T-L activity), respectively [290]. These results were again in agreement with the lack of substantial differences in β5, β1, and β2 expression levels or basal CT-L, C-L, and T-L activities between the parental and bortezomib-resistant cells, as well as the absence of mutations in the *PSMB5*, *PSMB6*, or *PSMB7* genes [290]. The authors concluded that neither differences in proteasome catalytic subunit levels or mutational status, nor in basal or residual proteasome activities, could account for the resistance phenotype of their model. Instead, bortezomib resistance was attributed to enhanced elimination of ubiquitin-containing protein aggregates via the autophagy pathway, assisted by overexpression of the small heat shock protein HSPB8 [290].

b. Epoxomicin and Carfilzomib Resistance

In contrast to the many reports describing proteasome catalytic subunit expression levels and activity patterns in cell line models of acquired bortezomib resistance, information on these properties in epoxomicin- or carfilzomib-resistant cell lines is currently limited to just a few reports. An early report showed increased proteasome subunit expression in epoxomicin-resistant variants of the A431 squamous cell carcinoma cell line relative to parental A431 cells, accompanied by an ~2.5-fold elevation of CT-L activity over parental levels. Accordingly, exposure to even 20 nM epoxomicin did not cause polyubiquitinated proteins to accumulate in these epoxomicin-resistant cells, in contrast to the obvious accumulation of these species that occurred in the parental A431 cells under these conditions [279]. In contrast to the epoxomicin-resistant KMS-11 cells

reported by Gutman et al. [278], the resistance phenotype of the epoxomicin-resistant A431 cell line was concluded to be P-glycoprotein independent [279]. Riz et al. found that the levels of the mRNAs encoding primary carfilzomib targets β5 and β5i were not substantially altered from parental levels in KMS-11 and KMS-34 multiple myeloma cell lines which had acquired resistance to 12 nM carfilzomib, indicating that the upregulation of these mRNAs is not necessary for acquisition of carfilzomib resistance. However, the protein levels of these subunits were not reported [306].

Compared with parental AMO-1 multiple myeloma cells, increased basal levels of active proteasome subunits, especially β2/β2i, were detected in carfilzomib-resistant AMO-1 cells, resulting in higher residual levels of these active subunits in the carfilzomib-resistant cells than in the parental cells following treatment with proteasome inhibitors [184]. However, the proportion of the basal levels of these active subunits inhibited by bortezomib or carfilzomib was similar in the parental and carfilzomib-resistant cell lines, indicating that the binding of these inhibitors to the proteasome's active sites was not impaired in the carfilzomib-resistant cells. Consistent with this conclusion, no active site mutations in the β5 subunit were detected in the carfilzomib-resistant cell line. These findings were similar to those obtained with bortezomib-resistant AMO-1 cells [184]. Interestingly, co-treatment of the bortezomib- or carfilzomib-resistant cells with bortezomib or carfilzomib and the β2/β2i-selective inhibitor LU-102 achieved greater inhibition of total proteasome activity than treatment with bortezomib or carfilzomib alone, consistent with the synergistic cytotoxic effects of these combinations observed in the inhibitor-resistant cell lines. Combining bortezomib or carfilzomib with LU-102 also had synergistic cytotoxic activity in primary malignant plasma cells that were resistant to bortezomib, at least two of which were also resistant to carfilzomib *in vitro* [184]. The mechanism by which combined treatment of bortezomib- or carfilzomib-resistant multiple myeloma cells with bortezomib or carfilzomib and LU-102 can overcome bortezomib or carfilzomib resistance was suggested to be a stronger and more prolonged inhibition of total proteasome activity, which causes greater accumulation of proteasome substrates and therefore a more robust activation of the UPR, leading to an increase in apoptosis [184]. This supports the notion that addition of a β2/β2i-selective inhibitor to bortezomib- or carfilzomib-containing therapeutic regimens may benefit patients resistant to these β5/β5i-selective inhibitors [184]. Although P-glycoprotein-mediated efflux has been found to contribute to carfilzomib resistance in other studies, its impact on carfilzomib resistance in the carfilzomib-resistant AMO-1 cell line was not assessed [184].

In conclusion, adjustments in overall proteasome levels, subunit composition, and catalytic activities were seen in most cell lines following the onset of acquired proteasome inhibitor resistance, highlighting the adaptability of the proteasome complex itself as an important contributor to this resistance. However, many permutations on this theme were observed. Although the disparate results reported could have, in some cases, resulted from differences in the experimental methodologies applied, they collectively indicate that this adaptation can be achieved via multiple routes, so long as the end result allows the cell to maintain sufficient proteasome activity to carry out essential tasks required for continued survival and proliferation during proteasome inhibitor exposure. As one would expect, proteasome adaptation does not appear to be the sole mediator of acquired proteasome inhibitor resistance, and the relative importance of this and other mechanisms may vary on a case-by-case basis. Nevertheless, the frequency with which alterations in the proteasome complex were observed suggests that proteasome-mediated resistance mechanisms may be of paramount importance.

1.8.5 Stability of Proteasome Inhibitor-Resistance Phenotypes

Different conclusions were reached regarding the stability of the resistance phenotypes described above. The bortezomib-resistance phenotype was maintained following a >2 month bortezomib withdrawal in the bortezomib-resistant Jurkat T lymphoblastic lymphoma/leukemia cells described by Lu et al., consistent with the finding that bortezomib-mediated inhibition of the proteasome's CT-L activity in these cells was still inferior to that achievable in parental Jurkat cells. However, the once increased *PSMB5* mRNA levels and CT-L activity of the bortezomib-resistant cells had normalized over this time period [286, 312]. These findings suggest that the *PSMB5* mutations identified in these cells are sufficient to maintain bortezomib resistance in the absence of sustained increases in β5 expression. Furthermore, after removing bortezomib-resistant THP-1 myelomonocytic leukemia cells from bortezomib-containing culture conditions, no major changes in β5 mRNA levels were observed, but β5 protein levels were gradually reduced over a 7 day period [246]. The increased proteasome gene expression detected in bortezomib-resistant THP-1 cells by microarray analysis had normalized during a 6 month withdrawal period, indicating the transient nature of these changes [246]. The decrease in β5 protein levels was even more pronounced following the 6 month bortezomib withdrawal, but β5 upregulation could be rapidly reinduced at the mRNA and protein levels when the bortezomib-resistant cells were reexposed to bortezomib,

consistent with the >35-fold resistance reportedly retained in these cells. Blocking bortezomib-induced β5 upregulation in the bortezomib-withdrawn cells via siRNA-mediated silencing led to a more robust inhibition of cell growth and induction of apoptosis, further implicating the rapid induction of this (mutant) subunit in the stability of bortezomib resistance in this cell line model [246].

Similarly, β5 and β5i levels were reduced, but remained higher than parental levels, in bortezomib-resistant HT-29 colorectal adenocarcinoma cells after a 40 day bortezomib withdrawal. β2 and β2i levels were also reduced to baseline levels, but the increased β1 levels that had been observed after only a 14 day withdrawal period were maintained after the 40 day withdrawal [298]. Interestingly, the degree of bortezomib resistance increased rather than decreased over this 40 day withdrawal period, leading the authors to conclude that elevated levels of proteasome subunits only partially account for bortezomib resistance [298]. However, consistent with the observations of Oerlemans et al. regarding the β5 subunit, reintroducing bortezomib-resistant HT-29 cells to bortezomib-containing culture conditions reportedly again led to an increase in catalytic proteasome subunit levels in the bortezomib-resistant cells [298]. De Wilt et al. also indicated that bortezomib resistance remained stable in their bortezomib-adapted NSCLC cell lines following a 2 month bortezomib withdrawal, consistent with *PSMB5* gene mutations contributing to the bortezomib resistance mechanisms of these cell lines [289].

In contrast to the results obtained with bortezomib-resistant Jurkat, THP-1, and HT-29 cells, it was concluded that the altered expression levels of proteasome subunits observed in bortezomib-resistant HL-60 myeloid leukemia, ARH-77 plasmacytoid lymphoma, and AMO-1 multiple myeloma cells were not directly influenced by whether or not the cells were incubated in bortezomib-containing medium or not, or by removing the cells from bortezomib-containing medium for up to 7 days, which the authors suggested reflected adaptive changes rather than reactive ones [209]. Additionally, the altered proteasome activity patterns in the bortezomib-resistant HL-60 cell line were stable for at least 7 days after removal from bortezomib-containing medium. Consistently, the authors indicated that resistance was stable in the bortezomib-resistant HL-60 cells after a 14 day bortezomib withdrawal [209]. As these cells were apparently devoid of *PSMB5* mutations [184, 209, 338], these results suggest that stable resistance is achievable in the absence of such mutations. In further support of this, the resistance phenotype was reportedly maintained in bortezomib-resistant I-45 mesothelioma cells—which lacked *PSMB5* mutations—following a 2 month bortezomib withdrawal period [287]. Additionally,

Stessman et al. reported that bortezomib resistance was stable for 1 year following bortezomib withdrawal in their mouse cell line model of acquired bortezomib resistance, which was also devoid of *PSMB5* mutations [333]. On the other hand, acquired bortezomib resistance in cell culture models derived from the JEKO and HBL2 mantle cell lymphoma cell lines was found to gradually decrease after bortezomib was withdrawn, which, together with the gradual acquisition of resistance and the lack of *PSMB5* gene mutations, was suggested to reflect a reversible adaptation to bortezomib-containing culture conditions [329].

These observations indicate that *PSMB5* mutations can mediate stable resistance to proteasome inhibitors, yet this can also be achieved without these mutations. Perhaps other stable changes in the proteasome complex can account for the stability of bortezomib resistance in some instances of the latter (e.g., in the bortezomib-resistant HL-60, ARH-77, and AMO-1 cells), or, perhaps other proteasome-independent mechanisms can be credited (e.g., in the bortezomib-resistant I-45 cells). Alternatively, in some cases (e.g., in the bortezomib-resistant JEKO and HBL2 cells), transient cellular changes can lead to reversible bortezomib resistance.

1.8.6 Cross-Resistance to Other Agents

Significant cross-resistance of bortezomib-resistant cell lines to non-proteasome-targeting chemotherapeutics was not observed in most cases in which it was reported [209, 246, 286, 287, 290, 314, 329, 330, 333]. No major change in sensitivity to daunorubicin was observed in bortezomib-resistant HL-60 myeloid leukemia or ARH-77 plasmacytoid lymphoma cells, but some cross-resistance to this agent was observed for bortezomib-resistant AMO-1 multiple myeloma cells. Despite the latter finding, the authors suggested these results to indicate that bortezomib resistance in these cell lines is likely not attributable to increased bortezomib efflux via multidrug resistance transporters [209]. Conversely, Fuchs et al. reported that their bortezomib-resistant Namalwa Burkitt lymphoma cell line was cross-resistant to the pro-apoptotic effects of γ-irradiation and staurosporine. This led the authors to suggest that, in the bortezomib-resistant cells, the upregulation of anti-apoptotic Hsp27 consequent to continuous bortezomib-mediated proteasome inhibition, as well as the reduced capacity to stabilize the pro-apoptotic protein p53 due to the elevated proteasome activities, conferred a general resistance to apoptosis [285].

In contrast to the predominant lack of cross-resistance of bortezomib-resistant cell lines to non-proteasome-targeting chemotherapeutic drugs, cross-resistance to other proteasome-targeting agents was commonly reported. Bortezomib-resistant cell lines were cross-resistant to several reversibly-binding proteasome inhibitors, including the peptide aldehydes ALLN [246] and MG-132 [246, 289, 290, 298, 313-315, 329], as well as the peptide boronate MG-262 [246]. While two bortezomib-resistant plasma cell lines derived by Stessman et al. from a mouse model of multiple myeloma were cross-resistant to the peptide boronate ixazomib, one of these cell lines was cross-resistant to MG-132 but the other was not [333]. Bortezomib-resistant HT-29 colorectal adenocarcinoma cells also lacked cross-resistance to the peptide boronate LLL-Bor [298]. The observed cross-resistance of bortezomib-resistant HL-60, ARH-77, and AMO-1 cell lines to reversibly-binding proteasome inhibitors led Rückrich et al. to conclude that treating bortezomib-resistant cancer cells with different proteasome inhibitors may be effective in cases where resistance is attributed to overexpression and/or active site mutations of β5, but, in those in which resistance is mediated by a general increase in proteasome components, this strategy may not be effective [209]. Bortezomib-resistant cell lines were also cross-resistant to a variety of irreversibly-binding proteasome inhibitors, such as the peptide vinyl sulfones ZL_3VS [209] and NLVS [209, 329], the β-lactones lactacystin [209, 285, 290] and marizomib [337], and the peptide epoxyketones epoxomicin [209, 290], carfilzomib [280, 313, 333, 338], ONX 0912 [280, 289, 313], ONX 0914 [280, 313, 315], and PR-924 [318].

Still, the levels of cross-resistance of bortezomib-resistant cell lines to alternative proteasome inhibitors were typically lower than the levels of resistance to bortezomib itself [246, 280, 285, 318, 329]. For example, bortezomib-resistant Namalwa cells were less resistant to the pro-apoptotic effects of lactacystin than to those of bortezomib [285]. This was consistent with the retained ability of lactacystin to inhibit the CT-L activity in the bortezomib-resistant cells, presumably due to its irreversible binding to the β5 subunit [285].

A similar conclusion was reached by Suzuki et al., whose bortezomib-resistant HT-29 cells remained relatively sensitive to carfilzomib, indicating that irreversible proteasome inhibitors can overcome bortezomib resistance. Additionally, the authors noted that the 3-4-fold decrease in carfilzomib sensitivity was in line with the 3-4-fold increase in proteasome catalytic activities observed in these cells [298]. Likewise, the 2-3-fold increase in the levels of constitutive catalytic subunits detected in bortezomib-resistant THP-1 myelomonocytic leukemia cells was suggested to contribute, together with amino

acid substitutions in the β5 active site, to the cross-resistance of these cells to other β5/β5i-targeting inhibitors. Cross-resistance to carfilzomib was observed in these cells, but to a lesser extent than that observed for the other inhibitors examined [280]. Also in accord with these findings, bortezomib-resistant JY B lymphoblast cells remained sensitive to carfilzomib and were only somewhat less sensitive to ONX 0914 and MG-132 [315]. Multiple bortezomib-resistant cell lines also retained full sensitivity to the α7 subunit-targeting proteasome inhibitor 5AHQ [289, 313], leading Franke et al. to recommend α7-targeting inhibitors for efforts to overcome cases of bortezomib resistance mediated by upregulation of proteasomes containing a mutant β5 subunit [313].

The reduced sensitivity of the bortezomib-resistant CCRF-CEM acute lymphoblastic leukemia, THP-1 myelomonocytic leukemia, and RPMI 8226 multiple myeloma cell lines to PR-924 appeared to be at least partially attributed to the weaker inhibition of the catalytic activities of β5i and β5, the latter of which was, in turn, at least partially attributed to β5 active site mutations [318]. That cell lines harboring mutant β5 subunits were less sensitive to both the β5-inhibitory and cytotoxic effects of PR-924 was in line with the finding that the cytotoxic effects of this β5i-selective inhibitor require co-inhibition of β5, consistent with results reported by Parlati et al. [186, 318]. However, if reduced efficacy of β5 inhibition by bortezomib was the predominant mechanism underlying bortezomib resistance in the bortezomib-resistant cell lines, the reduced efficacy of β5 inhibition by PR-924 observed in these cell lines would be expected to lead to a higher level of cross-resistance to PR-924. Instead, the levels of resistance to this inhibitor were much lower than those for bortezomib, which led the authors to suggest that much of the bortezomib-resistance phenotypes of these cell lines may be mediated by mechanisms independent of mutant β5 subunits [318]. Similarly, despite the reduced β5 inhibitory efficacy of marizomib in bortezomib-resistant CCRF-CEM cells, it was still more effective in inhibiting the CT-L and (especially) T-L activities in these cells than bortezomib, which may be reflected in the much lower level of resistance to marizomib than to bortezomib [337].

Not all bortezomib-resistant cell lines displayed greater resistance to bortezomib than to alternative proteasome inhibitors. While bortezomib-resistant KMS-11 multiple myeloma cells were less resistant to MG-132 than to bortezomib, a bortezomib-resistant variant of the multiple myeloma cell line OPM-2 displayed equivalent resistance to both inhibitors [314]. Additionally, bortezomib-resistant CCRF-CEM and RPMI 8226 cells were less resistant to most of the alternative proteasome inhibitors examined, including

MG-132, ONX 0912, and carfilzomib, than to bortezomib; however, although bortezomib-resistant CCRF-CEM cells were less resistant to ONX 0914 than to bortezomib, bortezomib-resistant RPMI 8226 cells were more resistant to the former inhibitor than to the latter [313]. The differences between the cross-resistance profiles of the bortezomib-resistant CCRF-CEM and RPMI 8226 cell lines were suggested to possibly reflect different β-subunit-mediated mechanisms of proteasome inhibitor resistance [313]. Similarly, bortezomib-resistant A549 NSCLC cells displayed equivalent resistance to carfilzomib and equivalent or greater resistance to ONX 0912, and SW1573 NSCLC cells resistant to 150 nM bortezomib were more resistance to ONX 0912 than to bortezomib [289]. Further differences in the cross-resistance profiles of the bortezomib-resistant NSCLC cell lines reported by de Wilt et al. were also observed. For example, while bortezomib-resistant H460 cells were not cross-resistant to ONX 0914, SW1573 cells resistant to 150 nM bortezomib and bortezomib-resistant A549 cells were. In addition, bortezomib-resistant H460 cells were not cross-resistant to carfilzomib, while A549 and SW1573 cells were. Finally, A549 cells resistant to 100 nM bortezomib and SW1573 cells resistant to 150 nM bortezomib were highly cross-resistant to ONX 0912 (to an even greater extent than to carfilzomib), while bortezomib-resistant H460 cells were cross-resistant to ONX 0912 to a much lesser extent [289].

Cell line models of resistance to second-generation proteasome inhibitors were also cross-resistant to other general and subunit-selective proteasome inhibitors. Cal33 and UMSCC-1 head and neck squamous cell carcinoma cell lines that had acquired resistance to 1 μM carfilzomib were highly cross-resistant to oprozomib [283]. They were also highly cross-resistant to paclitaxel—as were the carfilzomib-resistant NSCLC and colon adenocarcinoma cell lines previously developed in our laboratory [281]—but were only slightly cross-resistant to cisplatin [283]. Conversely, just as carfilzomib and oprozomib were found to retain considerable activity against cancer cells which have acquired bortezomib resistance [262, 266, 267, 274], the cell line models of acquired carfilzomib/oprozomib resistance employed in this study displayed only relatively low levels of cross-resistance to bortezomib, suggesting that bortezomib may retain clinical efficacy against cancers that have acquired resistance to carfilzomib and/or oprozomib [283].

Collectively, these results suggest that carfilzomib-resistant cancer cells are more likely to be resistant to chemotherapeutic agents that do not target the proteasome than are those resistant to bortezomib due to the greater probability of P-glycoprotein

overexpression contributing to carfilzomib resistance. Importantly, they also indicate that proteasome inhibitor-resistant cell lines differ in their cross-resistance profiles to alternative proteasome inhibitors, which may be mediated by differences in proteasome-dependent mechanisms of resistance. This is further supported by clinical observations demonstrating that second-generation proteasome inhibitors can be effective in treating bortezomib-resistant cancers and suggests that, as more proteasome inhibitors are developed for clinical use and our understanding of the resistance mechanisms to each inhibitor increases, identifying patients that will best respond to a given inhibitor may improve clinical outcomes.

1.9 Summary and Study Rationale

Much has been learned about the functions of the proteasome since the discovery of the UPP decades ago, in large part due to the development and discovery of both broad-spectrum and subunit-selective proteasome inhibitors. Furthermore, proteasomes were validated as anticancer targets when the first-in-class proteasome inhibitor bortezomib was approved by the FDA for use as an anticancer agent almost fifteen years ago. However, dose-limiting toxicities and intrinsic and acquired resistance have emerged as major clinical challenges associated with bortezomib treatment. It is believed that bortezomib's toxicity profile may result from off-target inhibition of nonproteasomal proteases and/or from inhibition of constitutive proteasomes in healthy cells. On the other hand, largely based on findings obtained from cell line models of acquired bortezomib resistance, a number of proteasome-mediated and non-proteasome-mediated resistance mechanisms have been proposed. Second-generation proteasome inhibitors such as carfilzomib and ixazomib were subsequently developed to overcome these limitations and have recently received the FDA's approval. Although they are generally more active than bortezomib against bortezomib-resistant cancer cells in both the laboratory and clinic, these inhibitors were designed to target the same active sites as bortezomib; this may limit their efficacy and may not prevent side effects that result from targeting proteasomes in healthy cells.

The discovery of the immunoproteasome as a second proteasome subtype and findings implicating this subtype in the pathogenesis of autoimmune diseases and cancers inspired researchers to develop inhibitors that selectively target the immunoproteasome over its constitutive counterpart. It was proposed that such inhibitors would target proteasomes present in diseased cells while sparing those in most healthy cells, thereby

creating a greater therapeutic window than that associated with inhibitors targeting both subtypes. Selective inhibitors of immunosubunits β1i and β5i have been successfully developed and have been shown to be effective in laboratory models of autoimmune diseases and cancers.

It is now understood that, in addition to constitutive proteasomes and immunoproteasomes, at least two additional proteasome subtypes comprising mixtures of constitutive subunits and immunosubunits are present in varying proportions across diverse tissues. It also appears that the distinct catalytic subunit combinations of each subtype imparts its unique activity profile, which may be optimized for specialized cellular functions. Furthermore, evidence demonstrating that proteasome inhibitors vary inhibitor-dependently in their inhibitory efficacies against the different proteasome subtypes of murine tissues has been reported. Together, these findings suggest that each subtype of proteasome carries out some discrete cellular functions and may be more effectively targeted by one inhibitor over another. Importantly, the proteasome's catalytic subunit expression levels and activities are frequently altered when cancer cell lines acquire bortezomib resistance; this is consistent with a shift in the ratios of discrete proteasome subtypes upon establishment of bortezomib resistance. We hypothesized that such a shift plays a causative role in acquired resistance to proteasome inhibitors, and that the subtypes involved in conferring resistance vary inhibitor-dependently. Evaluating which subtypes of proteasomes are present in diseased cells displaying resistance to a given proteasome inhibitor and identifying or developing inhibitor(s) that more effectively target those subtypes may provide necessary insight to ultimately improve the therapeutic efficacy of proteasome inhibitors.

2 HYPOTHESIS AND SPECIFIC AIMS

The overall goal of this project is to elucidate the functions and adaptive responses of distinct proteasome subtypes in cancer cells. It has become increasingly clear that mammalian cells contain at least four distinct proteasome subtypes in various proportions [186, 224-229, 233]. These subtypes are defined by their unique combinations of catalytic subunits and therefore differ in their activity profiles and effects on the MHC class I-mediated presentation of certain antigenic peptides, including clinically relevant tumor epitopes [224-226, 229, 232, 236, 238]. However, aside from antigen presentation, much regarding the unique functions of each subtype, or their roles as drug targets, remains poorly understood. This is in large part due to difficulties in differentiating between individual subtypes in complex biological samples, which frequently contain more than one subtype [224].

Changes in the levels of expression or activity of catalytic proteasome subunits are typically observed when cells acquire proteasome inhibitor resistance [184, 204, 209, 246, 280, 285, 288, 289, 298, 313, 315, 329, 330, 332, 333] and are often associated with the incomplete suppression of proteasome activities by the inhibitor to which resistance was acquired [184, 204, 209, 246, 285, 289, 313, 337]. It has frequently been concluded that the reduced sensitivities of the proteasome complexes within these cells to inactivation results from overexpression of specific subunits or of proteasome complexes as a whole [209, 246, 285, 289, 313]. Considering the findings of these studies, together with the observed differences in proteasome inhibitor sensitivity between distinct proteasome subtypes isolated from murine tissues [231, 232], the changes in the expression levels and activity patterns of catalytic proteasome subunits detected upon acquisition of proteasome inhibitor resistance may reflect a relative increase in proteasome subtypes that are more resistant to inhibition by the inhibitor applied, and a relative decrease in those that are more sensitive. We therefore hypothesized that changes in the relative abundances of individual proteasome subtypes serve as a mechanism of acquired proteasome inhibitor resistance. Our study had the following aims:

Aim 1. Develop a set of bifunctional activity-based probes for use in identifying distinct proteasome subtypes. A lack of practical, straightforward techniques for identifying distinct proteasome subtypes has been an important factor limiting studies of their biological functions. We therefore set out to develop new chemical probes for use in determining which proteasome subtypes are present within cell or tissue samples.

Building on earlier work by Moroder and colleagues [197] and Vidal, Reboud-Ravaux, and colleagues [198, 199], and utilizing several subunit-selective proteasome inhibitors, we developed a set of bifunctional activity-based probes capable of crosslinking specific pairs of catalytic proteasome subunits when they coexist within individual proteasome complexes and compatible with an immunoblotting-based readout of the crosslinked subunit pairs. We hypothesized that the information gained from experiments conducted with these probes would allow us to deduce the identity of proteasome subtypes present in a given sample.

Aim 2. Assess whether changes in the relative abundances of specific proteasome subtypes are associated with acquired resistance of cancer cells to bortezomib and carfilzomib. We established non-small cell lung cancer cell line models of acquired bortezomib and carfilzomib resistance. Proteasome activity assays and immunoblotting analyses were used to detect changes in proteasome complexes that had occurred upon acquisition of resistance to each inhibitor. These assays also allowed us to assess whether, and to what extent, the individual catalytic activities of proteasomes were suppressed under bortezomib or carfilzomib exposure in the inhibitor-resistant cells and in the parental cell line from which they were generated. We also conducted experiments with the bifunctional probes described in Aim 1 to determine whether changes in the relative abundances of particular proteasome subtypes had occurred during the development of bortezomib and carfilzomib resistance.

3 METHODS

Some of the methods described in this chapter were previously reported [239].

3.1 Synthesis of Bifunctional Proteasome Probes

Bifunctional proteasome probes were synthesized as reported [239, 341].

3.2 Proteasome Inhibitors

Epoxomicin [169], YU-102 [177], Ac-nLPnLD-CHO, Ac-PAL-ek [239], NC-012 [180], and PR-924 (IPSI) [186] were synthesized by following previously-reported procedures. Bortezomib was purchased from LC Laboratories (Woburn, MA), and carfilzomib was synthesized by previously reported methods [174] or purchased from ChemieTek (Indianapolis, IN).

3.3 Cell Culture and Whole Cell Lysis

The U266 human multiple myeloma and H23 non-small cell lung cancer (NSCLC) cell lines were purchased from the American Type Culture Collection and cultured as recommended in RPMI-1640 medium (Invitrogen) supplemented with 10% fetal bovine serum (Atlanta Biologicals) and 1 mM sodium pyruvate (Sigma-Aldrich) at 37°C and 5% CO_2. The cells were collected by centrifugation and lysed in Passive Lysis Buffer (Promega) following the manufacturer's protocol. Protein concentrations of the resulting lysates were determined using the Bio-Rad Protein Assay.

3.4 Treatment of Cell Lysates or Purified Proteasomes with Bifunctional Proteasome Probes

Cell lysates were diluted in Passive Lysis Buffer (Promega) to a final concentration of 1 μg/μL, or purified human 20S constitutive proteasome or immunoproteasome preparations (Boston Biochem) were diluted in 20S proteasome assay buffer to a final concentration of 5-15 ng/μL. The resulting samples were incubated with DMSO, 5 μM epoxomicin (a broadly-acting proteasome inhibitor used as a positive control for covalent modification of all catalytic proteasome subunits except for β1), 10 μM YU-102 (a β1/β1i-selective inhibitor [177, 178] used as a positive control for covalent modification of β1), or 1-10 μM of the indicated bifunctional probe for 4 h at room temperature. Where indicated, the samples were pretreated with DMSO, 3 μM Ac-nLPnLD-CHO (β1-selective) [239],

3 μM NC-012 (β2/β2i-selective) [180], 0.02 μM carfilzomib (β5/β5i-selective) [262], 1 μM Ac-PAL-ek (β1i-selective) [239], or 0.1 μM IPSI (PR-924; β5i-selective) [186] for 1 h at room temperature before adding the bifunctional probes.

3.5 Generating Cell Line Models of Acquired Bortezomib and Carfilzomib Resistance

Proteasome inhibitor-naïve parental H23 cells were cultured in the presence of increasing concentrations of bortezomib (3.2-150 nM) over a period of ~15 mo, or increasing concentrations of carfilzomib (8.7-1,000 nM) over a period of ~6-8 mo. Replicate cell lines resistant to each inhibitor were generated to assess the consistency of experimental results. Cells growing in the presence of 150 nM bortezomib (2 replicate cell lines) or 1 μM carfilzomib (3 replicate cell lines) were collected by centrifugation. In addition, cells growing at these concentrations of bortezomib or carfilzomib were similarly collected following inhibitor removal and further culture in inhibitor-free medium for 7 d. Cell pellets were stored at -80°C until required for use, at which point the cells were lysed and their protein concentrations determined as described above.

3.6 Treatment of Parental H23 Cells with Bortezomib or Carfilzomib

Parental H23 cells were plated on 3 100-mm culture dishes and incubated at 37°C until they became ~80% confluent. Separate dishes were then treated with DMSO, 150 nM bortezomib, or 1 μM carfilzomib for 4 h. Following the 4 h treatment, the cells were collected by centrifugation, and cell pellets were stored at -80°C until required for further use, at which point the cells were lysed and their protein concentrations determined as described above.

3.7 Proteasome Activity Assays

Purified human 20S constitutive proteasome or immunoproteasome (Boston Biochem) (50 ng/well) or cell lysates (5 μg of protein/well) were incubated in 96 well plates with DMSO, 20 μM epoxomicin, 10 μM YU-102, or increasing concentrations of each bifunctional proteasome probe in 20S proteasome assay buffer (20 mM Tris-HCl, pH 8.0, 0.5 mM EDTA, 0.035% SDS) in a total volume per well of 90 μL for 1 h at room temperature. SDS was omitted from the 20S proteasome assay buffer in assays in which the β2/β2i-selective substrate was used. Each substrate was diluted in 20S assay buffer, and 10 μL of the resulting solutions were added to the appropriate wells to give a final volume per

well of 100 µL. Substrates Ac-nLPnLD-AMC (β1-selective), Boc-LRR-AMC (β2/β2i-selective), Suc-LLVY-AMC (β5/β5i-selective) [181], Ac-PAL-AMC (β1i-selective), and Ac-ANW-AMC (β5i-selective) [76] were used at a final concentration of 100 µM, while Ac-RLR-AMC (β2/β2i-selective) [181] and Ac-WLA-AMC (β5-selective) [76] were employed at a final concentration of 20 µM. Fluorescence produced by AMC release was measured once per minute over a 1 h period with a SpectraMax M5 microplate reader (Molecular Devices) using excitation and emission wavelengths of 360 nm and 460 nm, respectively. Residual hydrolysis of each substrate measured in lysates treated with 20 µM epoxomicin (for all substrates except Ac-nLPnLD-AMC) or 10 µM YU-102 (for Ac-nLPnLD-AMC) was regarded as nonproteasomal and subtracted from each experimental measurement of proteasome activity. Hydrolysis rates were determined by linear regression in GraphPad Prism, and those of the DMSO-treated controls were designated as 100%. For the Ac-RLR-AMC substrate, only data points collected within the first 20 min following substrate addition were analyzed for the H23 parental and bortezomib-resistant cell lines due to the early plateau of the reaction progress curves obtained for the bortezomib-resistant cell lines. IC_{50} values of the bifunctional proteasome probes were determined by nonlinear regression in GraphPad Prism and represent the averages of three replicates.

3.8 Immunoblotting

Each sample was mixed with Laemmli Sample Buffer (2X; Sigma-Aldrich), and proteins were subsequently denatured at 100°C for 10 min. Equivalent protein amounts of each sample were resolved by 14% SDS-PAGE (for experiments with bifunctional proteasome probes) or 12% SDS-PAGE (for evaluating expression levels of catalytic proteasome subunits), and proteins were subsequently transferred from the gels onto PVDF membranes (Bio-Rad). Membranes were blocked in 5% non-fat dry milk (Bio-Rad) in Tris-buffered saline with 0.05% Tween-20 (TBST) for 1 h at room temperature. Primary antibodies against β1 (Enzo Life Sciences; PW8140), β2 (Enzo Life Sciences; PW8145), β5 (Thermo Scientific; PA1-977), β1i (Abcam; ab3328), β5i (Abcam; ab3329), and β-actin (Novus Biologicals, NB600-501) were diluted 3% BSA in TBST. The primary antibody against β2i (Santa Cruz, sc-133236) was diluted in 3% milk in TBST. Membranes were incubated in the appropriate primary antibody solutions overnight at 4°C. Anti-rabbit or anti-mouse horseradish peroxidase-conjugated secondary antibodies (GE Healthcare) were diluted in 3% milk in TBST, and membranes were incubated in the appropriate secondary antibody solutions for 1 h at room temperature. Protein visualization was

facilitated by SuperSignal West Femto Chemiluminescent Substrate (Thermo Scientific) and X-ray film (Thermo Scientific or GeneMate).

4 DEVELOPMENT OF BIFUNCTIONAL ACTIVITY-BASED PROBES FOR DETECTING DISTINCT PROTEASOME SUBTYPES

Some of the contents of this chapter were previously published [239].

4.1 Introduction

Due to technical difficulties in evaluating the catalytic subunit compositions of individual proteasome complexes, much about the cellular functions of each subtype, or their importance to the cellular response to proteasome inhibitors, remains to be determined. So far, most researchers have evaluated the relative abundances of individual catalytic proteasome subunits via immunoblotting, 2D PAGE [191, 223, 227, 231, 234, 342], or label-free LC-MS- or ELISA-based quantification [226, 228, 231, 233], and used the information obtained to draw conclusions regarding which subtypes may be present in a given cell or tissue sample. However, drawing conclusions based solely on these types of studies is complicated by the typical coexistence of multiple distinct subtypes [224]. Characterizing individual proteasome subtypes in greater detail has typically involved separating purified 20S proteasome complexes by anion-exchange or hydrophobic interaction chromatographic procedures [224, 225, 229, 232, 235], free-flow isoelectric focusing electrophoresis [230], or immunoprecipitation of tagged forms of catalytic β-subunits that were exogenously expressed [223, 342], coupled with immunoblotting- [223, 224, 229, 230, 342] or 2D PAGE-based [225, 232, 235] readouts of catalytic subunit composition. Additionally, Guillaume et al. developed antibodies that bind the native states of certain catalytic proteasome subunits, enabling proteasome subtypes to be separated via sequential immunoprecipitation steps for subsequent immunoblotting analysis of their catalytic subunit compositions [226]. They thereby confirmed the existence of two intermediate proteasome subtypes that had been previously identified in transfected cell lines and in cells derived from immunosubunit-deficient mice [220-223]: one containing immunosubunit β5i together with constitutive subunits β1 and β2, and another containing immunosubunits β1i and β5i together with constitutive subunit β2 [226].

Investigations using all of these techniques have yielded valuable information that has greatly enhanced our understanding of 20S proteasome diversity. We now know that there are at least four distinct 20S proteasome subtypes that differ in their catalytic activity profiles and contributions to producing a given antigenic epitope [224-226, 229, 230, 232, 235, 236, 238]. The abundance of each subtype appears to be cell type- or tissue-specific,

with intermediate proteasome subtypes comprising a greater proportion of the proteasome population in many cell and tissue types than was previously appreciated [224, 226, 228, 229, 233]. Specific subtypes of proteasomes may be associated with pathological processes and have been suggested to be of potential utility as disease biomarkers [190]. They may also play a role in defining the cellular repercussions of treatment with a given proteasome inhibitor [231, 232]. However, while only the more detailed examinations can truly provide information regarding the identity of specific proteasome subtypes, the techniques used so far require multiple technically challenging steps, and the approach described by Guillaume et al. depends on the availability and affinity of antibodies that recognize the proteasome's catalytic subunits in their native states.

Our laboratory thus set out to develop more practical methods to examine the catalytic subunit compositions of individual proteasome subtypes contained within cell or tissue samples. The first of these to be reported was a fluorescence resonance energy transfer (FRET)-based approach, which involves using pairs of fluorescently-labeled inhibitors that selectively bind to specific catalytic proteasome subunits to detect instances of catalytic subunit colocalization via a fluorescence readout [343]. Our second approach to be reported [239] will be the focus of this chapter.

As described in Chapter 1.4.8, Moroder and colleagues [197] and Vidal, Reboud-Ravaux, and colleagues [198, 199] developed several reversibly-binding bifunctional proteasome inhibitors with the goal of optimizing inhibitory potency. Their work, combined with our ongoing interest in developing proteasome-targeting activity-based probes, sparked the idea of coupling pairs of irreversibly-binding, subunit-selective proteasome inhibitors to generate a series of bifunctional proteasome inhibitors with utility as activity-based probes. Therefore, building upon the designs of the bifunctional proteasome inhibitors previously described [197-199], we designed, synthesized, and characterized a set of bifunctional, activity-based proteasome probes that can be used to crosslink different pairs of catalytic subunits that coexist within discrete proteasome complexes. We envisioned that treating cells or cell lysates with these bifunctional probes and the resulting catalytic subunit crosslinking would allow us to visualize the crosslinked subunit pairs via immunoblotting analyses, providing us with the direct information required to deduce which proteasome subtypes were present in the cell population under study (Figure 4.1).

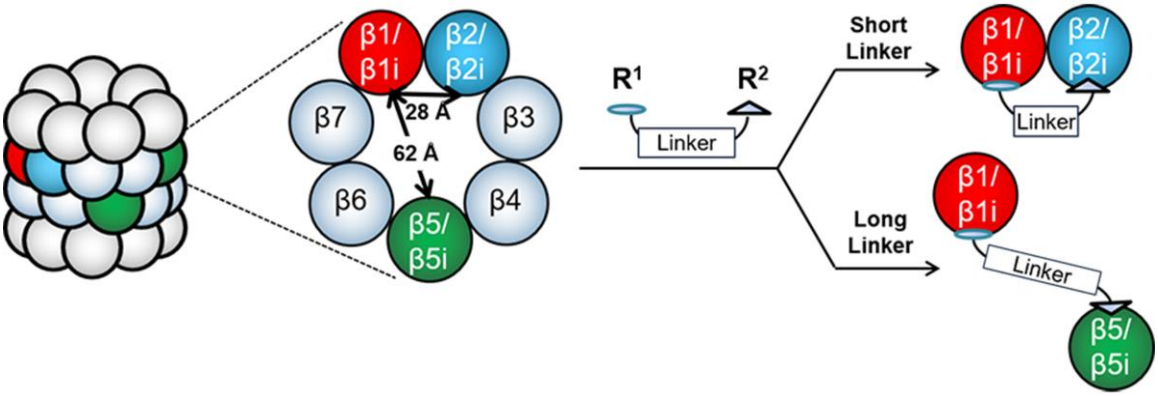

Figure 4.1 Crosslinking strategy for proteasome subtype identification
Bifunctional proteasome probes, composed of two peptide epoxyketone proteasome inhibitors coupled by a linker, crosslink different pairs of catalytic proteasome subunits when they are present within the same 20S core complex. Crosslinking efficiency of a particular subunit pair is determined by the subunit selectivity of the two inhibitors, as well as the length of the linker by which they are coupled. Following treatment of cell lysates or purified 20S proteasomes with a bifunctional proteasome probe, the crosslinked subunit pairs can be identified by immunoblotting analysis. *This figure was published in our previous report [239].*

4.2 Results

4.2.1 Design of Bifunctional Proteasome Probes

The most definitive evidence has been provided for the existence of four distinct proteasome subtypes: pure constitutive proteasomes of catalytic subunit composition β1-β2-β5, two intermediate proteasome subtypes of compositions β1-β2-β5i and β1i-β2-β5i, and pure immunoproteasomes of composition β1i-β2i-β5i [220-224, 226]. Consistent with this, it has been shown that the formation of proteasome subtypes containing β5 with immunosubunits or β2i with constitutive subunits is prohibited during the proteasome assembly process [221-223]. Therefore, we set out to develop bifunctional proteasome probes that can be used to discriminate between these four subtypes. The two β1-containing proteasome subtypes are distinguishable by whether they also contain β5 or β5i, while the two β1i-containing proteasome subtypes are distinguishable by whether they also contain β2 or β2i. It thus follows that probes capable of crosslinking the β1-type (β1 and β1i) subunits with the β5-type (β5 and β5i) subunits, and those capable of crosslinking the β1-type subunits with the β2-type (β2 and β2i) subunits, should be sufficient to allow the detection of each individual subtype. To generate such probes, we utilized several subunit-selective peptide epoxyketone proteasome inhibitors that had previously been developed in our laboratory and in others [101, 177, 180, 185, 186, 214, 343] (Figure 4.2).

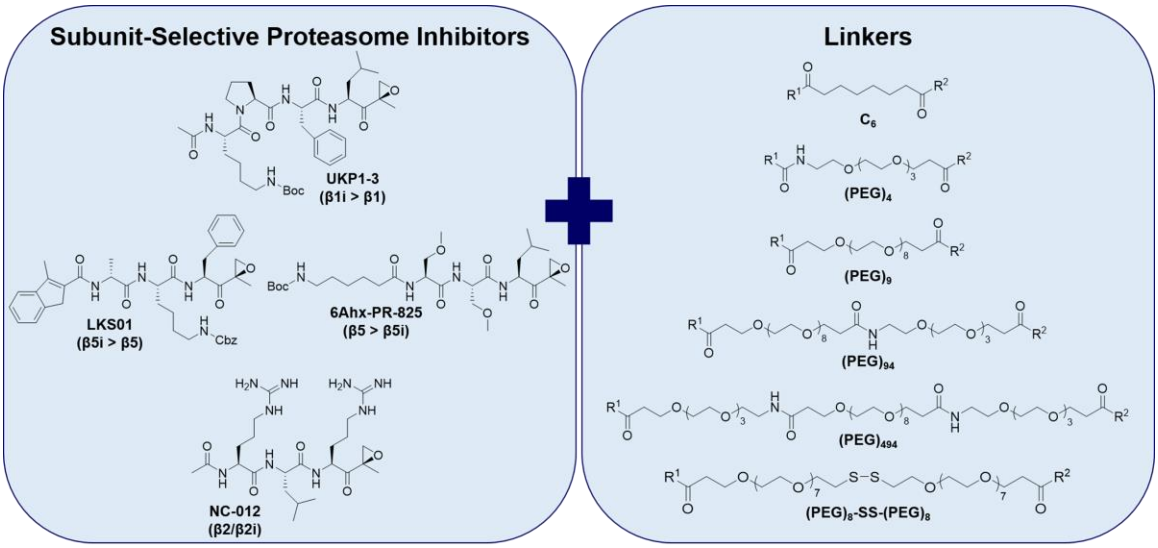

Figure 4.2 Design of bifunctional proteasome probes
Two of the depicted four subunit-selective proteasome inhibitors *(left panel*) were combined in various iterations via linkers of varying lengths and chemical compositions *(right panel*) to generate a series of bifunctional activity-based probes that target the proteasome's catalytic subunits.

UKP1-3 [343] was derived from the β1/β1i-selective inhibitor YU-102 [177, 178], and LKS01 [214] from the β5/β5i-selective inhibitor PR-924 (referred to in this chapter as IPSI) [186], by replacing their P4 glycine or P2 tryptophan side chains, respectively, with that of lysine to enable their coupling to a second inhibitor via amine-reactive linkers. We also synthesized a derivative of the β5-selective inhibitor PR-825 [101, 185] (6Ahx-PR825) in which PR-825's N-cap was replaced with a 6-aminohexanoyl group to allow linker attachment through its N-terminal amine. Finally, we derivatized the β2/β2i-selective inhibitor NC-012 [180] to facilitate linker attachment at its N-terminus. Different combinations of these inhibitors were coupled via linkers of varying lengths and chemical compositions to generate a set of 13 bifunctional probes (Table 4.1). We used the distances between the catalytic threonine O^{γ} atoms of each targeted catalytic subunit pair, which were previously derived from X-ray structure data for mammalian 20S proteasome complexes [75, 344], to assist us in selecting linkers of the appropriate lengths to facilitate crosslinking of these subunits (Figure 4.1). We chose peptide epoxyketone inhibitors because they form irreversible covalent bonds with the proteasome's catalytic threonine residues [170], which would thereby allow us to detect instances of crosslinking between catalytic proteasome subunits via immunoblotting analyses.

Table 4.1 List of the 13 bifunctional proteasome probes generated in this study

Probe	R^1	R^2	Linker
1	UKP1-3	LKS01	C_6
2			$(PEG)_9$
3			$(PEG)_{494}$
4			$(PEG)_8$-SS-$(PEG)_8$
5	UKP1-3	6Ahx-PR-825	$(PEG)_{494}$
6	UKP1-3	NC-012	$(PEG)_4$
7	LKS01	NC-012	$(PEG)_{94}$
8			$(PEG)_{494}$
9	UKP1-3	UKP1-3	$(PEG)_9$
10			$(PEG)_8$-SS-$(PEG)_8$
11	LKS01	LKS01	$(PEG)_9$
12			$(PEG)_{494}$
13	NC-012	NC-012	$(PEG)_{494}$

The two inhibitors comprising R^1 and R^2 and the linker of each bifunctional probe (see Figures 4.1 and 4.2) are listed. *These probes were synthesized by Dr. Lalit Kumar Sharma and Do-Min Lee, with assistance from Dr. Ying Wu and Ji Eun Park. Probes 1, 4, 5, and 6 were previously reported [239].*

4.2.2 Probes for β1/β1i-β2/β2i Crosslinking

a. Probe 1

Design

We began by making use of two inhibitors—the β1/β1i-selective inhibitor UKP1-3 and the β5/β5i-selective inhibitor LKS01—that were readily available in our laboratory at the time in order to test the feasibility of our crosslinking approach to identifying proteasome subtypes. UKP1-3 and LKS01 were coupled via a short hydrocarbon linker (C_6, with an estimated length of ~11.4 Å) to yield the bifunctional probe UKP13-C_6-LKS01 (probe **1**) (Figures 4.1 and 4.2, Table 4.1).

Subunit Binding Preferences

Prior to evaluating its crosslinking capabilities via immunoblotting analyses, we first wanted to confirm that probe **1** exhibited the proteasome inhibitory profile expected based on the known preferences of its parent compounds. Activity assays with a series of subunit-selective fluorogenic peptide substrates [76, 181] were conducted in purified human 20S proteasomes and in lysates of U266 multiple myeloma cells, which abundantly

express all three constitutive catalytic subunits as well as all three immunosubunits [345]. The results revealed that probe **1** does, in fact, preferentially inhibit the β1i and β5i subunits when incubated with the purified immunoproteasome, and the β1 and β5 subunits when incubated with the purified constitutive proteasome. Conversely, inhibiting 50% of β2 or β2i activity required concentrations of 10 μM or higher (Table 4.2). Probe **1** also selectively inhibits β1/β1i and β5/β5i activity in U266 cell lysates, with nearly complete inhibition being achieved at a concentration of 1 μM, while inhibiting β2/β2i activity by ~50% required a concentration of 10 μM (Table 4.3).

Crosslinking Capabilities

With probe **1** established as an active proteasome inhibitor displaying the expected inhibitory preferences, we conducted immunoblotting experiments with antibodies against individual catalytic proteasome subunits to examine whether this probe can crosslink one or more pairs of catalytic subunits. All of the proteasome's catalytic subunits fall within the molecular weight range of 20-30 kDa; therefore, covalent modification of a given subunit can be detected as an upward shift of an immunoreactive band within this molecular weight range. On the other hand, we expected to visualize crosslinking in the form of immunoreactive bands with molecular weights between 40-60 kDa, representing the combined molecular weights of two catalytic proteasome subunits. After treating the purified immunoproteasome with probe **1**, a single immunoreactive band at ~45 kDa was detected upon immunoblotting with an antibody against immunosubunit β1i, suggesting that β1i had been crosslinked with another catalytic proteasome subunit (Figure 4.3 A). When we treated U266 lysates with probe **1** to confirm the consistency of these results within a more complex system, we detected two anti-β1i-immunoreactive bands at ~45-50 kDa (Figure 4.3 B). This latter result suggested that probe **1** had crosslinked β1i with two different catalytic subunits within the U266 lysate. Despite the observed preference of this probe for inhibiting β5 and β5i over β2 and β2i (Tables 4.2 and 4.3), the apparent molecular weights of the crosslinked subunit pairs and the known molecular weights of each individual catalytic subunit led us to suspect that the two subunits crosslinked with β1i were actually β2 and β2i instead of β5 and β5i. This was further supported by our failure to detect crosslinking of β5 or β5i in probe **1**-treated U266 lysates (data not shown). These findings were not surprising, given that the linker used to couple the two inhibitors in probe **1** was likely too short to allow the probe to span the distance required for

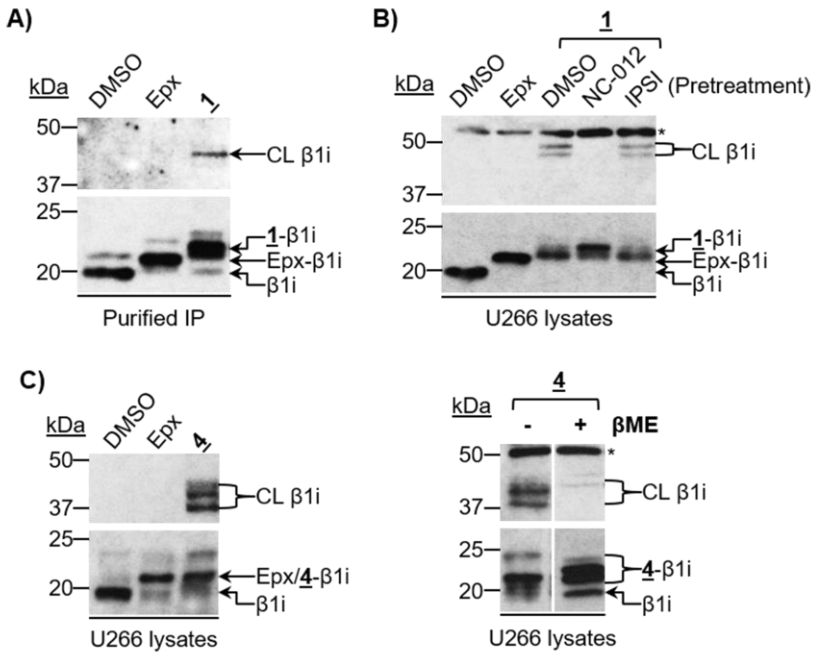

Figure 4.3 Probe 1 crosslinks β1i with β2/β2i
A) The purified 20S immunoproteasome (IP) was treated with DMSO, the broadly-acting proteasome inhibitor epoxomicin (Epx), or probe **1** prior to immunoblotting for β1i. **B)** U266 cell lysates were treated with DMSO or epoxomicin, or were pretreated with DMSO or the indicated subunit-selective inhibitor prior to treatment with probe **1**, as indicated. β1i was detected by immunoblotting. **C)** High-molecular-weight immunoblot signals detected following treatment with bifunctional proteasome probes result from crosslinking of catalytic proteasome subunits. *Left panel.* U266 cell lysates were treated with DMSO, epoxomicin, or probe **4** prior to immunoblotting for β1i. *Right panel.* U266 cell lysates were treated with probe **4**, and proteins were subsequently denatured in sample buffer with or without β-mercaptoethanol (βME), which cleaved the internal disulfide bond of the linker. β1i was detected by immunoblotting. Irrelevant lanes were removed from the blot shown in the right panel of **C**. CL = crosslinked β-subunit, * = nonspecific band. *Portions of this figure were published in our previous report [239].*

crosslinking β1-type subunits with β5-type subunits. We tested whether or not this was the case by pretreating U266 lysates with the proteasome inhibitor NC-012, which binds selectively to the β2 and β2i subunits, or with the β5i-selective proteasome inhibitor IPSI, before treating with probe **1**. Pretreating with NC-012 completely blocked probe **1**-mediated β1i crosslinking, as seen by the complete abolishment of the two ~45-50 kDa bands on the β1i immunoblot, whereas pretreating with IPSI did not (Figure 4.3 B). These results confirmed our suspicion that probe **1** crosslinks β1i with both β2 and β2i, which, despite the finding that the β2 and β2i subunits are not the preferred targets of this probe, likely results from the C_6 hydrocarbon linker restricting crosslinking to adjacent subunits within the 20S proteasome complex. Importantly, our findings indicate the presence of

intermediate proteasome subtypes harboring immunosubunit β1i together with constitutive subunit β2 in U266 myeloma cells, substantiating previous results demonstrating that intermediate proteasomes are formed even under situations in which all of the proteasome's catalytic subunits are simultaneously expressed [223].

b. Probe 4

To provide additional assurance that the anti-β1i-immunoreactive bands that appeared between ~45-50 kDa for probe **1**-treated U266 lysates actually represent crosslinked β1i, a second bifunctional proteasome probe, UKP13-SS-LKS01 (probe **4**), was synthesized in which we replaced the C_6 linker of probe **1** with a poly(ethylene glycol) (PEG) linker containing a scissile disulfide bond (Figure 4.2, Table 4.1). We anticipated that a reducing agent such as β-mercaptoethanol, when added to cell lysates following treatment with probe **4**, would break the intersubunit crosslinks that the probe had formed, and that this could be visualized by the depletion of the higher-molecular-weight bands detected for probe **4**-treated samples to which the reducing agent had not been added. A proteasome activity assay demonstrated that, as observed for probe **1**, probe **4** selectively binds β5i and β1i within the context of the purified immunoproteasome, and β1 and β5 within that of the purified constitutive proteasome. Substantially higher concentrations of this probe were required for inhibiting 50% of β2 or β2i activity (Table 4.2). Additionally, we detected anti-β1i immunoreactive bands with molecular weights between 37-50 kDa upon immunoblotting analysis of probe **4**-treated U266 lysates, indicating that, as observed with probe **1**, probe **4** mediates β1i crosslinking (Figure 4.3 C, *left panel*). We next incubated U266 lysates with probe **4** and denatured their proteins with or without β-mercaptoethanol. The two major anti-β1i-immunoreactive bands between 37-50 kDa that were detected for the probe **4**-treated sample denatured without added β-mercaptoethanol could not be detected in the probe **4**-treated sample denatured in the presence of β-mercaptoethanol, providing further evidence supporting the conclusion that the higher-molecular-weight bands observed represent crosslinked β1i (Figure 4.3 C, *right panel*).

c. Probe 6

Design and Subunit Binding Preferences

Now that we had confirmed that our compounds were, in fact, capable of crosslinking pairs of catalytic proteasome subunits, we decided to synthesize a third bifunctional probe in attempt to improve upon the β1/β1i-β2/β2i crosslinking efficiency of

probe **1**. To this end, we replaced the LKS01 component of probe **1** with the β2/β2i-selective inhibitor NC-012, and its C_6 linker with a more flexible and water-soluble PEG linker. The distance between the catalytic threonine O^{γ} atoms of β1/β1i and β2/β2i within each β-ring is relatively short (~28 Å) [75, 344] (Figure 4.1); we therefore chose a short $(PEG)_4$ linker of an estimated length of ~23.2 Å for use in coupling the two inhibitors (Figure 4.2, Table 4.1). Results of proteasome activity assays in purified constitutive proteasomes and immunoproteasomes confirmed that β1/β1i inhibition by the newly synthesized probe, UKP13-$(PEG)_4$-NC012 (probe **6**), is similar to that observed for probe **1**. On the other hand, probe **6**'s preference for inhibiting β2/β2i is greatly improved over that of probe **1**, and its preference for inhibiting β5/β5i is reduced (Table 4.2). Similar conclusions can be drawn from the results of proteasome activity assays with these probes in U266 lysates (Table 4.3).

Crosslinking Capabilities

Immunoblotting analysis showed that treatment of the purified constitutive proteasome with probe **6** produced an anti-β1-immunoreactive band just below 50 kDa, consistent with β1-β2 crosslinking (Figure 4.4 A). A similar anti-β1-immunoreactive band was detected for U266 cell lysates following treatment with probe **6** (Figure 4.4 B). Probe **6** was also found to crosslink β1i with β2i, but not with β5i, in the purified immunoproteasome, as shown by the ability of the β2/β2i-selective inhibitor NC-012, but not the β5i-selective inhibitor IPSI, to attenuate the anti-β1i-immunoreactive band representing crosslinked β1i (Figure 4.4 C). We also detected probe **6**-mediated β1i crosslinking in U266 lysates. In this case, two immunoreactive bands between ~45-50 kDa were observed on a β1i immunoblot (Figure 4.4 D), as previously observed when U266 lysates were treated with probe **1** (Figure 4.3 B). This latter result strongly indicates that probe **6**, like probe **1**, crosslinks β1i with both β2 and β2i in U266 lysates.

Our results obtained with probes **1** and **6** collectively demonstrate that, despite their structural differences, both probes crosslink β1/β1i with β2/β2i. They also highlight the presence of proteasome subtypes containing both β1i and β2i, and those containing both β1i and β2, in U266 cells. Conversely, while our results reflect the presence of proteasome subtypes containing both β1 and β2 in these cells, they indicate the absence of proteasome subtypes containing both β1 and β2i. The lack of evidence for the formation

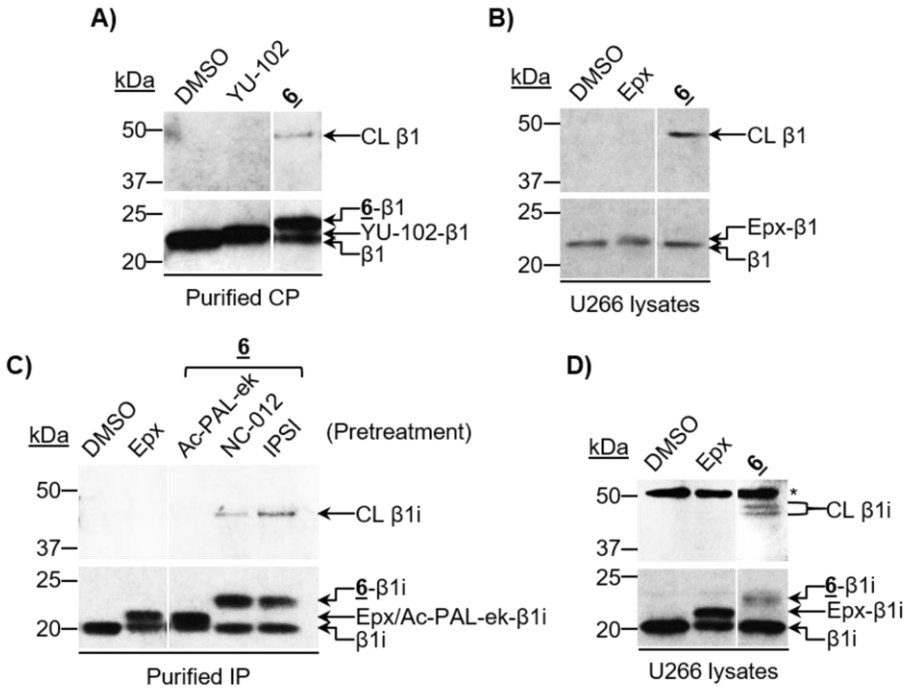

Figure 4.4 Probe 6 crosslinks β1/β1i with β2/β2i
A) The purified 20S constitutive proteasome (CP) was incubated with DMSO, the β1/β1i-selective proteasome inhibitor YU-102, or probe **6** prior to immunoblotting for β1. **B)** U266 cell lysates were incubated with DMSO, epoxomicin (Epx), or the indicated bifunctional probe prior to immunoblotting for β1. **C**) The purified 20S immunoproteasome (IP) was treated with DMSO, epoxomicin, or was pretreated with the indicated subunit-selective inhibitor prior to treatment with probe **6**, as indicated. β1i was detected by immunoblotting. **D)** U266 cell lysates were incubated with DMSO, epoxomicin, or probe **6** prior to immunoblotting for β1i. Irrelevant lanes were removed. CL = crosslinked β-subunit. * = nonspecific band. *These data were published in our previous report [239].*

of proteasome subtypes containing the β1-β2i combination agrees with previous observations suggesting that β2i is efficiently incorporated into proteasome complexes only when it is co-incorporated with β1i [220, 221, 223].

4.2.3 Probes for β1/β1i-β5/β5i Crosslinking

a. Probes 3 and 5

Design and Subunit Binding Preferences

Our next goal was to generate a bifunctional proteasome probe capable of crosslinking β1 or β1i with β5 or β5i. We therefore synthesized two UKP1-3-containing bifunctional probes: one in which the β5i-selective inhibitor LKS01 was used as the second inhibitory moiety, and another in which the β5-selective inhibitor PR-825 was used (Figure 4.2). The estimated length of the PEG linker we chose to incorporate into these probes is

~83.9 Å. We felt this length would be more than sufficient to facilitate crosslinking of the targeted subunits, whose catalytic threonine residues are separated by ~62 Å [75, 344] (Figures 4.1 and 4.2). The first of these two probes, UKP13-$(PEG)_{494}$-LKS01 (probe **3**) (Table 4.1), was found to selectively inhibit the β1-type and β5-type subunits in U266 lysates, whereas >10 μM of this probe was required to inhibit the β2/β2i activity by 50% (Table 4.3). The second of these probes, UKP13-$(PEG)_{494}$-6Ahx-PR825 (probe **5**) (Table 4.1) selectively binds the β5 and β1 subunits and the β1i and β5i subunits of the purified constitutive proteasome and immunoproteasome, respectively (Table 4.2). Furthermore, a 5 μM concentration of this probe completely inhibits the β1/β1i and β5/β5i activities in U266 lysates (Table 4.3).

Crosslinking Capabilities

1. Probe 3

Following treatment of the purified immunoproteasome with probe **3**, crosslinked β5i was detected on a β5i immunoblot as a single immunoreactive band with a molecular weight consistent with β5i-β1i crosslinking (Figure 4.5, *left panel*). Providing further evidence for this species, we detected a band of approximately the same molecular weight on a β1i immunoblot (Figure 4.5, *right panel*). Pretreating the purified immunoproteasome with the β5i-selective inhibitor IPSI effectively suppressed the emergence of this higher-molecular-weight band following treatment with probe **3**, verifying that this band represents crosslinked β5i (Figure 4.5, *left panel*). Additionally, pretreating with the β1i-selective inhibitor Ac-PAL-ek produced the same effect, indicating that probe **3** crosslinks β5i with β1i (Figure 4.5, *left panel*).

Pretreating with Ac-PAL-ek also blocked the appearance of the higher-molecular-weight band on the β1i immunoblot, demonstrating that it represents β1i (Figure 4.5, *right panel*). Conversely, pretreating with the β2/β2i-selective inhibitor NC-012 had no effect on this band, suggesting that probe **3**, unlike probes **1** and **6**, does not crosslink β1i with β2i (Figure 4.5, *right panel*). Interestingly, although we expected that pretreating with IPSI would block the appearance of this crosslinked β1i band, this was not the case. However, this band did appear to shift upward in molecular weight under these conditions (Figure 4.5, *right panel*). This suggests that the β1i-immunoreactive band seen for the DMSO- and NC-012-pretreated samples resulted from crosslinking of β1i with β5i, but that a different crosslinked species was formed when β5i's active site is blocked. Based on

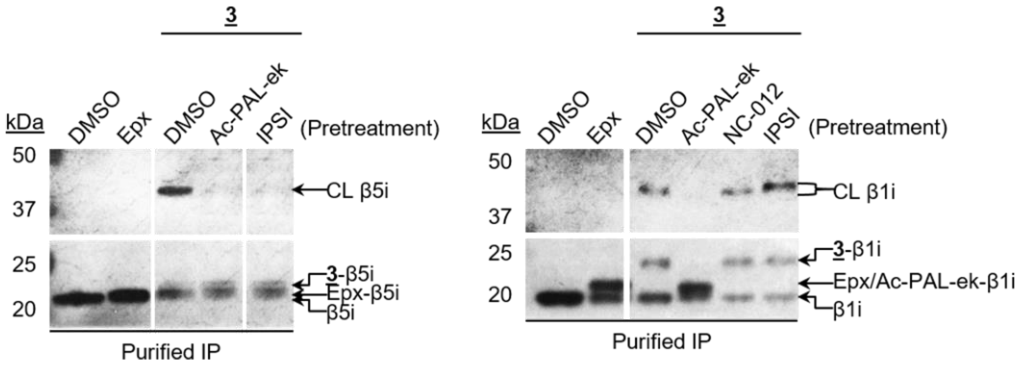

Figure 4.5 Probe 3-mediated crosslinking of catalytic proteasome subunits
The purified 20S immunoproteasome (IP) was incubated with DMSO or epoxomicin (Epx), or was pretreated with DMSO or the indicated subunit-selective inhibitor prior to treatment with probe **3**, as indicated. β5i (*left panel*) or β1i (*right panel*) was detected by immunoblotting. Irrelevant lanes were removed. CL = crosslinked β-subunit.

molecular weight, this new species is likely a β1i-β2i pair rather than a β1i-β1i pair, as β2i is of higher molecular weight than β5i, while β1i is of lower molecular weight.

Collectively, these results suggest that probe **3** crosslinks β1i with β5i, and, if β5i's active site is blocked, it crosslinks β1i with β2i instead. Conversely, it does not appear to crosslink β5i with β2i when β1i's active site is blocked. It is unclear if this is due to the probe's inability to reach the β2i active site when bound to that of β5i, or to the inefficient binding of one end of the probe (presumably the UKP1-3 end) to β2i. Regardless, it appears that the long, flexible PEG linker can facilitate probe **3**-mediated crosslinking of multiple subunit pairs within the purified immunoproteasome. On the other hand, despite its ability to bind both of the constitutive subunits β1 and β5 individually, probe **3** was not able to perceptibly crosslink either of these subunits with one another, or with β2, when incubated with the purified constitutive proteasome (data not shown).

2. Probe 5

In contrast to the single band observed following treatment with probe **3**, two anti-β1i-immunoreactive bands were observed between ~40-50 kDa by immunoblotting analysis of the probe **5**-treated purified immunoproteasome: one major band and one minor band (Figure 4.6 A, *left panel*). We detected a band with a comparable molecular weight to that of the major crosslinked β1i band on a β5i immunoblot, suggesting that these bands arose from crosslinking of β1i with β5i (Figure 4.6 A, *middle panel*). Based

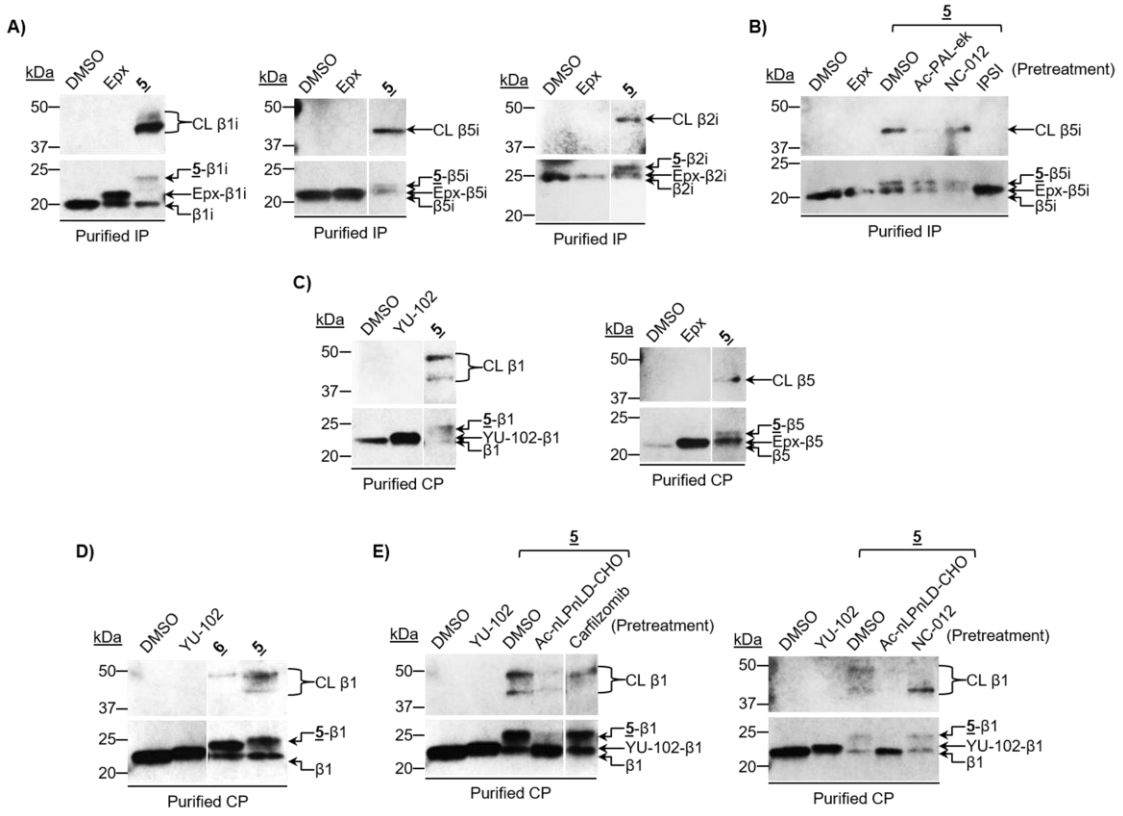

Figure 4.6 Probe 5 crosslinks β1/β1i with β5/β5i and β2/β2i
A) The purified 20S immunoproteasome (IP) was treated with DMSO, epoxomicin (Epx), or probe **5** prior to immunoblotting for β1i (*left panel*), β5i (*middle panel*), or β2i (*right panel*). **B)** The purified 20S immunoproteasome was treated with DMSO or epoxomicin, or was pretreated with DMSO or the indicated subunit-selective inhibitor prior to treatment with probe **5**, as indicated. β5i was detected by immunoblotting. **C)** The purified 20S constitutive proteasome (CP) was treated with DMSO, YU-102, epoxomicin, or probe **5** prior to immunoblotting for β1 (*left panel*) or β5 (*right panel*). **D)** The purified 20S constitutive proteasome was treated with DMSO, YU-102, probe **6**, or probe **5** prior to immunoblotting for β1. **E)** The purified 20S constitutive proteasome was treated with DMSO or YU-102, or was pretreated with DMSO or the indicated subunit-selective inhibitor prior to treatment with probe **5**, as indicated. β1 was detected by immunoblotting. Irrelevant lanes were removed from blots shown in **A**, **C**, **D**, and **E**. CL = crosslinked β-subunit. *These data were published in our previous report [239].*

on the results of the β1i immunoblot and of one for β2i, the minor band on the β1i immunoblot appears to reflect crosslinking between β1i and β2i (Figure 4.6 A, *right panel*). Together, these results indicate that probe **5** crosslinks β1i preferentially with β5i, but also, to a lesser extent, with β2i. The higher-molecular-weight β5i band was no longer detectable when the purified immunoproteasome was pretreated with the β5i-selective inhibitor IPSI before it was treated with probe **5**, confirming that this band represents crosslinked β5i (Figure 4.6 B). This band could also be attenuated by pretreating with the

β1i-selective inhibitor Ac-PAL-ek, providing further evidence that it resulted from crosslinking between β5i and β1i (Figure 4.6 B).

Also contrasting probe **3**-mediated crosslinking was the ability of probe **5** to crosslink catalytic subunits within the purified constitutive proteasome. We detected two immunoreactive bands on a β1 immunoblot with the probe **5**-treated constitutive proteasome that arose from β1 crosslinking (Figure 4.6 C, *left panel*). A crosslinked band with a molecular weight comparable to that of the lower of these crosslinked β1 bands was detected on a β5 immunoblot, indicating that probe **5** crosslinks β1 with β5 (Figure 4.6 C, *right panel*). On the other hand, the upper crosslinked β1 band was found to align with the crosslinked β1 band generated following treatment of the purified constitutive proteasome with probe **6**. Their comparable molecular weights suggested that the upper crosslinked β1 band observed for the probe **5**-treated constitutive proteasome reflects crosslinking between β1 and β2 (Figure 4.6 D). Both of the higher-molecular-weight β1 bands could be substantially depleted by pretreating the purified constitutive proteasome with the β1-selective inhibitor Ac-nLPnLD-CHO before treating with probe **5**, confirming that these bands arose from β1 crosslinking (Figure 4.6 E). Only the lower of these bands was depleted by pretreating with the β5/β5i-selective inhibitor carfilzomib [262] (Figure 4.6 E, *left panel*), while pretreating with the β2/β2i-selective inhibitor NC-012 depleted only the upper band (Figure 4.6 E, *right panel*). These results confirm that probe **5** crosslinks β1 with both β5 and β2 and again indicate that the long, flexible PEG linker can mediate crosslinking of multiple pairs of catalytic proteasome subunits.

4.2.4 Probes for β2/β2i-β5/β5i Crosslinking

Design and Subunit Binding Preferences

Although it was outside of our original goal of generating probes for crosslinking the β1-type subunits with the β2- or β5-type subunits, we also attempted to develop probes capable of crosslinking the β5-type subunits with the β2-type subunits. We felt that adding such probes to our repertoire would be helpful in determining the catalytic subunit compositions of the various proteasome subtypes more conclusively. Specifically, their use could provide the evidence required for deciding whether we could truly rule out the presence of mature proteasome complexes containing β2i together with β5 [220, 221, 223, 226], and, if not, allow us to detect those subtypes as well. We therefore synthesized probes **7** (LKS01-$(PEG)_{94}$-NC012) and **8** (LKS01-$(PEG)_{494}$-NC012), with the former having a shorter linker than the latter (estimated lengths: ~62.7 Å vs. ~83.9 Å) (Figure 4.2, Table

4.1). Still, we anticipated that the length of either of these linkers would likely be sufficient for crosslinking of the targeted subunits, whose catalytic residues are separated by ~63 Å within each β-ring. As observed for probe **6** (Tables 4.2 and 4.3), incorporating the β2/β2i-selective inhibitor NC-012 into these bifunctional probes substantially increased their potency against these subunits (Table 4.3). Both probe **7** and probe **8** prefer binding to β5, β5i, β2, and β2i over β1 and β1i in U266 lysates (Table 4.3).

Immunoblotting Analyses

Although immunoblotting analyses demonstrated that probe **7** does, in fact, covalently modify its preferred targets in U266 lysates—consistent with the activity assay results—crosslinking of these subunits could not be readily detected using their respective antibodies (data not shown). Conversely, we did observe faint crosslinking of β1i, whereas no significant β1 crosslinking was detected (data not shown). We did not go forward with discerning which subunit was crosslinked with β1i by probe **7**, but, based on the molecular weight of the crosslinked β1i band, the unknown subunit is unlikely to be a β2-type subunit and likely to be either a β5-type or β1-type subunit (data not shown). On the other hand, probe **8** did appear to weakly crosslink β5i (in addition to β1i) within the purified immunoproteasome, but it is unlikely that this probe crosslinks β5i with β2i (data not shown). Our efforts to definitively determine the identity of the subunits crosslinked with β5i and β1i by this probe have so far been unsuccessful.

4.2.5 Homobifunctional Proteasome Probes

Finally, we synthesized five homobifunctional proteasome probes: UKP13-$(PEG)_9$-UKP13 (probe **9**), UKP13-$(PEG)_8$-SS-$(PEG)_8$-UKP13 (probe **10**), LKS01-$(PEG)_9$-LKS01 (probe **11**), LKS01-$(PEG)_{494}$-LKS01 (probe **12**), and NC012-$(PEG)_{494}$-NC012 (probe **13**) (Figure 4.2, Table 4.1). Given the variability in proteasome catalytic subunit composition, it has been questioned whether the two β-rings within a 20S proteasome complex need be identical, or whether so-called 'asymmetric' core particles containing two β-rings of differing catalytic subunit content can form [73, 225]. We reasoned that our homobifunctional probes would allow these possibilities to be further examined.

Subunit Binding Preferences

We found that probe **9** strongly inhibits β1 and β1i in U266 lysates; it also exhibits reduced potency toward β5 and β5i compared with probes in which UKP1-3 was combined

with LKS01 or PR-825. Additionally, this probe poorly inhibits β2/β2i activity, with only 9% of this activity being inhibited at a probe concentration of 10 μM (Table 4.3). Probe **10** also completely inhibits β1i activity at a concentration of 1 μM. This probe is a more potent inhibitor of β5/β5i activity than probe **9** (Table 4.3). Probe **11** strongly inhibits β5/β5i activity and displays much weaker activity against β1/β1i and β2/β2i (Table 4.3). Probe **12** appears to inhibit β5/β5i activity more potently than probe **11**, but it also shows increased inhibitory potency toward β1/β1i and β2/β2i (Table 4.3). The results obtained with probes **9**-**12** suggest that coupling two UKP1-3 moieties, or two LKS01 moieties, via longer linkers gives rise to less specific probes than those in which the same inhibitory moieties are coupled by shorter linkers. Lastly, probe **13** is the most potent β2/β2i inhibitor among the bifunctional probes. Conversely, it poorly inhibits β1 and shows reduced β1i inhibitory potency compared with the UKP1-3-containing probes (Table 4.3).

Crosslinking Capabilities

1. Probes 9, 2, and 11

Strong β1i crosslinking was observed when U266 lysates were treated with probe **9** (Figure 4.7 A). A competition assay confirmed the subunit crosslinked with β1i by this probe to be the β1i subunit on the opposing β-ring (Figure 4.7 B). Surprisingly, similar results were obtained for probes **2** (UKP13-$(PEG)_9$-LKS01) (Figure 4.7 C) and **11** (Figure 4.7 D), suggesting that the $(PEG)_9$ linker directs crosslinking between the two β1i subunits within a 20S core complex. Conversely, probes **2** and **11** do not crosslink β5i or β5 (data not shown), consistent with their linker length (estimated to be ~35.8 Å), although longer than the C_6 linker of probe **1**, being insufficient for crosslinking between the β5-type and β1-type subunits (Figures 4.1 and 4.2). Interestingly, the $(PEG)_9$ linker of probe **2** leads to a loss of the β1i-β2/β2i crosslinking observed with probe **1**, further demonstrating that properties of the linker can have a meaningful influence on the subunits crosslinked by bifunctional probes with identical inhibitory moieties (Figure 4.7 A).

2. Probe 10

Like probe **4**, probe **10** was synthesized for use as a control to show that the higher-molecular-weight bands seen upon immunoblotting analysis of bifunctional probe-treated samples resulted from crosslinking of two catalytic proteasome subunits (Figure 4.2, Table 4.1). Like probe **9**, probe **10** produced strong bands on a β1i immunoblot that

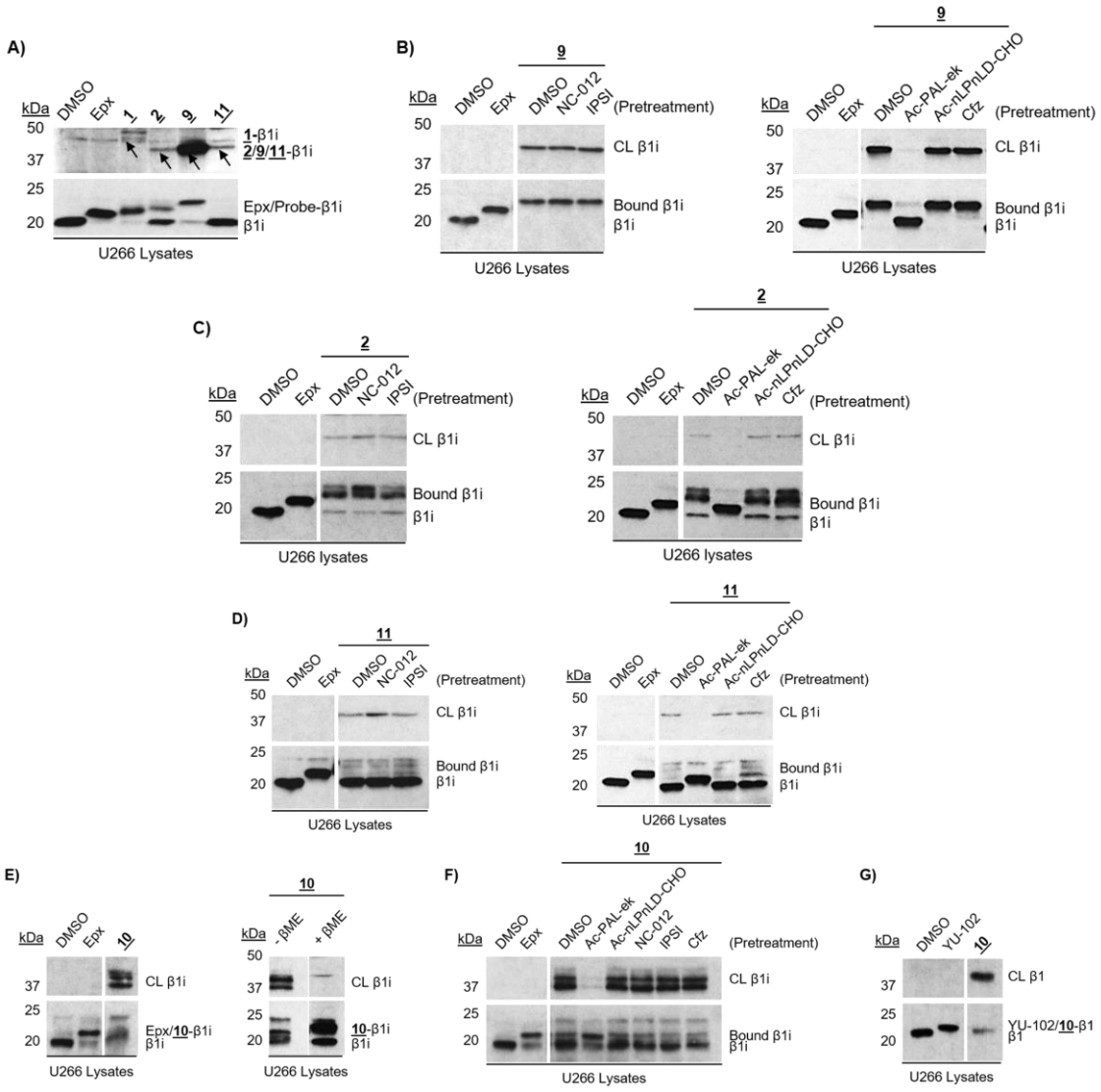

Figure 4.7 Probes 9, 2, 11, and 10 crosslink β1/β1i with β1/β1i on the opposing β-ring

A) U266 cell lysates were treated with DMSO, epoxomicin (Epx), or the indicated bifunctional probe prior to immunoblotting for β1i. **B-D)** U266 cell lysates were treated with DMSO or epoxomicin, or were pretreated with DMSO or the indicated subunit-selective inhibitor prior to treatment with probe **9 (B)**, **2 (C)**, or **11 (D)**, as indicated. β1i was detected by immunoblotting. **E)** *Left panel.* U266 cell lysates were treated with DMSO, epoxomicin, or probe **10** prior to immunoblotting for β1i. *Right panel.* U266 cell lysates were treated with probe **10**, and proteins were subsequently denatured in sample buffer with or without β-mercaptoethanol (βME), which cleaved the internal disulfide bond of the linker. β1i was detected by immunoblotting. **F)** U266 cell lysates were treated with DMSO or epoxomicin, or were pretreated with DMSO or the indicated subunit-selective inhibitor prior to treatment with probe **10**, as indicated. β1i was detected by immunoblotting. **G)** U266 cell lysates were treated with DMSO, YU-102, or probe **10** prior to immunoblotting for β1. Irrelevant lanes were removed from blots shown in **B**-**G**. CL = crosslinked β-subunit.

appeared to represent crosslinked β1i (Figure 4.7 E, *left panel*). This was confirmed by immunoblotting with probe **10**-treated samples whose proteins had been denatured in the absence or presence of β-mercaptoethanol (Figure 4.7 E, *right panel*). Despite its long and flexible PEG linker, β1i crosslinking by probe **10** seems to occur, based on competition assay results, exclusively with the β1i on the opposing β-ring (Figure 4.7 F); the multiple bands observed for crosslinked β1i appear to result from the non-reducing conditions under which this gel was run (Figure 4.7 E and F). This probe also crosslinks β1, most likely with β1 on the opposing β-ring (Figure 4.7 G). Although probe **10** was found to crosslink β1 (Figure 4.7 G), we did not observe crosslinking between β1i and β1 (Figure 4.7 F); these results suggest that proteasomes in U266 cells are symmetric rather than asymmetric, at least with respect to their β1 and β1i content.

3. Probe 12

In contrast to probe **11**, the longer linker of probe **12** facilitates crosslinking of β5i upon incubation of the purified immunoproteasome with this probe (Figure 4.8, *left panel*). This probe also crosslinks β1i (Figure 4.8, *right panel*). Results of competition assays suggest that probe **12** crosslinks β5i with both β5i (likely the predominant species) and β1i (Figure 4.8).

4. Probe 13

Assessments with the purified constitutive proteasome and immunoproteasome showed that probe **13**, like probe **8**, covalently modifies all detectable β2 and β2i (data not shown). It also binds β1i and β1 to a lesser extent, but does not bind β5i (data not shown). Unfortunately, however, we were unable to detect crosslinking of any subunit by this probe (data not shown).

4.3 Discussion

We designed and synthesized a set of bifunctional activity-based probes for use in a crosslinking-based strategy to elucidate the catalytic subunit compositions of individual proteasome subtypes (Figures 4.1 and 4.2, Table 4.1). We conducted proteasome activity assays (Tables 4.2 and 4.3) and immunoblotting analyses (Figures 4.3-4.8) to characterize the subunit binding and crosslinking preferences of these probes within the context of the purified constitutive proteasome or immunoproteasome, or of lysates

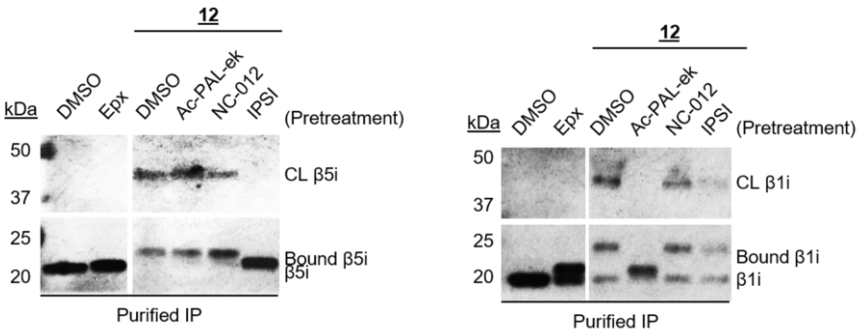

Figure 4.8 Probe 12-mediated crosslinking of catalytic proteasome subunits
The purified 20S immunoproteasome (IP) was incubated with DMSO or epoxomicin (Epx), or was pretreated with DMSO or the indicated subunit-selective inhibitor prior to treatment with probe **12**, as indicated. β5i (*left panel*) or β1i (*right panel*) was detected by immunoblotting. Irrelevant lanes were removed. CL = crosslinked β-subunit.

prepared from a multiple myeloma cell line (U266) that abundantly expresses all of the constitutive subunits and immunosubunits. Our results revealed that the bifunctional proteasome probes maintain the subunit binding preferences of the individual parent inhibitors of which they are composed. Additionally, they showed that all of the probes (except for the NC-012 homodimer [probe **13**]) are capable of crosslinking pairs of catalytic subunits within intact proteasome complexes, allowing us to detect instances of catalytic subunit colocalization within these complexes via immunoblotting analyses. A major advantage of this approach is that it does not necessitate proteasome purification or separation of individual proteasome subtypes from one another via chromatographic methods, free-flow isoelectric focusing electrophoresis, or immunoprecipitation [223-230, 232, 235, 342]; it requires fewer processing steps, yet provides more information on the identity of individual proteasome subtypes than techniques simply assessing overall expression levels of individual catalytic subunits [191, 223, 226-228, 231, 233, 234, 342], most of which may exist in more than one proteasome subtype [224]. Additionally, when using our previously-reported fluorescent proteasome probes in a FRET-based strategy for identifying proteasome subtypes [343], one must be sure to use concentrations of these probes that are subunit-specific for the experimental results to be accurately interpreted; conversely, this limitation does not necessarily apply to the use of our bifunctional probes in the approach discussed here.

We found that both the inhibitory moieties and the linker of a given bifunctional probe influence the subunits it preferentially crosslinks. By joining different combinations of subunit-selective inhibitors via linkers of varying lengths and chemical compositions, we

were able to meet our goal of developing bifunctional proteasome probes that crosslink β1/β1i with β2/β2i (e.g., probes **1** and **6**) or with β5/β5i (e.g., probes **3** and **5**). Using probes **1** and **6**, we identified two β1i-containing proteasome subtypes in U266 cells: one containing β2i, consistent with a pure immunoproteasome, and one containing β2, consistent with intermediate proteasome subtype β1i-β2-β5i [226]. Conversely, subtypes containing β1 together with β2i were not detected, which is in accord with prior results demonstrating that formation of subtypes containing both of these subunits within a single complex is precluded by the proteasome assembly process [220, 221, 226]. These results demonstrate the utility of these probes in discerning the identities of the proteasome subtypes that can be formed in a given cell or tissue type. We also developed bifunctional probes that crosslink β1/β1i with β1/β1i on the opposing β-ring within a single 20S proteasome complex (e.g., probes **2**, **9**, **10**, and **11**), and one (probe **12**) that appears to crosslink β5i with β5i on the opposing β-ring. These probes can be used to determine whether proteasome complexes are symmetric or asymmetric in terms of the catalytic subunit compositions of their two β-rings. Results obtained with probe **10** in U266 cell lysates (Figure 4.7 F and G) indicate that, although both β1- and β1i-containing proteasome complexes are present in this cell line, both β-rings within these complexes are identical with respect to whether they contain β1 or β1i—that is, our results are consistent with a lack of asymmetric proteasome complexes, at least with respect to the β1-type subunits. Whether this is true for other catalytic proteasome subunits or holds across multiple cell lines or tissue samples could be further explored using this approach, and the successful development of a probe that crosslinks the two β2-type subunits on opposing β-rings with one another would complete the set of bifunctional probes required for a full analysis. Although this conclusion contrasts that of Klare et al., who, following IFNγ stimulation, detected both β1 and β1i in proteasomes purified via a tagged β1 subunit from transfected HeLa cells [225], it is in line with that of Guillaume et al., who, by analyzing proteasomes immunoprecipitated with an antibody recognizing β5 in its native state via β5i immunoblotting, were unable to detect asymmetric proteasome complexes containing both β5 and β5i in melanoma cells or in kidney [226].

Although our approach offers several advantages over others that are currently available, it has several limitations worth addressing. First, the crosslinking efficiency of our probes stands to be improved. This would provide a greater probability of detecting subtypes that may be present in low amounts, which can still be of biological importance [226]. Additionally, our bifunctional proteasome probes containing the longest PEG linkers

used in our study (~83.9 Å) tend to crosslink multiple pairs of catalytic subunits (e.g., probes **5** and **12**), or appear to readily crosslink a given subunit with a non-preferred target when the active site of a preferred target is blocked (e.g., probe **3**). Unfortunately, this latter finding renders drawing definitive conclusions from the competition assays used to identify the subunit pairs crosslinked by these probes more difficult, especially when the next-preferred target for crosslinking is of similar molecular weight to the one whose active site was blocked.

Further optimization of linker lengths or inhibitor sequences may overcome these barriers. Additionally, our laboratory has been working to develop two modified approaches. In one approach, biotin-labeled versions of the various bifunctional proteasome probes are used to facilitate streptavidin-mediated purification of the crosslinked subunit pairs. This strategy would allow a mass spectrometry-based identification of the crosslinked catalytic subunits, bypassing the need for competition assays to confirm the identities of the subunits crosslinked by a given probe. The other approach involves using monomeric subunit-selective proteasome inhibitors that have been functionalized with biorthogonal reactive groups. Treatment of cells with these inhibitors, cell lysis, and incubation of the resulting lysates with a linker that has compatible reactive groups on either end to those of each inhibitor leads to joining of the two inhibitors by the linker. It is hoped that using these smaller inhibitors will provide greater subunit selectivity compared with the large bifunctional probes, thereby assisting the more straightforward interpretation of experimental results.

We anticipate that the bifunctional proteasome probes described here and the second-generation proteasome probes our lab is developing will continue to assist in answering many open yet important questions regarding proteasome biology. For example, the development of probes that crosslink β2/β2i with β5/β5i will allow generation of the evidence required to firmly establish whether formation of proteasome subtypes containing β2i together with β5 is permissible. Additionally, further experiments with the probes capable of crosslinking β1/β1i-β5/β5i may answer the question of whether proteasome complexes containing β1i together with β5 exist. Improving our knowledge regarding which proteasome subtypes can and cannot form in specific cell types and/or under specific conditions will improve our collective understanding of proteasome structure and function in both normal and diseased cells. Our probes can also be used in investigating the specific cellular functions of each proteasome subtype. Finally, they can be used to determine whether specific subtypes can serve as disease biomarkers or

indicators of relative sensitivity to proteasome inhibitors. If so, they may provide useful tools to screen for the relevant subtypes in patient samples. If certain subtypes of proteasomes do in fact confer sensitivity or resistance to particular proteasome inhibitors, such an approach may ultimately allow the personalized selection of the proteasome inhibitor that will most effectively target the subtypes present in diseased cells of each patient.

Table 4.2 Inhibitory potencies of bifunctional probes 1, 4, 5, and 6 towards individual catalytic subunits of the purified constitutive proteasome or immunoproteasome

	IC_{50} (μM)					
Probe	**β5**	**β5i**	**β1**	**β1i**	**β2**	**β2i**
UKP13-C_6-LKS01 (**1**)	0.895	0.349	0.655	0.402	10.64	>10
UKP13-$(PEG)_8$-SS-$(PEG)_8$-LKS01 (**4**)	0.165	0.017	0.094	0.038	6.669	>10
UKP13-$(PEG)_{494}$-6Ahx-PR825 (**5**)	0.075	0.380	0.188	0.130	15.28	28.07
UKP13-$(PEG)_4$-NC012 (**6**)	3.93	4.35	1.153	0.803	0.128	0.03

The purified constitutive proteasome or immunoproteasome was incubated with increasing concentrations of each bifunctional probe for 1 h. Proteasome activities were then assessed using fluorogenic peptide substrates selectively hydrolyzed by the indicated subunit. *These data were obtained with the help of Ji Eun Park and were previously reported [239].*

Table 4.3 Subunit binding preferences of the bifunctional proteasome probes in lysates of U266 multiple myeloma cells

		Relative Activity (% DMSO Control)					
Probe	**Conc. (μM)**	**β5/β5i**	**β5**	**β5i**	**β1**	**β1i**	**β2/β2i**
UKP13-C_6-LKS01 (**1**)	0.5	N.D.	N.D.	N.D.	N.D.	N.D.	104%
	1	4%	N.D.	4%	3%	0%	91%
	5	0%	N.D.	0%	0%	0%	71%
	10	0%	N.D.	1%	0%	0%	47%
UKP13-$(PEG)_9$-LKS01 (**2**)	0.5	N.D.	N.D.	N.D.	N.D.	N.D.	107%
	1	2%	N.D.	4%	13%	2%	108%
	5	0%	N.D.	0%	0%	0%	97%
	10	0%	N.D.	0%	0%	0%	70%
UKP13-$(PEG)_{494}$-LKS01 (**3**)	0.1	N.D.	4%	7%	2%	0%	N.D.
	0.5	N.D.	2%	0%	0%	0%	N.D.
	1	N.D.	2%	0%	0%	0%	108%
	5	N.D.	0%	0%	0%	0%	69%
	10	N.D.	0%	0%	0%	0%	65%
UKP13-$(PEG)_{494}$-6Ahx-PR825 (**5**)	0.5	N.D.	0%	5%	5%	0%	N.D.
	1	N.D.	0%	2%	3%	0%	N.D.
	5	N.D.	0%	0%	0%	0%	N.D.
	10	N.D.	0%	0%	0%	0%	N.D.
UKP13-$(PEG)_4$-NC012 (**6**)	1	N.D.	77%	101%	15%	7%	23%
	5	N.D.	33%	88%	2%	1%	6%
	10	N.D.	8%	61%	0%	0%	0%
LKS01-$(PEG)_{94}$-NC012 (**7**)	1	N.D.	0%	7%	N.D.	70%	21%
	5	N.D.	0%	0%	81%	28%	0%
	10	N.D.	0%	0%	62%	12%	0%
LKS01-$(PEG)_{494}$-NC012 (**8**)	0.1	N.D.	28%	40%	N.D.	95%	68%
	0.5	N.D.	1%	13%	N.D.	72%	48%
	1	N.D.	1%	5%	106%	71%	41%
	5	N.D.	1%	0%	80%	31%	10%
	10	N.D.	1%	0%	72%	12%	0%
UKP13-$(PEG)_9$-UKP13 (**9**)	0.5	N.D.	N.D.	N.D.	N.D.	N.D.	102%
	1	34%	N.D.	44%	0%	0%	106%
	5	2%	N.D.	18%	0%	0%	97%
	10	1%	N.D.	15%	0%	0%	91%

Table 4.3 (continued)

		Relative Activity (% DMSO Control)					
Probe	**Conc. (μM)**	**β5/β5i**	**β5**	**β5i**	**β1**	**β1i**	**β2/β2i**
UKP13-$(PEG)_8$-SS-$(PEG)_8$-UKP13 (**10**)	1	3%	N.D.	N.D.	N.D.	0%	N.D.
	5	1%	N.D.	N.D.	N.D.	0%	N.D.
	10	1%	N.D.	N.D.	N.D.	0%	N.D.
LKS01-$(PEG)_9$-LKS01 (**11**)	0.5	25%	N.D.	5%	89%	91%	105%
	1	4%	N.D.	5%	90%	95%	108%
	5	1%	N.D.	0%	73%	56%	87%
	10	1%	N.D.	0%	45%	36%	61%
LKS01-$(PEG)_{494}$-LKS01 (**12**)	0.1	N.D.	1%	0%	59%	15%	N.D.
	0.5	N.D.	1%	0%	35%	1%	N.D.
	1	N.D.	0%	0%	23%	0%	88%
	5	N.D.	0%	0%	11%	0%	54%
	10	N.D.	0%	0%	8%	0%	27%
NC012-$(PEG)_{494}$-NC012 (**13**)	0.1	N.D.	N.D.	N.D.	N.D.	N.D.	32%
	0.5	N.D.	N.D.	N.D.	N.D.	N.D.	13%
	1	N.D.	N.D.	N.D.	110%	56%	0%
	5	N.D.	N.D.	N.D.	84%	29%	0%
	10	N.D.	N.D.	N.D.	60%	11%	0%

Cell lysates were incubated with the indicated concentrations of each bifunctional probe for 1 h. Proteasome activities were then assessed using fluorogenic peptide substrates selectively hydrolyzed by the indicated subunit(s). N.D. = not determined. *Data for probes 1, 4, 5, and 6 were previously reported [239].*

5 EVALUATING PROTEASOME COMPOSITION AND FUNCTION IN CELL LINE MODELS OF ACQUIRED BORTEZOMIB AND CARFILZOMIB RESISTANCE

5.1 Introduction

Despite the markedly improved clinical outcomes achieved with proteasome inhibitor-based treatment regimens, acquired resistance to these inhibitors has emerged as a major clinical challenge [257, 258, 260, 267]. While multifarious conclusions have been drawn from preclinical studies of proteasome inhibitor resistance mechanisms (as described in Chapter 1.8), distinct expression and activity patterns of catalytic proteasome subunits have frequently been observed in cancer cells displaying both intrinsic [204, 289, 334, 346] and acquired [184, 204, 209, 246, 280, 285, 288, 289, 298, 313, 315, 329, 330, 332, 333] resistance to these agents. In cell line models of acquired bortezomib resistance, these properties are frequently accompanied by an inferior bortezomib-mediated suppression of proteasome activities [184, 204, 209, 246, 285, 289, 313, 337]. The consistency of these findings, especially those obtained with the same cell line before and after resistance was acquired, as well as previous findings linking distinct proteasome subtypes of murine cells with the differential inhibitory efficacies of bortezomib and other proteasome inhibitors [231, 232], led us to hypothesize that increases in the relative proportions of specific subtypes may serve as an important mechanism of acquired proteasome inhibitor resistance due to the inability of the proteasome inhibitors currently in clinical use to efficiently inhibit their activities. Additionally, given the structural and mechanistic differences between inhibitors, we hypothesized that the subtypes conferring resistance would differ in a manner depending on the inhibitor to which resistance was acquired. We therefore sought to test this hypothesis by following changes in proteasome composition and activities in a single, proteasome inhibitor-sensitive cell line once resistance to the clinically-relevant proteasome inhibitors bortezomib and carfilzomib was acquired, and assessing how these changes correlate with the effects of bortezomib and carfilzomib on the proteasome's various catalytic activities.

5.2 Results

5.2.1 Cell Line Models of Acquired Proteasome Inhibitor Resistance

We first generated cell line models of acquired bortezomib and carfilzomib resistance for use in testing our hypothesis. The H23 non-small cell lung cancer (NSCLC) cell line was selected for this purpose for the following reasons: (1) While a number of research groups have investigated mechanisms of acquired bortezomib resistance using

hematologic cancer cell line models, only a few have examined these mechanisms in solid cancer cell lines, and therefore a greater knowledge gap exists in this area, (2) Encouraging results of preclinical and clinical studies have rationalized further examining the applications of proteasome inhibitors in NSCLC therapy [347, 348], (3) Prior immunoblotting analyses conducted by members of our laboratory showed that, in comparison with other NSCLC cell lines, H23 cells express immunosubunits β1i and β5i at relatively high levels; as the constitutive subunits are also expressed in H23 cells, this indicates their potential to form multiple proteasome subtypes, and (4) Cell viability assays previously conducted in our laboratory demonstrated that H23 cells are, in comparison with other NSCLC cell lines, relatively intrinsically sensitive to bortezomib and carfilzomib, therefore allowing a comparison of the changes that occur when an initially sensitive cell line becomes resistant to these inhibitors. H23 cells were cultured in the continuous presence of gradually increasing concentrations of bortezomib or carfilzomib until they were able to survive and proliferate in the presence of a final concentration of 150 nM bortezomib or 1 μM carfilzomib. These concentrations exceed the respective IC_{50} values of these inhibitors in parental H23 cells by ~28- and ~55-fold, respectively (Table 5.1). We then collected the cells when they were growing in the presence of bortezomib or carfilzomib, or following a 7 day recovery period, for our analyses. Replicate cell lines resistant to each inhibitor (referred to as bortezomib-resistant cell lines #1 and #2 [BtzR#1 and #2] and carfilzomib-resistant cell lines #1-3 [CfzR #1-3]) were generated to evaluate the consistency of the experimental results.

Table 5.1 Cell line models of acquired bortezomib (BtzR) and carfilzomib (CfzR) resistance

Cell Lines	Parental Cell Line IC_{50} (nM)	Final Concentration (nM)
H23 BtzR	5.4	150 (~28X parental IC_{50})
H23 CfzR	18.3	1,000 (~55X parental IC_{50})

The IC_{50} values of bortezomib and carfilzomib in parental H23 cells, and the final concentrations of each inhibitor to which resistance was established, are listed. *Cell viability (IC_{50}) data for the parental H23 cell line were acquired by Min Jae Lee.*

5.2.2 Proteasome Catalytic Activities of Inhibitor-Exposed Cells

While some cancer cells tolerate partial inhibition of proteasome activity better than others, prolonged exposure to inhibitor concentrations that achieve stronger inhibition of total proteasome activity should induce growth arrest and cell death even in relatively insensitive cells. As a first step in determining how our bortezomib- and carfilzomib-resistant cell lines are able to survive the continuous presence of high concentrations of bortezomib or carfilzomib, respectively, we first assessed which of the proteasome's catalytic subunits were inhibited in these cell lines, and to what extents, under conditions of continuous exposure to 150 nM bortezomib or 1 μM carfilzomib, respectively, reasoning that insufficient proteasome inhibition could contribute to their survival under such conditions. The use of fluorogenic peptide substrates that are selectively hydrolyzed by specific catalytic proteasome subunits [76, 181] allowed us to selectively measure the activities of individual subunits in lysates obtained from the parental, bortezomib-, and carfilzomib-resistant cells. Each activity measured in the resistant cell lines was expressed as a percentage of that measured in untreated parental H23 cells. For comparison, we treated parental H23 cells with these same concentrations of bortezomib or carfilzomib. The treatment period for the parental cells was reduced to 4 hours to prevent the onset of cell death pathways [242]. We envisioned that any differences in activity patterns between the inhibitor-exposed parental and resistant cell lines could provide insight into underlying resistance mechanisms. Additionally, as such differences could result from the enhanced formation of specific proteasome subtypes in the inhibitor-resistant cell lines from those formed in the parental cell line, their detection would be in keeping with our hypothesis.

a. Effects of Bortezomib Exposure

As expected [174, 180, 207, 243-245], 150 nM bortezomib inhibited most of the β5 and β5i activities in parental H23 cells (Figure 5.1 A). It also almost completely inhibited the β1 and β1i activities, which were previously reported to be secondary targets that are bound at clinically relevant concentrations of bortezomib [200, 204, 207, 243] (Figure 5.1 A). In contrast, the β2/β2i activity was only inhibited by ~50%, which is in agreement with previous results showing the poor targeting of these subunits by bortezomib [174, 180, 204, 207, 243-245] (Figure 5.1 A).

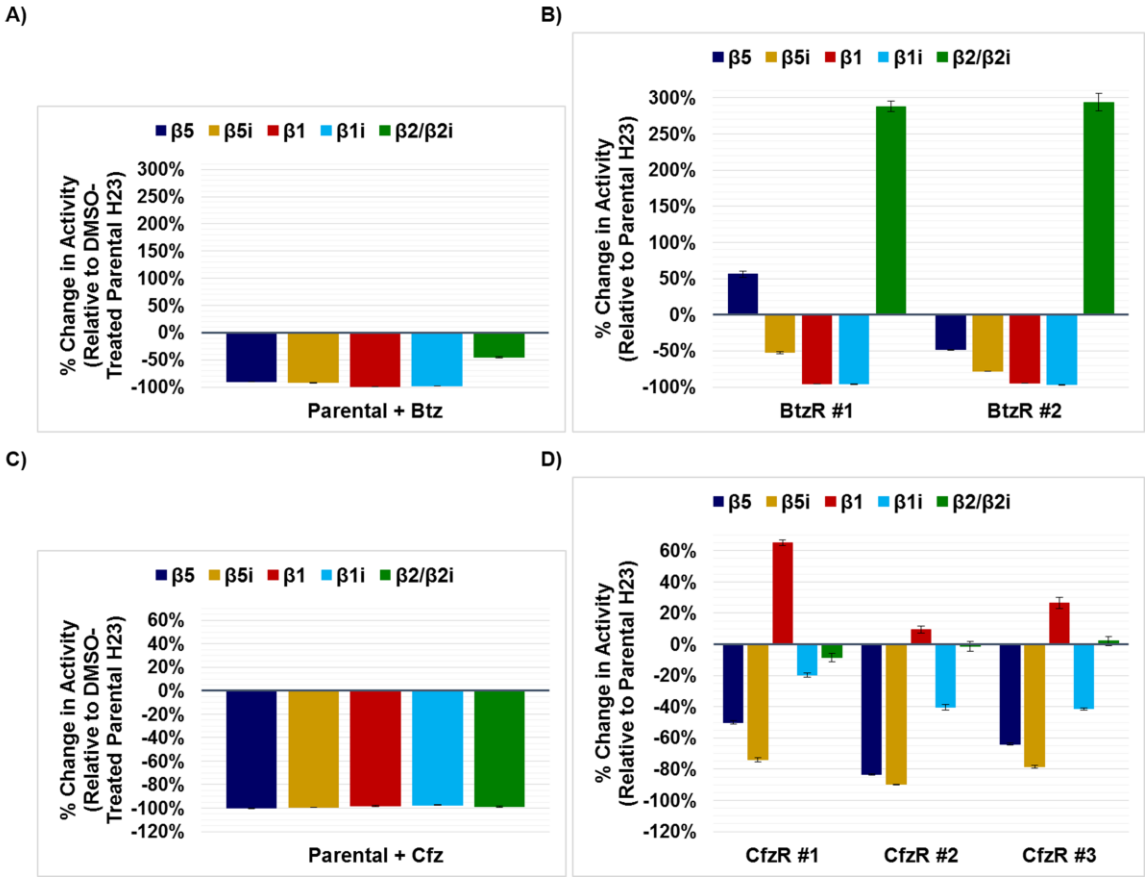

Figure 5.1 Effects of bortezomib or carfilzomib exposure on proteasome catalytic activities in the parental, BtzR, and CfzR H23 cell lines
A) Activity profile of parental H23 cells exposed to 150 nM bortezomib. **B)** Activity profile of BtzR H23 cells continuously maintained in the presence of 150 nM bortezomib. **C)** Activity profile of parental H23 cells exposed to 1 μM carfilzomib. **D)** Activity profile of CfzR H23 cells continuously maintained in the presence of 1 μM carfilzomib. Values represent the averages of three replicates, and error bars indicate standard deviations.

When we examined the activity profiles of the BtzR cells maintained under continuous bortezomib exposure, clear differences from that of the bortezomib-treated parental cells were observed. Although secondary bortezomib targets β1 and β1i were fully inhibited in both BtzR cell lines (Figure 5.1 B), as observed in the bortezomib-treated parental cells (Figure 5.1 A), we detected residual activities of primary targets β5 and β5i (Figure 5.1 B), in contrast to the near complete inhibition of these activities by bortezomib in the parental cells (Figure 5.1 A). β5 activity was even increased in bortezomib-exposed BtzR#1 cells relative to that of the untreated parental cells (Figure 5.1 B). Strikingly, the β2/β2i activity of both BtzR cell lines was considerably increased over that of the untreated parental cells, despite the presence of bortezomib (Figure 5.1 B). Although the responses

of the β5 and β5i activities to bortezomib differed between the two BtzR cell lines, the rank order of proteasome activities detected, ranging from strongly elevated to completely inhibited, was similar in both: β2/β2i > β5 > β5i > β1 = β1i (Figure 5.1 B). These results indicate that enhanced β2/β2i activity and residual β5 and β5i activities may be important in surviving continuous bortezomib exposure.

b. Effects of Carfilzomib Exposure

In contrast to the effects of 150 nM bortezomib on parental H23 cells, which left the β2/β2i activity partially intact (Figure 5.1 A), treatment of parental H23 cells with 1 μM carfilzomib abolished all proteasome catalytic activity (Figure 5.1 C), on par with previous findings [174]. However, residual activities of all of the constitutive proteasome and immunoproteasome catalytic subunits were detected in all three CfzR cell lines, despite their prolonged exposure to carfilzomib (Figure 5.1 D). As observed in both BtzR cell lines cultured in the presence of bortezomib (Figure 5.1 B), residual activities of primary carfilzomib targets β5 and β5i were detectable in all three CfzR cell lines (Figure 5.1 D). However, the suppression of β5 activity by at least 50% relative to parental levels in all three CfzR cell lines (Figure 5.1 D) contrasted the elevated β5 activity over parental levels detected in the bortezomib-exposed BtzR#1 cell line (Figure 5.1 B).

While both the BtzR and the CfzR cell lines displayed residual β5 and β5i activities in the presence of bortezomib and carfilzomib, respectively, the activities of the remaining catalytic subunits were differentially impacted under these conditions in the CfzR cell lines than in the BtzR cell lines. The β2/β2i activity, which was strongly increased over parental levels in both BtzR cell lines (Figure 5.1 B), remained similar to parental levels in all three CfzR cell lines (Figure 5.1 D). β1 activity was elevated, while the activity of its immunosubunit counterpart, β1i, was incompletely suppressed, in all three CfzR cell lines in comparison with those of untreated parental H23 cells (Figure 5.1 D). This contrasts the complete inhibition of both β1 and β1i activities by bortezomib in both BtzR cell lines (Figure 5.1 B). Despite variations in the degree to which certain catalytic activities were altered in these cell lines in the presence of carfilzomib, the rank order of residual activities, ranging from elevated (<2-fold) to predominantly suppressed, was similar across all three cell lines: β1 > β2/β2i > β1i > β5 > β5i (Figure 5.1 D). Of note, the preferred targets of carfilzomib were, in fact, those whose activities were suppressed to the greatest extent (Figure 5.1 D) (unlike what we observed for bortezomib [Figure 5.1 B]). These findings

suggest that elevated β1 activity and fully retained β2/β2i activity may allow the CfzR cells to tolerate continuous carfilzomib exposure.

5.2.3 Proteasome Catalytic Subunit Expression Levels of Inhibitor-Exposed Cells

a. Bortezomib-Resistant Cells

To determine whether the differential impacts of bortezomib on the various proteasomal catalytic activities in the parental and BtzR cell lines (Figure 5.1 A and B) may be attributed to the differential expression of the subunits responsible for these activities, we assessed the expression levels of these subunits via immunoblotting. In comparison with untreated parental H23 cells, the most prominent changes observed were the upregulation of constitutive catalytic subunits β5, β1, and β2 in both BtzR cell lines (Figure 5.2 A). The structural proteasome subunit α5 was also upregulated in both BtzR cell lines (Figure 5.2 A). Alternatively, immunosubunit β5i was downregulated in BtzR#1 and, to a lesser extent, in BtzR#2, while β1i was downregulated only in BtzR#1 (Figure 5.2 A). As the most striking result of the proteasome activity assays was the marked increase in β2/β2i activity in both bortezomib-exposed BtzR cell lines in comparison with that of parental H23 cells (Figure 5.1 B), we expected to see a strong increase in β2 and/or β2i levels in the BtzR cell lines. In contrast, we observed a comparable increase in β2 to that observed for β5 and β1 (Figure 5.2 A), while β2i expression remained below readily detectable levels (data not shown). Furthermore, the upregulation of β1 in both BtzR cell lines (Figure 5.2 A) apparently could not protect against its full inhibition by bortezomib (Figure 5.1 B). Finally, despite the higher levels of proteasome subunit α5—which is common to all proteasome subtypes—in BtzR#2 than in BtzR#1 (Figure 5.2 A), overall proteasome activity under continuous bortezomib exposure was higher in BtzR#1 (possibly indicating weaker inhibition) than in BtzR#2 (Figure 5.1 B). Collectively, these results indicate that changes in the expression levels of the catalytic proteasome subunits had occurred in the BtzR cell lines during prolonged exposure to bortezomib, but that these changes alone cannot fully explain the proteasome activity profiles observed.

b. Carfilzomib-Resistant Cells

A comparison of the proteasome catalytic subunit expression levels between the parental and CfzR cell lines revealed that, despite the detection of residual β5 activity in all three CfzR cell lines under continuous carfilzomib exposure (Figure 5.1 D), β5 expression appeared to remain largely unaltered from parental levels (Figure 5.2 B). This

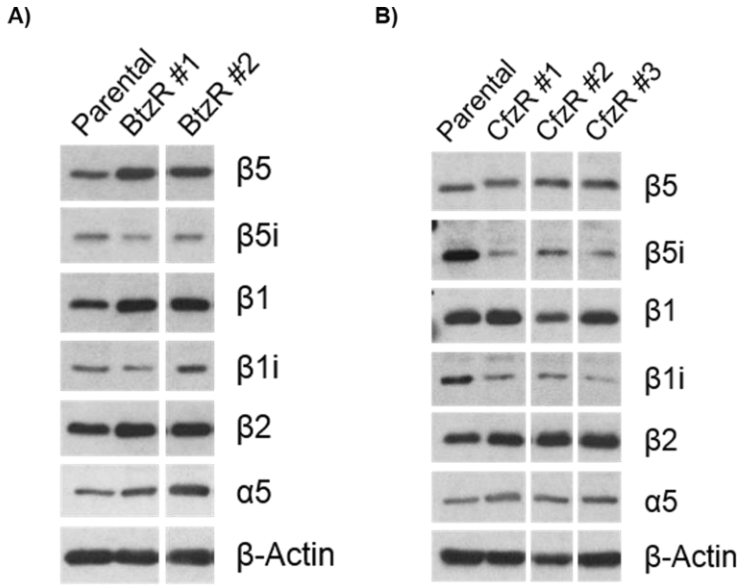

Figure 5.2 Effects of continuous bortezomib or carfilzomib exposure on the expression levels of catalytic proteasome subunits
A) The expression levels of catalytic proteasome subunits are altered BtzR cells maintained under continuous bortezomib exposure relative to those of bortezomib-naïve parental H23 cells. **B)** The expression levels of catalytic proteasome subunits are altered CfzR cells maintained under continuous carfilzomib exposure relative to those of carfilzomib-naïve parental H23 cells.

contrasts the overexpression of β5 seen in both BtzR cell lines (Figure 5.2 A) and indicates that overexpression of this subunit cannot explain the residual β5 activity observed. Furthermore, all of the β5 detectable by immunoblotting appeared to be covalently modified by carfilzomib, as indicated by the upward shift of the β5 band for the CfzR cell lines in comparison with that for the parental H23 cell line (Figure 5.2 B and data not shown). As observed for both BtzR cell lines (Figure 5.2 A), β5i expression was decreased in all three CfzR cell lines in comparison with that of parental H23 cells (Figure 5.2 B). Like β5, all of the β5i detectable by immunoblotting appeared to be covalently modified by carfilzomib (Figure 5.2 B and data not shown). Additionally, the failure of carfilzomib to completely inhibit the β1i activity (Figure 5.1 D) was not due to an upregulation of β1i, since the expression of this subunit was reduced in all three CfzR cell lines when grown under continuous carfilzomib exposure (Figure 5.2 B). Decreases in these two immunosubunits appeared to be greater than those observed in the BtzR cell lines (Figure 5.2 A and B).

In contrast to the bortezomib-exposed BtzR cell lines (Figure 5.2 A), increases in β1 expression over parental levels in the carfilzomib-exposed CfzR cells were more

modest (Figure 5.2 B). This indicates that the high residual β1 activity detected in these cell lines (Figure 5.1 D) cannot be attributed to a strong upregulation of the β1 subunit. β2 expression was also increased in all three CfzR cell lines relative to that of parental H23 cells (Figure 5.2 B), similar to our observations in the BtzR cell lines (Figure 5.2 A). We were again unable to readily detect the β2i subunit in the CfzR cells (data not shown). Finally, α5 expression levels were elevated (although only slightly) in all three CfzR cell lines (Figure 5.2 B), as observed in the BtzR cell lines (Figure 5.2 A). In contrast to the BtzR cell lines, however, the rank order of α5 expression across the three CfzR cell lines (Figure 5.2 B) appeared to agree with the rank order of total residual proteasome activity in these cell lines in the presence of carfilzomib (Figure 5.1 D). However, these results collectively indicate that, as for the bortezomib-exposed BtzR cell lines, the observed changes in expression of the individual catalytic proteasome subunits cannot fully account for the activity profiles observed for the CfzR cell lines maintained under continuous carfilzomib exposure. Additionally, they confirm a lack of (at least complete) covalent modification of β1, β1i, and β2 by carfilzomib in the CfzR cell lines, which is consistent with the activity assay results and suggests that the binding of carfilzomib to these subunits is somehow impeded in the CfzR cell lines.

Our activity assays revealed an incomplete suppression or an elevation of specific proteasome activities in the BtzR and CfzR H23 cells maintained under continuous inhibitor exposure (Figure 5.1 B and D). Additionally, our immunoblotting analyses of these cells revealed that the expression levels of individual catalytic proteasome subunits were altered relative to those of the parental H23 cells, indicating a shift in the abundances of particular proteasome subtypes (Figure 5.2 A and B). Although, for many of these cell lines, the immunoblotting data obtained may be consistent with an overall downregulation of immunoproteasomes (especially for the CfzR cell lines) and upregulation of constitutive proteasomes (especially for the BtzR cell lines), these data alone are insufficient to definitively determine which subtypes of proteasomes are formed in each cell line. Since most of the catalytic proteasome subunits are incorporated into more than one proteasome subtype [226], a change in the level of a given subunit could reflect a change in the abundance(s) of one, or of more than one, subtype into which that subunit incorporates. As the individual catalytic activities of distinct proteasome subtypes appear to be differentially impacted by proteasome inhibitors [231, 232], a relative increase in subtypes that are less efficiently inhibited by bortezomib or carfilzomib and a relative

decrease in those that are more efficiently inhibited could, at least partially, explain the incomplete inhibition of specific proteasome activities observed and, therefore, the reduced sensitivities of the BtzR and CfzR cell lines to bortezomib and carfilzomib, respectively.

5.2.4 Proteasome Activity Profiles of Inhibitor-Resistant Cells

Different subtypes of proteasomes have been shown to display different proteolytic activity profiles [224-226, 229-232, 235], and these differences may contribute to the apparent discrepancies between our activity assay and immunoblotting data. However, such differences in activity profiles are difficult to identify in samples from inhibitor-exposed cells, as it is difficult to discern whether a particular activity is elevated or suppressed due to the effects of inhibitor binding, altered catalytic subunit composition, or both. Therefore, to further examine whether the relative levels of particular subtypes may differ between the inhibitor-resistant and parental H23 cell lines, we again measured the various proteasome activities in the inhibitor-resistant cell lines, this time following a 7 day inhibitor withdrawal to exclude the effects of the inhibitors on these activities.

a. Proteasome Activity Profiles of Bortezomib-Resistant Cells

Following bortezomib withdrawal, we again noted differences in the regulation of β5 activity in the two BtzR cell lines: this activity returned to parental levels in BtzR#1, while it was elevated >2-fold over parental levels in BtzR#2 (Figure 5.3 A). We also observed differences in the regulation of β5i activity, which, relative to parental levels, remained reduced in BtzR#1 to levels similar to those observed in the presence of bortezomib, but was increased in BtzR#2 (Figure 5.3 A). Interestingly, the higher β5 and β5i activities following bortezomib withdrawal were observed for the cell line in which they were most suppressed in the presence of bortezomib (Figures 5.1 B and 5.3 A). Conversely, β1 activity, which was completely inhibited in the presence of bortezomib (Figure 5.1 B), was increased following bortezomib withdrawal in both BtzR cell lines (Figure 5.3 A). However, in contrast to β1 activity, β1i activity, which was also completely inhibited in the presence of bortezomib (Figure 5.1 B), was differentially regulated following withdrawal in the two BtzR cell lines: this activity was decreased in BtzR#1, but increased in BtzR#2, relative to parental levels, following suit the trend observed for β5i activity (Figure 5.3 A). Interestingly, β2/β2i activity remained highly elevated

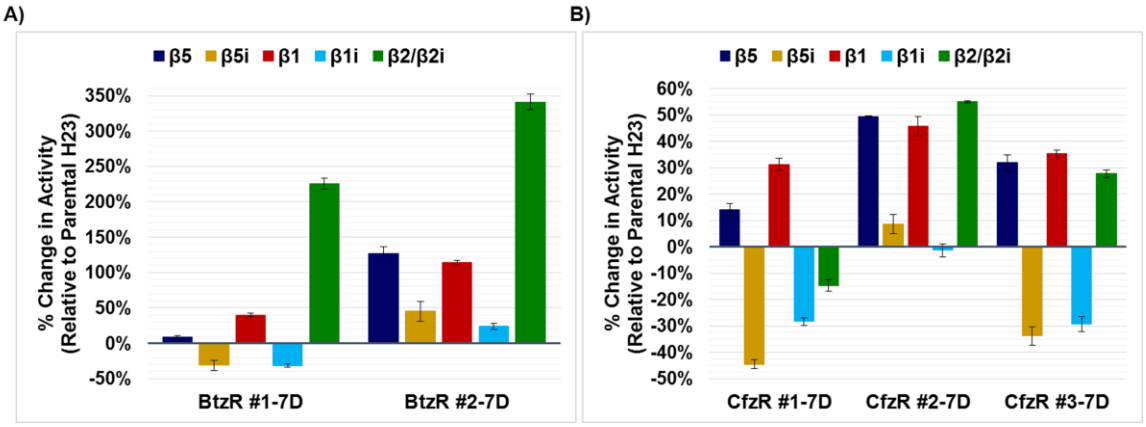

Figure 5.3 Proteasome activity profiles in inhibitor-withdrawn BtzR and CfzR H23 cell lines
A) Proteasome activity profiles of BtzR H23 cells following a 7 d withdrawal from bortezomib. **B)** Proteasome activity profiles of CfzR H23 cells following a 7 d withdrawal from carfilzomib. Values represent the averages of three replicates, and error bars indicate standard deviations.

relative to parental levels in both BtzR cell lines following bortezomib withdrawal (Figure 5.3 A). However, relative to the level of β2/β2i activity observed in each cell line in the presence of bortezomib (Figure 5.1 B), the level of this activity following withdrawal was decreased in BtzR#1 and further increased in BtzR#2 (Figure 5.3 A). These results show that the proteasome activity patterns of the BtzR cell lines measured following bortezomib withdrawal remained altered in comparison with that of the parental cell line (Figure 5.3 A), demonstrating that the effects observed in cells maintained under continuous bortezomib exposure (Figure 5.1 B) were not solely a direct result of inhibitor binding. This is consistent with our hypothesis that the abundances of specific proteasome subtypes become altered when cells acquire resistance to bortezomib, and that these alterations persist after removal of this inhibitor. Intriguingly, our findings obtained with the BtzR cell lines also demonstrate that, with respect to overall proteasome activity, stronger inhibition in the presence of bortezomib is associated with a larger increase following bortezomib withdrawal.

b. Proteasome Activity Profiles of Carfilzomib-Resistant Cells

A similar examination in the CfzR cell lines following carfilzomib withdrawal also revealed that the proteasome activity patterns of these cell lines remained altered in comparison with that of the parental cell line. We found β5 activity to be increased in all three CfzR cell lines (Figure 5.3 B). β1 activity, which was increased over parental levels

even in cells continuously exposed to carfilzomib (Figure 5.1 D), remained elevated in all three CfzR cell lines following carfilzomib withdrawal (Figure 5.3 B). β1 activity was also increased in the BtzR cell lines following bortezomib withdrawal (Figure 5.3 A), albeit following substantial inactivation of this activity in the presence of bortezomib (Figure 5.1 B). β2/β2i activity, which remained similar to parental levels in all three CfzR cell lines under continuous carfilzomib exposure (Figure 5.1 D), did vary from parental levels in these cell lines following carfilzomib withdrawal. The activity of these subunits was slightly decreased relative to parental levels in CfzR#1, but was increased in the other two CfzR cell lines (Figure 5.3 B). This contrasts the more strongly enhanced β2/β2i activity observed in the BtzR cell lines cultured in both the presence and absence of bortezomib (Figures 5.1 B and 5.3 A). Finally, β5i and β1i activities were both reduced relative to parental levels in CfzR#1 and CfzR#3, but remained similar to parental levels in CfzR#2, following carfilzomib withdrawal (Figure 5.3 B). As observed for the BtzR cell lines (Figures 5.1 B and 5.3 A), the greater the β5 and β5i activities were suppressed in the presence of carfilzomib, the more they were increased relative to parental levels following carfilzomib withdrawal (Figures 5.1 D and 5.3 B). The β1 and β1i activities followed this trend as well (Figures 5.1D and 5.3 B). Collectively, these altered activity patterns are, again, in line with the hypothesis that the CfzR cells contain altered amounts of specific proteasome subtypes relative to those of the parental cells, and suggest that a greater suppression of proteasome activity during carfilzomib exposure leads to a greater elevation of proteasome activity following withdrawal of the inhibitor.

5.2.5 Proteasome Catalytic Subunit Expression Levels of Inhibitor-Withdrawn Cells

To determine whether these differences in proteasome activity profiles between parental and inhibitor-resistant cell lines were reflected by differences in the overall expression levels of the catalytic proteasome subunits that persisted following inhibitor withdrawal, we again analyzed the expression levels of these subunits in each cell line following the 7 day inhibitor withdrawal period via immunoblotting.

a. Bortezomib-Resistant Cells

We did, in fact, observe that proteasome catalytic subunit composition remained altered in the BtzR cell lines, relative to that of the parental cells, following bortezomib withdrawal, especially with respect to immunosubunits β5i and β1i. The differential

regulation observed for the β5i and β1i activities in the two BtzR cell lines (Figure 5.3 A) was reflected by their expression levels, which both remained decreased relative to parental levels in BtzR#1 yet were increased above parental levels in BtzR#2 (Figure 5.4 A). β1 expression was also relatively consistent with the β1 activity data, with expression being higher in the cell line with higher β1 activity (BtzR#2) (Figures 5.3 A and 5.4 A). However, despite the observed differential regulation of β5 activity in the two BtzR cell lines following bortezomib withdrawal (Figure 5.3 A), their levels of expression of this subunit was similar (Figure 5.4 A). As observed for the BtzR cell lines under continuous bortezomib exposure (Figures 5.1 B and 5.2 A), the β2 expression data obtained following bortezomib withdrawal is difficult to reconcile with the β2/β2i activity measured; while β2 expression was slightly decreased and increased in BtzR#1 and BtzR#2, respectively, relative to parental levels (Figure 5.4 A), the β2/β2i activity remained elevated to ~330-440% of parental levels (Figure 5.3 A). In contrast to our observations obtained with the BtzR cells continuously exposed to bortezomib (Figures 5.1 B and 5.2 A), following bortezomib withdrawal, α5 expression remained elevated in the cell line with the highest overall proteasome activity (BtzR#2) but reverted to parental levels in the cell line with lower overall proteasome activity (BtzR#1) (Figures 5.3 A and 5.4 A). Collectively, these findings indicate that the proteasome activity patterns of these cell lines are partially, but not solely, determined by their overall expression levels of each catalytic proteasome subunit. That overall proteasome activity following bortezomib withdrawal was higher in the cell line in which it was most suppressed during continuous bortezomib exposure indicates that cellular mechanisms are in place to sense the extent to which proteasome activity is impaired and to adjust proteasome complexes accordingly to allow the appropriate degree of compensation following removal of the inhibitor.

b. Carfilzomib-Resistant Cells

As observed for the BtzR cell lines (Figure 5.4 A), the overall proteasome catalytic subunit composition in the CfzR cell lines, when compared against that of the parental cell line, also remained altered following carfilzomib withdrawal. Again, there were some discrepancies between the expression levels and activities of certain catalytic proteasome subunits. For instance, the sustained increase in β1 activity detected in all three CfzR cell lines following carfilzomib withdrawal (Figure 5.3 B) was apparently not obtained by an increase in β1 expression under these conditions (Figure 5.4 B). Additionally, while the increased β5 activity observed in CfzR#3 following carfilzomib withdrawal was paralleled

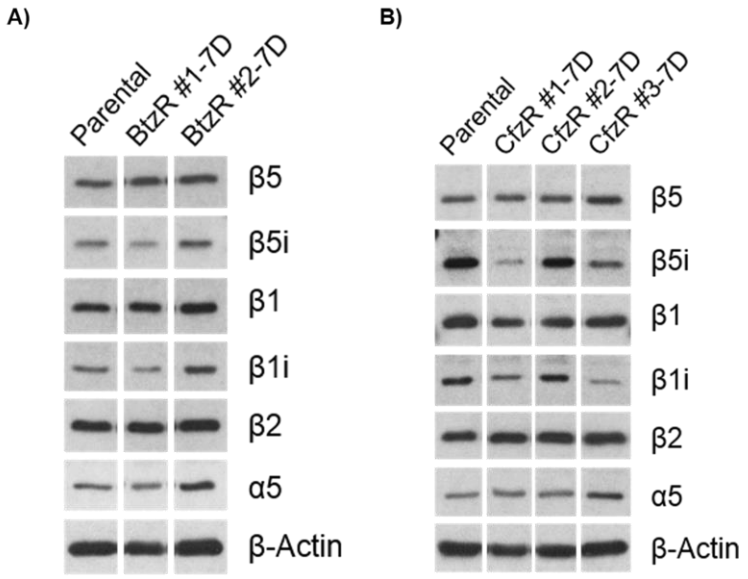

Figure 5.4 Expression levels of catalytic proteasome subunits in inhibitor-withdrawn BtzR and CfzR H23 cell lines
A) Expression levels of catalytic proteasome subunits and structural proteasome subunit α5 in the BtzR cell lines following a 7 d bortezomib withdrawal are compared with those of bortezomib-naïve parental H23 cells. **B)** Expression levels of catalytic proteasome subunits and structural proteasome subunit α5 in the CfzR cell lines following a 7 d carfilzomib withdrawal are compared with those of carfilzomib-naïve parental H23 cells.

by an increase in β5 expression, a comparable increase in β5 activity was observed in CfzR#2 in the absence of a similar β5 upregulation (Figures 5.3 B and 5.4 B). Conversely, the reduced β5i activities, relative to that of the parental cells, observed in CfzR#1 and CfzR#3, and the near parental levels of this activity in CfzR#2, following carfilzomib withdrawal (Figure 5.3 B) were reflected at the protein level (Figure 5.4 B). Like the β5i activity, β1i activity was reduced relative to parental levels in CfzR#1 and CfzR#3, but remained similar to parental levels in CfzR#2, following carfilzomib withdrawal (Figure 5.3 B). This was also in relatively good agreement with the levels of the β1i protein; however, the similar levels of β1i activity in CfzR#1 and CfzR#3 were not reflected by similar levels of β1i expression, which were lower in CfzR#3 than in CfzR#1 (Figures 5.3 B and 5.4 B). The levels of β2/β2i activity observed in the CfzR cell lines following carfilzomib withdrawal did not correlate with the expression levels of the β2 subunit. Although the β2/β2i activity was increased to differing extents in CfzR#2 and CfzR#3, and was slightly decreased in CfzR#1, relative to parental levels (Figure 5.3 B), β2 expression was elevated to a similar extent above parental levels in all three of these cell lines (Figure 5.4 B). Conversely, β2i expression remained below readily detectable levels (data not shown). Finally, α5

expression was increased above parental levels to a similar extent in CfzR#1 and CfzR#2, but was increased to a greater extent in CfzR#3 (Figure 5.4 B). Collectively, these results indicate that, as observed for the bortezomib-withdrawn BtzR cells, the expression levels of each catalytic proteasome subunit in the carfilzomib-withdrawn CfzR cells, taken at face value, are only partially consistent with the activity profiles observed. This suggests that other factors aside from the overall cellular levels of each subunit modulate their catalytic activities. Additionally, these results, too, are consistent with the ability of the CfzR cells to sense the degree of proteasome inhibition and to compensate accordingly following carfilzomib withdrawal.

5.2.6 Identifying Proteasome Subtypes

Our activity assay and immunoblotting analyses clearly demonstrated that the emergence of bortezomib and carfilzomib resistance in H23 cells was accompanied by changes in the overall levels of expression and activity of the various catalytic proteasome subunits. While this supports a shift in the relative abundances of specific proteasome subtypes in the inhibitor-resistant cell lines, the identity of the subtypes formed in each cell line remained elusive. We thus began experiments with the bifunctional proteasome probes described in Chapter 4 to identify, and to determine the relative abundances of, the discrete proteasome subtypes present in the parental and inhibitor-resistant cells. First, we treated lysates from the parental, BtzR#1, and CfzR#2 cell lines with UKP13-$(PEG)_4$-NC012 (probe **6**). U266 cell lysates were also treated with this probe for use as a positive control for detecting catalytic subunit crosslinking. Upon immunoblotting analysis, we found that probe **6** crosslinks β1i in all three H23 cell lines with a single catalytic subunit (Figure 5.5). The band representing crosslinked β1i migrated similarly on the SDS-PAGE gel to the top crosslinked β1i band detected for the U266 cell line, which represents a β1i-β2 crosslinked subunit pair [239] (see also Chapter 4). However, the intensity of this band varied across the three cell lines in a manner that was relatively consistent with the expression level of β1i itself—it was lower than that detected for the parental cells in BtzR#1 and higher in CfzR#2—consistent with most or all β1i-containing subtypes in all three H23 cell lines also containing β2. If, as indicated by previous findings [221-223], β1i-β2-containing subtypes also contain β5i and not β5, then our results indicate that all 3 cell lines predominantly or exclusively harbor β1i-containing subtypes of the β1i-β2-β5i variety but vary in their levels of this subtype.

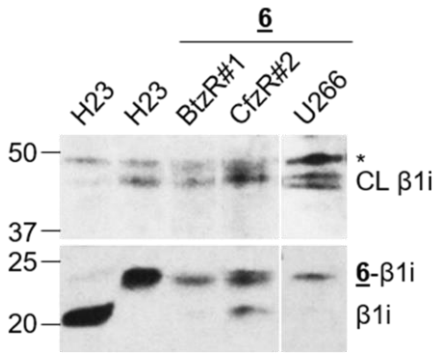

Figure 5.5 Differential regulation of an intermediate proteasome subtype in BtzR and CfzR cell lines
Lysates obtained from the H23 parental, BtzR#1 and CfzR#2 cell lines cultured in the absence of inhibitor for 7 d were treated with probe **6** to crosslink β1i with β2 and/or β2i, and the identity and abundance of the crosslinked subunit pair was evaluated via immunoblotting. A probe **6**-treated lysate obtained from U266 cells, which are known to harbor β1i-containing proteasome subtypes containing either β2 or β2i [239], served as a positive control, while untreated H23 cells (lane 1) served as a negative control. Crosslinked β1i is represented by the band(s) just below 50 kDa. The top crosslinked β1i band detected for the U266 cell line results from β1i-β2 crosslinking, while the bottom crosslinked β1i band results from β1i-β2i crosslinking [239]. The single crosslinked β1i band for the three H23 cell lines aligns with the top crosslinked β1i band detected for the U266 cell line, indicating that the majority of the β1i-containing proteasome subtypes present in the H23 cell lines also contain β2 rather than β2i. Irrelevant lanes were removed. CL = crosslinked β-subunit. * = nonspecific band. *Data acquired with the assistance of Min Jae Lee.*

Our failure to detect β1i-containing subtypes that also contain β2i in any of the H23 cell lines is in agreement with our difficulty in detecting the β2i subunit in these cell lines via immunoblotting with an anti-β2i antibody (Figure 5.5 and data not shown). Whether these cell lines fail to assemble detectable levels of proteasome subtypes containing both β1i and β2i due to their inability to express sufficient levels of β2i remains unknown. As β5i can more promiscuously incorporate into proteasome subtypes containing multiple combinations of catalytic subunits (i.e., β1-β2-β5i, β1i-β2-β5i, and β1i-β2i-β5i) [220-223], it would be interesting to determine whether the relative levels of these β5i-containing subtypes differ between the parental and resistant cell lines, especially since all three cell lines detectably express all of the subunits of the former two subtypes. Although we attempted to evaluate this, we have so far been unable to obtain clear results due to technical difficulties that arose during the immunoblotting experiments. This may be further pursued by other members of our laboratory in the future. Based on the lack of detectable β2i expression, one may expect to find one or two β5i-containing subtypes in these cell lines—β1-β2-β5i and/or β1i-β2-β5i [226]—and, if the relative levels of these

subtypes are altered in the inhibitor-resistant cells, this would indicate that whether β5i is preferentially assembled into β1- or β1i-containing proteasomes when all of these subunits are co-expressed may play a causal role in the resistance phenotypes observed.

5.3 Discussion

We conducted the experiments described in this chapter to test the hypothesis that the altered abundances of specific proteasome subtypes serve as a mechanism of acquired bortezomib and carfilzomib resistance. We were able to establish variants of the H23 NSCLC cell line that survive exposure to a concentration of bortezomib that almost completely inhibits the activities of four of the six catalytic proteasome subunits, and inhibits half of that of the β2-type subunits, in the parental cell line. Additionally, we successfully established variants of this cell line that are resistant to a concentration of carfilzomib that fully inactivates all proteasome activities in the parental cells. We identified specific alterations in the levels of expression and activity of the various catalytic proteasome subunits that were associated with acquired resistance to each inhibitor. These changes were accompanied by the retention of substantial levels of specific proteasome activities in the resistant cell lines under exposure to these inhibitors, consistent with our hypothesis that changes in proteasome composition contribute to acquired proteasome inhibitor resistance.

The most obvious changes in proteasome composition emerging in the BtzR H23 cells following prolonged bortezomib exposure were increases in β5, β1, and β2 expression. We also observed decreased β5i expression in these cells (Figure 5.2 A). These findings are consistent with those obtained with other bortezomib-resistant cell lines [209, 246, 280, 285, 288, 289, 298, 313, 315, 329, 330, 332, 333], indicating that these changes may be generally important in conferring bortezomib resistance.

As observed in bortezomib-exposed parental H23 cells, full inactivation of the β1 and β1i subunits was achieved under continuous bortezomib exposure in both BtzR cell lines (Figure 5.1 A and B). However, residual activities of primary targets β5 and β5i, and especially of weakly-targeted β2 and β2i, appear to compensate for this loss (Figure 5.1 B). Notably, while β5 activity was partially impaired in the bortezomib-exposed BtzR#2 cell line, this activity was in fact elevated over that of untreated parental cells in the BtzR#1 cell line, despite the presence of bortezomib (Figure 5.1 B). The increased rather than suppressed β5 activity detected in BtzR#1 may be attributed in part to upregulation of the β5 subunit; however, a similar effect on β5 activity was not observed in BtzR#2 under

these conditions, despite a comparable degree of β5 upregulation (Figures 5.1 B and 5.2 A). It is possible that BtzR#1 cells could harbor a β5 mutation that impairs bortezomib binding to the β5 active site [246, 289, 298, 311, 313-315], although such a mutation may be expected to similarly impair substrate binding, an effect that has, in fact, been reported for the β5/β5i-selective substrate Suc-LLVY-AMC by other research groups [246, 289, 313]. Therefore, the finding that our BtzR#1 cell line displayed enhanced and not reduced hydrolysis of this substrate may argue against a β5 mutation. Nevertheless, this effect may differ depending on the specific mutation as well as on the substrate used to measure the β5 activity. As inhibitors with different structural properties from those of bortezomib have been suggested to retain greater efficiency in binding mutant β5 subunits than bortezomib itself [246, 280, 298, 315, 318, 337], perhaps the ability of our BtzR cells to hydrolyze the Ac-WLA-AMC substrate could remain largely intact, even if a β5 active site mutation that impairs the hydrolysis of Suc-LLVY-AMC is present. Despite this possibility, bortezomib also inhibited the β5i activity of BtzR#1 more weakly than that of BtzR#2 (Figure 5.1 B), perhaps suggesting a more general mechanism of resilience of these two activities.

We were surprised to find that bortezomib completely inhibited the activities of its secondary targets (β1 and β1i), but not those of its primary targets (β5 and β5i) (Figure 5.1 B). Presuming that bortezomib binding to β5 and β5i is not impaired, and, because free β5 and β5i subunits are not active in the cell (their active forms are instead confined to intact proteasomes, which also contain β1 or β1i), our results may suggest that bortezomib is able to dissociate more readily from the active sites of β5 and β5i than from those of β1 and β1i in the BtzR cell lines. Furthermore, upregulation of β1 in both BtzR cell lines (Figure 5.2 A) was insufficient to prevent the complete depletion of the catalytic activity of this subunit under continuous bortezomib exposure (Figure 5.1 B). This suggests that the upregulation of specific catalytic proteasome subunits alone is insufficient to prevent their full inhibition by exogenous inhibitors, which in turn implies that the upregulation observed may merely be part of a general stress response to proteasome inhibition rather than a cause of resistance. However, the up- and downregulation of specific catalytic proteasome subunits may promote the increased assembly of specific proteasome subtypes whose activities are more resistant to total inhibition by the proteasome inhibitor applied and thereby indirectly contribute to the mechanism of resistance.

Although the observed increase in β2/β2i activity over parental levels in the bortezomib-exposed BtzR cell lines is itself unsurprising, its scale is somewhat surprising. Previously-reported increases in this activity in bortezomib-exposed cells were typically <2-fold [245, 246], whereas we observed an ~4-fold increase (Figure 5.1 B). Additionally, in bortezomib-naïve H23 cells, such an increase was not observed; instead, 150 nM bortezomib partially reduced the β2/β2i activity in the parental cells (Figure 5.1 A). Furthermore, despite the strong elevation of β2/β2i activity above parental levels in both bortezomib-exposed BtzR cell lines (Figure 5.1 B), the increase in β2 expression under these conditions was comparable to that of β1 and β5, and we were still unable to readily detect expression of β2i (Figure 5.2 A and data not shown). This is in further agreement with the conclusion that β2 and β2i expression levels alone cannot account for the observed alterations in β2/β2i activity; other factors likely contributed. For example, it has been reported that inhibiting the proteasome's C-L activity (which is attributed to the β1 subunit) leads to an increase in its T-L activity (which is attributed to the β2 and β2i subunits), an effect that directly results from binding of an inhibitor to the β1 active site [349]. It is possible that such an effect could have contributed to the observed increase in β2/β2i activity in our BtzR cell lines, although, if this were the case, it is unclear why a similar effect was not observed in the parental cell line. Alternatively, an increase in the abundances of proteasome subtypes with high T-L activity, or the association of proteasomes within these cells with a factor that activates this activity, may also account for our observations.

While the higher α5 expression detected for bortezomib-exposed BtzR#2 than for bortezomib-exposed BtzR#1 (Figure 5.2 A) may seem inconsistent with this cell line's comparatively lower proteasome activity (Figure 5.1 B), the latter observation may simply result from stronger proteasome inhibition in BtzR#2 than in BtzR#1. However, unlike the catalytic β-subunits, the α5 subunit is not synthesized with an N-terminal propeptide that is cleaved during the proteasome assembly process, and the unincorporated versus proteasome-incorporated α5 subunits therefore do not differ in molecular weight and are indistinguishable based on immunoblotting. As a result, it is possible that some of the detected α5 has not yet been incorporated into proteasome complexes. Either way, the increased α5 expression of BtzR#2 compared with that of BtzR#1 could indicate that BtzR#1 cells are attempting to compensate for their greater suppression of proteasome activity by further upregulating proteasome expression. This is consistent with the higher

overall expression levels and activities of catalytic proteasome subunits observed in BtzR#2 than in BtzR#1 following withdrawal from bortezomib (as discussed below).

Collectively, these results suggest that the BtzR cells can survive and proliferate without the catalytic activities of β1 and β1i. Perhaps this is only possible due to their high β2/β2i activity and residual β5 and β5i activities, which appear to be important in surviving continuous bortezomib exposure. Residual proteasome activities were also concluded to be important for surviving bortezomib exposure by other research groups [184, 204, 209, 246, 285, 289, 311-313, 337]. Our results also demonstrate that the expression levels of the various catalytic proteasome subunits are altered in bortezomib-resistant cells cultured under continuous bortezomib exposure in comparison with those of untreated parental H23 cells, but that these changes alone cannot account for the observed changes in proteasome activities. These findings are consistent with our hypothesis that changes in proteasome composition contribute to the resistance phenotype by ensuring that substantial catalytic activity is maintained during bortezomib exposure.

We were initially surprised to find that H23 cells could acquire resistance to a concentration of carfilzomib that renders the proteasome completely inactive in the parental cells (Figure 5.1 C). However, the ability of carfilzomib to produce such a profound effect in parental H23 cells was clearly not retained in the CfzR cell lines. As was the case for our BtzR cell lines (Figure 5.1 B), our CfzR cell lines were able to maintain significant proteasome function while under carfilzomib exposure (Figure 5.1 D), although this end was achieved through different means.

All three CfzR cell lines maintained some residual β5 and β5i activities under continuous carfilzomib exposure (Figure 5.1 D), as did both bortezomib-exposed BtzR cell lines (Figure 5.1 B). The finding that β5 expression remained largely similar to parental levels in the three carfilzomib-exposed CfzR cell lines (Figure 5.2 B) contrasts the elevated expression of this subunit observed in our bortezomib-exposed BtzR cell lines (Figure 5.2 A) and demonstrates that β5 overexpression cannot account for the residual β5 activity detected under these conditions. Likewise, the residual β5i activity is not attributable to an upregulation of β5i in the CfzR cells (Figure 5.2 B). Also inconsistent with the residual β5 and β5i activities was our finding that all of the β5 and β5i in these cells detectable by immunoblotting analysis was covalently modified by carfilzomib (Figure 5.2 B). It is therefore possible that these subunits remain completely bound by carfilzomib in the CfzR cell lines, and the perceived residual β5 and β5i activities are, in fact, mediated by non-specific hydrolysis of the substrates used to measure their activities by the uninhibited

subunits. This would be consistent with the notion that uninhibited subunits can compensate for the impaired catalytic activities of those that are inhibited. A similar analysis of bortezomib binding could not be performed for the BtzR cells because, as a consequence of bortezomib's irreversible binding mode, it dissociates from the proteasome's active sites during immunoblotting sample preparation.

Unlike the marked increase in β2/β2i activity detected in our BtzR cell lines cultured under continuous bortezomib exposure (Figure 5.1 B), the activity of these subunits was not upregulated in the carfilzomib-exposed CfzR cell lines (Figure 5.1 D), despite the elevated levels of β2 (Figure 5.2 B). This can be highlighted as a major difference in the responses of H23 cells to the doses of bortezomib and carfilzomib to which resistance could be acquired: β2/β2i activity was only partially inhibited in the parental cells and was strongly increased in our BtzR cell lines, even in the presence of bortezomib (Figures 5.1 A and B), whereas β2/β2i activity was fully inhibited by carfilzomib in the parental cells and remained at approximately parental levels in our CfzR cell lines (Figure 5.1 C and D). Although β2i has been reported as a secondary binding target of carfilzomib, our collective immunoblotting data seem to indicate a lack of significant levels of β2i-containing subtypes in any of these H23 cell lines. Therefore, β2i binding by carfilzomib may not measurably impact the β2/β2i activity detected in our CfzR cell lines. Unfortunately, a better discrimination of catalysis by β2 versus β2i awaits the development of substrates or inhibitors that can effectively distinguish between their two highly similar active sites [75].

In contrast to the unaltered β2/β2i activity, we did observe that β1 activity was elevated above parental levels in the CfzR cell lines, despite the presence of carfilzomib (Figure 5.1 D), an effect associated with only slight increases in β1 expression (Figure 5.2 B). This is also a major difference between the influence of bortezomib and carfilzomib on proteasome activities in the inhibitor-resistant cell lines, as bortezomib completely inhibited this activity in the BtzR lines (Figure 5.1 B). Alternatively, the β1i activity was reduced in comparison with that of the parental cells, although it was not completely suppressed (Figure 5.1 D), unlike the complete inhibition of this activity in the BtzR cell lines under continuous bortezomib exposure (Figure 5.1 B). Finally, the only slight increase observed in α5 levels in the CfzR cell lines (Figure 5.2 B) contrasts the more pronounced upregulation observed in the BtzR cell lines (Figure 5.2 A) and indicates that these cell lines are not compensating for impaired proteasome activity by massively overproducing proteasomes in general.

While activities of shared primary bortezomib and carfilzomib targets β5 and β5i were not those exhibiting the greatest degree of inactivation in our bortezomib-exposed BtzR cell lines (Figure 5.1 B), these were indeed the activities suppressed to the largest extent in our carfilzomib-exposed CfzR cell lines (Figure 5.1 D). This could be due to the irreversible binding mode of carfilzomib, in contrast to the reversible one of bortezomib. Alternatively, it could be due to changes in the proteasome complexes in the BtzR cell lines that lower bortezomib's binding affinity for the β5 and β5i subunits. Also notable is the finding that, despite complete inhibition of all proteasome activities in parental cells treated with 1 μM carfilzomib (Figure 5.1 C), none of these activities were completely inhibited by carfilzomib in the CfzR cell lines (Figure 5.1 D). These results may be consistent with the extrusion of carfilzomib from the CfzR cells by an efflux transporter such as P-glycoprotein, as we have previously observed in an independently generated carfilzomib-resistant H23 cell line [281] and has been reported as a resistance mechanism to carfilzomib [281-283] and epoxomicin [278]. Additionally or alternatively, they may be consistent with other cellular mechanisms operating to similarly prevent sufficient levels of carfilzomib from reaching the proteasome's active sites to achieve a more complete proteasome inhibition in the CfzR cell lines (e.g., altered carfilzomib metabolism). However, our results suggest that at least enough carfilzomib is maintained within the CfzR cells to suppress the activities of its preferred binding targets by a considerable extent. While selectively suppressing these activities was found to be cytotoxic to hematologic cancer cell lines [186], it was found in another study to poorly correlate with proteasome inhibitor-induced cytotoxicity [244]. It is therefore probable that inhibition of only the CT-L activity of the CfzR cell lines—especially while the T-L activity remains unaffected and the C-L activity is activated—is insufficient to arrest cell growth or induce cell death. To what extent the inferior inhibition of proteasome activity in these cell lines results from P-glycoprotein-mediated efflux of carfilzomib, thereby only allowing sufficient levels to accumulate within these cells to inhibit β5 and β5i, from structural changes in proteasome complexes that lower carfilzomib's binding affinity for the β1-type and β2-type subunits, or from some other mechanism, is worth further investigating.

Taken together, our results suggest that increased β1 activity and full retention of β2/β2i activity (perhaps together with residual activities of primary carfilzomib targets β5 and β5i) may be important in surviving continuous exposure to high concentrations of carfilzomib. However, the increased β1 activity of the CfzR cells was not as pronounced as the increased β2/β2i activity observed in the BtzR cells. Perhaps this is due to the

more selective reduction of β5 and β5i activities by carfilzomib in the CfzR cell lines (aside from those of β5 and β5i, carfilzomib did not inhibit any other catalytic activities in the CfzR cells beyond 20-40%) than by bortezomib in the BtzR cell lines (β1 and β1i activities were completely inhibited by bortezomib in the BtzR cells). Therefore, the large increase in one particular activity appears to be less important in maintaining sufficient proteasome activity in the CfzR cells than in the BtzR cells, as, in the CfzR cells, substantial levels of the β1, β1i, β2, and β2i activities remain.

Our findings also confirm that, as for the BtzR cell lines, catalytic proteasome subunit expression levels, in comparison with those of untreated parental H23 cells, are altered in the CfzR cell lines maintained under continuous carfilzomib exposure. Decreased expression of immunosubunits β1i and β5i was perhaps the most pronounced difference observed. This is consistent with a recent report suggesting that immunosubunit expression is important for the cytotoxic effects of carfilzomib in mantle cell lymphoma cells [346]. Furthermore, as observed for the BtzR cell lines, the expression levels of individual catalytic subunits alone cannot account for the observed proteasome activity patterns of the CfzR cells cultured in the continuous presence of carfilzomib. Based on our collective observations, we conclude that these results are consistent with the hypothesis that changes in proteasome composition contribute to the apparently inferior inhibition of total proteasome activity by carfilzomib in the CfzR cell lines, and, therefore, to carfilzomib resistance. However, it is very possible that P-glycoprotein-mediated efflux of carfilzomib also plays a role in dampening its inhibitory efficacy by reducing its intracellular concentrations.

Altered proteasome activity patterns and catalytic subunit expression levels remained apparent in the BtzR and CfzR cell lines following a 7 day inhibitor withdrawal. Since this withdrawal period was sufficient to allow full recovery of the proteasome's catalytic activities, the activity patterns observed under these conditions were uninfluenced by bound inhibitor and, therefore, the level of each catalytic activity measured represents the average level of that activity conferred by the various proteasome subtypes present [224].

The individual proteasome activities of the two BtzR cell lines, relative to those of the parental cell line, were differentially altered: all proteasome activities were increased in BtzR#2, whereas only specific activities (β1 and β2) were elevated in BtzR#1, following bortezomib withdrawal (Figure 5.3 A). Some of the activity assay results did not appear to be in accord with the immunoblotting results obtained. Most notably, although a strong

increase in β2/β2i activity over parental levels was maintained in both BtzR cell lines (Figure 5.3 A), this does not appear to result from a marked overexpression of β2 (Figure 5.4 A). This disparity is also unlikely to be attributed to a large increase in the β2i subunit, since expression of this subunit remained below readily detectable levels (data not shown). Furthermore, we were unable to detect proteasome subtypes containing both β1i and β2i in BtzR#1 (Figure 5.5), and the formation of proteasome subtypes containing β2i combined with constitutive catalytic subunits is disfavored during proteasome assembly [220, 221, 223]. Therefore, other factors in addition to β2 and β2i expression levels likely contributed to the increased β2/β2i activity observed.

As observed for the BtzR cell lines (Figures 5.3 A and 5.4 A), proteasome activity patterns and catalytic subunit expression levels in all three CfzR cell lines following carfilzomib withdrawal differed from those of the parental cell line. Again, some of the immunoblotting results appear to be inconsistent with those obtained via proteasome activity assays. For example, the β1 activity measured following carfilzomib withdrawal (Figure 5.3 B) may be higher than suggested based on β1 expression (Figure 5.4 B). Additionally, despite their differential regulation of β2/β2i activity (Figure 5.3 B), β2 was similarly overexpressed in all three CfzR cell lines following carfilzomib withdrawal (Figure 5.4 B), while we were still unable to readily detect β2i expression (data not shown). Furthermore, our crosslinking results indicate that, in CfzR#2, the cell line with the highest β1i and β5i expression levels and activities and therefore the most likely candidate to harbor β2i-containing proteasomes [221, 223], all detectable β1i-containing subtypes contain β2 rather than β2i (Figure 5.5). Another inconsistency is that, while both CfzR#1 and CfzR#3 displayed equivalent β1i activity following carfilzomib withdrawal, higher levels of the β1i subunit were detected in CfzR#1 than in CfzR#3 (Figure 5.4 B), with both cell lines having an equivalent level of β1i activity (Figure 5.3 B). Interestingly, the β5i expression in these two cell lines was found to bear an inverse relationship to that of β1i—it was higher in CfzR#3 than in CfzR#1 (Figure 5.4 B). This is consistent with the conclusion that these discrepancies are, at least in part, caused by differences in the activity profiles of the more abundant proteasome subtypes formed in each of these cell lines against the fluorogenic peptide substrates used in our study.

Interestingly, in both the BtzR and CfzR cell lines, the more strongly overall proteasome activity was suppressed under inhibitor exposure, the higher overall proteasome activity became following inhibitor withdrawal (Figures 5.1 B and D and 5.3 A and B). However this was achieved (e.g., by a general upregulation of proteasomes,

assembly of altered proteasome subtypes with higher overall activity, association with specific regulatory factors, etc.), it suggests that cells can detect to what extent proteasome activity is suppressed and can respond accordingly to ensure that proteasome activity is increased to the extent required to regain protein homeostasis once the inhibitor has been removed. The finding that BtzR#2 maintained elevated α5 levels, while the levels of this subunit returned from their elevated state back to parental levels in BtzR#1, following bortezomib withdrawal is in line with the conclusion that the greater overall proteasome inhibition by bortezomib in BtzR#2 resulted in a general increase in proteasome components; this is further supported by the higher levels of expression and activity of all proteasome catalytic subunits in BtzR#2 than in BtzR#1 following bortezomib withdrawal (Figure 5.3 A and 5.4 A). Additionally, that CfzR#2 was, following carfilzomib withdrawal, the cell line with the greatest expression levels and activities of immunosubunits β1i and β5i is consistent with the notion that immunosubunit-containing proteasomes may assist in restoring protein homeostasis following withdrawal from proteasome inhibitors [289].

These data indicate that the catalytic subunit composition of proteasomes remains altered in the BtzR and CfzR cell lines after bortezomib and carfilzomib withdrawal. Additionally, they show that the proteolytic activity profiles observed in these cells under these conditions cannot be fully accounted for by the expression levels of each active subunit. These discrepancies may arise from differences in the overall architecture of each proteasome subtype that result from the incorporation of catalytic subunits in distinct permutations; such differences could result in each subtype interacting uniquely with each of the fluorogenic substrates, thereby impacting overall proteasome activity in a manner that does not solely correlate with the expression levels of each individual subunit. Based on these findings, we conclude that the ratios of the various proteasome subtypes are altered in the inhibitor-resistant cell lines from those found in the parental cell line, which supports our hypothesis that such changes may contribute to the reduced efficacy with which proteasome activity is inhibited by bortezomib and carfilzomib. Our crosslinking results are consistent with a reduction in intermediate proteasome subtype β1i-β2-β5i in BtzR#1, which may indicate a relative increase in constitutive proteasomes and/or intermediate proteasomes of composition β1-β2-β5i (Figure 5.5). Alternatively, they indicate an increase in the levels of intermediate proteasome subtype β1i-β2-β5i in CfzR#2, potentially reflecting inhibitor-dependent effects (Figure 5.5). It is therefore possible that differences in the relative levels of distinct proteasome subtypes in each cell

line may contribute to their disparate activity profiles as well as their ability to maintain substantial proteasome activity in the presence of bortezomib and carfilzomib and to regain adequate proteasome activity following inhibitor withdrawal.

In summary, our cell line models of acquired resistance to the proteasome inhibitors bortezomib and carfilzomib exhibited altered proteasome activities and catalytic subunit expression patterns compared with those of the parental cell line from which they were generated, both in the presence or absence of these inhibitors. The changes in these properties seen in the BtzR cell lines differed from those seen in the CfzR cell lines, which is consistent with the different mechanisms by which these inhibitors bind to the proteasome's active sites as well as their different subunit binding preferences. In both BtzR and CfzR cells, these changes appear to reflect a reorganization of proteasome composition, resulting in a shift in the relative ratios of particular proteasome subtypes. Our findings also indicate that the changes observed help to protect the inhibitor-resistant cells from an intolerable extent of proteasome inactivation. That these alterations were observed in all of the inhibitor-resistant cell lines and differed inhibitor-dependently supports the hypothesis that they play a role in conferring bortezomib and carfilzomib resistance. Finally, in both BtzR and CfzR H23 cells, a more pronounced inhibition of proteasome activity was associated with a stronger elevation of total proteasome activity following inhibitor withdrawal, further highlighting the adaptability of the proteasome complexes within these cells.

It is highly likely that multiple mechanisms contribute to the proteasome inhibitor-resistant phenotypes of our BtzR and CfzR cell lines. If P-glycoprotein or other efflux pumps contribute, the effect is not pronounced enough to prevent sufficient accumulation of bortezomib within the BtzR cell lines to fully inactivate their β1 and β1i subunits and partially impair the activities of their β5i (and, for BtzR#2, β5) subunit(s), or to prevent sufficient accumulation of carfilzomib within the CfzR cell lines to cause substantial inhibition of primary carfilzomib targets β5 and β5i. If β5 active site mutations contribute, we may also expect them to impair β5 activity, which we did not observe, and such mutations cannot account for the impaired suppression of β5i activity that was also observed in the inhibitor-exposed BtzR and CfzR cells. Additionally, nonproteasomal proteolytic pathways such as autophagy may also help cells survive when their proteasome activities are reduced [290, 303-306]. However, the ability of our proteasome inhibitor-resistant cells to enhance the activities of the weakly-targeted proteasome subunits—while maintaining at least residual activities of others—suggests that

proteasome activity remains important for their continued survival and proliferation under the continuous pressure exerted by these inhibitors. Future studies of these cell lines should be conducted to evaluate the contribution of each of these other potential resistance mechanisms. Additionally, they should further evaluate whether specific subtypes of proteasomes play a causative role in resistance to each of these inhibitors. The use of the bifunctional probes described in Chapter 4, and of the second-generation probes our laboratory is currently developing, can assist in these studies. Other members of our laboratory are using genetic approaches to evaluate the influence of specific proteasome subtypes on proteasome inhibitor resistance. Finally, determining whether inhibiting the β2/β2i activity in the BtzR cell lines, or inhibiting the β1 activity in the CfzR cell lines, can sensitize them to bortezomib or carfilzomib, respectively, should shed further light upon the relative importance of the upregulation of these activities in acquiring resistance to these inhibitors. The findings from these analyses could provide a rationale for the further development of β2/β2i- and/or β1-selective inhibitors to overcome or circumvent proteasome inhibitor resistance.

The mammalian proteasome is a highly evolved and exquisitely specialized complex that provides critical assistance to a massive array of essential cellular functions. It is therefore not surprising that residual proteasome activities are typically detected in cell line models of acquired proteasome inhibitor resistance upon exposure to their selective inhibitor concentrations. Armed with the ability to recruit different combinations of proteolytically active subunits into assembling 20S core particles, to remain unbound or to associate with a variety of activator complexes at one or both ends, to be allosterically regulated by its substrates or inhibitors, and to have its subunits be upregulated by a feedback loop when its activities have been inhibited, the proteasome is well suited to adapt itself to meet the needs of the cell in the face of a diverse range of cellular insults. Gaining a better understanding of the adaptive responses of the proteasome complex to inhibition of specific proteasome activities will in turn guide the development of proteasome-targeting approaches to block these responses and thereby thwart the onset of proteasome inhibitor resistance.

6 SUMMARY

It is now well-understood that proteasome inhibitor resistance is a major limitation associated with the clinical use of these agents in treating cancers, yet there is currently no consensus regarding the most important factors contributing to clinical cases of this resistance. Mounting evidence has demonstrated that proteasome populations are diverse and can adapt to meet cellular demands. This would be expected to pose challenges for proteasome inhibitor-based therapies. In fact, this is supported by results from an increasing number of studies demonstrating that alterations in proteasome composition and catalytic activities occur when cancer cells acquire proteasome inhibitor resistance, and that these changes are associated with greater proteasome functionality when exposed to these inhibitors. It thus follows that proteasome composition may play an important role in such adaptive responses, since the up- and downregulation of specific proteasome subunits may result in a relative increase in the abundances of proteasome subtypes that are more resilient to inactivation by the drug applied, and a relative decrease in the levels of those that are less resilient. We set out to test this hypothesis in cell line models of acquired bortezomib and carfilzomib resistance derived from the H23 NSCLC cell line.

Methodologies to identify distinct proteasome subtypes were limited when we began our study. We therefore sought to develop new chemical tools to aid us in this process. We generated a series of bifunctional activity-based probes that can crosslink distinct pairs of catalytic proteasome subunits within intact proteasome complexes and facilitate immunoblotting-based detection of the crosslinked subunit pairs. These probes proved useful in detecting proteasome subtypes with distinct combinations of catalytic subunits. Additionally, results obtained using these probes provided further evidence to support previously drawn conclusions regarding which combinations of catalytic subunits are permissible and which are discouraged when all six of these subunits are coexpressed. Our bifunctional proteasome probes should be useful not only in associating specific subtypes with sensitivity or resistance to a particular proteasome inhibitor, but also in other studies of proteasome function in both normal and diseased cells.

We also derived cell line models of acquired bortezomib and carfilzomib resistance from the H23 NSCLC cell line in order to test our hypothesis that proteasome catalytic subunit composition is an important mediator of resistance to these inhibitors. We identified changes in the expression levels and activities of individual catalytic proteasome subunits that were associated with the onset of acquired resistance to each inhibitor.

These changes were consistent with a shift in the relative abundances of the various proteasome subtypes, and their inhibitor-dependency and consistency across cell lines support a causative role in the resistance phenotypes observed. Additionally, we observed a graded response to inhibition across these cell lines in which stronger inhibition of total proteasome activity was associated with a greater enhancement following inhibitor withdrawal, highlighting the ability of the proteasome complex to adapt to the appropriate degree to restore protein homeostasis when it is no longer under attack. Finally, the initial dataset obtained using one of our bifunctional proteasome probes indicates that β1i-containing proteasome subtypes in the parental and inhibitor-resistant H23 cells are predominantly intermediate proteasomes that also contain the constitutive catalytic subunit β2. We found that this subtype was downregulated in a bortezomib-resistant cell line, and upregulated in a carfilzomib-resistant cell line. Taken together, our results indicate that alterations in the levels of specific proteasome subtypes occur when cells acquire resistance to either bortezomib or carfilzomib, and support the hypothesis that these changes play a role in conferring resistance to these inhibitors.

Although we initiated experiments to examine the relative abundances of specific proteasome subtypes in our parental and inhibitor-resistant cell lines, additional efforts are needed in this realm to gain a true understanding of which specific proteasome subtypes are important in conferring resistance to each inhibitor. Experiments involving the use of our bifunctional probes in inhibitor-sensitive and -resistant cell lines, as well as those involving genetic approaches, are underway in our laboratory to further investigate this. Additionally, our laboratory is working to determine whether the elevated proteasome activities detected in inhibitor-resistant cell lines can serve as co-targets for inhibitors and thereby allow improved anticancer activity to be achieved. Furthermore, it is unlikely that changes in the proteasome complex serve as the sole mediator of bortezomib or carfilzomib resistance. Moving forward, it will therefore be important to evaluate to what extent each potential resistance mechanism contributes to the resistance phenotypes observed. If specific subtypes involved in conferring resistance to each inhibitor can be identified, the development of inhibitors that specifically target those subtypes, rather than a specific subunit or set of subunits, may be worthwhile.

REFERENCES

1. Ciechanover, A., *Proteolysis: from the lysosome to ubiquitin and the proteasome.* Nature Reviews: Molecular Cell Biology, 2005. **6**(1): p. 79-87.
2. Ciechanover, A., *Intracellular Protein Degradation: From a Vague Idea, through the Lysosome and the Ubiquitin–Proteasome System, and onto Human Diseases and Drug Targeting (Nobel Lecture).* Angewandte Chemie International Edition, 2005. **44**(37): p. 5944-5967.
3. Hershko, A., et al., *Proposed role of ATP in protein breakdown: conjugation of protein with multiple chains of the polypeptide of ATP-dependent proteolysis.* Proceedings of the National Academy of Sciences, 1980. **77**(4): p. 1783-1786.
4. Hershko, A., A. Ciechanover, and I.A. Rose, *Identification of the active amino acid residue of the polypeptide of ATP-dependent protein breakdown.* Journal of Biological Chemistry, 1981. **256**(4): p. 1525-1528.
5. Ciechanover, A., et al., *Activation of the heat-stable polypeptide of the ATP-dependent proteolytic system.* Proceedings of the National Academy of Sciences, 1981. **78**(2): p. 761-765.
6. Ciechanover, A., et al., *"Covalent affinity" purification of ubiquitin-activating enzyme.* Journal of Biological Chemistry, 1982. **257**(5): p. 2537-2542.
7. Hershko, A., et al., *Components of ubiquitin-protein ligase system. Resolution, affinity purification, and role in protein breakdown.* Journal of Biological Chemistry, 1983. **258**(13): p. 8206-14.
8. Chau, V., et al., *A Multiubiquitin Chain is Confined to Specific Lysine in a Targeted Short-Lived Protein.* Science, 1989. **243**(4898): p. 1576-1583.
9. Finley, D., et al., *Inhibition of proteolysis and cell cycle progression in a multiubiquitination-deficient yeast mutant.* Molecular and Cellular Biology, 1994. **14**(8): p. 5501-5509.
10. Thrower, J.S., et al., *Recognition of the polyubiquitin proteolytic signal.* The EMBO Journal, 2000. **19**(1): p. 94-102.
11. Wilk, S., S. Pearce, and M. Orlowski, *Identification and partial purification of a cation-sensitive neutral endopeptidase from bovine pituitaries.* Life Sciences, 1979. **24**(5): p. 457-64.
12. Wilk, S. and M. Orlowski, *Cation-Sensitive Neutral Endopeptidase: Isolation and Specificity of the Bovine Pituitary Enzyme.* Journal of Neurochemistry, 1980. **35**(5): p. 1172-1182.
13. Orlowski, N. and S. Wilk, *A multicatalytical protease complex from pituitary that forms enkephalin and enkephalin containing peptides.* Biochemical and Biophysical Research Communications, 1981. **101**(3): p. 814-822.
14. Kisselev, A.F., et al., *Proteasome Active Sites Allosterically Regulate Each Other, Suggesting a Cyclical Bite-Chew Mechanism for Protein Breakdown.* Molecular Cell, 1999. **4**(3): p. 395-402.
15. Orlowski, M., C. Cardozo, and C. Michaud, *Evidence for the presence of five distinct proteolytic components in the pituitary multicatalytic proteinase complex. Properties of two components cleaving bonds on the carboxyl side of branched chain and small neutral amino acids.* Biochemistry, 1993. **32**(6): p. 1563-1572.
16. Peters, J.-M., et al., *Structural Features of the 26 S Proteasome Complex.* Journal of Molecular Biology, 1993. **234**(4): p. 932-937.
17. Deveraux, Q., et al., *A 26 S protease subunit that binds ubiquitin conjugates.* Journal of Biological Chemistry, 1994. **269**(10): p. 7059-7061.
18. Husnjak, K., et al., *Proteasome subunit Rpn13 is a novel ubiquitin receptor.* Nature, 2008. **453**(7194): p. 481-488.

19. Braun, B.C., et al., *The base of the proteasome regulatory particle exhibits chaperone-like activity.* Nature Cell Biology, 1999. **1**(4): p. 221-226.
20. Liu, C.-w., et al., *Conformational Remodeling of Proteasomal Substrates by PA700, the 19 S Regulatory Complex of the 26 S Proteasome.* Journal of Biological Chemistry, 2002. **277**(30): p. 26815-26820.
21. Verma, R., et al., *Role of Rpn11 Metalloprotease in Deubiquitination and Degradation by the 26S Proteasome.* Science, 2002. **298**(5593): p. 611-615.
22. Yao, T. and R.E. Cohen, *A cryptic protease couples deubiquitination and degradation by the proteasome.* Nature, 2002. **419**(6905): p. 403.
23. Śledź, P., et al., *Structure of the 26S proteasome with ATP-γS bound provides insights into the mechanism of nucleotide-dependent substrate translocation.* Proceedings of the National Academy of Sciences, 2013. **110**(18): p. 7264-7269.
24. Dahlmann, B., et al., *The multicatalytic proteinase (prosome) is ubiquitous from eukaryotes to archaebacteria.* FEBS Letters, 1989. **251**(1-2): p. 125-131.
25. Pühler, G., et al., *Subunit stoichiometry and three-dimensional arrangement in proteasomes from Thermoplasma acidophilum.* The EMBO Journal, 1992. **11**(4): p. 1607-1616.
26. Heinemeyer, W., et al., *PRE5 and PRE6, the Last Missing Genes Encoding 20S Proteasome Subunits from Yeast? Indication for a Set of 14 Different Subunits in the Eukaryotic Proteasome Core.* Biochemistry, 1994. **33**(40): p. 12229-12237.
27. Kopp, F., et al., *Subunit arrangement in the human 20S proteasome.* Proceedings of the National Academy of Sciences, 1997. **94**(7): p. 2939-2944.
28. Groll, M., et al., *A gated channel into the proteasome core particle.* Nature Structural Biology, 2000. **7**(11): p. 1062-1067.
29. Brannigan, J.A., et al., *A protein catalytic framework with an N-terminal nucleophile is capable of self-activation.* Nature, 1995. **378**(6555): p. 416-419.
30. Lowe, J., et al., *Crystal structure of the 20S proteasome from the archaeon T. acidophilum at 3.4 A resolution.* Science, 1995. **268**(5210): p. 533-9.
31. Heinemeyer, W., et al., *The Active Sites of the Eukaryotic 20 S Proteasome and Their Involvement in Subunit Precursor Processing.* Journal of Biological Chemistry, 1997. **272**(40): p. 25200-25209.
32. Seemuller, E., et al., *Proteasome from Thermoplasma acidophilum: a threonine protease.* Science, 1995. **268**(5210): p. 579-582.
33. Groll, M., et al., *Structure of 20S proteasome from yeast at 2.4 A resolution.* Nature, 1997. **386**(6624): p. 463-71.
34. Früh, K., et al., *Alternative exon usage and processing of the major histocompatibility complex-encoded proteasome subunits.* Journal of Biological Chemistry, 1992. **267**(31): p. 22131-40.
35. Frentzel, S., et al., *Isolation and characterization of the MHC linked β-type proteasome subunit MC13 cDNA.* FEBS Letters, 1992. **302**(2): p. 121-125.
36. Frentzel, S., et al., *20 S proteasomes are assembled via distinct precursor complexes processing of LMP2 and LMP7 proproteins takes place in 13–16 S preproteasome complexes.* Journal of Molecular Biology, 1994. **236**(4): p. 975-981.
37. Seemuller, E., A. Lupas, and W. Baumeister, *Autocatalytic processing of the 20S proteasome.* Nature, 1996. **382**(6590): p. 468-470.
38. Chen, P. and M. Hochstrasser, *Autocatalytic Subunit Processing Couples Active Site Formation in the 20S Proteasome to Completion of Assembly.* Cell, 1996. **86**(6): p. 961-972.

39. Schmidtke, G., et al., *Analysis of mammalian 20S proteasome biogenesis: the maturation of beta-subunits is an ordered two-step mechanism involving autocatalysis.* The EMBO Journal, 1996. **15**(24): p. 6887-6898.
40. Schmidtke, G., M. Schmidt, and P.M. Kloetzel, *Maturation of mammalian 20 S proteasome: purification and characterization of 13 S and 16 S proteasome precursor complexes.* Journal of Molecular Biology, 1997. **268**(1): p. 95-106.
41. Ditzel, L., et al., *Conformational constraints for protein self-cleavage in the proteasome.* Journal of Molecular Biology, 1998. **279**(5): p. 1187-1191.
42. Kisselev, A.F., et al., *The Sizes of Peptides Generated from Protein by Mammalian 26 and 20 S Proteasomes: IMPLICATIONS FOR UNDERSTANDING THE DEGRADATIVE MECHANISM AND ANTIGEN PRESENTATION.* Journal of Biological Chemistry, 1999. **274**(6): p. 3363-3371.
43. Cascio, P., et al., *26S proteasomes and immunoproteasomes produce mainly N-extended versions of an antigenic peptide.* EMBO Journal, 2001. **20**(10): p. 2357-2366.
44. Saric, T., C.I. Graef, and A.L. Goldberg, *Pathway for Degradation of Peptides Generated by Proteasomes: A KEY ROLE FOR THIMET OLIGOPEPTIDASE AND OTHER METALLOPEPTIDASES.* Journal of Biological Chemistry, 2004. **279**(45): p. 46723-46732.
45. Beninga, J., K.L. Rock, and A.L. Goldberg, *Interferon-γ Can Stimulate Post-proteasomal Trimming of the N Terminus of an Antigenic Peptide by Inducing Leucine Aminopeptidase.* Journal of Biological Chemistry, 1998. **273**(30): p. 18734-18742.
46. Stoltze, L., et al., *Generation of the vesicular stomatitis virus nucleoprotein cytotoxic T lymphocyte epitope requires proteasome-dependent and -independent proteolytic activities.* European Journal of Immunology, 1998. **28**(12): p. 4029-4036.
47. Yewdell, J.W., E. Reits, and J. Neefjes, *Making sense of mass destruction: quantitating MHC class I antigen presentation.* Nature Reviews: Immunology, 2003. **3**(12): p. 952-961.
48. Groll, M. and R. Huber, *Inhibitors of the eukaryotic 20S proteasome core particle: a structural approach.* Biochimica et Biophysica Acta (BBA) - Molecular Cell Research, 2004. **1695**(1–3): p. 33-44.
49. Groll, M., et al., *The catalytic sites of 20S proteasomes and their role in subunit maturation: A mutational and crystallographic study.* Proceedings of the National Academy of Sciences of the United States of America, 1999. **96**(20): p. 10976-10983.
50. Groettrup, M., et al., *The Interferon-γ-inducible 11 S Regulator (PA28) and the LMP2/LMP7 Subunits Govern the Peptide Production by the 20 S Proteasome in Vitro.* Journal of Biological Chemistry, 1995. **270**(40): p. 23808-23815.
51. Etlinger, J.D. and A.L. Goldberg, *A soluble ATP-dependent proteolytic system responsible for the degradation of abnormal proteins in reticulocytes.* Proceedings of the National Academy of Sciences of the United States of America, 1977. **74**(1): p. 54-58.
52. Hershko, A., et al., *Immunochemical analysis of the turnover of ubiquitin-protein conjugates in intact cells. Relationship to the breakdown of abnormal proteins.* Journal of Biological Chemistry, 1982. **257**(23): p. 13964-70.
53. Ciechanover, A., D. Finley, and A. Varshavsky, *Ubiquitin dependence of selective protein degradation demonstrated in the mammalian cell cycle mutant ts85.* Cell, 1984. **37**(1): p. 57-66.

54. Glotzer, M., A.W. Murray, and M.W. Kirschner, *Cyclin is degraded by the ubiquitin pathway.* Nature, 1991. **349**(6305): p. 132-138.
55. Ciechanover, A., et al., *Degradation of nuclear oncoproteins by the ubiquitin system in vitro.* Proceedings of the National Academy of Sciences of the United States of America, 1991. **88**(1): p. 139-143.
56. Shkedy, D., et al., *Complete reconstitution of conjugation and subsequent degradation of the tumor suppressor protein p53 by purified components of the ubiquitin proteolytic system.* FEBS Letters, 1994. **348**(2): p. 126-130.
57. Monaco, J.J. and H.O. McDevitt, *Identification of a fourth class of proteins linked to the murine major histocompatibility complex.* Proceedings of the National Academy of Sciences of the United States of America, 1982. **79**(9): p. 3001-3005.
58. Monaco, J.J. and H.O. McDevitt, *H-2-linked low-molecular weight polypeptide antigens assemble into an unusual macromolecular complex.* Nature, 1984. **309**(5971): p. 797-799.
59. Monaco, J.J. and H.O. McDevitt, *The LMP antigens: A stable MHC-controlled multisubunit protein complex.* Human Immunology, 1986. **15**(4): p. 416-426.
60. Brown, M.G., J. Driscoll, and J.J. Monaco, *Structural and serological similarity of MHC-linked LMP and proteasome (multicatalytic proteinase) complexes.* Nature, 1991. **353**(6342): p. 355-357.
61. Monaco, J., S. Cho, and M. Attaya, *Transport protein genes in the murine MHC: possible implications for antigen processing.* Science, 1990. **250**(4988): p. 1723-1726.
62. Monaco, J.J., *A molecular model of MHC class-I-restricted antigen processing.* Immunology Today, 1992. **13**(5): p. 173-179.
63. Brown, M., J. Driscoll, and J. Monaco, *MHC-linked low-molecular mass polypeptide subunits define distinct subsets of proteasomes. Implications for divergent function among distinct proteasome subsets.* Journal of Immunology, 1993. **151**(3): p. 1193-1204.
64. Aki, M., et al., *Interferon-gamma Induces Different Subunit Organizations and Functional Diversity of Proteasomes.* The Journal of Biochemistry, 1994. **115**(2): p. 257-269.
65. Akiyama, K., et al., *Replacement of proteasome subunits X and Y by LMP7 and LMP2 induced by interferon-γ for acquirement of the functional diversity responsible for antigen processing.* FEBS Letters, 1994. **343**(1): p. 85-88.
66. Früh, K., et al., *Displacement of housekeeping proteasome subunits by MHC-encoded LMPs: a newly discovered mechanism for modulating the multicatalytic proteinase complex.* The EMBO Journal, 1994. **13**(14): p. 3236-3244.
67. Gaczynska, M., K.L. Rock, and A.L. Goldberg, *[gamma]-Interferon and expression of MHC genes regulate peptide hydrolysis by proteasomes.* Nature, 1993. **365**(6443): p. 264-267.
68. Gaczynska, M., et al., *Peptidase activities of proteasomes are differentially regulated by the major histocompatibility complex-encoded genes for LMP2 and LMP7.* Proceedings of the National Academy of Sciences of the United States of America, 1994. **91**(20): p. 9213-9217.
69. Gaczynska, M., et al., *Proteasome Subunits X and Y Alter Peptidase Activities in Opposite Ways to the Interferon-γ-induced Subunits LMP2 and LMP7.* Journal of Biological Chemistry, 1996. **271**(29): p. 17275-17280.
70. Groettrup, M., et al., *A third interferon-γ-induced subunit exchange in the 20S proteasome.* European Journal of Immunology, 1996. **26**(4): p. 863-869.

71. Hisamatsu, H., et al., *Newly identified pair of proteasomal subunits regulated reciprocally by interferon gamma.* The Journal of Experimental Medicine, 1996. **183**(4): p. 1807-1816.
72. Larsen, F., et al., *A tight cluster of five unrelated human genes on chromosome 16q22.1.* Human Molecular Genetics, 1993. **2**(10): p. 1589-1595.
73. Nandi, D., H. Jiang, and J. Monaco, *Identification of MECL-1 (LMP-10) as the third IFN-gamma-inducible proteasome subunit.* Journal of Immunology, 1996. **156**(7): p. 2361-2364.
74. Unno, M., et al., *The Structure of the Mammalian 20S Proteasome at 2.75 Å Resolution.* Structure, 2002. **10**(5): p. 609-618.
75. Huber, Eva M., et al., *Immuno- and Constitutive Proteasome Crystal Structures Reveal Differences in Substrate and Inhibitor Specificity.* Cell, 2012. **148**(4): p. 727-738.
76. Blackburn, C., et al., *Characterization of a new series of non-covalent proteasome inhibitors with exquisite potency and selectivity for the 20S β5-subunit.* Biochemical Journal, 2010. **430**(3): p. 461-476.
77. Frentzel, S., et al., *The major-histocompatibility-complex-encoded β-type proteasome subunits LMP2 and LMP7.* European Journal of Biochemistry, 1993. **216**(1): p. 119-126.
78. Stohwasser, R., et al., *Molecular cloning of the mouse proteasome subunits MC14 and MECL-1: reciprocally regulated tissue expression of interferon-γ-modulated proteasome subunits.* European Journal of Immunology, 1997. **27**(5): p. 1182-1187.
79. Foss, G.S., et al., *Constitutive and interferon-γ-induced expression of the human proteasome subunit multicatalytic endopeptidase complex-like 11.* Biochimica et Biophysica Acta (BBA) - Molecular Cell Research, 1998. **1402**(1): p. 17-28.
80. Rock, K.L., et al., *Inhibitors of the proteasome block the degradation of most cell proteins and the generation of peptides presented on MHC class I molecules.* Cell, 1994. **78**(5): p. 761-771.
81. Craiu, A., et al., *Lactacystin and clasto-Lactacystin β-Lactone Modify Multiple Proteasome β-Subunits and Inhibit Intracellular Protein Degradation and Major Histocompatibility Complex Class I Antigen Presentation.* Journal of Biological Chemistry, 1997. **272**(20): p. 13437-13445.
82. Schwarz, K., et al., *Overexpression of the Proteasome Subunits LMP2, LMP7, and MECL-1, But Not PA28α/β, Enhances the Presentation of an Immunodominant Lymphocytic Choriomeningitis Virus T Cell Epitope.* The Journal of Immunology, 2000. **165**(2): p. 768-778.
83. Fehling, H., et al., *MHC class I expression in mice lacking the proteasome subunit LMP-7.* Science, 1994. **265**(5176): p. 1234-1237.
84. Tu, L., et al., *Critical role for the immunoproteasome subunit LMP7 in the resistance of mice to Toxoplasma gondii infection.* European Journal of Immunology, 2009. **39**(12): p. 3385-3394.
85. Van Kaer, L., et al., *Altered peptidase and viral-specific T cell response in LMP2 mutant mice.* Immunity, 1994. **1**(7): p. 533-541.
86. Caudill, C.M., et al., *T Cells Lacking Immunoproteasome Subunits MECL-1 and LMP7 Hyperproliferate in Response to Polyclonal Mitogens.* The Journal of Immunology, 2006. **176**(7): p. 4075-4082.
87. Basler, M., et al., *An Altered T Cell Repertoire in MECL-1-Deficient Mice.* The Journal of Immunology, 2006. **176**(11): p. 6665-6672.

88. Hayashi, T. and D.L. Faustman, *Development of Spontaneous Uterine Tumors in Low Molecular Mass Polypeptide-2 Knockout Mice.* Cancer Research, 2002. **62**(1): p. 24-27.
89. Zaiss, D.M.W., et al., *Proteasome Immunosubunits Protect against the Development of CD8 T Cell-Mediated Autoimmune Diseases.* The Journal of Immunology, 2011. **187**(5): p. 2302-2309.
90. Arnold, D., et al., *Proteasome subunits encoded in the MHC are not generally required for the processing of peptides bound by MHC class I molecules.* Nature, 1992. **360**(6400): p. 171-174.
91. Momburg, F., et al., *Proteasome subunits encoded by the major histocompatibility complex are not essential for antigen presentation.* Nature, 1992. **360**(6400): p. 174-177.
92. Schmidtke, G., et al., *Inactivation of a Defined Active Site in the Mouse 20S Proteasome Complex Enhances Major Histocompatibility Complex Class I Antigen Presentation of a Murine Cytomegalovirus Protein.* The Journal of Experimental Medicine, 1998. **187**(10): p. 1641-1646.
93. Chen, W., et al., *Immunoproteasomes Shape Immunodominance Hierarchies of Antiviral Cd8+ T Cells at the Levels of T Cell Repertoire and Presentation of Viral Antigens.* The Journal of Experimental Medicine, 2001. **193**(11): p. 1319-1326.
94. Pang, K.C., et al., *Immunoproteasome Subunit Deficiencies Impact Differentially on Two Immunodominant Influenza Virus-Specific CD8+ T Cell Responses.* The Journal of Immunology, 2006. **177**(11): p. 7680-7688.
95. Chapiro, J., et al., *Destructive Cleavage of Antigenic Peptides Either by the Immunoproteasome or by the Standard Proteasome Results in Differential Antigen Presentation.* The Journal of Immunology, 2006. **176**(2): p. 1053-1061.
96. Morel, S., et al., *Processing of Some Antigens by the Standard Proteasome but Not by the Immunoproteasome Results in Poor Presentation by Dendritic Cells.* Immunity, 2000. **12**(1): p. 107-117.
97. Basler, M., et al., *Immunoproteasomes Down-Regulate Presentation of a Subdominant T Cell Epitope from Lymphocytic Choriomeningitis Virus.* Journal of Immunology, 2004. **173**(6): p. 3925-3934.
98. Nussbaum, A.K., et al., *Immunoproteasome-Deficient Mice Mount Largely Normal CD8+ T Cell Responses to Lymphocytic Choriomeningitis Virus Infection and DNA Vaccination.* Journal of Immunology, 2005. **175**(2): p. 1153-1160.
99. Zaiss, D.M.W., N. de Graaf, and A.J.A.M. Sijts, *The Proteasome Immunosubunit Multicatalytic Endopeptidase Complex-Like 1 Is a T-Cell-Intrinsic Factor Influencing Homeostatic Expansion.* Infection and Immunity, 2008. **76**(3): p. 1207-1213.
100. Moebius, J., et al., *Immunoproteasomes are essential for survival and expansion of T cells in virus-infected mice.* European Journal of Immunology, 2010. **40**(12): p. 3439-3449.
101. Muchamuel, T., et al., *A selective inhibitor of the immunoproteasome subunit LMP7 blocks cytokine production and attenuates progression of experimental arthritis.* Nature Medicine, 2009. **15**(7): p. 781-787.
102. Kalim, K.W., et al., *Immunoproteasome Subunit LMP7 Deficiency and Inhibition Suppresses Th1 and Th17 but Enhances Regulatory T Cell Differentiation.* The Journal of Immunology, 2012. **189**(8): p. 4182-4193.
103. Hensley, S.E., et al., *Unexpected Role for the Immunoproteasome Subunit LMP2 in Antiviral Humoral and Innate Immune Responses.* Journal of Immunology, 2010. **184**(8): p. 4115-4122.

104. Basler, M., et al., *Prevention of Experimental Colitis by a Selective Inhibitor of the Immunoproteasome.* The Journal of Immunology, 2010. **185**(1): p. 634-641.
105. Rockwell, C.E., J.J. Monaco, and N. Qureshi, *A Critical Role for the Inducible Proteasomal Subunits LMP7 and MECL1 in Cytokine Production by Activated Murine Splenocytes.* Pharmacology, 2012. **89**(3-4): p. 117-126.
106. Basler, M., et al., *Inhibition of the immunoproteasome ameliorates experimental autoimmune encephalomyelitis.* EMBO Molecular Medicine, 2014. **6**(2): p. 226-238.
107. Ferrington, D.A., et al., *Immunoproteasome responds to injury in the retina and brain.* Journal of Neurochemistry, 2008. **106**(1): p. 158-169.
108. Díaz-Hernández, M., et al., *Neuronal Induction of the Immunoproteasome in Huntington's Disease.* Journal of Neuroscience, 2003. **23**(37): p. 11653-11661.
109. Mishto, M., et al., *Immunoproteasome and LMP2 polymorphism in aged and Alzheimer's disease brains.* Neurobiology of Aging, 2006. **27**(1): p. 54-66.
110. Kotamraju, S., et al., *Upregulation of immunoproteasomes by nitric oxide: Potential antioxidative mechanism in endothelial cells.* Free Radical Biology and Medicine, 2006. **40**(6): p. 1034-1044.
111. Pickering, Andrew M., et al., *The immunoproteasome, the 20S proteasome and the PA28αβ proteasome regulator are oxidative-stress-adaptive proteolytic complexes.* Biochemical Journal, 2010. **432**(3): p. 585-595.
112. Seifert, U., et al., *Immunoproteasomes Preserve Protein Homeostasis upon Interferon-Induced Oxidative Stress.* Cell, 2010. **142**(4): p. 613-624.
113. Zu, L., et al., *Evidence for a role of immunoproteasomes in regulating cardiac muscle mass in diabetic mice.* Journal of Molecular and Cellular Cardiology, 2010. **49**(1): p. 5-15.
114. Hayashi, T. and D. Faustman, *NOD Mice Are Defective in Proteasome Production and Activation of NF-κB.* Molecular and Cellular Biology, 1999. **19**(12): p. 8646-8659.
115. Kessler, B.M., et al., *LMP2 expression and proteasome activity in NOD mice.* Nature Medicine, 2000. **6**(10): p. 1064.
116. Runnels, H.A., W.A. Watkins, and J.J. Monaco, *LMP2 expression and proteasome activity in NOD mice.* Nature Medicine, 2000. **6**(10): p. 1064.
117. Hayashi, T., S. Kodama, and D.L. Faustman, *Reply to 'LMP2 expression and proteasome activity in NOD mice'.* Nature Medicine, 2000. **6**(10): p. 1065.
118. Jang, E.R., et al., *Revisiting the role of the immunoproteasome in the activation of the canonical NF-κB pathway.* Molecular BioSystems, 2012. **8**(9): p. 2295-2302.
119. Fujiwara, T., et al., *Proteasomes are essential for yeast proliferation. cDNA cloning and gene disruption of two major subunits.* Journal of Biological Chemistry, 1990. **265**(27): p. 16604-13.
120. Salter, R.D., D.N. Howell, and P. Cresswell, *Genes regulating HLA class I antigen expression in T-B lymphoblast hybrids.* Immunogenetics, 1985. **21**(3): p. 235-46.
121. Ortiz-Navarrete, V., et al., *Subunit of the '20S' proteasome (multicatalytic proteinase) encoded by the major histocompatibility complex.* Nature, 1991. **353**(6345): p. 662-664.
122. Murata, S., et al., *Regulation of CD8+ T Cell Development by Thymus-Specific Proteasomes.* Science, 2007. **316**(5829): p. 1349-1353.
123. Nitta, T., et al., *Thymoproteasome Shapes Immunocompetent Repertoire of $CD8^+$ T Cells.* Immunity, 2010. **32**(1): p. 29-40.

124. Xing, Y., S.C. Jameson, and K.A. Hogquist, *Thymoproteasome subunit-β5T generates peptide-MHC complexes specialized for positive selection.* Proceedings of the National Academy of Sciences of the United States of America, 2013. **110**(17): p. 6979-6984.
125. Sasaki, K., et al., *Thymoproteasomes produce unique peptide motifs for positive selection of CD8+ T cells.* Nature Communications, 2015. **6**.
126. Murata, S., Y. Takahama, and K. Tanaka, *Thymoproteasome: probable role in generating positively selecting peptides.* Current Opinion in Immunology, 2008. **20**(2): p. 192-196.
127. Bevan, M.J., *The Cutting Edge of T Cell Selection.* Science, 2007. **316**(5829): p. 1291-1292.
128. Vinitsky, A., et al., *Inhibition of the chymotrypsin-like activity of the pituitary multicatalytic proteinase complex.* Biochemistry, 1992. **31**(39): p. 9421-9428.
129. Maki, C.G., J.M. Huibregtse, and P.M. Howley, *In Vivo Ubiquitination and Proteasome-mediated Degradation of p53.* Cancer Research, 1996. **56**(11): p. 2649-2654.
130. Pagano, M., et al., *Role of the ubiquitin-proteasome pathway in regulating abundance of the cyclin-dependent kinase inhibitor p27.* Science, 1995. **269**(5224): p. 682-685.
131. Sadoul, R., et al., *Involvement of the proteasome in the programmed cell death of NGF-deprived sympathetic neurons.* EMBO Journal, 1996. **15**(15): p. 3845-52.
132. Grimm, L.M., et al., *Proteasomes play an essential role in thymocyte apoptosis.* EMBO Journal, 1996. **15**(15): p. 3835-44.
133. Palombella, V.J., et al., *The ubiquitinproteasome pathway is required for processing the NF-κB1 precursor protein and the activation of NF-κB.* Cell, 1994. **78**(5): p. 773-785.
134. Adams, J., et al., *Proteasome Inhibitors: A Novel Class of Potent and Effective Antitumor Agents.* Cancer Research, 1999. **59**(11): p. 2615-2622.
135. Shinohara, K., et al., *Apoptosis induction resulting from proteasome inhibition.* Biochemical Journal, 1996. **317**(2): p. 385-388.
136. Drexler, H.C.A., *Activation of the cell death program by inhibition of proteasome function.* Proceedings of the National Academy of Sciences of the United States of America, 1997. **94**(3): p. 855-860.
137. Orlowski, R.Z., et al., *Tumor Growth Inhibition Induced in a Murine Model of Human Burkitt's Lymphoma by a Proteasome Inhibitor.* Cancer Research, 1998. **58**(19): p. 4342-4348.
138. Kudo, Y., et al., *p27Kip1 Accumulation by Inhibition of Proteasome Function Induces Apoptosis in Oral Squamous Cell Carcinoma Cells.* Clinical Cancer Research, 2000. **6**(3): p. 916-923.
139. Soligo, D., et al., *The apoptogenic response of human myeloid leukaemia cell lines and of normal and malignant haematopoietic progenitor cells to the proteasome inhibitor PSI.* British Journal of Haematology, 2001. **113**(1): p. 126-135.
140. Saito, Y., et al., *The structure-function relationship between peptide aldehyde derivatives on initiation of neurite outgrowth in PC12h cells.* Neuroscience Letters, 1990. **120**(1): p. 1-4.
141. Tsubuki, S., et al., *Purification and Characterization of a Z-Leu-Leu-Leu-MCA Degrading Protease Expected to Regulate Neurite Formation: A Novel Catalytic Activity in Proteasome.* Biochemical and Biophysical Research Communications, 1993. **196**(3): p. 1195-1201.

142. Adams, J., et al., *Potent and selective inhibitors of the proteasome: Dipeptidyl boronic acids.* Bioorganic & Medicinal Chemistry Letters, 1998. **8**(4): p. 333-338.
143. Adams, J., *Preclinical and clinical evaluation of proteasome inhibitor PS-341 for the treatment of cancer.* Current Opinion in Chemical Biology, 2002. **6**(4): p. 493-500.
144. Mc Cormack, T., et al., *Active Site-directed Inhibitors of Rhodococcus 20 S Proteasome: KINETICS AND MECHANISM.* Journal of Biological Chemistry, 1997. **272**(42): p. 26103-26109.
145. Groll, M., et al., *Crystal Structure of the Boronic Acid-Based Proteasome Inhibitor Bortezomib in Complex with the Yeast 20S Proteasome.* Structure, 2006. **14**(3): p. 451-456.
146. Adams, J., *The development of proteasome inhibitors as anticancer drugs.* Cancer Cell, 2004. **5**(5): p. 417-421.
147. Fenteany, G., et al., *A beta-lactone related to lactacystin induces neurite outgrowth in a neuroblastoma cell line and inhibits cell cycle progression in an osteosarcoma cell line.* Proceedings of the National Academy of Sciences of the United States of America, 1994. **91**(8): p. 3358-3362.
148. Fenteany, G., et al., *Inhibition of proteasome activities and subunit-specific amino-terminal threonine modification by lactacystin.* Science, 1995. **268**(5211): p. 726-31.
149. Dick, L.R., et al., *Mechanistic Studies on the Inactivation of the Proteasome by Lactacystin: A CENTRAL ROLE FOR clasto-LACTACYSTIN β-LACTONE.* Journal of Biological Chemistry, 1996. **271**(13): p. 7273-7276.
150. Ostrowska, H., et al., *Lactacystin, a Specific Inhibitor of the Proteasome, Inhibits Human Platelet Lysosomal Cathepsin A-like Enzyme.* Biochemical and Biophysical Research Communications, 1997. **234**(3): p. 729-732.
151. Granot, Z., et al., *Turnover of Mitochondrial Steroidogenic Acute Regulatory (StAR) Protein by Lon Protease: The Unexpected Effect of Proteasome Inhibitors.* Molecular Endocrinology, 2007. **21**(9): p. 2164-2177.
152. Schwarz, K., et al., *The Selective Proteasome Inhibitors Lactacystin and Epoxomicin Can Be Used to Either Up- or Down-Regulate Antigen Presentation at Nontoxic Doses.* The Journal of Immunology, 2000. **164**(12): p. 6147-6157.
153. Imajoh-Ohmi, S., et al., *Lactacystin, a Specific Inhibitor of the Proteasome, Induces Apoptosis in Human Monoblast U937 Cells.* Biochemical and Biophysical Research Communications, 1995. **217**(3): p. 1070-1077.
154. Soldatenkov, V.A. and A. Dritschilo, *Apoptosis of Ewing's Sarcoma Cells Is Accompanied by Accumulation of Ubiquitinated Proteins.* Cancer Research, 1997. **57**(18): p. 3881-3885.
155. Delic, J., et al., *The proteasome inhibitor lactacystin induces apoptosis and sensitizes chemo- and radioresistant human chronic lymphocytic leukaemia lymphocytes to TNF-α-initiated apoptosis.* British Journal of Cancer, 1998. **77**(7): p. 1103-1107.
156. Masdehors, P., et al., *Ubiquitin-Proteasome System and Increased Sensitivity of B-CLL Lymphocytes to Apoptotic Death Activation.* Leukemia & Lymphoma, 2000. **38**(5-6): p. 499-504.
157. U.S. National Library of Medicine and U.S. National Institutes of Health. *ClinicalTrials.gov*. [cited 2016 February 3]; Available from: https://clinicaltrials.gov/.
158. Bogyo, M., et al., *Covalent modification of the active site threonine of proteasomal β subunits and the Escherichia coli homolog HslV by a new class*

of inhibitors. Proceedings of the National Academy of Sciences of the United States of America, 1997. **94**(13): p. 6629-6634.
159. Bogyo, M., et al., *Substrate binding and sequence preference of the proteasome revealed by active-site-directed affinity probes.* Chemistry & Biology, 1998. **5**(6): p. 307-320.
160. Nazif, T. and M. Bogyo, *Global analysis of proteasomal substrate specificity using positional-scanning libraries of covalent inhibitors.* Proceedings of the National Academy of Sciences of the United States of America, 2001. **98**(6): p. 2967-2972.
161. Screen, M., et al., *Nature of Pharmacophore Influences Active Site Specificity of Proteasome Inhibitors.* Journal of Biological Chemistry, 2010. **285**(51): p. 40125-40134.
162. Kessler, B.M., et al., *Extended peptide-based inhibitors efficiently target the proteasome and reveal overlapping specificities of the catalytic β-subunits.* Chemistry & Biology, 2001. **8**(9): p. 913-929.
163. Carmony, K.C. and K. Kim, *Activity-Based Imaging Probes of the Proteasome.* Cell Biochemistry and Biophysics, 2013. **67**(1): p. 91-101.
164. Palmer, J.T., et al., *Vinyl Sulfones as Mechanism-Based Cysteine Protease Inhibitors.* Journal of Medicinal Chemistry, 1995. **38**(17): p. 3193-3196.
165. Meng, L., et al., *Eponemycin Exerts Its Antitumor Effect through the Inhibition of Proteasome Function.* Cancer Research, 1999. **59**(12): p. 2798-2801.
166. Meng, L., et al., *Epoxomicin, a potent and selective proteasome inhibitor, exhibits in vivo antiinflammatory activity.* Proceedings of the National Academy of Sciences of the United States of America, 1999. **96**(18): p. 10403-10408.
167. Sugawara, K., et al., *Eponemycin, a new antibiotic active against B16 melanoma. I. Production, isolation, structure and biological activity.* The Journal of Antibiotics (Tokyo), 1990. **43**(1): p. 8-18.
168. Hanada, M., et al., *Epoxomicin, a new antitumor agent of microbial origin.* The Journal of Antibiotics (Tokyo), 1992. **45**(11): p. 1746-52.
169. Sin, N., et al., *Total synthesis of the-potent proteasome inhibitor epoxomicin: a useful tool for understanding proteasome biology.* Bioorganic & Medicinal Chemistry Letters, 1999. **9**(15): p. 2283-2288.
170. Groll, M., et al., *Crystal Structure of Epoxomicin:20S Proteasome Reveals a Molecular Basis for Selectivity of α',β'-Epoxyketone Proteasome Inhibitors.* Journal of the American Chemical Society, 2000. **122**(6): p. 1237-1238.
171. Kim, K.B., et al., *Proteasome inhibition by the natural products epoxomicin and dihydroeponemycin: Insights into specificity and potency.* Bioorganic & Medicinal Chemistry Letters, 1999. **9**(23): p. 3335-3340.
172. Steele, J.M., *Carfilzomib: A new proteasome inhibitor for relapsed or refractory multiple myeloma.* Journal of Oncology Pharmacy Practice, 2013. **19**(4): p. 348-354.
173. Elofsson, M., et al., *Towards subunit-specific proteasome inhibitors: synthesis and evaluation of peptide α'β'-epoxyketones.* Chemistry & Biology, 1999. **6**(11): p. 811-822.
174. Demo, S.D., et al., *Antitumor Activity of PR-171, a Novel Irreversible Inhibitor of the Proteasome.* Cancer Research, 2007. **67**(13): p. 6383-6391.
175. Momose, I., et al., *Structure-based design of derivatives of tyropeptin A as the potent and selective inhibitors of mammalian 20S proteasome.* Bioorganic & Medicinal Chemistry Letters, 2005. **15**(7): p. 1867-1871.

176. Britton, M., et al., *Selective Inhibitor of Proteasome's Caspase-like Sites Sensitizes Cells to Specific Inhibition of Chymotrypsin-like Sites.* Chemistry & Biology, 2009. **16**(12): p. 1278-1289.
177. Myung, J., et al., *Lack of Proteasome Active Site Allostery as Revealed by Subunit-Specific Inhibitors.* Molecular Cell, 2001. **7**(2): p. 411-420.
178. Miller, Z., et al., *Inhibitors of the immunoproteasome: current status and future directions.* Current Pharmaceutical Design, 2013. **19**(22): p. 4140-51.
179. van Swieten, P.F., et al., *A cell-permeable inhibitor and activity-based probe for the caspase-like activity of the proteasome.* Bioorganic & Medicinal Chemistry Letters, 2007. **17**(12): p. 3402-3405.
180. Mirabella, Anne C., et al., *Specific Cell-Permeable Inhibitor of Proteasome Trypsin-like Sites Selectively Sensitizes Myeloma Cells to Bortezomib and Carfilzomib.* Chemistry & Biology, 2011. **18**(5): p. 608-618.
181. Kisselev, A.F. and A.L. Goldberg, *Monitoring Activity and Inhibition of 26S Proteasomes with Fluorogenic Peptide Substrates*, in *Methods in Enzymology*, R.J. Deshaies, Editor. 2005, Academic Press. p. 364-378.
182. Marastoni, M., et al., *Peptidyl Vinyl Ester Derivatives: New Class of Selective Inhibitors of Proteasome Trypsin-Like Activity.* Journal of Medicinal Chemistry, 2005. **48**(15): p. 5038-5042.
183. Geurink, P.P., et al., *Incorporation of Non-natural Amino Acids Improves Cell Permeability and Potency of Specific Inhibitors of Proteasome Trypsin-like Sites.* Journal of Medicinal Chemistry, 2013. **56**(3): p. 1262-1275.
184. Kraus, M., et al., *The novel β2-selective proteasome inhibitor LU-102 synergizes with bortezomib and carfilzomib to overcome proteasome inhibitor resistance of myeloma cells.* Haematologica, 2015. **100**(10): p. 1350-1360.
185. Zhou, H.-J., et al., *Design and Synthesis of an Orally Bioavailable and Selective Peptide Epoxyketone Proteasome Inhibitor (PR-047).* Journal of Medicinal Chemistry, 2009. **52**(9): p. 3028-3038.
186. Parlati, F., et al., *Carfilzomib can induce tumor cell death through selective inhibition of the chymotrypsin-like activity of the proteasome.* Blood, 2009. **114**(16): p. 3439-3447.
187. Ichikawa, H.T., et al., *Beneficial effect of novel proteasome inhibitors in murine lupus via dual inhibition of type I interferon and autoantibody-secreting cells.* Arthritis & Rheumatism, 2012. **64**(2): p. 493-503.
188. Fitzpatrick, L., et al., *Dextran Sulfate Sodium-Induced Colitis Is Associated with Enhanced Low Molecular Mass Polypeptide 2 (LMP2) Expression and Is Attenuated in LMP2 Knockout Mice.* Digestive Diseases and Sciences, 2006. **51**(7): p. 1269-1276.
189. Fitzpatrick, L., et al., *Enhanced Intestinal Expression of the Proteasome Subunit Low Molecular Mass Polypeptide 2 in Patients with Inflammatory Bowel Disease.* Diseases of the Colon & Rectum, 2007. **50**(3): p. 337-350.
190. Visekruna, A., et al., *Expression of catalytic proteasome subunits in the gut of patients with Crohn's disease.* International Journal of Colorectal Disease, 2009. **24**(10): p. 1133-1139.
191. Visekruna, A., et al., *Comparative expression analysis and characterization of 20S proteasomes in human intestinal tissues: The proteasome pattern as diagnostic tool for IBD patients.* Inflammatory Bowel Diseases, 2009. **15**(4): p. 526-33.
192. Ho, Y.K., et al., *LMP2-Specific Inhibitors: Chemical Genetic Tools for Proteasome Biology.* Chemistry & Biology, 2007. **14**(4): p. 419-430.

193. Kuhn, D.J., et al., *Targeted inhibition of the immunoproteasome is a potent strategy against models of multiple myeloma that overcomes resistance to conventional drugs and nonspecific proteasome inhibitors.* Blood, 2009. **113**(19): p. 4667-4676.
194. Singh, A.V., et al., *PR-924, a selective inhibitor of the immunoproteasome subunit LMP-7, blocks multiple myeloma cell growth both in vitro and in vivo.* British Journal of Haematology, 2011. **152**(2): p. 155-163.
195. Wehenkel, M., et al., *A selective inhibitor of the immunoproteasome subunit LMP2 induces apoptosis in PC-3 cells and suppresses tumour growth in nude mice.* British Journal of Cancer, 2012. **107**(1): p. 53-62.
196. Loidl, G., et al., *Bifunctional inhibitors of the trypsin-like activity of eukaryotic proteasomes.* Chemistry & Biology, 1999. **6**(4): p. 197-204.
197. Loidl, G., et al., *Bivalency as a principle for proteasome inhibition.* Proceedings of the National Academy of Sciences, USA, 1999. **96**(10): p. 5418-5422.
198. Maréchal, X., et al., *Noncovalent inhibition of 20S proteasome by pegylated dimerized inhibitors.* European Journal of Medicinal Chemistry, 2012. **52**(0): p. 322-327.
199. Desvergne, A., et al., *Dimerized Linear Mimics of a Natural Cyclopeptide (TMC-95A) Are Potent Noncovalent Inhibitors of the Eukaryotic 20S Proteasome.* Journal of Medicinal Chemistry, 2013. **56**(8): p. 3367-3378.
200. Berkers, C.R., et al., *Activity probe for in vivo profiling of the specificity of proteasome inhibitor bortezomib.* Nature Methods, 2005. **2**(5): p. 357-362.
201. Verdoes, M., et al., *A Fluorescent Broad-Spectrum Proteasome Inhibitor for Labeling Proteasomes In Vitro and In Vivo.* Chemistry & Biology, 2006. **13**(11): p. 1217-1226.
202. Chauhan, D., et al., *A novel orally active proteasome inhibitor induces apoptosis in multiple myeloma cells with mechanisms distinct from Bortezomib.* Cancer Cell, 2005. **8**(5): p. 407-419.
203. Crawford, L.J.A., et al., *Comparative Selectivity and Specificity of the Proteasome Inhibitors BzLLLCOCHO, PS-341, and MG-132.* Cancer Research, 2006. **66**(12): p. 6379-6386.
204. Kraus, M., et al., *Activity patterns of proteasome subunits reflect bortezomib sensitivity of hematologic malignancies and are variable in primary human leukemia cells.* Leukemia, 2006. **21**(1): p. 84-92.
205. Gu, C., et al., *Proteasome activity profiling: a simple, robust and versatile method revealing subunit-selective inhibitors and cytoplasmic, defense-induced proteasome activities.* Plant Journal, 2010. **62**(1): p. 160-170.
206. Verdoes, M., et al., *A panel of subunit-selective activity-based proteasome probes.* Organic & Biomolecular Chemistry, 2010. **8**(12): p. 2719-2727.
207. Berkers, C.R., et al., *Probing the Specificity and Activity Profiles of the Proteasome Inhibitors Bortezomib and Delanzomib.* Molecular Pharmaceutics, 2012. **9**(5): p. 1126-1135.
208. Berkers, C.R., et al., *Profiling Proteasome Activity in Tissue with Fluorescent Probes.* Molecular Pharmaceutics, 2007. **4**(5): p. 739-748.
209. Ruckrich, T., et al., *Characterization of the ubiquitin-proteasome system in bortezomib-adapted cells.* Leukemia, 2009. **23**(6): p. 1098-1105.
210. Crawford, L.J., et al., *Proteasome proteolytic profile is linked to Bcr-Abl expression.* Experimental Hematology, 2009. **37**(3): p. 357-366.
211. Kristiansen, M., et al., *Disease-Associated Prion Protein Oligomers Inhibit the 26S Proteasome.* Molecular Cell, 2007. **26**(2): p. 175-188.

212. Florea, B.I., et al., *Activity-Based Profiling Reveals Reactivity of the Murine Thymoproteasome-Specific Subunit β5t.* Chemistry & Biology, 2010. **17**(8): p. 795-801.
213. Carmony, K.C., et al., *A bright approach to the immunoproteasome: Development of LMP2/β1i-specific imaging probes.* Bioorganic & Medicinal Chemistry, 2012. **20**(2): p. 607-613.
214. Sharma, L.K., et al., *Activity-Based Near-Infrared Fluorescent Probe for LMP7: A Chemical Proteomics Tool for the Immunoproteasome in Living Cells.* ChemBioChem, 2012. **13**(13): p. 1899-1903.
215. Hirano, Y., et al., *A heterodimeric complex that promotes the assembly of mammalian 20S proteasomes.* Nature, 2005. **437**(7063): p. 1381-1385.
216. Hirano, Y., et al., *Cooperation of Multiple Chaperones Required for the Assembly of Mammalian 20S Proteasomes.* Molecular Cell, 2006. **24**(6): p. 977-984.
217. Hirano, Y., et al., *Dissecting β-ring assembly pathway of the mammalian 20S proteasome.* The EMBO Journal, 2008. **27**(16): p. 2204-2213.
218. Nandi, D., et al., *Intermediates in the formation of mouse 20S proteasomes: implications for the assembly of precursor β subunits.* The EMBO Journal, 1997. **16**(17): p. 5363-5375.
219. Bai, M., et al., *Assembly Mechanisms of Specialized Core Particles of the Proteasome.* Biomolecules, 2014. **4**(3): p. 662-677.
220. Groettrup, M., et al., *The subunits MECL-1 and LMP2 are mutually required for incorporation into the 20S proteasome.* Proceedings of the National Academy of Sciences, USA, 1997. **94**(17): p. 8970-8975.
221. Griffin, T.A., et al., *Immunoproteasome Assembly: Cooperative Incorporation of Interferon γ (IFN-γ)–inducible Subunits.* Journal of Experimental Medicine, 1998. **187**(1): p. 97-104.
222. Kingsbury, D.J., T.A. Griffin, and R.A. Colbert, *Novel Propeptide Function in 20 S Proteasome Assembly Influences β Subunit Composition.* Journal of Biological Chemistry, 2000. **275**(31): p. 24156-24162.
223. De, M., et al., *β2 Subunit Propeptides Influence Cooperative Proteasome Assembly.* Journal of Biological Chemistry, 2003. **278**(8): p. 6153-6159.
224. Dahlmann, B., et al., *Different proteasome subtypes in a single tissue exhibit different enzymatic properties.* Journal of Molecular Biology, 2000. **303**(5): p. 643-653.
225. Klare, N., et al., *Intermediate-type 20 S Proteasomes in HeLa Cells: "Asymmetric" Subunit Composition, Diversity and Adaptation.* Journal of Molecular Biology, 2007. **373**(1): p. 1-10.
226. Guillaume, B., et al., *Two abundant proteasome subtypes that uniquely process some antigens presented by HLA class I molecules.* Proceedings of the National Academy of Sciences, USA, 2010. **107**(43): p. 18599-18604.
227. Wang, X., et al., *Gel-based proteomics analysis of the heterogeneity of 20S proteasomes from four human pancreatic cancer cell lines.* Proteomics: Clinical Applications, 2011. **5**(9-10): p. 484-492.
228. Fabre, B., et al., *Subcellular Distribution and Dynamics of Active Proteasome Complexes Unraveled by a Workflow Combining in Vivo Complex Cross-Linking and Quantitative Proteomics.* Molecular & Cellular Proteomics, 2013. **12**(3): p. 687-699.
229. Gohlke, S., et al., *Adult human liver contains intermediate-type proteasomes with different enzymatic properties.* Ann Hepatol, 2014. **13**(4): p. 429-38.

230. Drews, O., et al., *Mammalian Proteasome Subpopulations with Distinct Molecular Compositions and Proteolytic Activities.* Molecular & Cellular Proteomics, 2007. **6**(11): p. 2021-2031.
231. Gomes, A.V., et al., *Contrasting Proteome Biology and Functional Heterogeneity of the 20 S Proteasome Complexes in Mammalian Tissues.* Molecular & Cellular Proteomics, 2009. **8**(2): p. 302-315.
232. Kloß, A., et al., *Multiple cardiac proteasome subtypes differ in their susceptibility to proteasome inhibitors.* Cardiovascular Research, 2010. **85**(2): p. 367-375.
233. Pelletier, S., et al., *Quantifying cross-tissue diversity in proteasome complexes by mass spectrometry.* Molecular BioSystems, 2010. **6**(8): p. 1450-1453.
234. Zheng, J., A. Dasgupta, and O.A. Bizzozero, *Changes in 20S subunit composition are largely responsible for altered proteasomal activities in experimental autoimmune encephalomyelitis.* Journal of Neurochemistry, 2012. **121**(3): p. 486-494.
235. Gohlke, S., et al., *Molecular alterations in proteasomes of rat liver during aging result in altered proteolytic activities.* Age, 2014. **36**(1): p. 57-72.
236. Guillaume, B., et al., *Analysis of the Processing of Seven Human Tumor Antigens by Intermediate Proteasomes.* Journal of Immunology, 2012. **189**(7): p. 3538-3547.
237. Vigneron, N. and B.J. Van den Eynde, *Proteasome subtypes and the processing of tumor antigens: increasing antigenic diversity.* Current Opinion in Immunology, 2012. **24**(1): p. 84-91.
238. Zanker, D., et al., *Mixed Proteasomes Function To Increase Viral Peptide Diversity and Broaden Antiviral CD8+ T Cell Responses.* Journal of Immunology, 2013. **191**(1): p. 52-59.
239. Carmony, K.C., et al., *Elucidating the Catalytic Subunit Composition of Distinct Proteasome Subtypes: A Crosslinking Approach Employing Bifunctional Activity-Based Probes.* ChemBioChem, 2015. **16**(2): p. 284-292.
240. Goldberg, A.L., *Development of proteasome inhibitors as research tools and cancer drugs.* The Journal of Cell Biology, 2012. **199**(4): p. 583-588.
241. Masdehors, P., et al., *Deregulation of the ubiquitin system and p53 proteolysis modify the apoptotic response in B-CLL lymphocytes.* Blood, 2000. **96**(1): p. 269-274.
242. Hideshima, T., et al., *The Proteasome Inhibitor PS-341 Inhibits Growth, Induces Apoptosis, and Overcomes Drug Resistance in Human Multiple Myeloma Cells.* Cancer Research, 2001. **61**(7): p. 3071-3076.
243. Altun, M., et al., *Effects of PS-341 on the Activity and Composition of Proteasomes in Multiple Myeloma Cells.* Cancer Research, 2005. **65**(17): p. 7896-7901.
244. Kisselev, A.F., A. Callard, and A.L. Goldberg, *Importance of the Different Proteolytic Sites of the Proteasome and the Efficacy of Inhibitors Varies with the Protein Substrate.* Journal of Biological Chemistry, 2006. **281**(13): p. 8582-8590.
245. Piva, R., et al., *CEP-18770: A novel, orally active proteasome inhibitor with a tumor-selective pharmacologic profile competitive with bortezomib.* Blood, 2008. **111**(5): p. 2765-2775.
246. Oerlemans, R., et al., *Molecular basis of bortezomib resistance: proteasome subunit β5 (PSMB5) gene mutation and overexpression of PSMB5 protein.* Blood, 2008. **112**(6): p. 2489-2499.
247. Mitsiades, N., et al., *Molecular sequelae of proteasome inhibition in human multiple myeloma cells.* Proceedings of the National Academy of Sciences of the United States of America, 2002. **99**(22): p. 14374-14379.

248. Ruiz, S., et al., *The proteasome inhibitor NPI-0052 is a more effective inducer of apoptosis than bortezomib in lymphocytes from patients with chronic lymphocytic leukemia.* Molecular Cancer Therapeutics, 2006. **5**(7): p. 1836-1843.
249. Aghajanian, C., et al., *A Phase I Trial of the Novel Proteasome Inhibitor PS341 in Advanced Solid Tumor Malignancies.* Clinical Cancer Research, 2002. **8**(8): p. 2505-2511.
250. Orlowski, R.Z., et al., *Phase I Trial of the Proteasome Inhibitor PS-341 in Patients With Refractory Hematologic Malignancies.* Journal of Clinical Oncology, 2002. **20**(22): p. 4420-4427.
251. Papandreou, C.N., et al., *Phase I Trial of the Proteasome Inhibitor Bortezomib in Patients With Advanced Solid Tumors With Observations in Androgen-Independent Prostate Cancer.* Journal of Clinical Oncology, 2004. **22**(11): p. 2108-2121.
252. Hamilton, A.L., et al., *Proteasome Inhibition With Bortezomib (PS-341): A Phase I Study With Pharmacodynamic End Points Using a Day 1 and Day 4 Schedule in a 14-Day Cycle.* Journal of Clinical Oncology, 2005. **23**(25): p. 6107-6116.
253. Reece, D.E., et al., *Pharmacokinetic and pharmacodynamic study of two doses of bortezomib in patients with relapsed multiple myeloma.* Cancer chemotherapy and pharmacology, 2011. **67**(1): p. 57-67.
254. Bross, P.F., et al., *Approval Summary for Bortezomib for Injection in the Treatment of Multiple Myeloma.* Clinical Cancer Research, 2004. **10**(12): p. 3954-3964.
255. *VELCADE® (bortezomib) [package insert]*. 2015, Millennium Pharmaceuticals, Inc., USA.
256. Arastu-Kapur, S., et al., *Nonproteasomal Targets of the Proteasome Inhibitors Bortezomib and Carfilzomib: a Link to Clinical Adverse Events.* Clinical Cancer Research, 2011. **17**(9): p. 2734-2743.
257. Richardson, P.G., et al., *Bortezomib or High-Dose Dexamethasone for Relapsed Multiple Myeloma.* New England Journal of Medicine, 2005. **352**(24): p. 2487-2498.
258. Cheriyath, V., B.S. Jacobs, and M.A. Hussein, *Proteasome Inhibitors in the Clinical Setting: Benefits and Strategies to Overcome Multiple Myeloma Resistance to Proteasome Inhibitors.* Drugs in R&D, 2007. **8**(1): p. 1-12.
259. Richardson, P.G., et al., *Single-Agent Bortezomib in Previously Untreated Multiple Myeloma: Efficacy, Characterization of Peripheral Neuropathy, and Molecular Correlations With Response and Neuropathy.* Journal of Clinical Oncology, 2009. **27**(21): p. 3518-3525.
260. Hrusovsky, I., et al., *Bortezomib Retreatment in Relapsed Multiple Myeloma – Results from a Retrospective Multicentre Survey in Germany and Switzerland.* Oncology, 2010. **79**(3-4): p. 247-254.
261. Huang, Z., et al., *Efficacy of therapy with bortezomib in solid tumors: a review based on 32 clinical trials.* Future Oncology, 2014. **10**(10): p. 1795-1807.
262. Kuhn, D.J., et al., *Potent activity of carfilzomib, a novel, irreversible inhibitor of the ubiquitin-proteasome pathway, against preclinical models of multiple myeloma.* Blood, 2007. **110**(9): p. 3281–3290.
263. O'Connor, O.A., et al., *A Phase 1 Dose Escalation Study of the Safety and Pharmacokinetics of the Novel Proteasome Inhibitor Carfilzomib (PR-171) in Patients with Hematologic Malignancies.* Clinical Cancer Research, 2009. **15**(22): p. 7085-7091.
264. Alsina, M., et al., *A Phase I Single-Agent Study of Twice-Weekly Consecutive-Day Dosing of the Proteasome Inhibitor Carfilzomib in Patients with Relapsed or*

Refractory Multiple Myeloma or Lymphoma. Clinical Cancer Research, 2012. **18**(17): p. 4830-4840.
265. Vij, R., et al., *An open-label, single-arm, phase 2 (PX-171-004) study of single-agent carfilzomib in bortezomib-naive patients with relapsed and/or refractory multiple myeloma.* Blood, 2012. **119**(24): p. 5661-5670.
266. Vij, R., et al., *An open-label, single-arm, phase 2 study of single-agent carfilzomib in patients with relapsed and/or refractory multiple myeloma who have been previously treated with bortezomib.* British Journal of Haematology, 2012. **158**(6): p. 739-748.
267. Siegel, D.S., et al., *A phase 2 study of single-agent carfilzomib (PX-171-003-A1) in patients with relapsed and refractory multiple myeloma.* Blood, 2012. **120**(14): p. 2817-2825.
268. Papadopoulos, K.P., et al., *A phase I/II study of carfilzomib 2–10-min infusion in patients with advanced solid tumors.* Cancer Chemotherapy and Pharmacology, 2013. **72**(4): p. 861-868.
269. Jagannath, S., et al., *An Open-Label Single-Arm Pilot Phase II Study (PX-171-003-A0) of Low-Dose, Single-Agent Carfilzomib in Patients With Relapsed and Refractory Multiple Myeloma.* Clinical Lymphoma Myeloma and Leukemia, 2012. **12**(5): p. 310-318.
270. Kupperman, E., et al., *Evaluation of the Proteasome Inhibitor MLN9708 in Preclinical Models of Human Cancer.* Cancer Research, 2010. **70**(5): p. 1970-1980.
271. Chauhan, D., et al., *In Vitro and In Vivo Selective Antitumor Activity of a Novel Orally Bioavailable Proteasome Inhibitor MLN9708 against Multiple Myeloma Cells.* Clinical Cancer Research, 2011. **17**(16): p. 5311-5321.
272. Muz, B., et al., *Spotlight on ixazomib: potential in the treatment of multiple myeloma.* Drug Design, Development and Therapy, 2016. **10**: p. 217-226.
273. Gallerani, E., et al., *A first in human phase I study of the proteasome inhibitor CEP-18770 in patients with advanced solid tumours and multiple myeloma.* European Journal of Cancer, 2013. **49**(2): p. 290-296.
274. Chauhan, D., et al., *A novel orally active proteasome inhibitor ONX 0912 triggers in vitro and in vivo cytotoxicity in multiple myeloma.* Blood, 2010. **116**(23): p. 4906-4915.
275. Sharma, R.C., et al., *Peptide transport by the multidrug resistance pump.* Journal of Biological Chemistry, 1992. **267**(9): p. 5731-4.
276. de Jong, M.C., et al., *Peptide Transport by the Multidrug Resistance Protein MRP1.* Cancer Research, 2001. **61**(6): p. 2552-2557.
277. Sasaki, T., et al., *Inhibitory effect of di- and tripeptidyl aldehydes on calpains and cathepsins.* Journal of Enzyme Inhibition, 1990. **3**(3): p. 195-201.
278. Gutman, D., A.A. Morales, and L.H. Boise, *Acquisition of a multidrug-resistant phenotype with a proteasome inhibitor in multiple myeloma.* Leukemia, 2009. **23**(11): p. 2181-2183.
279. Ohkawa, K., et al., *Establishment and some characteristics of epoxomicin (a proteasome inhibitor) resistant variants of the human squamous cell carcinoma cell line, A431.* International Journal of Oncology, 2004. **24**(2): p. 425-433.
280. Verbrugge, S.E., et al., *Inactivating PSMB5 Mutations and P-Glycoprotein (Multidrug Resistance-Associated Protein/ATP-Binding Cassette B1) Mediate Resistance to Proteasome Inhibitors: Ex Vivo Efficacy of (Immuno)Proteasome Inhibitors in Mononuclear Blood Cells from Patients with Rheumatoid Arthritis.* Journal of Pharmacology and Experimental Therapeutics, 2012. **341**(1): p. 174-182.

281. Ao, L., et al., *Development of Peptide-Based Reversing Agents for P-Glycoprotein-Mediated Resistance to Carfilzomib.* Molecular Pharmaceutics, 2012. **9**(8): p. 2197-2205.
282. Hawley, T.S., et al., *Identification of an ABCB1 (P-glycoprotein)-positive carfilzomib-resistant myeloma subpopulation by the pluripotent stem cell fluorescent dye CDy1.* American journal of hematology, 2013. **88**(4): p. 265-272.
283. Zang, Y., C.J. Kirk, and D.E. Johnson, *Carfilzomib and oprozomib synergize with histone deacetylase inhibitors in head and neck squamous cell carcinoma models of acquired resistance to proteasome inhibitors.* Cancer Biology & Therapy, 2014. **15**(9): p. 1142-1152.
284. Zheng, B., et al., *Proteasome inhibitor bortezomib overcomes P-gp-mediated multidrug resistance in resistant leukemic cell lines.* International Journal of Laboratory Hematology, 2012. **34**(3): p. 237-247.
285. Fuchs, D., et al., *Increased expression and altered subunit composition of proteasomes induced by continuous proteasome inhibition establish apoptosis resistance and hyperproliferation of Burkitt lymphoma cells.* Journal of Cellular Biochemistry, 2008. **103**(1): p. 270-283.
286. Lü, S., et al., *Overexpression of the PSMB5 gene contributes to bortezomib resistance in T-lymphoblastic lymphoma/leukemia cells derived from Jurkat line.* Experimental Hematology, 2008. **36**(10): p. 1278-1284.
287. Zhang, L., et al., *Characterization of bortezomib-adapted I-45 mesothelioma cells.* Molecular Cancer, 2010. **9**(110).
288. Kuhn, D.J., et al., *Targeting the insulin-like growth factor-1 receptor to overcome bortezomib resistance in preclinical models of multiple myeloma.* Blood, 2012. **120**(16): p. 3260-3270.
289. de Wilt, L.H.A.M., et al., *Proteasome-based mechanisms of intrinsic and acquired bortezomib resistance in non-small cell lung cancer.* Biochemical Pharmacology, 2012. **83**(2): p. 207-217.
290. Hamouda, M.-A., et al., *The small heat shock protein B8 (HSPB8) confers resistance to bortezomib by promoting autophagic removal of misfolded proteins in multiple myeloma cells.* Oncotarget, 2014. **5**(15): p. 6252-6266.
291. Minderman, H., et al., *Bortezomib activity and in vitro interactions with anthracyclines and cytarabine in acute myeloid leukemia cells are independent of multidrug resistance mechanisms and p53 status.* Cancer Chemotherapy and Pharmacology, 2007. **60**(2): p. 245-55.
292. Rumpold, H., et al., *Knockdown of PgP resensitizes leukemic cells to proteasome inhibitors.* Biochemical and Biophysical Research Communications, 2007. **361**(2): p. 549-554.
293. O'Connor, R., et al., *The interaction of bortezomib with multidrug transporters: implications for therapeutic applications in advanced multiple myeloma and other neoplasias.* Cancer chemotherapy and pharmacology, 2013. **71**(5): p. 1357-1368.
294. Bentires-Alj, M., et al., *NF-κB transcription factor induces drug resistance through MDR1 expression in cancer cells.* Oncogene, 2003. **22**(1): p. 90-97.
295. Fujita, T., et al., *Proteasome inhibitors can alter the signaling pathways and attenuate the P-glycoprotein-mediated multidrug resistance.* International Journal of Cancer, 2005. **117**(4): p. 670-682.
296. Inoue, S., et al., *Cellular detoxification of tripeptidyl aldehydes by an aldo-keto reductase.* Journal of Biological Chemistry, 1993. **268**(8): p. 5894-8.

297. Xu, D., et al., *Dll1/Notch activation contributes to bortezomib resistance by upregulating CYP1A1 in multiple myeloma.* Biochemical and Biophysical Research Communications, 2012. **428**(4): p. 518-524.
298. Suzuki, E., et al., *Molecular Mechanisms of Bortezomib Resistant Adenocarcinoma Cells.* PLoS ONE, 2011. **6**(12): p. e27996.
299. Glas, R., et al., *A proteolytic system that compensates for loss of proteasome function.* Nature, 1998. **392**(6676): p. 618-622.
300. Geier, E., et al., *A Giant Protease with Potential to Substitute for Some Functions of the Proteasome.* Science, 1999. **283**(5404): p. 978-981.
301. Wang, E.W., et al., *Integration of the ubiquitin-proteasome pathway with a cytosolic oligopeptidase activity.* Proceedings of the National Academy of Sciences of the United States of America, 2000. **97**(18): p. 9990-9995.
302. Princiotta, M.F., et al., *Cells adapted to the proteasome inhibitor 4-hydroxy- 5-iodo-3-nitrophenylacetyl-Leu-Leu-leucinal-vinyl sulfone require enzymatically active proteasomes for continued survival.* Proceedings of the National Academy of Sciences of the United States of America, 2001. **98**(2): p. 513-518.
303. Milani, M., et al., *The Role of ATF4 Stabilization and Autophagy in Resistance of Breast Cancer Cells Treated with Bortezomib.* Cancer Research, 2009. **69**(10): p. 4415-4423.
304. Zhu, K., K. Dunner, Jr., and D.J. McConkey, *Proteasome inhibitors activate autophagy as a cytoprotective response in human prostate cancer cells.* Oncogene, 2009. **29**(3): p. 451-462.
305. Min, H., et al., *Bortezomib induces protective autophagy through AMP-activated protein kinase activation in cultured pancreatic and colorectal cancer cells.* Cancer Chemother Pharmacol, 2014. **74**(1): p. 167-76.
306. Riz, I., T.S. Hawley, and R.G. Hawley, *KLF4-SQSTM1/p62-associated prosurvival autophagy contributes to carfilzomib resistance in multiple myeloma models.* Oncotarget, 2015. **6**(17): p. 14814-14831.
307. Lin, K.-I., J.M. Baraban, and R.R. Ratan, *Inhibition versus induction of apoptosis by proteasome inhibitors depends on concentration.* Cell Death & Differentiation, 1998. **5**(7): p. 577.
308. Meiners, S., et al., *Nontoxic proteasome inhibition activates a protective antioxidant defense response in endothelial cells.* Free Radical Biology and Medicine, 2006. **40**(12): p. 2232-2241.
309. Shabaneh, T.B., et al., *Molecular Basis of Differential Sensitivity of Myeloma Cells to Clinically Relevant Bolus Treatment with Bortezomib.* PLoS ONE, 2013. **8**(2): p. e56132.
310. Voortman, J., A. Checinska, and G. Giaccone, *The proteasomal and apoptotic phenotype determine bortezomib sensitivity of non-small cell lung cancer cells.* Molecular Cancer, 2007. **6**(1): p. 73.
311. Lü, S., et al., *Point Mutation of the Proteasome β5 Subunit Gene Is an Important Mechanism of Bortezomib Resistance in Bortezomib-Selected Variants of Jurkat T Cell Lymphoblastic Lymphoma/Leukemia Line.* Journal of Pharmacology and Experimental Therapeutics, 2008. **326**(2): p. 423-431.
312. Lü, S., et al., *Different mutants of PSMB5 confer varying bortezomib resistance in T lymphoblastic lymphoma/leukemia cells derived from the Jurkat cell line.* Experimental Hematology, 2009. **37**(7): p. 831-837.
313. Franke, N.E., et al., *Impaired bortezomib binding to mutant β5 subunit of the proteasome is the underlying basis for bortezomib resistance in leukemia cells.* Leukemia, 2011.

314. Ri, M., et al., *Bortezomib-resistant myeloma cell lines: a role for mutated PSMB5 in preventing the accumulation of unfolded proteins and fatal ER stress.* Leukemia, 2010. **24**(8): p. 1506-1512.
315. Verbrugge, S.E., et al., *Overcoming bortezomib resistance in human B cells by anti-CD20/rituximab-mediated complement-dependent cytotoxicity and epoxyketone-based irreversible proteasome inhibitors.* Experimental Hematology & Oncology, 2013. **2**(1): p. 1-12.
316. Heinemeyer, W., et al., *PRE2, highly homologous to the human major histocompatibility complex-linked RING10 gene, codes for a yeast proteasome subunit necessary for chrymotryptic activity and degradation of ubiquitinated proteins.* Journal of Biological Chemistry, 1993. **268**(7): p. 5115-5120.
317. Wang, L., et al., *Proteasome β Subunit Pharmacogenomics: Gene Resequencing and Functional Genomics.* Clinical Cancer Research, 2008. **14**(11): p. 3503-3513.
318. Niewerth, D., et al., *Anti-leukemic activity and mechanisms underlying resistance to the novel immunoproteasome inhibitor PR-924.* Biochemical Pharmacology, 2014. **89**(1): p. 43-51.
319. Politou, M., et al., *No evidence of mutations of the PSMB5 (beta-5 subunit of proteasome) in a case of myeloma with clinical resistance to Bortezomib.* Leukemia Research, 2006. **30**(2): p. 240-241.
320. Shuqing, L., et al., *Upregulated expression of the PSMB5 gene may contribute to drug resistance in patient with multiple myeloma when treated with bortezomib-based regimen.* Experimental Hematology, 2011. **39**(12): p. 1117-1118.
321. Lichter, D.I., et al., *Sequence analysis of β-subunit genes of the 20S proteasome in patients with relapsed multiple myeloma treated with bortezomib or dexamethasone.* Blood, 2012. **120**(23): p. 4513-4516.
322. Fleming, J.A., et al., *Complementary whole-genome technologies reveal the cellular response to proteasome inhibition by PS-341.* Proceedings of the National Academy of Sciences of the United States of America, 2002. **99**(3): p. 1461-1466.
323. Ju, D., et al., *Homeostatic regulation of the proteasome via an Rpn4-dependent feedback circuit.* Biochemical and Biophysical Research Communications, 2004. **321**(1): p. 51-57.
324. Wójcik, C. and G.N. DeMartino, *Analysis of Drosophila 26 S Proteasome Using RNA Interference.* Journal of Biological Chemistry, 2002. **277**(8): p. 6188-6197.
325. Meiners, S., et al., *Inhibition of Proteasome Activity Induces Concerted Expression of Proteasome Genes and de Novo Formation of Mammalian Proteasomes.* Journal of Biological Chemistry, 2003. **278**(24): p. 21517-21525.
326. Radhakrishnan, S.K., et al., *Transcription Factor Nrf1 Mediates the Proteasome Recovery Pathway after Proteasome Inhibition in Mammalian Cells.* Molecular Cell, 2010. **38**(1): p. 17-28.
327. Sha, Z. and Alfred L. Goldberg, *Proteasome-Mediated Processing of Nrf1 Is Essential for Coordinate Induction of All Proteasome Subunits and p97.* Current Biology, 2014. **24**(14): p. 1573-1583.
328. Steffen, J., et al., *Proteasomal Degradation Is Transcriptionally Controlled by TCF11 via an ERAD-Dependent Feedback Loop.* Molecular Cell, 2010. **40**(1): p. 147-158.
329. Pérez-Galán, P., et al., *Bortezomib resistance in mantle cell lymphoma is associated with plasmacytic differentiation.* Blood, 2011. **117**(2): p. 542-552.

330. Balsas, P., et al., *Bortezomib resistance in a myeloma cell line is associated to PSMβ5 overexpression and polyploidy.* Leukemia Research, 2012. **36**(2): p. 212-218.
331. Kale, A.J. and B.S. Moore, *Molecular Mechanisms of Acquired Proteasome Inhibitor Resistance.* Journal of Medicinal Chemistry, 2012. **55**(23): p. 10317-10327.
332. Niewerth, D., et al., *Interferon-γ-induced upregulation of immunoproteasome subunit assembly overcomes bortezomib resistance in human hematological cell lines.* Journal of Hematology & Oncology, 2014. **7**(1): p. 1-15.
333. Stessman, H.A.F., et al., *Profiling Bortezomib Resistance Identifies Secondary Therapies in a Mouse Myeloma Model.* Molecular Cancer Therapeutics, 2013. **12**(6): p. 1140-1150.
334. Busse, A., et al., *Sensitivity of tumor cells to proteasome inhibitors is associated with expression levels and composition of proteasome subunits.* Cancer, 2008. **112**(3): p. 659-670.
335. Hendil, K.B., S. Khan, and K. Tanaka, *Simultaneous binding of PA28 and PA700 activators to 20 S proteasomes.* Biochemical Journal, 1998. **332**(3): p. 749-754.
336. Tanahashi, N., et al., *Hybrid Proteasomes: INDUCTION BY INTERFERON-γ AND CONTRIBUTION TO ATP-DEPENDENT PROTEOLYSIS.* Journal of Biological Chemistry, 2000. **275**(19): p. 14336-14345.
337. Niewerth, D., et al., *Antileukemic Activity and Mechanism of Drug Resistance to the Marine Salinispora tropica Proteasome Inhibitor Salinosporamide A (Marizomib).* Molecular Pharmacology, 2014. **86**(1): p. 12-19.
338. Kraus, M., et al., *Nelfinavir augments proteasome inhibition by bortezomib in myeloma cells and overcomes bortezomib and carfilzomib resistance.* Blood Cancer Journal, 2013. **3**(3): p. e103.
339. Roué, G., et al., *The Hsp90 inhibitor IPI-504 overcomes bortezomib resistance in mantle cell lymphoma in vitro and in vivo by down-regulation of the prosurvival ER chaperone BiP/Grp78.* Blood, 2011. **117**(4): p. 1270-1279.
340. Ling, S.C.W., et al., *Response of myeloma to the proteasome inhibitor bortezomib is correlated with the unfolded protein response regulator XBP-1.* Haematologica, 2012. **97**(1): p. 64-72.
341. Kumar, L. *Development of Novel Chemical Tools for Proteasome Biology & a New Approach to 1-Azaspirocyclic Ring System*. Theses and Dissertations--Chemistry 2012; Available from: http://uknowledge.uky.edu/chemistry_etds/14/
342. Joeris, T., et al., *The Proteasome System in Infection: Impact of β5 and LMP7 on Composition, Maturation and Quantity of Active Proteasome Complexes.* PLoS One, 2012. **7**(6): p. e39827.
343. Park, J.E., et al., *A FRET-based approach for identification of proteasome catalytic subunit composition.* Molecular BioSystems, 2014. **10**(2): p. 196-200.
344. Lu, Y.F., et al., *Computational prediction of cleavage using proteasomal in vitro digestion and MHC I ligand data.* Journal of Zhejiang University, Science, B, 2013. **14**(9): p. 816-28.
345. Cenci, S., et al., *Pivotal Advance: Protein synthesis modulates responsiveness of differentiating and malignant plasma cells to proteasome inhibitors.* Journal of Leukocyte Biology, 2012. **92**(5): p. 921-931.
346. Zhang, L., et al., *In Vitro and In Vivo Therapeutic Efficacy of Carfilzomib in Mantle Cell Lymphoma: Targeting the Immunoproteasome.* Molecular Cancer Therapeutics, 2013. **12**(11): p. 2494-2504.
347. Scagliotti, G., *Proteasome inhibitors in lung cancer.* Critical Reviews in Oncology/Hematology, 2006. **58**(3): p. 177-189.

348. Escobar, M., et al., *The Role of Proteasome Inhibition in Nonsmall Cell Lung Cancer.* Journal of Biomedicine and Biotechnology, 2011. **2011**.
349. Kisselev, A.F., et al., *The Caspase-like Sites of Proteasomes, Their Substrate Specificity, New Inhibitors and Substrates, and Allosteric Interactions with the Trypsin-like Sites.* Journal of Biological Chemistry, 2003. **278**(38): p. 35869-35877.

VITA

KIMBERLY CORNISH CARMONY

EDUCATION

2003-2008	Bachelor of Science, Biology University of Kentucky, Lexington, KY *Magna Cum Laude*

PROFESSIONAL POSITIONS

2008	Undergraduate Researcher University of Kentucky, Department of Biology Supervisor: James Lund, Ph.D.
2008-2009	Laboratory Technician University of Kentucky Livestock Disease Diagnostic Center Supervisor: Steve Sells, M.S., Ph.D.
2009-2011	Teaching Assistant and Exam Proctor University of Kentucky, College of Pharmacy Supervisors: Val Adams, Pharm.D., FCCP, BCOP, Gregory Graf, Ph.D., and Jim Pauly, Ph.D.
2010-Present	Research Assistant Supervisor: Kyung-Bo Kim, Ph.D.

PUBLICATIONS

1. **Kimberly Cornish Carmony** and Kyung-Bo Kim (2012). PROTAC-Induced Proteolytic Targeting. *Methods in Molecular Biology* edited by R. Jürgen Dohmen and Martin Scheffner, **832**: 627-638.

2. **Kimberly Cornish Carmony**, Do-Min Lee, Ying Wu, Na-Ra Lee, Marie Wehenkel, Jason Lee, Beilei Lei, Chang-Guo Zhan, and Kyung-Bo Kim (2012). A bright approach to the immunoproteasome: Development of LMP2/β1i-specific imaging probes. *Bioorganic & Medicinal Chemistry*, **20**(2): 607-613.

3. Marie Wehenkel, Jung-Ok Ban, Yik-Khuan Ho, **Kimberly Cornish Carmony**, Jin Tae Hong, and Kyung-Bo Kim (2012). A selective inhibitor of the immunoproteasome subunit LMP2 induces apoptosis in PC-3 cells and suppresses tumor growth in nude mice. *British Journal of Cancer*, **107**(1): 53-62.

4. Eun Ryoung Jang, Na-Ra Lee, Songhee Han, Ying Wu, Lalit Kumar Sharma, **Kimberly Cornish Carmony**, James Marks, Do-Min Lee, Jung-Ok Ban, Marie Wehenkel, Jin Tae Hong, Kyung Bo Kim, and Wooin Lee (2012). Revisiting the role of the immunoproteasome in the activation of the canonical NF-κB pathway. *Molecular BioSystems*, **8**(9): 2295-2302.

5. **Kimberly Cornish Carmony** and Kyung Bo Kim (2013). Activity-Based Imaging Probes of the Proteasome. *Cell Biochemistry and Biophysics*, **67**(1): 91-101.

6. Ji Eun Park, Ying Wu, **Kimberly Cornish Carmony**, Zachary Miller, Lalit Kumar Sharma, Do-Min Lee, Doo-Young Kim, Wooin Lee, and Kyung-Bo Kim (2014). A FRET-based approach for identification of proteasome catalytic subunit composition. *Molecular BioSystems*, **10**(2): 196-200.

7. **Kimberly Cornish Carmony**, Lalit Kumar Sharma, Do-Min Lee, Ji Eun Park, Wooin Lee, and Kyung-Bo Kim (2015). Elucidating the Catalytic Subunit Composition of Distinct Proteasome Subtypes: A Crosslinking Approach Employing Bifunctional Activity-Based Probes. *ChemBioChem*, **16**(2): 284-292.

8. Zachary Miller, Keun-Sik Kim, Do-Min Lee, Vinod Kasam, Si-Eun Baek, Kwang Hyun Lee, Yan-Yan Zhang, Lin Ao, **Kimberly Carmony**, Na-Ra Lee, Shuo Zhou, Qingquan Zhao, Yujin Jang, Hyun-Young Jeong, Chang-Guo Zhan, Wooin Lee, Dong-Eun Kim, and Kyung Bo Kim (2015). Proteasome inhibitors with pyrazole scaffolds from structure-based virtual screening. *Journal of Medicinal Chemistry*, **58**(4): 2036-2041.

AWARDS AND HONORS

2003-2007	Kentucky Educational Excellence Scholarship
2007	Inducted into Golden Key International Honour Society
2007-2008	Academic Excellence Scholarship from the University of Kentucky
2011	Inducted into the Rho Chi Society
2013-2014	AFPE Pre-Doctoral Fellowship in the Clinical Pharmaceutical Sciences
2014-2015	AFPE Pre-Doctoral Fellowship in the Clinical Pharmaceutical Sciences *Renewal of fellowship award for the 2014-2015 academic year.*

ABSTRACTS AND PRESENTATIONS
(denotes the presenter)*

1. Markey Cancer Center Research Day, 2010
   April 14, University of Kentucky, Lexington, Kentucky
   Poster Presentation: Revisiting the Role of LMP2 in the NF-κB Activation Pathway. (Abstract #81) **Kimberly Cornish***, Samantha Mangold, Marie Wehenkel, Jee Eun Kim, Abby Ho, and Kyung-Bo Kim

2. Proteomics of Protein Degradation and Ubiquitin Pathways, 2010
   June 6-8, Vancouver, British Columbia, Canada
   Poster Presentation: Effect of the chemical genetic inhibition of LMP2 on nuclear factor-κB (NF-κB) activation. (Abstract #44) **Kimberly Cornish***, Samantha Mangold, Marie Wehenkel, Jee Eun Kim, Abby Ho, and Kyung-Bo Kim

3. Symposium on Drug Discovery and Development, 2010
   October 15, University of Kentucky, Lexington, Kentucky
   Poster Presentation: Revisiting the Role of LMP2 in the NF-κB Activation Pathway. **Kimberly Cornish***, Samantha Mangold, Marie Wehenkel, Jee Eun Kim, Abby Ho, and Kyung-Bo Kim

4. American Association for Cancer Research Annual Meeting, 2011
   April 2-6, Orlando, Florida
   Poster Presentation: Development of Immunoproteasome-Targeting Activity-Based Fluorescent Probes. (Abstract #2621) **Kimberly Cornish Carmony***, Ying Wu, Do-Min Lee, Na-Ra Lee, Marie Wehenkel, Jason Lee, and Kyung-Bo Kim

5. American Association for Cancer Research Annual Meeting, 2012
   March 31-April 4, Chicago, Illinois
   Poster Presentation: Development of an immunoproteasome fluorescent substrate: A functional proteomics tool. (Abstract #4744) Na-Ra Lee, **Kimberly C. Carmony***, Ying Wu, Zachary Miller, and Kyung-Bo Kim

6. American Association for Cancer Research Annual Meeting, 2013
   April 6-10, Washington, D.C.
   Poster Presentation: Development of bifunctional cross-linking agents to identify intermediate proteasomes. (Abstract #2231) **Kimberly Cornish Carmony***, Lalit Kumar Sharma, Wooin Lee, and Kyung-Bo Kim

7. Rho Chi Research Day, 2013
   April 11, University of Kentucky, Lexington, Kentucky
   Poster Presentation: Development of bifunctional cross-linking agents to identify intermediate proteasomes. **Kimberly Cornish Carmony***, Lalit Kumar Sharma, and Kyung-Bo Kim
   Awarded 3rd Place in the Graduate Student Category

8. American Association for Cancer Research Annual Meeting, 2014
   April 5-9, San Diego, California
   Poster Presentation: Development of a novel cross-linking strategy to identify distinct proteasome subtypes. (Abstract #3236) **Kimberly Carmony***, Do-Min Lee, Lalit Kumar Sharma, Jieun Park, Wooin Lee, and Kyung-Bo Kim

9. Pharmaceutics Graduate Student Research Meeting, 2015
   June 11-13, University of Kentucky, Lexington, Kentucky
   Poster Presentation: Development of a novel cross-linking strategy to identify distinct proteasome subtypes. **Kimberly Carmony***, Do-Min Lee, Lalit Kumar Sharma, Jieun Park, Wooin Lee, and Kyung-Bo Kim